

Advancing Hyperacuity for Vision Screening

by

Mohammed, Abdul Rasheed

A thesis

presented to the University of Waterloo

in fulfillment of the

thesis requirement for the degree of

Doctor of Philosophy

in

Vision Science

Waterloo, Ontario, Canada, 2023

© Mohammed Abdul Rasheed 2023

EXAMINING COMMITTEE MEMBERSHIP

The following members served on the examining committee for this thesis.

The decision of the examining committee is by majority vote.

External Examiner

Dr. Vernon Odom

Professor
Department of Ophthalmology,
West Virginia University

Supervisor

Dr. Vasudevan Lakshminarayanan

Professor,
School of Optometry and Vision Science,
University of Waterloo

Co-supervisor

Dr. Kaamran Raahemifar

Associate Professor,
School of Optometry and Vision Science,
University of Waterloo

Committee Member

Dr. Kristine Dalton

Associate Professor,
School of Optometry and Vision Science,
University of Waterloo

Dr. Simar Saini

Associate Professor,
School of Electrical Engineering,
University of Waterloo

Internal-external Member

Dr. John Zelek

Associate Professor & Co-Director VIP
(Vision Image Processing) Lab,
Systems Design Engineering,
University of Waterloo

AUTHOR'S DECLARATION

This thesis consists of material all of which I authored or co-authored: see Statement of Contributions included in the thesis. This is a true copy of the thesis, including any required final revisions, as accepted by my examiners.

I understand that my thesis may be made electronically available to the public.

STATEMENT OF CONTRIBUTIONS

I, Mohammed Abdul Rasheed, was involved in the concept/design of this thesis project's data collection, data analysis, paper writing, and editing. My supervisor, Prof. Vasudevan Lakshminarayanan, and co-supervisor, Dr. Kaamran Raahemifar, were involved in the concept/design of the projects and article editing.

I, Mohammed Abdul Rasheed, certify that:

- The above statement correctly reflects the nature and extent of the candidate's contributions to this work and the nature of the contribution of each of the co-authors, and I wrote all the text for this thesis.

Abstract

Introduction:

The human visual system is extremely sensitive to certain spatial visual tasks. It can detect the subtle misalignment of closer objects to a degree of 2-5 arcseconds, which is smaller than the foveal cone diameter or spacing. This ability is referred to as hyperacuity, and one such visual task is the Vernier task, which involves misalignment detection of Vernier lines or dots. It is also called Vernier acuity and has a significant diagnostic value for screening various eye abnormalities. However, due to methodological and technical limitations, its utility was restricted to laboratory applications due to concerns over test reliability and testing time. I hypothesized that applying advanced psychophysical procedures, techniques, and modern technological interventions might improve the Vernier acuity testing standards for clinical consideration. Therefore, I attempted to address the challenges noticed in the literature by advancing the methodology and technicality to improve the Vernier acuity test efficiency for clinical application.

Aims:

- **Experiment 1** (Chapter-2): To develop a software application and assess the Vernier acuity program performance, measurements, and stimuli characteristics.
- **Experiment 2** (Chapter-3): To enhance the Vernier acuity program efficiency, assess program performance and reliability for technical validation.
- **Experiment 3** (Chapter-4): To modify the Vernier acuity program for the visual field quantification (Hyperacuity perimetry) and assess reliability for technical validation.
- **Experiment 4** (Chapter-5): To develop a software application for the visual distortions quantification (Metamorphopsia) using Vernier acuity-based bisectional program and assess reliability for technical validation.

Methods:

This study was performed through two pilot studies: the first pilot study had five adult volunteers with the best corrected visual acuity of 20/20 vision in the right eye (tested right eye only) and included all the experiments from Chapter 2, whereas the second pilot study was carried out on 21 adult emmetropes

(unaided 20/20 vision) volunteers (tested both eyes individually) and included all the experiments from Chapters-3, 4, and 5. I used PsychoPy3 to develop each software program. However, I employed two methods to provide the test results efficiently and reliably for clinical testing. I developed three software applications and could only perform technical validation because of the pandemic.

- **Experiment 1** (Chapter-2): I programmed a software program and employed a 3-Down, 1-Up adaptive staircase method and three alternative forced choices technique to quantify the Vernier acuity. The Vernier acuity was measured at seven vertical separations (gaps) to assess test performance. The initial testing was focused on determining test performance using stimuli shapes, followed by technical validation of the software application program and assessment of stimuli contrast for standardization.
- **Experiment 2** (Chapter-3): I adjusted the measurement parameters to improve test efficiency. I assessed the program performance from response accuracy, reaction time, and testing time, along with repeatability of measurements for technical validation of the Vernier acuity program.
- **Experiment 3** (Chapter-4): I modified the Vernier acuity program to quantify the hyperacuity perimetry in superior, inferior, nasal, and temporal visual fields. I assessed the repeatability of measurements for technical validation of this modified Vernier acuity program.
- **Experiment 4** (Chapter-5): I programmed a Vernier bisection program to quantify the metamorphopsia using a method of adjustment. The testing involved Vernier stimuli in two different orientations and referred to them as patterns (A and B), Pattern-A had a presentation of two vertical and horizontal line stimuli that are equally away from the center of the screen in either direction, whereas pattern B involved presentations of pattern-A at oblique angles to the screen center. Using both patterns, I measured the metamorphopsia in central 5 degrees and assessed the repeatability of the measurements and testing time for technical validation of the Vernier bisection program.

Results:

- **Experiment 1** (Chapter-2): In the initial experiment, the line stimuli achieved comparable measurements to dot stimuli at most gap sizes except at 32 arcminutes of gap size. The test detected the lowest misalignment of 2 arcseconds at 2 arcminutes of gap size. The mean lowest acuity was below 8 arcseconds at 2 arcminutes, and the highest acuity was within an arcminute at 128

arcminutes. The negative contrast line stimuli were comparably precise to positive line stimuli at most gap sizes except at 16 arcminutes.

- **Experiment 2** (Chapter-3): The right eyes were repeatable at most of the gap sizes except for the 32 and 64 gap sizes, whereas the left eyes were repeatable at all gap sizes except 128. The right and left eye measurements were statistically the same at both visits. Since no difference was observed between the eyes, results from both eyes were compiled to assess the test performance and response accuracy. The Vernier acuity measured at 16, 8, 4, and 2 gap sizes were statistically repeatable, and the correlation was positive but weak. The response accuracy was estimated to be above 90% for mean correct responses, below 3% for mean incorrect responses, and about 5% for mean aligned responses through the gap sizes at both visits. The estimated reaction time was just below a second for mean correct responses, below 0.75 seconds for the mean incorrect responses, and about 2.5 seconds for the mean aligned responses. The test time was below 2 minutes at each gap size at both visits.
- **Experiment 3** (Chapter-4): The right eye hyperacuity perimetry results were repeatable in all four quadrants of 15 gap size, and the correlation was positive but weak in all quadrants except the superior visual field, where the correlation was negative and weak. Whereas for gap size 30, the results were repeatable in all quadrants except the inferior visual field, where the results were not repeatable. However, results from all the quadrants had a positive but weak correlation. The left eye hyperacuity perimetry results were repeatable in all quadrants of 15 gap size, except the nasal visual field, where the results were not repeatable. However, results from all the quadrants had a positive but weak correlation. For gap size 30, the results were repeatable in all four quadrants, and all quadrants had a positive but weak correlation. The results from both eyes showed no significant difference for a gap of 15 arcminutes. However, there was a substantial difference between the eyes only at the inferior field for a gap of 30 arcminutes.
- **Experiment 4** (Chapter-5): The right eye metamorphopsia results were repeatable in the central 5 degrees using a pattern A with a positive but weak correlation at all degrees except 5 and 1 degrees, where the correlation was negative and weak. Similarly, the results were repeatable in the central 5 degrees using a pattern B except for 5 degrees, and the correlation was positive but weak at all degrees except 3 and 2 degrees, where there was a negative and weak correlation. On the other hand, the left eye results were repeatable in the central 5 degrees using a pattern A with positive and moderate to strong correlations at all degrees. Similarly, the results were repeatable in the central 5

degrees using a pattern B except for 4 degrees, and the correlation was positive and moderate to strong at all degrees. There was no difference between the eyes for individual patterns at both visits.

Conclusions:

- **Experiment 1** (Chapter-2): The developed software application program measured the Vernier acuity precisely using 3-down, 1-up, an adaptive staircase method, and the 3AFC technique. In addition, I standardized stimuli for shape and contrast to measure the Vernier acuity. The calculated results are precise and consistent with the previously reported data. Therefore, motivating to advance the test further for Vernier acuity testing. While performing the test, some areas for improvement were identified. By adjusting the necessary parameters, the test's efficiency can be enhanced. I plan to make those adjustments in the following pilot testing and perform technical validation.
- **Experiment 2** (Chapter-3): I adjusted the necessary parameters to improve the efficiency of the Vernier acuity testing. The results showed that the program is efficient, robust, and repeatable. The mean Vernier acuity measured at seven different gap sizes was consistent with previously reported data and comparable with pilot study 1 results. This cohort's Vernier acuity measured at smaller gap sizes was highly dependable. The measurements were significantly repeatable at most gap sizes but were poorly dependable. Therefore, this program may need further modifications to achieve better reliable results for clinical testing.
- **Experiment 3** (Chapter-4): I modified the Vernier acuity program to quantify the Vernier acuity in eccentric 5 degrees of the macula (para-foveal area). The right eye results were repeatable for 15 arc minutes of gap size, whereas the left eye results were repeatable for the 30 arc minutes of gap size. However, both eyes had poor reliability at most of the gap sizes except the superior field of gap 30, where the reliability was moderate. This inconsistency between the eyes could be due to distinct reasons and therefore, needs further investigations to address the underlying cause.
- **Experiment 4** (Chapter-5): I programmed a software application to quantify the metamorphopsia using a method of adjustment. The right eye results were repeatable at most gap sizes for both patterns. However, the measurements were poorly dependable at most gap sizes of both patterns. Similarly, the left eye results were repeatable at most gap sizes for both patterns. However, the measurements were poorly dependable at most gap sizes of both patterns, except at 3 degrees of pattern A and 5 and 2 degrees of pattern B, where the reliability was moderate. Further modifications in the program may provide better reliability for clinical testing.

Acknowledgments

I would like to express my sincere gratitude to the following individuals and organizations who have been instrumental in the completion of this research thesis:

My Advisor: I extend my deepest appreciation to my supervisor, Prof. Vasudevan Lakshminarayanan, and my co-supervisor Dr. Kaamran Raahemifar for their unwavering guidance, expertise, and mentorship throughout this research journey. Their insightful feedback and continuous support have been invaluable in shaping this thesis.

Faculty Members: I would like to thank my thesis committee members, Dr. Kristine Dalton, Dr. Simar Singh Saini, and Dr. John Zelek, for their time and thoughtful input during the thesis defense and review process. Their constructive criticism has significantly improved the quality of this work.

Research Participants: I am grateful to the participants who generously contributed their time and insights to this study. Their willingness to share their experiences was essential in gathering valuable data and drawing meaningful conclusions.

Grad Students and Peers: I want to acknowledge my fellow grad students and colleagues for their encouragement and support throughout this research endeavor. The exchange of ideas and collaborative spirit within our academic community has been inspiring.

Family and Friends: My heartfelt thanks go to my family for their unwavering belief in my abilities and constant encouragement. I am profoundly grateful to my friends, who provided moral support and understanding during this demanding period.

Financial Support: I would like to acknowledge the Canadian Optometric Education and Trust Fund (COETF) for providing financial support through a grant award that enabled me to conduct this research. Their investment in my work is deeply appreciated.

Institutional Support: The resources and facilities provided by the University of Waterloo have been indispensable to the successful completion of this thesis. I thank the university staff for their assistance.

Technical/Other Support: Dr. Jeffery Hovis for providing and explaining the digital spectrophotometer to measure the stimuli contrast on the experimental screen.

Dr. Andrew Silva for assisting in fixing the bugs in the code during the initial testing of the experiments.

I would like to thank Yutong for her help in seeking permission for an image used in this thesis.

I would like to acknowledge Dr. Andrew Silva, Cathy Le, and Hardeet Singh Saini for assisting with technical knowledge and skills in programming and fixing the bugs that eventually improved the code quality.

I acknowledge the co-op students, Suyog Joshi, Cedrick Mah, and Josh Kazi, for all their assistance in programming the code.

I would like to acknowledge the School of Optometry Clinic managers, Ann Girling, Vanessa Risser, and Shannon Oliu, for the administrative support and for assisting this research by providing necessary testing equipment, such as visual acuity charts and associated tools.

Anyone I May Have Omitted: To anyone whose contributions may not have been explicitly mentioned but who has played a part in this research, your efforts have not gone unnoticed, and I am thankful for your involvement.

Completing this research thesis has been a challenging yet rewarding endeavor, made possible by the collective efforts of those mentioned above. Your guidance, encouragement, and support have made this research a reality. I am indebted to each one of you.

Dedication

Though you are no longer with us in person, your presence remains eternally alive in our hearts and cherished memories. As I progress toward my dreams, I dedicate these achievements to you, my beloved late grandfather.

Your wisdom, kindness, and the profound love you showered upon our family have been a source of strength and inspiration throughout my life. The lessons you taught me through your words and actions continue to guide me on this journey.

As I reach my goals and aspire to make a difference in this world, I am reminded of your unwavering support and encouragement. Your belief in my potential, even when I doubted myself, has propelled me forward.

Though you may not be here to witness my accomplishments, I find solace in knowing you are watching over me from above. Every success, every milestone, and every moment of happiness is dedicated to your memory.

Your legacy of love, resilience, and the indomitable spirit you embodied lives on within me. I carry your name with honor and strive to uphold the values and principles you hold dear.

In your absence, your memory continues to be a guiding light, illuminating my path through life's challenges and triumphs. You are forever in my thoughts and forever a part of my journey.

With heartfelt love and enduring devotion, I dedicate this thesis to my grandfather, Late: Mohammed Abdul Wali, a retired health officer and a leader of my family.

Table of Contents

EXAMINING COMMITTEE MEMBERSHIP	ii
AUTHOR'S DECLARATION	iii
STATEMENT OF CONTRIBUTIONS	iv
Abstract	v
Acknowledgments	ix
Dedication	xi
List of Figures	xix
List of Tables	xxi
Chapter 1 Introduction.....	1
1.1 Vision Impairment.....	1
1.1.1 Prevalence of Visual Impairment	1
1.2 Human Vision.....	2
1.3 Visual System.....	4
1.4 Retina.....	5
1.4.1 Macula	7
1.4.2 Fovea	8
1.5 Photoreceptors	9
1.5.1 Phototransduction	11
1.5.2 Rods.....	12
1.5.3 Cones	13
1.6 Visual Perception	15
1.6.1 Visual Pathways	16
1.6.2 Colour Vision	17

1.6.3 Visual Fields.....	18
1.6.4 Binocular Vision.....	19
1.7 Receptive Fields	20
1.7.1 Bipolar Cells.....	21
1.7.2 Ganglion Cells.....	22
1.7.3 Lateral Geniculate Nucleus	23
1.7.4 Visual Cortex.....	23
1.8 Visual Functions.....	23
1.8.1 Vision Development	24
1.8.2 Visual Acuity (VA)	25
1.8.3 Contrast Sensitivity (CS).....	27
1.9 Eye: An Optical System	27
1.9.1 Diffraction Theory.....	28
1.10 Resolution Limits	28
1.10.1 Raleigh Criteria	30
1.10.2 Abbe Criterion.....	31
1.10.3 Sparrow Criterion.....	31
1.10.4 Retinal Mosaic.....	32
1.10.5 Visual Aliasing	32
1.11 Visual Psychophysics	33
1.12 Visual Hyperacuity.....	34
1.12.1 Definition.....	34
1.12.2 Hyperacuity and Visual Acuity	34
1.12.3 History of Hyperacuity	34

1.12.4 Hyperacuity Research.....	35
1.13 Vernier Acuity (VeA).....	35
1.13.1 Definition.....	35
1.13.2 Vernier Acuity Development.....	36
1.13.3 Neural Mechanism of Vernier Acuity	37
1.13.4 Vernier Acuity and Stereoacuity	38
1.13.5 Vernier Acuity and Aberrations	38
1.13.6 Vernier Acuity and Perceptual Learning	38
1.13.7 Vernier Acuity and Light conditions	38
1.14 Clinical Importance of Vernier Acuity.....	38
1.15 Lacunae	40
1.16 Hypothesis.....	41
1.17 Clinical Applications of Vernier Acuity.....	41
1.18 Thesis Plan	41
1.19 Thesis Synopsis	43
1.20 Research Ethics For Pilot Study 1 (Chapter 2).....	44
1.21 Research Ethics For Pilot Study 2 (Chapters 3, 4, and 5)	44
Chapter 2 Vernier Acuity Test (VAT).....	45
2.1 Introduction	45
2.2 Software Development	47
2.3 An Adaptive Staircase Method.....	49
2.4 Alternative Forced Choice Technique.....	51
2.5 Stimuli Configuration.....	53
2.5.1 Gap Sizes	53

2.5.2 Shapes.....	54
2.5.3 Contrast Polarity.....	54
2.6 Method.....	54
2.6.1 Study Subjects.....	54
2.6.2 Experimental Setup.....	55
2.6.3 Stimuli Configuration.....	55
2.6.4 Gap Sizes.....	55
2.6.5 Experiment Testing.....	56
2.7 Data Analysis.....	56
2.7.1 Data Interpretation.....	56
2.8 Results.....	57
2.8.1 Experiment-1: Software Program Testing (Positive Contrast).....	57
2.8.2 Experiment-2: Method Validation.....	58
2.8.3 Experiment-3: Stimuli Contrast Comparison (Positive vs. Negative).....	61
2.9 Discussion.....	63
2.10 Conclusion.....	65
Chapter 3 Vernier Acuity Test.....	66
3.1 Introduction.....	66
3.1.1 Impact of Covid-19 on this Research.....	67
3.1.2 Post-Pandemic Research Precautions.....	67
3.1.3 Technical Validation.....	67
3.1.4 Factors Affecting Vernier Acuity.....	68
3.1.5 Reproducibility.....	69
3.2 Method.....	70

3.2.1 Program Modification	70
3.2.2 Study Subjects	70
3.2.3 Experimental Setup	71
3.3 Data Acquisition.....	71
3.3.1 Data Categorization.....	72
3.3.2 Repeatability.....	72
3.3.3 Data Analysis.....	72
3.3.4 Data Interpretation.....	73
3.4 Results	73
3.4.1 Vernier Acuity Repeatability (Eyes)	73
3.4.2 Vernier Acuity Repeatability (Between Eyes)	77
3.4.3 Vernier Acuity Repeatability (Compiled)	81
3.4.4 Responses Accuracy Analysis	84
3.4.5 Reaction Time Analysis	87
3.4.6 Test Time Analysis.....	90
3.4.7 Vernier Acuity and Age.....	90
3.4.8 Vernier Acuity and Gender	95
3.5 Discussion	99
3.6 Conclusion.....	102
Chapter 4 Hyperacuity Perimetry.....	103
4.1 Introduction	103
4.2 Method.....	104
4.2.1 Study Subjects	104
4.2.2 Experimental Setup	104

4.2.3 Software Application.....	105
4.2.4 Stimuli Configuration.....	105
4.2.5 Gap sizes.....	105
4.2.6 Experiment Testing	106
4.2.7 Data Analysis.....	106
4.3 Results	106
4.3.1 Right Eyes HP (Visit 1).....	106
4.3.2 Right Eyes HP (Visit 2).....	108
4.3.3 Right Eyes HP (Repeatability)	110
4.3.4 Left Eyes HP (Visit 1)	112
4.3.5 Left Eyes HP (Visit 2)	113
4.3.6 Left Eyes (Repeatability).....	115
4.3.7 Right Eyes Verses Left Eyes	118
4.4 Discussion	119
4.5 Conclusion.....	120
Chapter 5 Metamorphopsia	121
5.1 Introduction	121
5.2 Method.....	122
5.2.1 Study Subjects	122
5.2.2 Experimental Setup	122
5.2.3 Software Application.....	122
5.2.4 Stimuli Configuration.....	122
5.2.5 The Method of Adjustment (MOA).....	122
5.2.6 Gap Sizes	123

5.2.7 Experiment Testing	123
5.2.8 Data Interpretation.....	124
5.2.9 Data Analysis.....	124
5.3 Results	124
5.3.1 Right Eye MMP (Visit 1)	124
5.3.2 Right Eye MMP (Visit 2)	125
5.3.3 Right Eye MMP (Repeatability).....	127
5.3.4 Left Eye MMP (Visit 1)	129
5.3.5 Left Eye MMP (Visit 2)	130
5.3.6 Left Eye MMP (Repeatability).....	132
5.3.7 Symmetry Between Eyes.....	134
5.4 Discussion	135
5.5 Conclusion.....	136
Chapter 6 Conclusion and Future Direction	137
6.1 Summary of the Dissertation	137
6.2 Limitations.....	139
6.3 Future Directions.....	140
References	141
Appendix A Permissions to Reproduce Figures.....	150
Appendix B Conference Presentations	164
Appendix C Software Program Codes	165

List of Figures

Figure 1-1 Visual experience of the perception of a colourful world (Modified from color_spectrum_by_chrisisl.jpg (900×563) (wixmp.com)).....	3
Figure 1-2 The visible light region of the electromagnetic spectrum showing variation in wavelength resulting in the perception of colours. (Adopted from 450px-Visible-light.png (450×143) (ascensionglossary.com))	3
Figure 2-1 The GUI window of the VAT model to add participant information in the left image and experimental settings in the right image.....	48
Figure 2-2 Graphical representation of staircase method using stimuli positioning example on the left and response on the right that drives the following presentation of the stimuli.	49
Figure 2-12-3 Graphical representation of mean VeT from positive and negative contrast line stimuli.	62
Figure 3-1 Repeatability of the Vernier acuity thresholds measured with right at both visits were plotted against gap sizes.	74
Figure 3-2 Mean VeT measured with the left eye at visits 1 and 2 were plotted against gap sizes.	76
Figure 3-3 Mean VeT measured with the right and left eye at visit 1 were plotted against gap sizes.	78
Figure 3-4 Mean VeT measured with the right and left eye at visit 2 were plotted against gap sizes.	80
Figure 3-5 The right and left eye (compiled) mean VeT at visits 1 and 2 were plotted against gap sizes.	82
Figure 3-6 Responses percentages across gap sizes estimated using ASM model at visit 1.....	84
Figure 3-7 Responses percentages across gap sizes estimated using ASM model at visit 2.....	85
Figure 3-8 Response reaction time across gaps using ASM program at visit 1.	87
Figure 3-9 Response reaction time across gaps using ASM program at visit 2.	88
Figure 3-10 VAT testing time across gap sizes at visits 1 and 2.....	90
Figure 3-11 Mean VeT measured in the 20 to 30 age group at visits 1 and 2 were plotted against gap sizes.	92
Figure 3-12 Mean VeT measured in 31 to 40 years of age group at visits 1 and 2 were plotted against gap sizes.	93
Figure 3-13 Mean VeT measured in females at visits 1 and 2 were plotted against gap sizes.....	96
Figure 3-14 Mean VeT measured in males at visits 1 and 2 were plotted against gap sizes.....	97

Figure 4-1 Graphical representation of hyperacuity perimetry position on the screen with respective central fixation target.....	105
Figure 4-2 Hyperacuity Perimetry with right eyes for eccentric 5 degrees across four viewing quadrants at 15 and 30 gap sizes at Visit 1.....	107
Figure 4-3 The mean VeT measured with right eyes for eccentric 5 degrees across four viewing quadrants at 15 and 30 gap sizes.	109
Figure 4-4 Repeatability of Hyperacuity Perimetry with right eye using 15 gap size.....	110
Figure 4-5 Repeatability of Hyperacuity Perimetry with right eye using 30 gap size.....	111
Figure 4-6 Hyperacuity Perimetry with left eyes for eccentric 5 degrees across four viewing quadrants using 15 and 30 gap sizes at Visit 1.	113
Figure 4-7 Hyperacuity Perimetry with left eyes for eccentric 5 degrees across four viewing quadrants using 15 and 30 gap sizes at Visit 2.	114
Figure 4-8 Repeatability of Hyperacuity Perimetry with left eye using gap 15.	116
Figure 4-9 Repeatability of Hyperacuity Perimetry with left eye using gap 30.	117
Figure 5-1 Stimuli presentation on screen for pattern A (left) and pattern B (right).....	123
Figure 5-2 Mean MMP thresholds measured with right eyes across central 5 degrees using patterns A and B at visit 1.....	125
Figure 5-3 Mean MMP thresholds measured with right eyes across central 5 degrees using patterns A and B at visit 2.....	126
Figure 5-4 Repeatability of Metamorphopsia with right eye for pattern-A.....	127
Figure 5-5 Repeatability of Metamorphopsia with right eye for pattern-B.....	128
Figure 5-6 Mean MMP thresholds measured with left eye across central 5 degrees using patterns A and B at visit 1.....	130
Figure 5-7 Mean MMP thresholds measured with left eye across central 5 degrees using patterns A and B at visit 2.....	131
Figure 5-8 Comparison of left eye MMP patter-A.	132
Figure 5-9 Comparison of left eye MMP patter-B.	132

List of Tables

Table 2-1 Mean VeT using positive and negative contrast, mean difference, and p-values at all gap sizes. 63

Table 3-1 Repeatability of Vernier acuity thresholds measured with right eyes at visits 1 and 2, mean difference and statistical significance are provided in the table below. 75

Table 3-2 Mean VeT measured with left eye at visits 1 and 2, mean difference, and statistical significance..... 77

Table 3-3 Mean VeT measured with right and left eyes were compared for symmetry between the eyes at visit 1. 79

Table 3-4 Mean VeT measured with right and left eyes were compared for symmetry between the eyes at visit 2. 81

Table 3-5 The right and left eye (compiled) mean VeT at visits 1 and 2, mean difference, p-value, and interclass correlation (ICC). 83

Table 3-6 The repeatability of mean percentage correct, incorrect, and aligned responses measured for all gap sizes. 86

Table 3-7 The mean response reaction time measured for all gap sizes at visits 1 and 2. 89

Table 3-8 Repeatability of Vernier acuity in 20 to 30 age group. 92

Table 3-9 Repeatability of Vernier acuity in 31 to 40 age group. 94

Table 3-10 Comparison of Vernier acuity between the age groups at both visits. 95

Table 3-11 Repeatability of Vernier acuity in females..... 96

Table 3-12 Vernier acuity repeatability in males 98

Table 3-13 Comparison of Vernier acuity between gender at both visits. 99

Table 3-14 Comparisons of Vernier acuity for all variables using statistical significance from repeatability (p-values)..... 101

Table 4-1 Hyperacuity Perimetry with Right Eye at Visit 1 108

Table 4-2 Hyperacuity Perimetry with Right Eye at Visit 2 109

Table 4-3 Repeatability of Hyperacuity Perimetry using right eye. 112

Table 4-4 Left eye Hyperacuity Perimetry comparison between the gap sizes at visit 2. 115

Table 4-5 Comparison of Hyperacuity Perimetry between the visits for both gap sizes..... 117

Table 4-6 Comparison of Hyperacuity perimetry between eyes at visit 1. 118

Table 4-7 Comparison of Hyperacuity perimetry between eyes at visit 2. 119

Table 5-1 Repeatability of MMP using pattern A and pattern B for right eye.....	129
Table 5-2 Repeatability of MMP using pattern A and pattern B for left eye.	133
Table 5-3 MMP Symmetry between the eyes for patter A and B at visit 1.....	134
Table 5-4 MMP symmetry between eyes for patter A and B at visit 2	135

Chapter 1

Introduction

In this chapter, I introduced the thesis with motivation and established the foundation of the thesis by delving into important background information. Topics covered in this chapter include the anatomy and physiology of important eye structures, vision functions, visual acuity, resolution, hyperacuity, and Vernier acuity. Furthermore, I emphasized Vernier acuity's clinical importance and outlined gaps in the literature. Finally, I conclude with a brief overview of the thesis in the last section of this chapter.

1.1 Vision Impairment

The International Classification of Functioning Disability and Health (ICF) states that the term "impaired" is typically used to refer to a problem with a person's body's structure or function due to a medical condition. Vision impairment occurs when an eye condition affects the visual system and one or more of its vision functions, according to the World Health Organization (WHO). It can also lead to disability, referring to the impairments, limitations, and restrictions that someone experiences while interacting with the environment. Vision loss can have a profound negative impact on an individual's overall well-being, including physical, emotional, social, and financial. Additionally, it may also result in a lower quality of life^{1,2}.

Several risk factors can contribute to visual impairment, including age, systemic health conditions, family history, lifestyle, environmental factors, and injury. Age is the primary factor contributing to visual impairment since certain eye conditions, including age-related macular degeneration, cataracts, and glaucoma, usually develop with aging. While diabetic retinopathy is the leading cause of visual impairment in younger and older individuals, as it can develop independently of age. Most of these eye conditions are particularly known to develop and progress subtly without apparent symptoms until significant damage to vision is experienced. Furthermore, these eye problems often cause permanent vision loss, increasing the prevalence of vision impairment globally.^{2,3}

1.1.1 Prevalence of Visual Impairment

According to the WHO's most recent global vision report on Blindness and Visual Impairment, there are more than 2.2 billion visually impaired individuals worldwide; at least half of those instances could have been avoided or managed^{4,5}. Age-related macular degeneration, glaucoma, and diabetic

retinopathy produce almost twenty million cases of irreversible vision impairment. The WHO resolution developed methods for glaucoma and diabetic retinopathy assessment services^{1,6}.

According to the Canadian National Institute for the Blind (CNIB), over a million Canadians suffer serious vision loss, which is expected to increase by 2031. According to the Centers for Disease Control and Prevention (CDC), more than twelve million Americans over forty have some form of visual impairment. By 2050, this number is predicted to rise to sixteen million. Age-related Macular degeneration, cataracts, and glaucoma are the primary causes of visual impairment in both nations. The key factors that increase the risk of visual impairment include smoking, high blood pressure, and diabetes⁷⁻¹⁰. **It is highly important to detect such conditions during the initial stages and treat them before it is too late. This thesis attempts to advance extraordinary visual functions that has the potential to detect visual abnormalities during the early stages of several eye conditions.**

1.2 Human Vision

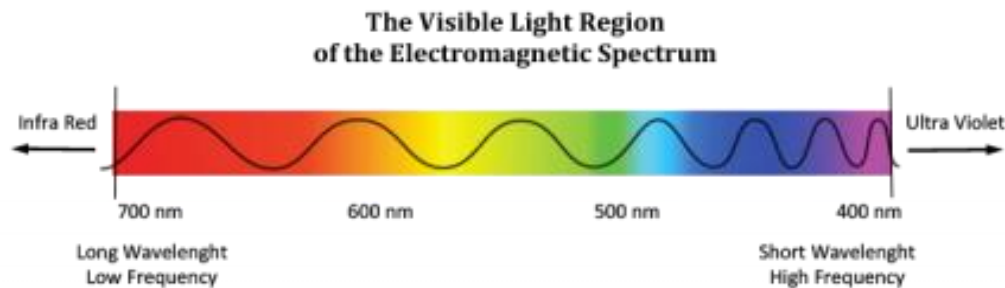
Humans evolved several primary senses through specialized sensory organs and nerve cells called sensory receptors^{11,12}. These receptors react to stimuli from both internal and external environments by producing nerve impulses¹³⁻¹⁵. One such remarkable sensory organ is the eye, which detects light and processes visual information, allowing us to experience a colourful world (Figure 1-1) through the sense of sight¹⁶. An eye can perceive light wavelengths from the visible spectrum (Figure 1-2), spanning approximately 400 to 700 nanometers, and translate them into neuronal signals that the brain can



[This Photo](#) by Unknown Author is licensed under [CC BY-NC](#)

process^{16,17}. Vision is considered the most significant and essential sense, as the eyes contain over fifty percent of all sensory receptors in the human body¹⁷. Additionally, a large portion of the cerebral cortex is involved in interpreting the visual information captured by the eye^{18,19}.

Figure 1-1 Visual experience of the perception of a colourful world (Modified from [color_spectrum_by_chrisilt.jpg \(900×563\) \(wixmp.com\)](#))



[This Photo](#) by Unknown Author is licensed under [CC BY-SA](#)

Figure 1-2 The visible light region of the electromagnetic spectrum showing variation in wavelength resulting in the perception of colours. (Adopted from [450px-Visible-light.png \(450×143\) \(ascensionglossary.com\)](#))

Our vision is essential in our daily lives, and its significance cannot be overstated. It is a critical element in our body's motor systems, allowing us to perform physical actions such as reaching, grabbing, navigating, and pushing efficiently²⁰⁻²². Our ability to see is also essential for communication through reading, media consumption, and technology^{23,24}. Furthermore, vision contributes significantly to the appreciation of visual art and entertainment²⁵. People with visual impairment face significant challenges that emphasize the importance of good eyesight²⁶. Good eyesight is crucial for our day-to-day life because it significantly impacts our overall well-being and quality of life^{26,27}. Throughout history, the ancient Egyptians utilized discernment between the twin stars Mizar and Alcor to gauge the quality of their vision²⁸. Scientists continue exploring various aspects of vision, including how the brain processes and integrates visual information with auditory and tactile inputs¹⁸.

Physiological optics is a branch of optics that explores the physiological and biological processes involved in vision and perception. On the other hand, geometric optics describes light propagation in terms of rays and their interactions with various media types, such as optical and non-optical objects. Physical optics delves into the physical properties of light, including diffraction, polarization, and

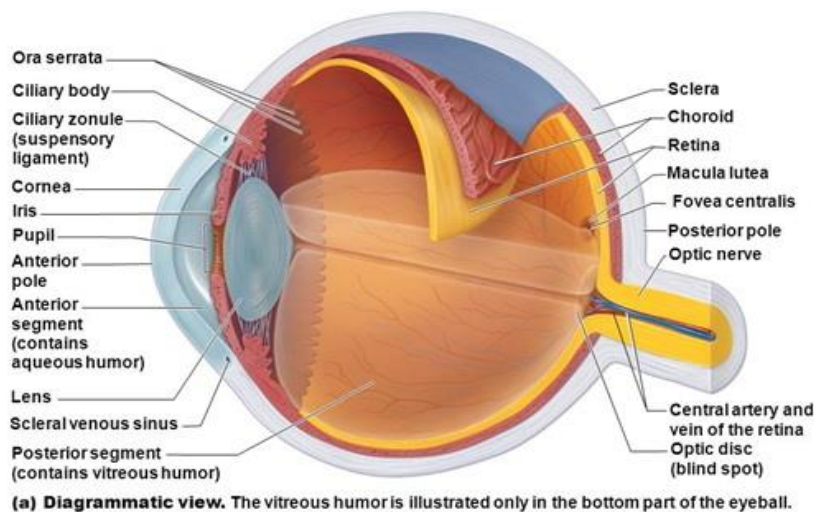
interference²⁹. Among the notable pioneers in the field of physiological optics, Ibn Al-Haytham Hasan is considered the father of modern optics. He contributed significantly to our understanding of how the eye perceives light and studied the physics of light and vision. In his book "Kitab Al-Manazir" (Book of Optics), he extensively discussed eye anatomy, properties of light, and laws of reflection using angles of incidence and deviations. Moreover, he conducted thorough studies on the dioptrics of the eye and the visual pathway from the eye to the cerebral cortex of the brain²⁹⁻³³.

This thesis dissertation is focused on susceptible visual functions. Before delving into the main topics, it is important to understand our visual system's essential structure and functioning.

1.3 Visual System

The human eye can be divided into two segments - anterior and posterior. The anterior segment includes various parts like the eyelids, cornea, conjunctiva, anterior sclera, iris, aqueous humor, pupil, ciliary body and crystalline lens, while the posterior segment comprises the vitreous humor, retina, choroid, and posterior sclera³⁴. An adult's eyeball has an average diameter of 2.5 centimeters, with 60% hidden under the front eyelids and surrounding structures situated posterior to the lids in the bony orbit. In contrast, the remaining 40% is visible outside between the eyelids^{17,35,36}. The orbit safeguards the

Figure 15.4a Internal structure of the eye (sagittal section).



© 2013 Pearson Education, Inc.

[This Photo](#) by Unknown Author is licensed under [CC BY-NC-ND](#)

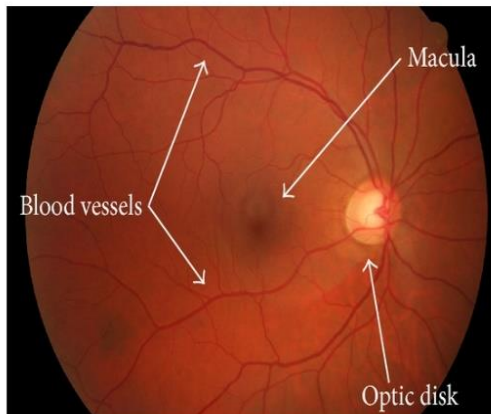
eyeball and permits it to move within a specific range. The wall of the eye can be classified into three anatomical layers^{16,34}. (Figure 1-3)

Figure 1-3 Anatomy of the human eye with labeled structures (Adopted from [EYE.jpg](#) (524×393) ([pharmacologyeducation.org](#)))

- 1. Outer:** The eye's outer layer is made of dense connective tissue that forms the cornea and sclera. The sclera maintains the shape of the eye and protects it from physical harm. It extends from the optic nerve to the anterior corneal margin, the limbus.
- 2. Uvea:** The middle layer between the retina and sclera is a vascular layer that supplies blood and nutrients. This pigmented layer includes the Choroid, Ciliary body, and Iris, arranged from the back to the front of the eye.
- 3. Retina:** The inner-neural sensory layer of the eye responsible for vision. It comprises two primary layers: the inner sensory layer and the outer pigmented epithelium. The inner layer, the more significant of the two, is responsible for transmitting visual information to the brain for interpretation. In contrast, the outer layer protects and nourishes the inner layer. Together, these two layers enable us to see and perceive the world around us³⁷.

1.4 Retina

The retina is the innermost layer of the eye that is responsible for visual perception. Its primary function is to capture light as it enters our eyes and translate it into three-dimensional images³⁸. The retina extends anteriorly to the point where the ciliary body and retina converge across 360 degrees, except for the optic disc. Although it is only **around 0.5 millimeters** thick, the retina comprises **over a hundred million neurons**, which is remarkable³⁹. The eye lens focuses the light entering the eye onto the retina. The outer layer of the retina is composed of pigmented epithelium and contains a sheet of melanin-containing epithelial cells known as retinal pigmented epithelium. On the other hand, the innermost and deepest layer of the retina is densely populated with light-sensitive sensory receptors referred to as photoreceptors. These cells are the only ones in the retina capable of converting light into nerve signals^{36,40,41}. (Figure 1-4)

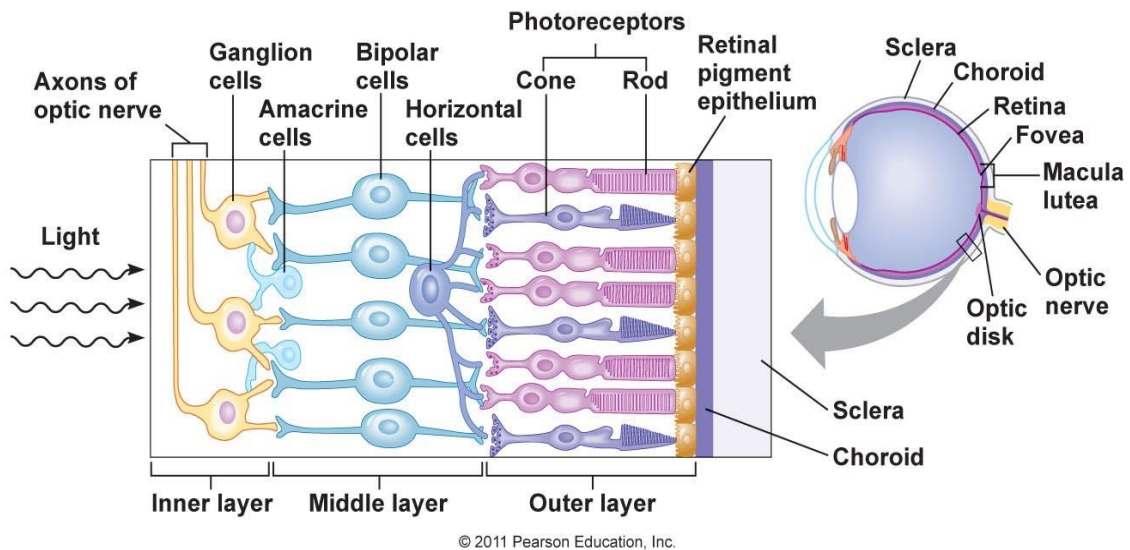


[This Photo](#) by Unknown Author is licensed under [CC BY](#)

Figure 1-4 Retinal Fundus image of the right eye with labeled structures (Adopted from [154860.fig.001.jpg \(600×413\) \(hindawi.com\)](#))

The retina comprises several layers of neurons that work together to process and transmit vision. Photoreceptor neurons are the first to process light and create a nerve signal through photochemical activation. This signal is then passed on to bipolar cells in the second layer and the ganglion cells in the third layer. Two intermediate layers of neurons primarily handle lateral interactions and early visual processing: horizontal cells and amacrine cells. The axons of the ganglion cells form the optic nerve, which carries nerve impulses to the brain through the optic disk, a small area on the retina that lacks photoreceptors and is commonly known as a blind spot^{37,38}. (Figure 1-5)

The retina has a unique blood supply system that provides it with sufficient oxygen and nutrients. It receives oxygen and nutrients through a dual blood supply system. The inner retinal arteries supply the inner layers except fovea, while the choroid supplies the outer layers and fovea³⁷. The retina is the only extension of the brain that can be externally viewed, providing real-time insights into retinal conditions. It can be divided into the central (macula) and peripheral retina. The peripheral retina fills the peripheral vision field, while the macula lets you view objects in the central vision^{42,43}. For example, when seated across a table from a friend, your macula enables you to view their face while your peripheral retina lets you see the rest of the room.



[This Photo](#) by Unknown Author is licensed under [CC BY-SA](#)

Figure 1-5 The graphical representation of various neuronal interactions of the retina in the eye. (Adopted from [KBYrq.jpg \(1344×648\) \(imgur.com\)](#))

1.4.1 Macula

The macula lutea, also known as the macula, is a circular and pigmented region that measures approximately five millimeters in diameter. Located in the retina's center, it plays a critical role in processing central vision, which refers to the clear and sharp images one sees directly in front. Additionally, the macula is responsible for most color vision, making it an essential component of our visual system. The macula can be divided into four distinct areas: parafovea, perifovea, fovea, and foveola (Figure 1-6). Understanding these subdivisions is crucial for comprehending the complex role that the macula plays in our vision^{37-41,44,45}.

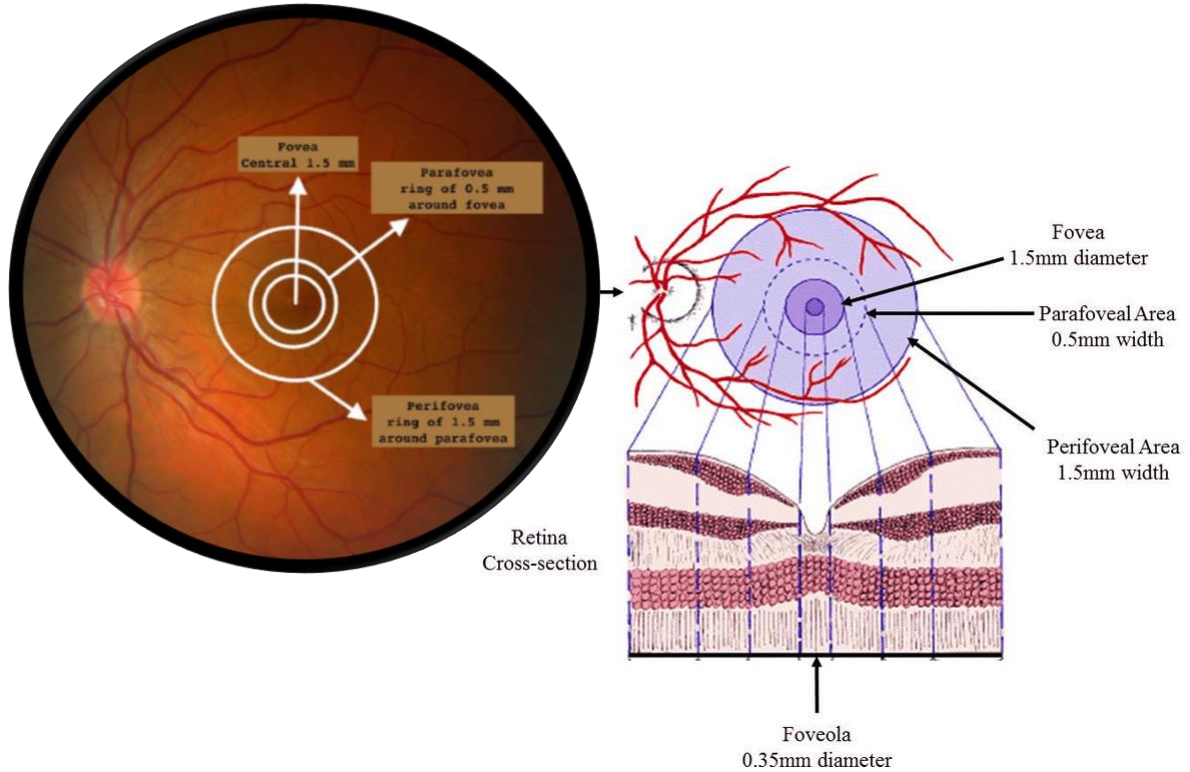


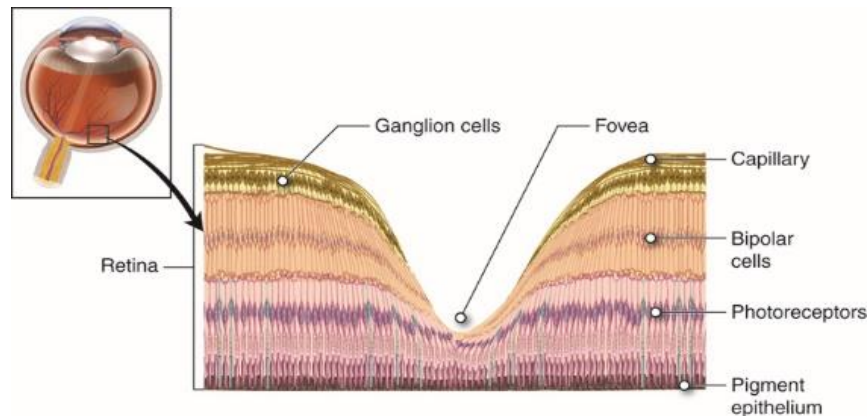
Figure 1-6 Left image: Retinal fundus image of the left eye with demarcated and labelled foveal regions, Modified with permission from Atlas of Inherited Retinal Diseases ([Figure 2 | Retinal Histology and Anatomical Landmarks | SpringerLink](#))

Right image: Depicting concentric foveal areas with respective cross-section segments to visualize the foveal cup and organization of retinal layer at fovea, Modified with permission from Remington 2012. (<https://ars-els-cdn-com.proxy.lib.uwaterloo.ca/content/image/3-s2.0-B9781437719260100049-f04-26-9781437719260.jpg>)

1.4.2 Fovea

The fovea also known as fovea centralis is a small pit extending about 1.5 millimeters at the center of the macula. The foveola is a slight depression measuring 0.35 millimeters in diameter, located at the center of the fovea. This area contains approximately 200,000 cones per square millimeter^{39,44}. The fovea possesses unique anatomical features that include the relocation of retinal components, such as synapses and the retinal blood supply, facilitating an unobstructed view of incoming light and enabling maximum light collection to produce sharp vision. Central vision, crucial for reading, writing, and safe

driving, is achieved through a clear foveal vision. Our visual system focuses the image on the fovea to ensure clarity, and as you read this sentence, our head or eyes move unconsciously to position the words on the fovea. This explains the rapid transfer of foveal gaze in our highly developed oculomotor system towards eccentric and moving targets^{35-39,41,44-46}. (Figure 1-7)



[This Photo](#) by Unknown Author is licensed under [CC BY-SA-NC](#)

Figure 1-7 The graphical representation of the Macula with the foveal cup where the layers of retina move aside and expose photoreceptors to the incoming light. Modified from [Nerv 24.jpg](#) (770×396)

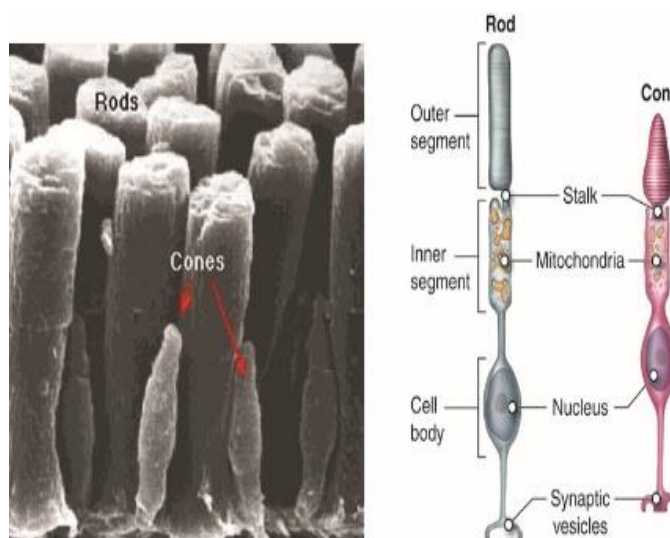
1.5 Photoreceptors

Photoreceptors are the specialized neuroepithelial cells in our eyes responsible for detecting light. These cells work in perfect harmony to create a clear and vivid image, tightly packed together to ensure that the retina can absorb a significant amount of light in a small area. Approximately 125 million photoreceptor cells synapse with surrounding 100 million bipolar cells and a small number of horizontal cells within the outer plexiform layer of the retina^{44,45,47-49}. This complex network of cells and synapses ensures that our eyes can perceive and interpret the world around us with incredible detail and accuracy.

The two types of photoreceptors are differentiated by their morphology and function. These are called rods and cones. Rods are cylindrical in shape, while cones are conical. They both are susceptible to the photons of light, as the name photoreceptors suggest; however, they have specific structures and perform different roles in visual perception⁴⁷⁻⁴⁹.

They consist of five common regions: (Figure 1-8)

1. Outer segment
2. Stalk
3. Inner segment
4. Nuclear region
5. Synaptic region



[This Photo](#) by Unknown Author is licensed under [CC BY-SA-NC](#)

Figure 1-8 The electron microscopic image of the rod and cone cells on the left and the graphical representation on the right with labeled parts. Modified from [Nerv 25.jpg \(770x439\)](#)

The photoreceptor cell is made up of several regions. The outer segment absorbs light and converts it into an electrical impulse, while the stalk (the connecting cilium) links the outer and inner segments. The inner segment contains metabolic organelles like mitochondria, lysosomes, and endoplasmic reticulum, while the nuclear region covers the cell's nucleus. The synaptic area is the last region, which assists in the movement of neurotransmitters between photoreceptor cells and secondary neurons like bipolar cells, with glutamate being a primary example. Rod cells are distributed throughout the retina, except for the foveola. The density of rod cells increases as I move away from the fovea, reaching a peak around 20 degrees before gradually declining towards the periphery, as shown in the graph. In

contrast, cone cells are highly concentrated in the fovea and are the only ones in the foveola. Cone concentration decreases from the fovea towards the periphery^{42-45,47-50}. (Figure 1-9)

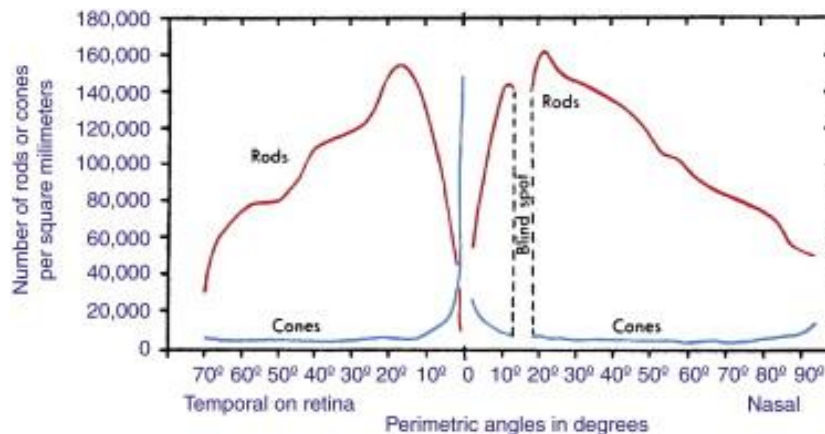
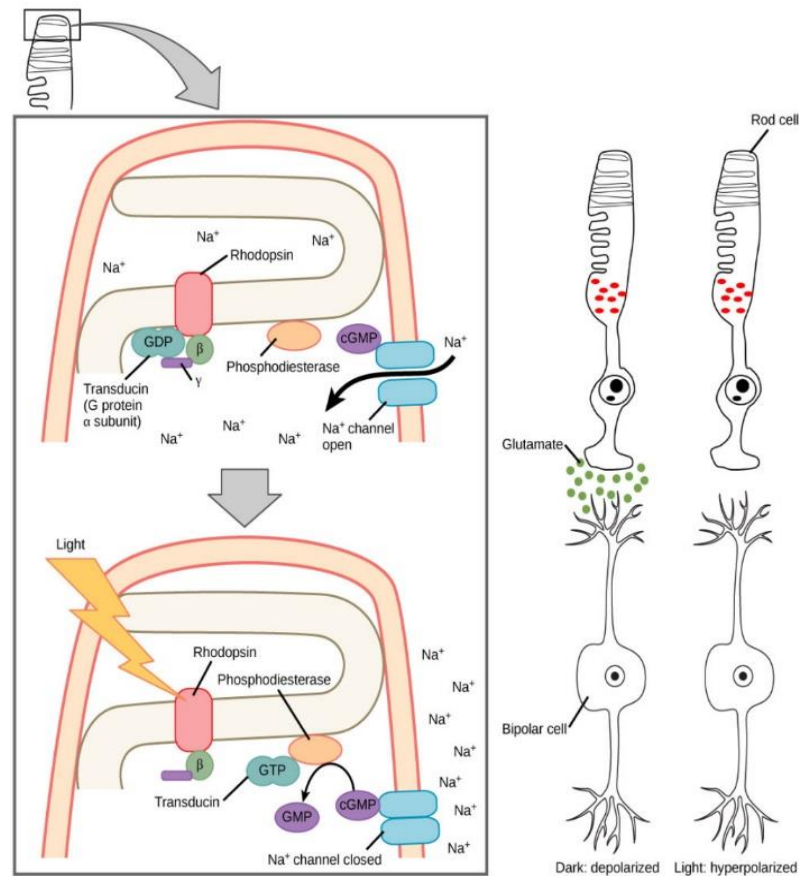


Figure 1-9 The graphical representation of rods and cone distribution across retina. Adopted with permission from Remington 2012: (<https://ars-els-cdn-com.proxy.lib.uwaterloo.ca/content/image/3-s2.0-B9781437719260100049-f04-23-9781437719260.jpg>)

1.5.1 Phototransduction

When light enters the eye, photoreceptors convert it into electrical signals the brain can understand as visual information. This process is known as phototransduction and is facilitated by a light-sensitive pigment called rhodopsin, found in photoreceptors. Rhodopsin comprises opsin, a protein, and a retinal molecule, an aldehyde of vitamin A^{51,52}. When light photons hit rhodopsin molecules in rod or cone cells, it changes the retinal and opsin structures, resulting in a chain reaction of chemical responses. This leads to activating an enzyme called phosphodiesterase, which breaks down cyclic guanosine monophosphate (cGMP), which is commonly found in high concentrations in rod or cone cells. (Figure 1-10) Consequently, the ion channels in the cell membrane close, causing a change in ion flow that generates an electric or nerve signal sent to the brain via the optic nerve. Macular fibers are associated with about 90 percent of all axons that travel from the eye to the brain. The brain interprets these signals as visual information, creating a visual image. The distinct photoreceptors in the retina process various

vision components, such as color perception, contrast perception, and motion detection. The brain integrates information from these cells to produce a complex and detailed visual experience^{13,36,47,51,53}.



[This Photo](#) by Unknown Author is licensed under [CC BY](#)

Figure 1-10 The graphical representation of phototransduction of the rod cell when exposed to the light leading to various chemical reactions. Adopted from [Figure 36 05 05-1008x1024.jpg](#) [\(1008x1024\)](#)

1.5.2 Rods

The cylindrical rod cells are sensitive to dim light and dark environments to produce scotopic vision (black-and-white vision). It is believed that they evolved approximately five hundred million years ago to supplement cones and improve the ability to survive in low-light conditions. In humans, there are more than one hundred million rods in the retina, about 95 percent of photoreceptors in the retina. The

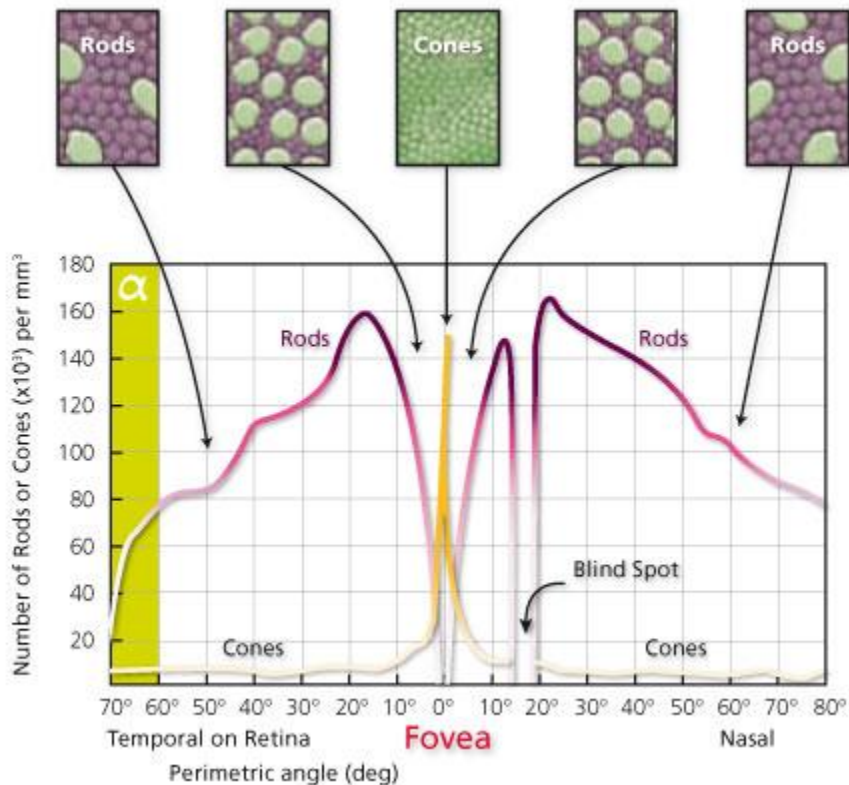
cylinder-shaped outer segments of rods comprise about a thousand flat, lobulated, membranous discs. The inner segment of the rod cell is split between an outer segment with numerous mitochondria and an inner segment with endoplasmic reticulum. The structure of rod cells is usually consistent across all the areas of the retina and is predominantly situated in the outer retina^{49,50,54}.

Rod's response speed is slow, and their spatial acuity and contrast sensitivity are relatively poor. This is typically due to the synaptic connection arrangement as three rods converge upon a single retinal ganglion cell (output neuron). They use glutamate as their neurotransmitter and make synapses with bipolar cells. They are often photobleached during the day and have a recovery time of approximately 20 to 40 minutes after sunset or complete darkness. They become functional and produce scotopic vision^{47-50,53,54}.

1.5.3 Cones

The cones respond differently to various wavelengths of light (photopic) to produce fine detailed color vision. Cones facilitate the brain's processing of photopic vision, which involves colour perception from visible light intensities used in most human interactions. In contrast to rods, cones are usually less sensitive to photons of dim light but more responsive to three specific (colour) wavelengths of light^{49,50,53,55,56}.

The opsin in the cone cells accounts for the ability to detect various light wavelengths and are classified into three types; S-cones detect a little blue light (2 %), M-cones detect green light (32 %), and L-cones majorly engage in detecting combinations of red light (64 %) to produce color vision⁵⁷. At the fovea centralis, the red and green cones are concentrated, while the blue cones are usually present outside the fovea and have the highest sensitivity. They collectively account for high resolution of vision. The retina has approximately 6 to 7 million cones, constituting only 5 percent of the total retinal photoreceptors; nevertheless, our visual acuity depends on as few as 100,000 cones. Humans have 50% of the cones within the central 30 degrees of the visual field, which corresponds to the macula region approximately. Across the retina, the cone density is relatively higher in the nasal when compared to the temporal field and slightly higher in the inferior visual field when compared to the superior^{43,47-50,53-56,58,59}.



[This Photo](#) by Unknown Author is licensed under [CC BY-SA](#)

Figure 1-11 The graph represents rod and cone distribution across the retina and cone density picture at the top at specific points. Adopted from [jjsDG.jpg \(483×407\) \(imgur.com\)](#)

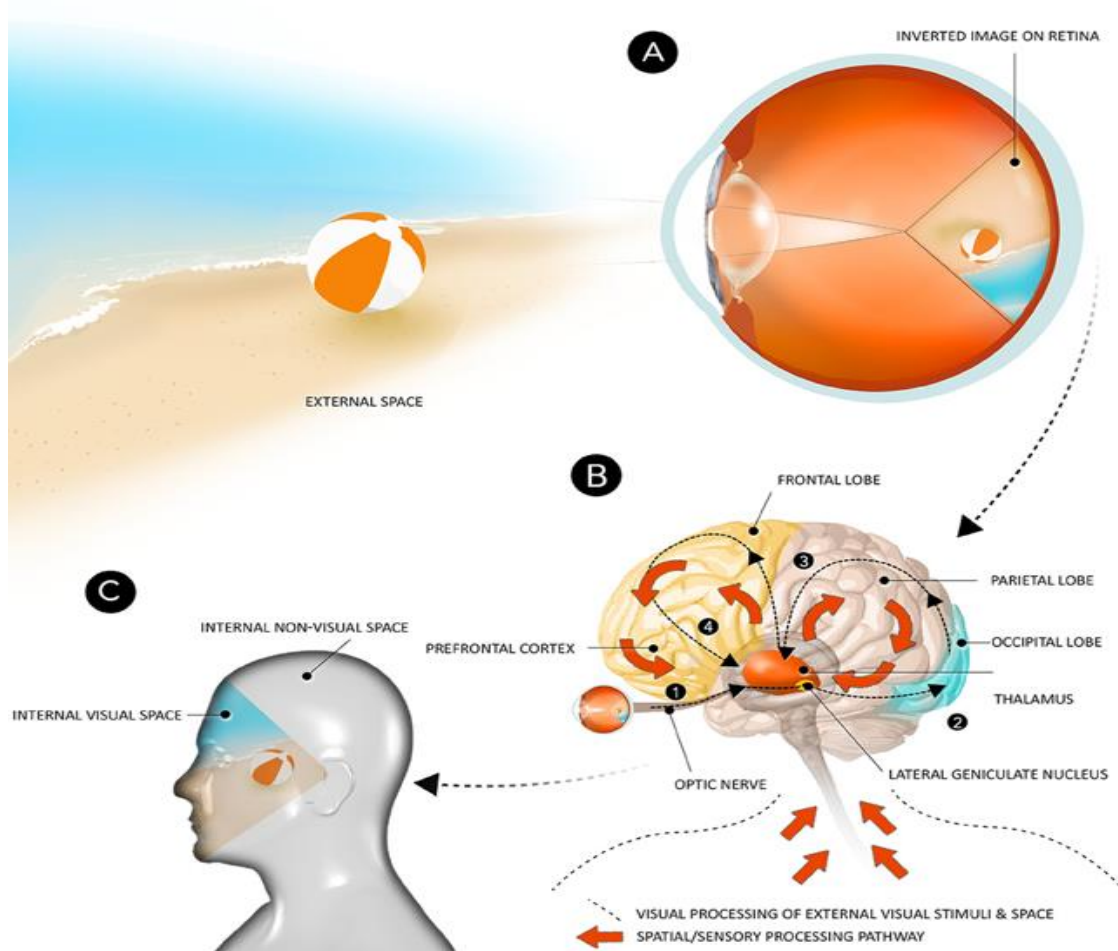
Like rods, Cones are also primarily situated in the outer retina. However, as their name suggests, cone outer segments are often conical in shape and are relatively shorter than rods. Like rods, the inner segment of the cone cells is also divided into an outer portion with many mitochondria and an inner portion with endoplasmic reticulum. Unlike rods, cones can immediately respond to light and do not saturate under constant illumination. Like rods, cones also discharge glutamate as their neurotransmitter and make synapses with bipolar cells. They can recover after photobleaching within twenty milliseconds. Cones are exceptionally sensitive to spatial and contrast acuity. Even though rods are more sensitive to photons, the high density of cones in the fovea, each of which with its own direct 1:1 synaptic connection to a retinal ganglion cell, enables each cone to contribute more visual information

to the overall image that the brain is attempting to interpret. Consequently, allowing the brain to distinguish between two close spots^{48-50,53,55}. (Figure 1-11)

1.6 Visual Perception

Visual perception can be understood as the ability to visualize the surrounding environment through the light that enters our eyes and is processed by the visual and cortical systems. It involves the components starting from the retina, the optic nerve, the lateral geniculate nucleus (LGN), and other visual association cortices. Initially, the photoreceptors process the light energy and convert it into nerve signals that are further fine-tuned in the retina neuronal layers. The axons of approximately 1 million neurons subsequently transmit these signals to the cell bodies of LGN neurons in the thalamus. Before branching into several connected stages of visual processing, these signals from the LGN axons are further dispersed to the primary visual cortex located in the striate cortex of the occipital lobe. The LGN of the thalamus sends the information to the primary visual cortex, commonly known as V1, which is the brain's first stage of visual processing. Most of the primary visual cortex is organized retinotopically, which makes it sensitive to the visual image's organization, topological, or spatial cognition. It controls edge detection, direction, and colour, crucial for developing a coherent visual perception^{19,60,61}. (Figure 1-12)

The secondary visual cortex, also known as V2, is responsible for advanced visual processing and is adjacent to the primary visual cortex or V1. It integrates information from V1 and other visual areas to provide a more precise image of the visual scene. V2 contributes to the experience of motion and depth and is involved in processing complex shapes, patterns, and textures. V1 and V2 work together to form the primary components of the brain's early visual processing system. In addition to that, it also involves several surrounding areas of the visual cortex, including V1, V2, V3-VP, V3a, V4-VA, and 7a, where the signals are processed as they all have different sensitivities individually¹⁸. Our visual system characterizes the images that stimulate adjacent parts of the retina by the surrounding neurons to create a cortical representation of the world. It first synthesizes the image into cues or features, then binds the encoded aspects of objects such as depth, colour, and motion to form our visual perception of the world. Most higher-level brain processes are also supported by vision. Our memories of places and individuals are frequently based on visual imagery or visual features⁶⁰⁻⁶².



[This Photo](#) by Unknown Author is licensed under [CC BY](#)

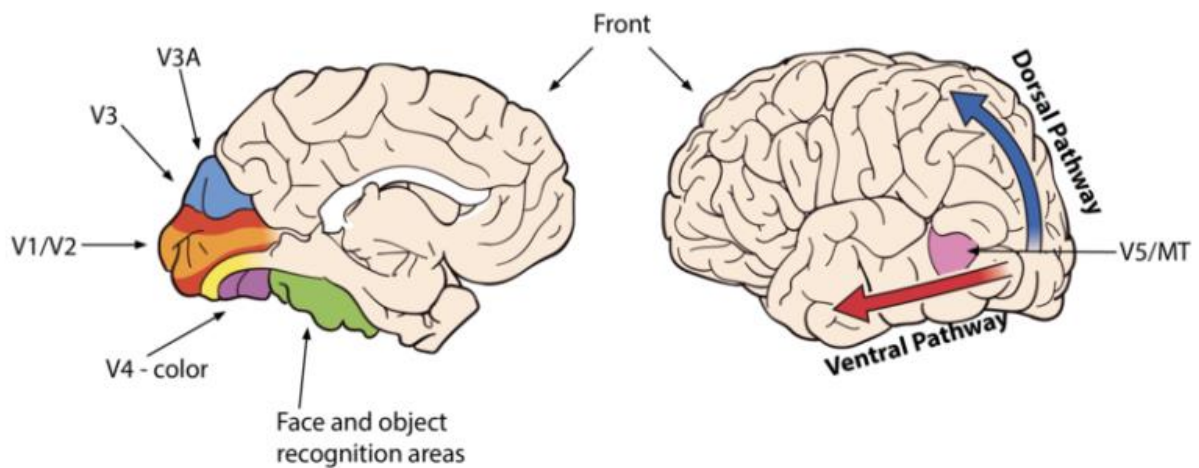
Figure 1-12 (A) The graphical representation of inverted image formation in the eye (B) Visual information is passed to different regions of the brain (C) Image perception in the visual space.

Adopted from [fpsyg-06-01204-g001.jpg \(666x694\) \(frontiersin.org\)](#)

1.6.1 Visual Pathways

There are two types of visual pathways: the dorsal and the ventral stream. The dorsal stream is responsible for processing information related to visual stimuli's location, movement, and spatial relationships. It is commonly referred to “where” pathway. It extends from the primary visual cortex to the posterior parietal cortex, which involves motor planning. The dorsal stream is crucial for navigation, tracking, and reaching objects. At the same time, the ventral stream is responsible for processing

information about the visual stimuli's identity, color, and shape. It is commonly referred to “what” pathway. It extends from the primary visual cortex to the inferior temporal cortex, involving object recognition and memory. The ventral stream is crucial for reading, facial recognition, and object identification. The interaction of the dorsal and ventral streams provides a complete image of the visual world. In addition to these two pathways, other visual pathways process specific types of information, such as the color-processing and motion-processing pathways⁶³⁻⁶⁷. (Figure 1-13)



[This Photo](#) by Unknown Author is licensed under [CC BY](#)

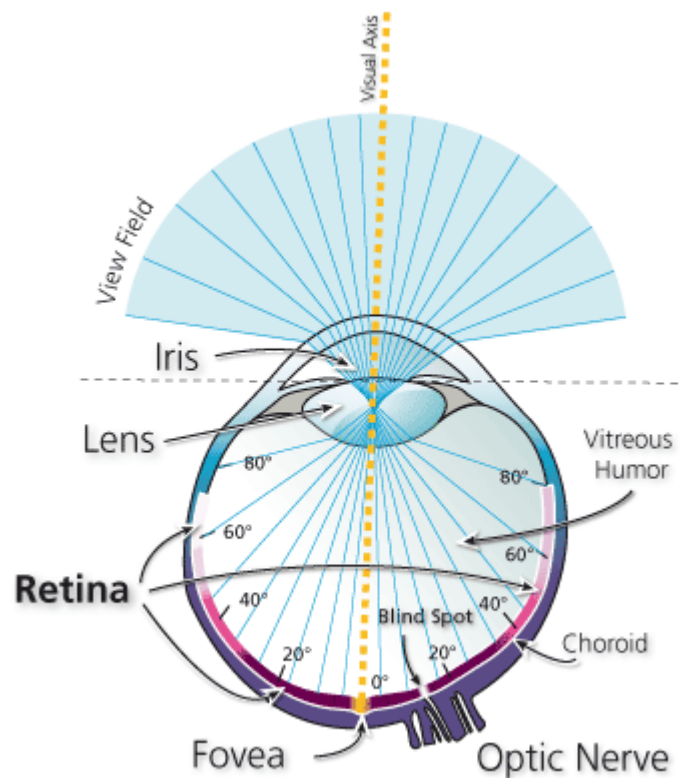
Figure 1-13 The graphical representation of human brain with labeled areas and the direction of the visual pathways of the brain. Adopted from [visualpathways-768x387.png \(768x387\)](#)

1.6.2 Colour Vision

Colour vision is achieved through the relative contribution of three different cones, as discussed in the cone section. Each type of cone is sensitive to a particular range of light wavelengths across the visible spectrum capturing the meaningful spectral information of the object being viewed. The factors that affect the ability to perceive colour are the light intensity and duration of exposure time, except for anomalies. Colour information makes up most of our visual interactions, making it an incredible sense among other senses to perceive and enjoy^{68,69}.

1.6.3 Visual Fields

The visual field, or the spatial extent to which the visual system is light-sensitive, is typically expressed in the visual angle—the angular distance the eye covers. The angle between the fixation point, or fovea, and spaces in the peripheral visual field is known as the eccentricity of the visual field. In normal eyes, the horizontal and vertical limits of the monocular visual field are around 160 degrees and 100 degrees, respectively. Except for the temporal visual area of each eye in the far distance, the two eyes' visual fields overlap. There is an inverse and reversal link between the retina and the VF. The nasal VF depends on the temporal retina, the temporal VF remains on the nasal retina, and the superior VF falls on the inferior retina (below the fovea)^{16,34,36,70}. (Figure 1-14)

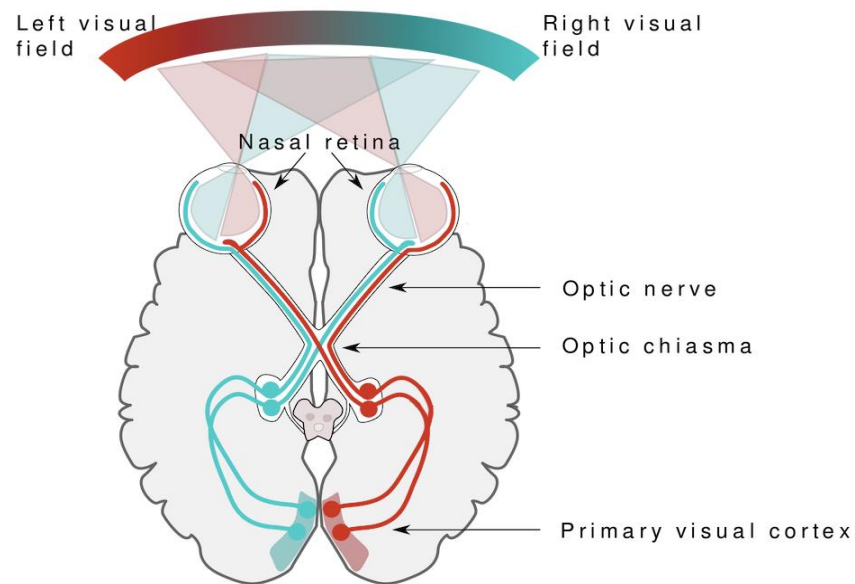


[This Photo](#) by Unknown Author is licensed under [CC BY-SA](#)

Figure 1-14 Graphical depiction of eyeball with visual field coverage and corresponding retinal location across the field. Adopted from [faOv5.gif \(367×410\) \(imgur.com\)](#)

1.6.4 Binocular Vision

The two-dimensional retinal surfaces of our two eyes' visual fields receive picture projections from slightly different angles as they concurrently see the world. The process of fusion, which merges vision from both eyes into a single perception, perceives the information present in the different and marginally dissimilar images appearing in each eye as a single image. For normal binocular single vision, the two eyes must be precisely coordinated for all gaze directions, and the visual cortical elements must be able to effectively combine the slightly different monocular inputs (sensory fusion). This ensures that corresponding points on the two retinas are aligned (motor fusion). Our visual cortex can recognize slight shifts between two-dimensional retinal images to recreate the third dimension in addition to single binocular vision (stereopsis)⁷¹. (Figure 1-15)



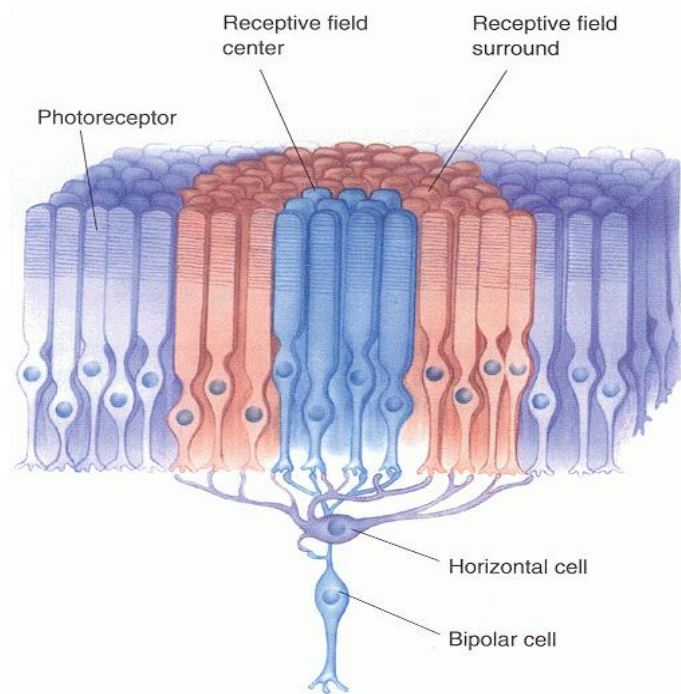
[This Photo](#) by Unknown Author is licensed under [CC BY](#)

Figure 1-15 Graphical depiction of binocular visual field and corresponding retinal areas that **perceive the visual information and pass it to the brain through optic nerve. The colour lines indicating the visual information track.**

The horizontal visual field of binocular vision is around 180-200 degrees. The peripheral visual field relates to eccentricities that are greater than 30° radius (60° diameter), whereas the macular region refers to eccentricities that are less than 5° radius (about 10° diameter) from fixation^{70,71}.

1.7 Receptive Fields

Receptive fields in the eye refer to the volume of visual space and are usually exhibited in two dimensions. Each neuron in the retina's layer covers an area in the field of vision. The area in space where the presence of the appropriate stimulus will influence this neuron's activity is referred to as the neuron's receptive field (sensory space). For example, a single photoreceptor cell's receptive field is confined to the tiny spot of light in the field of vision. It corresponds to the precise location of this photoreceptor on the retina. The receptive field in the fovea is the smallest and can be a few minutes of arc to tens of degrees. However, the receptive field size increases as neuron layers progress. It gets more complex and becomes even more complicated regarding the neurons in the visual cortex. Sir Charles Scott Sherrington, an English physiologist in 1906, was the first to use the term receptive fields in his discussion of the scratch reflex of dogs. The receptive fields of the retina are complex with each additional level, and they get more complicated when it comes to the neurons of the visual cortex^{43,55,63-66,72}. (Figure 1-16)



[This Photo](#) by Unknown Author is licensed under [CC BY-SA](#)

Figure 1-16 The graphical representation of photoreceptors and its connections with adjacent cells that forms a receptive field. Adopted from [SjQQV.gif \(511×579\) \(imgur.com\)](#)

1.7.1 Bipolar Cells

Anatomically, a bipolar cell's receptive field is determined by where and how many receptor cells it forms synapses with. At the fovea, direct connections exist between a single cone bipolar cell and a small network of cone cells. Consequently, Bipolar cells at the fovea have a tiny, color-sensitive receptive field. Gradient potentials rather than action potentials are produced by bipolar cells in response to the glutamate released by photoreceptors (i.e., by hyperpolarizing or depolarizing). Cone bipolar cells can be on- or off-type by being hyperpolarized or depolarized by glutamate. At the same time, the receptive field of the rod bipolar cells is relatively large due to synapses with a few to over fifty-rod receptor cells and lacks colour sensitivity. As glutamate hyperpolarizes all bipolar cells, they are all just on-type bipolar cells^{55,56,60,64,66,72}.

Bipolar cells has circular receptive fields, and their circle's center and periphery behave differently. For instance, a light ray encountering a photoreceptor that synapses with bipolar cells results in the center

response from the bipolar cell. However, stimulation from the surrounding receptors reduces the on-bipolar cell response to activation of the center receptor when both the center and surrounding receptor cells are exposed to light. In contrast, a light spot surrounded by a dark ring causes an on-bipolar cell to respond most strongly, whereas a dark area surrounded by a light ring causes an off-bipolar cell to depolarize the most. The horizontal cells are in pre- and post-synaptic interaction with the photoreceptor cells, contributing indirectly to the bipolar cell receptive field. These horizontal cells enhance spatial discrimination, the object's brightness to produce sharp images and contrast depending on the background^{50,55,72}.

1.7.2 Ganglion Cells

The receptive fields of retinal ganglion cells located in the fovea are the smallest compared to the periphery, where it is the largest. This explains why we have poor spatial resolution of vision outside the fixation point (foveal center). The receptive field of a specific ganglion cell encompasses the entire synapsing network of photoreceptors, bipolar, horizontal, and amacrine cells that converge to it. The retinal ganglion cells are the final components of the retina in the direct path from the eye to the brain. Since the retinal ganglion cells' axons transmit all the visual information from the eye, they have voltage-regulated sodium channels in their axonal membranes that can produce action potentials when they are depolarized by the glutamate released by the bipolar cells. On-Center OFF-Surround, OFF-Center, and On-Surround are the two main annular receptive fields in retinal ganglion cells. Like bipolar cells, the center and its surroundings are always antagonistic and tend to cancel each other's activity. A ganglion cell's receptive field arrangement is determined by the receptive fields of the bipolar cells with which it synapses. The shape and motion of things offer crucial information. Amacrine cells synapse with ganglion and bipolar cells and form lateral connections between reasonable neurons, such as connecting bipolar cells to other bipolar cells. It may also provide "vertical" connections between bipolar and ganglion cells, separating them from horizontal cells^{48,50,55,56,60}.

The center-surround receptive field framework enables ganglion cells to communicate the difference in response rates between cells in the center and surround and information about the photoreceptor's response. Retinal ganglion cell receptive fields offer information about discontinuities in the dispersion of light falling on the retina, frequently detecting objects' edges^{50,55,64,72}.

1.7.3 Lateral Geniculate Nucleus

A receptive field of cells in the LGN is made up of a collection of ganglion cells. With an antagonistic center-surround system and either on or off-center cells, it is comparable to those of ganglion cells⁶⁰.

1.7.4 Visual Cortex

The receptive fields of the neurons of the primary visual cortex are rectangular, and therefore they respond well to light rays that are oriented in a particular direction. Rectangular receptive fields typically have two OFF-side bands that react to darkness and an ON-center band that prompts responses to light. Compared to retinal ganglion cells, the visual cortex's cell receptive fields are larger and have more complex input needs. The visual cortex's receptive fields of cells were divided into simple, complex, and hypercomplex cells by Hubel and Wiesel (e.g., Hubel, 1963). Simple cell receptive fields are rectangular or elongated, with one long side excitatory and the other inhibitory, such as an excitatory middle oval and a surrounding inhibitory region. To excite the cell, images for these receptive fields must have a specific orientation. A correctly oriented light bar may need to move in a specific direction to excite the cell in complex-cell receptive fields. The bar might also need to be a certain length for receptive fields that are extremely complicated^{60,61,73,74}.

1.8 Visual Functions

Understanding vision requires collecting data from each visual component and comprehending how they work together to shape and interact with the visual world. The complexities of visual input are the foundation of visual function, as they determine the capability of a visual system to detect a specific stimulus. This often involves repeatedly testing a specific parameter in a controlled environment, such as the size of the target stimuli. A visual function can be assessed using several visual forms, and the most common forms include **visual acuity, visual field, colour, contrast, depth, and motion perception**. In contrast to visual function, there is another overlapping concept called functional vision. It refers to valuable vision interactions required to accomplish everyday activities in the visual environment. It involves the assessment of complex real-life conditions with varying parameters. Functional vision and visual function are connected concepts and evaluating one can frequently provide valuable information about the other. They both are assessed using behavioral methods and provide a complete assessment of vision-related abilities^{75,76}.

In clinics, various subjective tests assess various visual functions for diagnostics. It is crucial to record specific visual functions to evaluate visual performance, assess vision damage, estimate pre- and post-medical care, and classify visual impairment. Visual acuity is the most common visual function assessed in the clinics as it evaluates the macular function in the central visual field, which delivers the most demanding visual tasks, such as reading. Under typical lighting circumstances, there is a regional variation in visual function and sensitivity across the visual field. Under standard lighting, the fovea offers the best visual sensitivity and performance. This is primarily because of the fovea's low cone convergence and high cone density packing. However, as I go out from the fovea toward the periphery (with increasing peripheral eccentricity), visual sensitivity and other visual processes systematically deteriorate⁴⁵.

This thesis is focused on assessing macular functions using visual functions called hyperacuity.

The study of visual functions aims at understanding how a functioning, goal-directed organism reacts to its environment in a visual space. It is complicated research that can only be resolved by a multi-disciplinary approach. A combined effort of many scientific fields, including biology, vision science, optometry, ophthalmology, computer science, neuroscience, and physics, each of which approaches the issue from a different angle. Usually, these studies start with visual psychophysics and end with it in diverse ways^{18,75,76}. **The following sections discuss vision development, visual acuity, and contrast in more detail, as these topics are part of the thesis core. It is essential to advance the assessment of certain extremely sensitive vision functions, particularly for vision screening of various eye conditions.**

1.8.1 Vision Development

The literature makes it clear that infants have a weak visual resolution, but as the eye and brain mature, so does the visual system's total ability. To quantitatively measure visual function in infant children, clinicians rely on behavior or electrophysiological techniques that do not require verbal responses. Behavior techniques have been vastly used to measure infants' vision, mainly using grating acuity for clinical purposes. It relies on behavioral responses such as head or eye turn indicating the visual target is being seen. For example, when using Teller acuity cards, the card with grating acuity is positioned in front of a child, and only if the child sees the lines and makes an eye or head movement towards the lines, indicating the ability of the child to see the lines. However, many studies reported that grating

acuity only sometimes correlates with resolution acuity. Resolution acuity is likely channeled through different cortical mechanisms that follow the discrimination of different spatial patterns when compared with the grating acuity that involves simple pattern detection. Investigations using visual evoked potential (VEP)-a non-invasive electrophysiological measure of a visual target, **reported that Vernier acuity is a better approximation of resolution acuity than grating acuity**^{18,75,76}.

1.8.2 Visual Acuity (VA)

Visual acuity can be classified into various broad categories, including detection acuity, resolution acuity, localization acuity, and recognition acuity. Detection acuity deals with the ability of the visual system to reliably detect the smallest size target in the visual space. It is extremely sensitive relative to the resolving acuity as the target has an angle at the eye as small as one arcsecond (1/3600 degree). It is usually measured psychophysically using two alternative forced choices (Is an object present in the first/right or seconds/left screen?). The resolution acuity is the minimum spatial separation between objects to be detected as separate or resolved. The localization acuity is the ability of the visual system to spatially discriminate the visual targets⁷⁷⁻⁷⁹. The resolution and localization acuity are discussed in the following sections in detail. This thesis is focused on quantifying the localization acuity for clinical applications.

The ability of the visual system to spatially recognize optotypes such as letters, numbers, shapes, signs, pictures, and patterns from a given distance is a measurement of resolution acuity. The testing involves tasks such as target identification or reporting the object orientation. The separation of the target features affects these optotypes' acuity; if the targets are too close together, their point spread functions overlap, making it impossible to distinguish between them. The visual system can identify the stimuli characteristics approximately 1.75 millimeters apart from six meters of viewing distance. At this distance, the optotype subtends the visual angle of about five arc minutes with a critical detail of about one minute of arc (60/3600 degree), which is the resolution limit of the eye, and it is also known as the minimum angle of resolution (MAR)^{31,78-81}.

The optotypes of varying sizes are usually well-calibrated and printed in black-on-white background charts with sharp contrast. These charts are often referred to as visual acuity charts and are extensively used in clinics for testing distance and near VA. Over 150 years ago, in the 1860s, Hermann Snellen, a Dutch ophthalmologist, designed the first letter chart for the clinical measurement of visual acuity, and

it is commonly used in clinics today. VA is routinely assessed in clinics using a psychophysical procedure and a Snellen chart showing letters of various sizes against a white background. The observer reads the letters on the chart while seated far away, beginning with the largest letters, and working their way down. The observer's visual acuity is measured by the smallest row of letters they can read clearly and recorded in Snellen notation; that is, the ratio of the test distance to the distance at which the smallest optotype resolved would subtend MAR^{31,77-79}. Although popular and relatively straightforward, the Snellen chart test has numerous drawbacks, including a dependency on high contrast and the peculiarities of letter recognition.

The Landolt-C chart, which displays a gap in a ring with the gap oriented in various directions, and tumbling E chart are the additional tests that can be used to evaluate visual acuity. These techniques use distinct forms of neural processing than the Snellen chart and provide information on a different aspect of visual acuity^{77,80,82}. While recognition acuity is typically slower to develop than visual acuity in children as they often need to learn to recognize the features of objects before they can recognize the objects themselves. In addition, recognition acuity depends on cognitive and sensory factors, while visual acuity primarily measures sensory function. However, visual and recognition acuity are important aspects of visual development for children^{83,84}.

For several reasons, VA testing is still essential to an eye exam performed by an optometrist or ophthalmologist. This is useful for assessing refractive error, clinical diagnosis, and disease monitoring of most eye conditions. Over the years, visual acuity has been used as a primary indicator of the severity of functional impairment due to vision loss. In addition, several licensing authorities and employers also utilize visual acuity measurements to determine if someone is qualified for specific jobs such as police officers, pilots of airplanes, and activities like driving. A VA of 6/6 is widely considered the standard for normal acuity. However, provided that refractive error has been corrected, individuals with normal, healthy eyes often have acuities better than 6/6^{75,85}. Vision 6/12 means low performance, as the subject has half the spatial resolution and requires twice the size to discern the optotypes, while vision 6/3 means better visual acuity. Poor VA is likely to be a result of conditions that damage the macula or the optic nerve pathways that are associated with it. Visual acuity is known to deteriorate in several eye diseases or disorders that impair the transparency of the optical regularity of the cornea, lens, or vitreous^{31,70,77-79}. However, certain highly sensitive visual functions are not dependent on the optical quality of the ocular media and are discussed briefly in the following sections of this chapter.

1.8.3 Contrast Sensitivity (CS)

Contrast sensitivity is one of the visual functions related to the ability to see distinct, well-defined contours of relatively small-scale visual targets or objects. In other words, if two interspersed zones are not divided by borders, a visual system can detect slight illuminance variations between them. Campbell and Green studied it in 1968 using a sinusoidal luminance grating and concluded that it is a complicated and unique retinal function. Contrast is defined as the ratio of an object's darkness to its whiteness in spatial contrast, and the lowest contrast needed to recognize an object is known as the contrast threshold. CS highly depends on the stimuli's luminance characteristics and varies with luminance, target, grating shape, and motion. CS is the reciprocal of contrast thresholds of two types, spatial and temporal. It is known to be affected by several eye conditions, including refractive conditions, age, cataracts, glaucoma, diabetic retinopathy, optic neuropathies, pituitary adenoma, and eye surgeries. Snellen's test only measures the ability to distinguish sharp, distinct edges of tiny objects, not variations in illumination. Thus, it is possible to have 20/20 visual acuity with CS loss in several eye disorders. It can be measured using various tests, including the Pelli-Robson CS chart, Bailey Lovie chart, Vistech Chart, etc. ^{86,87}.

1.9 Eye: An Optical System

The human eye is a fascinating physiological organ with a dynamic lens optical focusing system guided by an aperture (pupil) regulated by light-intensity sensitive pigmented film (Iris). The cornea, aqueous humor, and crystalline lens are thought to act as thin lens collectively. The light-sensitive retina, located at a set distance from the lens on the back of the eye, must be projected with focused images to perceive clear vision. **The crystalline lens is flexible to adjust its thickness and curvature, thereby giving it optical power to project the image on the retina, particularly for objects near distances. This process is called accommodation.** The cornea and the lens of the eye work as a compound lens system that projects an inverted image of the visual scene. The center of the image falls on the fovea to provide the most excellent acuity or image sharpness in the visual field. Due to its variable aperture (pupil), the eye can perceive light intensities from the lowest to 10^{10} times greater without damaging its essential structures. Our eyes perform various visual tasks, including sensing direction, motion, sophisticated colors, and distance. Inter-connections in the retina are the starting point for processing visual nerve impulses, which continue in the brain. The optic nerve carries information from the eye's

sensors to the brain^{88,89}. **Though the eye has a remarkable detection range, it is subjected to diffraction laws that limit the image details that can be resolved.**

1.9.1 Diffraction Theory

The diffraction pattern is a pattern of bright and dark areas created when light spreads out and interacts with itself when it travels through a small aperture, such as the eye pupil. It forms a central bright, focused spot of light surrounded with dark and bright concentric rings, called the Airy disc pattern. In general, **the diffraction in the human eye depends on pupil diameter**; if the pupil is about two millimeters or less, a point object viewed through a circular aperture, such as our eye's iris, the outcome is a diffraction pattern rather than a point. This pattern restricts the overall amount of light that may reach the eye and the spatial resolution of the image that develops on the retina. This disk's diameter is influenced by the light's wavelength and aperture size, which is determined by the pupil's diameter. The two features in the observed object merge into a single image when the size of the Airy disc is larger than the distance between them^{16,19,34,50,90,91}.

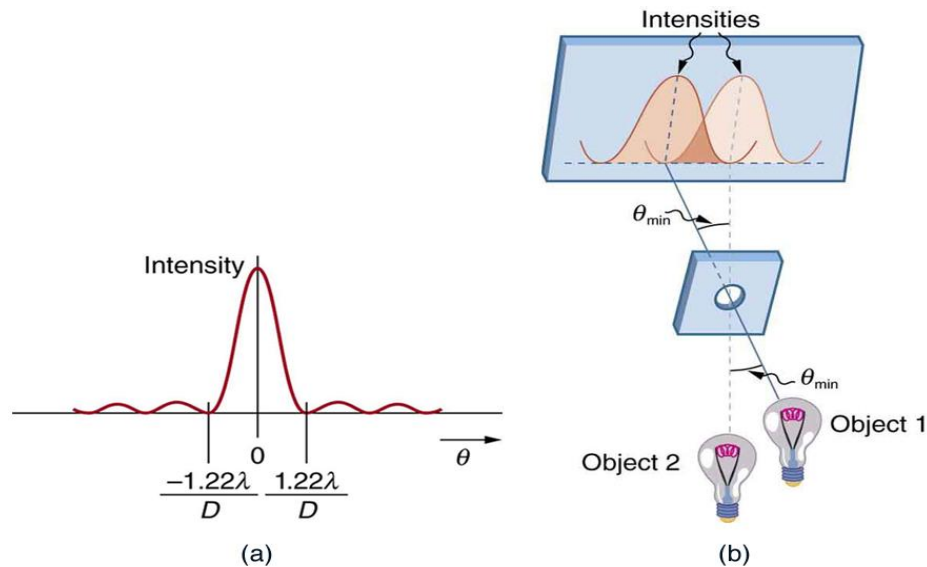
As illustrated in the figure 1-17, point sources near one another may overlap because of the airy discs, resulting in a fuzzy image. This establishes the theoretical upper bound on the resolution for imaging, known as the diffraction-limited resolution, which uses light with shorter wavelengths. Even for small wavelengths, there is a diffraction limit^{90,91}.

Several physical principles and anatomical structures control humans' spatial vision. The brain uses this spatial information to reconstruct a three-dimensional image of the visual world. The retinal cones are especially useful for visual tasks that require high spatial acuity, such as reading or discriminating small details. The retinotopic organization allows the visual system to calculate object locations using retinal light distribution differences. Binocular disparity, motion parallax, and perspective also help the visual system refine spatial localization and distance perception. The brain then combines this visual information with other sensory information to form a coherent percept of the world^{80,81}.

1.10 Resolution Limits

The concept of resolution limits relies on the physical distance in visual space that two-point sources would have to lie to distinguish their light intensity pattern or point spread function (PSF) from each other. (Figure 1-17) The stimulus must be recognized by a single receptor surrounded by two other receptors that receive a more significant light signal to distinguish the light from two visual stimuli as

independent. Therefore, the visual acuity-determined eye resolution limit corresponds to the distance between photoreceptors⁷⁷. The size of the photoreceptors on which the image is focused determines the eye's maximum resolution. The image quality would be impacted by optical crosstalk between adjacent photoreceptors if photoreceptors were any thinner or more closely spaced apart than two microns. The measured values of maximum visual acuity in various species, including humans, can be explained well by this type of photoreceptor spacing in conjunction with the eye's focal length⁵⁹.



[This Photo](#) by Unknown Author is licensed under [CC BY](#)

Figure 1-17 The graphical representation of point spread function and diffraction using two similar light sources.

Limits of resolution refer to the limit of maximum separation required for an optical system to resolve; it is also called the resolving power. It can also be defined as the inverse of the distance or angular separation between two objects that an optical instrument can resolve.

$$\text{Resolving power} = \frac{1}{\Delta\theta} = \frac{d}{1.22\lambda}$$

High-frequency fringes show curved stripes over more than 30 min of arc, indicating local regularity in the foveal lattice. This psychophysical evidence for a regular lattice of human foveal cones shows that the visual system can resolve and measure small differences in retinal photoreceptor placement. The photoreceptor mosaic, the eye's refractive error, the optical system's low-pass filter, neural

processing, and eye fixation can all limit human visual resolution. Retinal pigmentation and vascularization may also indirectly affect imaging precision⁹². There are mainly three criteria for resolution limits: the Rayleigh, Abbe, and Sparrow criteria.

1.10.1 Raleigh Criteria

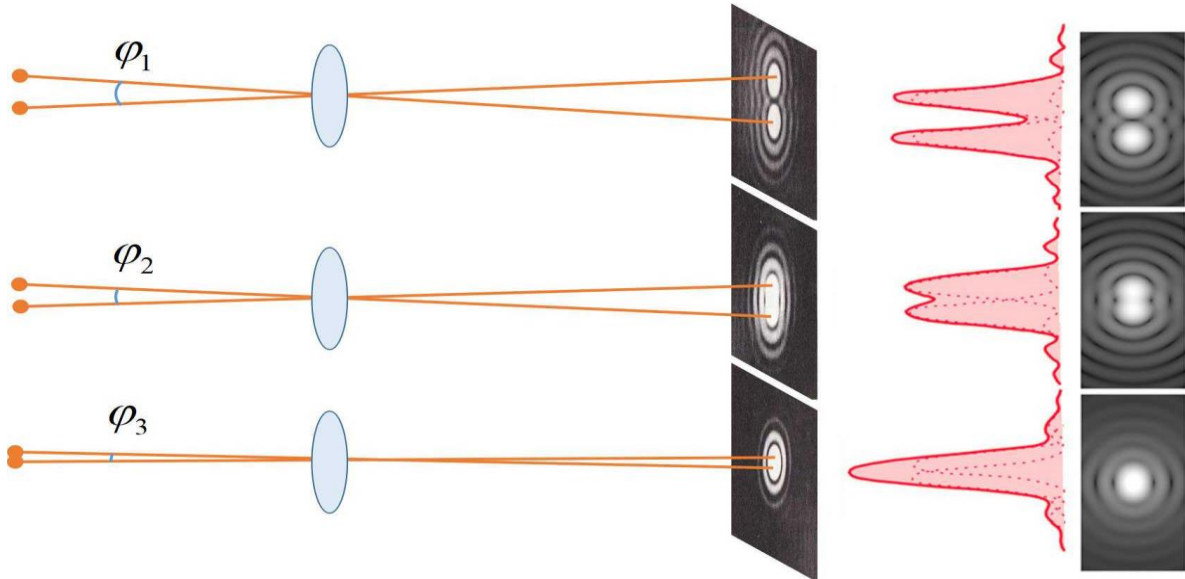
In 1879, John William Strutt (Baron Rayleigh III) investigated the resolution limit of several optical devices, including telescopes and spectroscopes. The Rayleigh criterion is the most common criterion for the minimum resolvable detail. It describes the receptive apparatus to signal the two peaks and the trough as distinct features, assuming the spatial grain is sufficiently refined. The intensity difference is detectable if two similar light sources are just resolvable when the center of the diffraction pattern of a light source is directly over the first minimum of the diffraction pattern of the other^{77,89,93}.

(Or)

Rayleigh's criteria state that spectral lines can only be judged as single or double if they are separated by at least the half-width of the diffraction distribution, which is widely used to measure performance. Rayleigh's Criteria for the diffraction-limited vision for an iris diameter of 5mm and a wavelength of

$$500 \text{ nanometers are: } \theta_R = 1.22 \frac{\lambda}{D} = \frac{1.22 \times 5 \times 10^{-5} \text{ cm}}{0.5 \text{ cm}} = 1.22 \times 10^{-4} \text{ rad}$$

Where θ is the angle in radians, λ is the wavelength of light, and D is the diameter of the circular aperture.



[This Photo](#) by Unknown Author is licensed under [CC BY-SA](#)

Figure 1-17 Graphical representation of two objects to be resolved using Rayleigh Criterion.
 Adopted from [20191230221553873.jpg \(2028×1038\) \(csdnimg.cn\)](#)

1.10.2 Abbe Criterion

The Abbe and Rayleigh criteria are two values for the diffraction limit that are closely related. The definition used in deriving what is meant by two objects being resolvable from each other is the basis for the distinction between the two. This distinction is negligible in practical applications. In the Abbe limit, a slight dip is still discernible between the two maxima. Both these criteria are most used in microscopy^{94,95}.

1.10.3 Sparrow Criterion

According to Sparrow criteria, two-point sources can only be resolved when the second derivative of the total illumination distribution in the diffraction image of the two points diminishes on-axis. A flat intensity profile is the result of adding two airy patterns. The distance at which a dip midway between such point objects of equal intensity stops is evident in the super-resolution of their pictures (the first two derivations of the intensity curve along the connecting line become zero). In contrast to the

Rayleigh resolution criteria, the Sparrow resolution criterion relies on the incident light's coherence characteristics.^{95,96} However, two sources separated by much less than the Rayleigh or Sparrow limit can still be distinguishable due to the wider image generated. The optical system's limiting spatial frequency, or cut-off frequency, is expressed through the optical transfer function. It is fixed at a value of a/λ cycles/radian in the object space, where a is the aperture diameter, and λ is the wavelength of light.

1.10.4 Retinal Mosaic

The cones in fovea centralis have been microscopically observed to be highly compact hexagonal (mosaic) with their centers are about 25 arcseconds apart and individual cone exhibit as a distinct unit. Human vision relies on the photoreceptor mosaic, which is the anatomical foundation of our visual acuity or resolution. Research indicates that the cone mosaic is a uniform arrangement of "sensors" that capture the optical image projected onto the retina, initiating specific photochemical reactions. Due to the sampling properties of the cone array, it is possible to observe distorting effects when viewing very fine gratings, i.e., stimuli whose light intensity varies according to a sinusoidal function. This is a consequence of the sampling theorem from linear systems analysis, and it is vulnerable to sampling artifacts and aliasing effects^{36,44,45,77,91,92,97}.

1.10.5 Visual Aliasing

Visual aliasing occurs when an image's resolution is too low to effectively capture the tiny features or high-frequency information, resulting in a stair-step-like pattern. It is observed when insufficient sampling or resolution causes an image to look wrapped or distorted. It is often referred to as aliasing or spatial aliasing and can be seen in various digital media such as pictures, films, and computer graphics. When high spatial frequencies in an image are inaccurately represented on the retinal image by the cone mosaic in the fovea, this phenomenon is known as aliasing in human foveal vision. This happens when the image's spatial frequency rises above the Nyquist limit of roughly 60 cycles per degree. Even under ideal conditions, the optics of the eye, the size, and the spacing of the cones in the fovea serve as low-pass filters that reduce the modulation available at the retina by roughly a factor of 10 at this frequency⁹².

The visual system solves aliasing's effects on human vision. Post-receptor filtering, such as the ganglion cell receptive field mosaic, can eliminate aliasing in the human visual system. This filtering removes useful information at frequencies above the cone Nyquist limit. The inner retina's light scattering may also reduce the contrast of high spatial frequencies in the aliasing range, reducing aliasing effects. Weak electrotonic coupling at the photoreceptor level may reduce aliasing by reducing spatial frequency contrast⁹⁸. The attenuation of high-frequency spatial components responsible for aliasing may also result from reducing high-frequency interference fringes and other elements such as irregularity in the cone mosaic and low pass filtering by individual photoreceptors. Studies demonstrated that the Moire pattern produced by the foveal cone mosaic with a sinusoidal grating in human foveal vision suggests high local regularity in the foveal lattice⁹⁸⁻¹⁰².

1.11 Visual Psychophysics

A classical subfield of psychology that studies and quantifies the relationship between physical stimuli and the perceptual experience they produce in human observers is known as visual psychophysics. The German physicist Gustav Theodor Fechner (1801 -1887) coined the term psychophysics. It aims to understand the sensory system's processing and interpretation of environmental information and how it influences behavior. Typically, “visual psychophysics” refers to the experimental methods and techniques used to quantify and examine the connection between physical inputs and visual perceptual experiences. These techniques include, for instance, threshold measurements, which determine the minimum intensity or duration of a stimulus required for a perceptual response, psychophysical scaling, **which involves asking participants to rate the intensity or quality of a perceptual experience; and reaction time measurements, which measure how quickly participants react to a stimulus**^{29,103}.

Fechner developed classical psychophysical methods that include the method of limits, the method of adjustment, and the method of constant stimuli. More recent methods are motivated by the signal detection theory, including the yes-no method and the forced-choice method⁶⁵. The first step in visual psychophysics involves a detailed assessment of the physical attributes of the stimulus environment through a range of presentation and measuring procedures. The relationship between the characteristics of the physical stimulus and the participant performance based on perception is then quantified. Measuring these interactions relies on locating these connections across different perceptual realms and understanding the decisions made for certain actions or task objectives. The outcome is an

understanding of the potential and limitations of functional behavior. It has applications in various research areas, including neuroscience, cognitive psychology, and vision science. It can investigate various visual phenomena, including optical illusions, color vision, depth perception, and visual attention. Psychophysical tests have a unique advantage in the clinical testing of vision as they provide information about visual functions in a non-invasive manner. It allows clinicians to assess various aspects of vision using psychophysical activities, including visual acuity^{18,54,90,93,103-107}.

1.12 Visual Hyperacuity

1.12.1 Definition

The human visual system is extremely sensitive to specific visual tasks and can precisely perceive subtle differences between relatively localized stimuli. Under ideal conditions, the perceived differences are measured to be smaller than the size or spacing of the foveal cone diameter beyond the optical and anatomical limits of the eye. Gerald Westheimer named such extremely sensitive visual functions' Hyperacuity' in 1975. Hyperacuity refers to a class of spatial visual tasks such as orientation discrimination and alignment detection^{54,78-82,91,108}.

1.12.2 Hyperacuity and Visual Acuity

Hyperacuity refers to the ability of the visual system to detect small displacements or differences in spatial stimuli that are beyond the theoretical limits of retinal resolution. It differs from visual acuity, which refers to resolving separate stimuli as distinct objects. While refractive correction lenses (positive or negative) can improve visual acuity, they cannot improve neural processing related to hyperacuity. Currently, measurement of hyperacuity can indicate various eye conditions, including diseases and neurological or developmental anomalies, so appropriate medical attention can be offered^{79,95,109}.

1.12.3 History of Hyperacuity

Hyperacuity was known for centuries and was the foundation for advancements in ancient tools used for astronomy and navigation, including the 'Astrolabe' in the 15th century, as reported by Pedro Nunes in 1542. In the 16th Century, the Vernier caliper was invented by Pierre Vernier, which allowed quantitative measurement of the object dimensions with high precision using the most sensitive visual task of human beings, alignment detection. The invention of the telescope by Sir Robert Hooke in the

17th century allowed him to notice that the observer's eye provides the resolution limit for double stars. While in the 18th Century, Volkmann first measured just detectable differences for retinal distances based on Weber's theory and reported that it could be measured up to twelve arc seconds: a fraction of photoreceptor diameter, In 1850. Later in 1861, Ewald Hering, a German physiologist who contributed significantly to the study of visual perception, proposed that Vernier acuity is obtained through spatial sampling, where the Vernier line stimuli simulate over a hundred photoreceptors. While in 1892, Wülfing conducted Vernier experiments quantitatively and believed that the photoreceptor cells in the fovea had to be much smaller than his anatomist colleagues thought. It has been reported that the diameter of photoreceptors is larger than the Vernier acuity thresholds (VeT) by a factor of 2 to 3^{79,97,110,111}.

In the 19th century, Ludvigh disproved Hering's explanation through his experiment in 1953; he performed Vernier experimentation using dots instead of line stimuli and achieved almost equal thresholds. As the dot stimuli are spatially small compared to the line and can simulate fewer photoreceptors, Hering's hypothesis was considered incorrect. Around the same time, an anatomist described that the resolution limit directly depends on the size of the photoreceptors. The unifying theory of visual acuity achieved recognition in the first half of the 20th century, which merges on the behaviorally determined value of little under one minute of arc from diffraction, photoreceptors distribution, and intensity discrimination^{79,97}.

1.12.4 Hyperacuity Research

Hyperacuity has been studied to explore other senses with similar sensitivity in the human body. Evidence from the literature suggests that cutaneous sensibility may have some functional similarity with vision. It has been suggested that vision's various spatial discriminative capacities, denoted as "hyperacuties," are matched by similar capacities in touch. This is due to the cutaneous sense, like vision, having as its first stage a two-dimensional receptive surface¹¹². Investigations examined the hyperacuity performances and cortical processing in cats and other animals¹¹³⁻¹¹⁸.

1.13 Vernier Acuity (VeA)

1.13.1 Definition

Vernier Acuity is one of the prime forms of hyperacuity that involves the alignment detection of two or more line or dot stimuli. The Vernier tasks involve two scales with markings; a stationary main scale

with reference marking and the moving scale that is adjusted to make alignment against reference marking. It has been observed that an individual can perceive the misalignment of markings up to 2-5 arcseconds of visual angle, which is 10-30 times smaller than the eye's natural resolution limit (60 arcseconds or one arcminute). In our day-to-day life, we exercise Vernier acuity using various tools, particularly for making quantitative measurements of various elements, including time, shape, dimensions, volume, power, etc.^{91,119}

1.13.2 Vernier Acuity Development

A study on the development of Vernier acuity in human infants and children between 2 months to 9 years of age found that it was present in all age groups¹²⁰. The development of Vernier acuity in infants has been extensively studied using a behavior technique called preferential looking in both normal and several childhood visual conditions, including developmental delays¹²¹ and cortical visual impairment¹²². Studies also indicate that Vernier acuity develops substantially later than grating acuity, suggesting that various visual systems constrain these two functions. Vernier acuity appears slightly poorer or equal to resolution acuity in the first three months of life. Investigators speculate this could be because of the mean sampling distance or the center-to-center distance between receptive fields. However, Vernier acuity improves (0.5 c/deg at 2 months to 12.0 c/deg at 8 months) to become better than resolution and grating acuities between 4-18 months. This could probably be due to the changes in the retina, cortex, or both^{78,123}.

A similar improvement in Vernier acuity is observed at five years of age. While the resolution acuity is close to adult levels, the Vernier acuity improves significantly between five years and adulthood. In addition, Females have significantly better Vernier acuity than males for 3-5 months. This difference is not due to behavioral factors but might be related to the neurotrophic effects of the early pulse of testosterone found in male infants. The ideal observer program predicts that Vernier acuity will be inversely proportional to the square root of photon capture. In contrast, resolution acuity will be inversely proportional to the fourth root of photon capture. As photon capture improves with age, Vernier acuity improves proportionally compared to the resolution acuity^{78,123}.

1.13.3 Neural Mechanism of Vernier Acuity

The sensitivity for hyperacuity tasks is due to cortical processing by the neuronal visual system because such accuracy exceeds the eye's optical or, in other words, foveal cone diameter or spacing limits. When we focus on Vernier acuity, different aspects of Vernier processing can be explained by the characteristics of oriented filters in the striate cortex (V1), as the neurons in the V1 area are highly selective to the orientation and size of the stimuli. In the visual cortex, many receptive fields are made up of elongated regions that, when stimulated, cause a cell to become activated and their sidebands, inhibiting the same neuron. These receptive fields may be oriented differently and are covered by a fine-grained layer that covers the visual fields. If the Vernier is centered on the cell's receptive field, a cell with a vertically oriented receptive field cannot tell the difference between a straight and an offset Vernier stimulus. The offset stimulus will activate a portion of the inhibitory surround. Still, because the receptive field centers of neighboring cells are slightly offset to the side of the first neuron, they can distinguish between these two stimuli. Receptive fields with a little gradient proportional to the orientation of the Vernier are regulated by the same rules. The ability to distinguish between straight and offset Verniers will be greatest in cells having receptive fields in this orientation^{58,78,91,108,124-130}.

Studies from several computational programs based on size and orientation filters and psychophysical masking support the assumption that striate mechanisms critically limit the extraction of hyperacuity-related information^{131,132}. However, studies utilizing functional magnetic resonance imaging (fMRI) and electroencephalogram (EEG) identified extra striate participation. They revealed a distributed network of frontal, parietal, occipital, and cerebellar cortical areas specifically activated by Vernier stimuli. In addition, VeT obtained using visual evoked potential (VEP) found that VEPs displayed an initial predominate reaction across medial occipital electrodes. Later, widely dispersed secondary responses took place, which was compatible with a convolutional pathway starting in the early visual cortex and moving to higher-order areas¹³³. A study using fMRI-informed EEG source imaging confirmed four visual regions, including V1, lateral occipital cortex, hV4, and middle temporal cortex, that are sensitive to detecting Vernier displacement. The lateral occipital cortex is the most sensitive cortical area to Vernier displacement stimuli and striate mechanisms^{51,63,132-136}.

1.13.4 Vernier Acuity and Stereoacuity

Vernier and stereo acuity are both hyper acuities with comparable thresholds well below the eye's resolution limit. However, the neural circuits for these two classes of visual responses do not identically process the signals. Vernier acuity involves discrimination of the relative location of visual features in a two-dimensional plane, while stereo acuity is based on the judgment of relative depth. Compared to stereo acuity, hyperacuity is more immune to image blur. It has been shown that the zones where two targets must be placed to meet their lowest thresholds are very different. The neural basis for the differences in processing between Vernier acuity and stereo acuity is not yet fully understood. However, it is known that they involve different neural circuits for processing the signals. It has been shown that blurring the targets results in a more severe deficit in stereo acuity than in hyper acuity, indicating that they are processed differently at some stage of visual processing. However, both involve as-yet-unknown cortical neural processing due to their yielding thresholds being much smaller than the spacing of the elements of the retinal mosaic ^{80,136-138}.

1.13.5 Vernier Acuity and Aberrations

A study that examined the relationship between optical flaws in the eye and visual acuity and Vernier acuity discovered that higher-order aberrations of the eye did not affect hyperacuity thresholds but that lower higher-order aberrations had a significant positive impact on Landolt acuity thresholds¹⁰⁸.

1.13.6 Vernier Acuity and Perceptual Learning

Several studies have investigated the learning effect on Vernier acuity and found a positive perceptual learning effect on Vernier acuity ^{127,139}.

1.13.7 Vernier Acuity and Light conditions

A study compared the difference between photopic (in the light environment) and scotopic (in the dark or absence of light environment) Vernier acuity thresholds and found they were the same in both environments⁵⁴.

1.14 Clinical Importance of Vernier Acuity

In clinics, vision is assessed majorly using three visual functions that deteriorate in these eye conditions. The three primary visual functions are Macular function in the form of visual acuity, visual field defects, and visual distortions. However, Vernier acuity is highly sensitive to detect subtle changes in the fovea,

and poor VeT can efficiently indicate disease-related changes much earlier than visual acuity. Therefore, it holds a vast potential to be used in clinics for vision screening of several conditions that can result in permanent blindness. In addition, Vernier acuity can be used to assess all three types of visual functions that provide disease-associated clinical information. Vernier acuity has been extensively studied since it possesses extraordinary clinical diagnostic properties, making it a very efficient vision screening tool. The three important clinical properties are:

- 1. Highly resistant to retinal image degradation:** The Vernier acuity thresholds can predict post-operative visual function in individuals with cataracts or similar media opacities. The thresholds are immune to optical media-related image degradation¹⁴⁰⁻¹⁴⁴.
- 2. Independent of age:** The Vernier acuity thresholds do not change significantly with age and thus can be used to evaluate a wide range of age groups¹⁴⁵⁻¹⁴⁹.
- 3. Vision screening potential:** Vernier acuity has been extensively investigated in the literature because of its high sensitivity characteristics for certain visual functions. Certain hyperacuties, including Vernier acuity, deteriorate during disease pathogenesis and abnormal eye conditions. Therefore, it can be used in the clinical screening of eye conditions^{58,119,138,150-153}. A few eye conditions that have been investigated in the literature include:

Glaucoma: The change in receptive fields due to the loss of ganglion cells in glaucoma has been studied using Vernier acuity as a substitute measure. The Vernier acuity can detect subtle pathological changes during the early phases before they can be detected using conventional visual acuity or visual field defects. These conditions are usually challenging to diagnose during the initial stages as they progress quietly and show no sign of visual acuity changes until considerable vision damage is experienced. Therefore, detecting such eye conditions at the initial stages and managing them promptly to fight irreversible blindness is particularly important^{154,155}.

Retinitis pigmentosa: Vernier acuity deteriorates to a similar extent as letter and grating acuities, suggesting that increased foveal inter-cone spacing is responsible for the decline in these acuities. A larger stimulus size is required for the increased retinal mosaic dimension¹⁰⁹.

Amblyopia: Vernier acuity deteriorates in the unilateral amblyopic eye while the fellow eye shows no deficiency, unlike other visual functions such as contrast sensitivity, motion perception, and stereopsis. It is due to cortical suppression of spatial information corresponding to the amblyopic

eye, causing spatial distortions and uncertainty. Therefore, a clinician may become aware of neurological or developmental issues by a higher Vernier acuity threshold, allowing for further investigations or referrals¹⁵⁶. In addition, Vernier acuity has also been investigated for vision-related cortical, neurological⁵⁸, and psychiatric conditions, including cortical visual impairment¹²², Down's syndrome¹⁵⁷, and schizophrenia. Furthermore, it can also provide access to a valuable outcome measure in clinical studies of novel neuro-ophthalmic treatments^{58,78,133,156,158,159}.

1.15 Lacunae

As discussed in the above sections, hyperacuity has tremendous potential to detect subtle changes in the central vision and thus can be efficient in clinical testing. In addition, Vernier acuity's ability to detect a broad spectrum of eye conditions makes it an exceptional tool for clinical vision screening and diagnostics. However, it is not routinely measured in clinical settings for the following reasons.

1. **Feasibility:** The psychophysical methods used in the literature involve stimuli adjustments ranging from a hundred to a few hundred times to achieve precision, resulting in fatigue, lack of interest, and boredom. Therefore, it is not feasible for clinical testing.
2. **Time:** The psychophysical procedures used in the literature are time-consuming, and it is not feasible to perform extremely long testing in clinical settings due to the importance of time.
3. **Technical tools:** The technical limitations of tools used in the literature to make stimuli alignment may affect the accuracy of the measurements.
4. **Lack of stimuli standards:** The VeT depends highly on stimuli characteristics such as shape, colour, contrast, and size. Therefore, it is important to have standard stimuli to achieve reliable results.
5. **Learning effect:** The Vernier acuity is known to have a strong practice effect on the magnitude of VeT. Therefore, it is not easy to generalize the results obtained from testing.
6. **Reliability:** The clinical community does not accept Vernier acuity well, mainly because of reliability issues arising from the reasons mentioned above.

1.16 Hypothesis

I hypothesize that the advanced psychophysical procedure, technique, and modern technological interventions might improve the Vernier acuity testing standards for clinical consideration. Therefore, I attempted to address the challenges noticed in the literature by advancing the methodology and technicality to improve the Vernier acuity test efficiency for clinical application.

1.17 Clinical Applications of Vernier Acuity

Vernier acuity can be used in clinics in three different formats/programs to assess three important visual functions of central vision susceptible to most eye abnormalities. They are:

- 1. Vernier acuity:** Can quantify macular function in the central 2 degrees.
- 2. Hyperacuity perimetry:** This can quantify the central 5 degrees of the visual field.
- 3. Metamorphopsia:** Can quantify central 5 degrees of visual field distortions.

1.18 Thesis Plan

In this thesis, I plan to develop three computer-based software application programs that quantitatively assess three different visual functions using sophisticated hyperacuity paradigms. Each program is built with a focus on quantifying a unique visual function of the macula that is highly valuable in the clinical diagnosis of several eye abnormalities. I further plan to perform technical validation of the developed programs by assessing repeatability to ensure that the programs produce consistent results.

Three hyperacuity-based modules are listed below:

Program-1: Vernier Acuity Thresholds (VAT)

Program-2: Hyperacuity Perimetry (HP)

Program-3: Metamorphopsia (MMP)

Initially, this research study was planned to achieve thesis objectives that included the development of a software program using an advanced method to measure Vernier acuity, followed by clinical testing for validation. A month before the pandemic, the VAT program was first assessed for precision, gap functions, and ideal stimuli configuration in the laboratory through a small pilot study (pilot study 1). The program achieved promising results and motivated further testing. However, due to the COVID-

19 restrictions, I could not perform the clinical testing of this program for validation. Consequently, I limited program testing to the laboratory for technical validation. Alternatively, I planned to extend the hyper-acuity paradigms by developing two additional software programs, HP and MMP, and testing them with the VAT program.

I performed an extensive pilot study (pilot study 2) to assess the performance of all three programs for technical validation. All three programs were assessed for program precision, testing time, and repeatability. The testing was performed on both eyes individually; results from individual eyes were assessed for repeatability and compared between eyes at each visit for symmetry. The correlation between the repeated measurements was estimated to verify the result's consistency for reliability. The programs that can produce consistent results were considered for technical validation. In addition, the results obtained from each program can serve as baseline data for future comparisons. A discrepancy between the measurement and prediction implies the presence of a possible retinal/neural dysfunction. The VAT program was additionally assessed for performance through the subject's response accuracy and response time. In addition, I further classified the results into age and gender groups to verify similarities and differences.

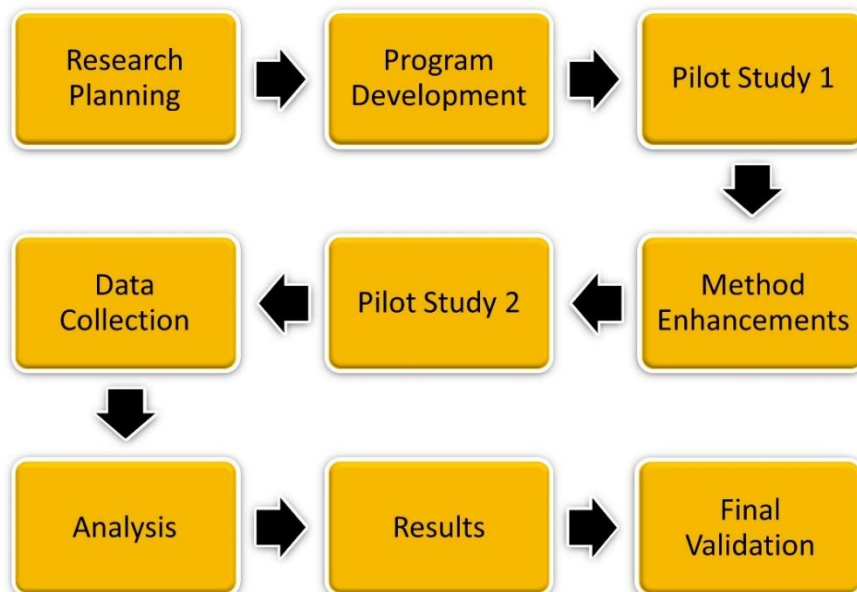


Figure 1-18 Graphical presentation of research flow chart of this thesis.

1.19 Thesis Synopsis

A summary of each chapter is listed below for a quick review.

Chapter 1: Introduction

This first chapter of the thesis lays comprehensive background information before moving on to the thesis topics, its clinical importance, and research aims. It clearly outlines the research problem, the motivation behind the investigation, and the research question that will be addressed throughout the thesis. It also offers a short synopsis of the chapter that follows.

Chapter 2: Vernier Acuity Test: Software Program Development, Method Implementation, and Stimuli Standardization

The second chapter details the software program development and implementation of an adaptive staircase method. It describes the testing process, experimental setup, and response collection technique to address the research questions. This chapter justifies the chosen methodology and explains its suitability for the research objectives. In addition, it details program performance and verification of ideal stimuli configuration for standardization through pilot study 1.

Chapter-3: Vernier Acuity Test: Program Enhancement, Test Performance Analysis, and Results Repeatability

The third chapter focuses on program enhancement and performance assessment using four different metrics, including precision (lowest detectable measurements and mean measurements), Response accuracy (Percentage), time (Responses time and test time), and repeatability of results. It also compares the results between demographics, including eyes (Right and Left), age groups (≤ 30 and >30 years), and gender (Females and Males) for similarities and differences. In addition, it also outlines possible limitations and potential issues during the research process.

Chapter-4: Hyperacuity Perimetry: Modifying VAT and Results Repeatability

The fourth chapter of this thesis focuses on modifying the VAT program and assessing hyperacuity-based visual fields across central 5 degrees. The measurements were taken in four quadrant positions using two gap sizes and repeated to assess reliability.

Chapter-5: Metamorphopsia: Software Program Development and Results Repeatability

The fifth chapter of this thesis focuses on programming a program to quantify visual field distortions using a method of adjustment. The measurements were taken from 1 to 5 degrees using two orientations and repeated to assess reliability.

Chapter-6: Final Discussions, Conclusions, Recommendations, and Future Directions

The final chapter of this thesis summarizes the main findings, reiterates the research objectives, and the answer to the research questions. It provides a concise conclusion that reflects the overall research process and its outcomes. Additionally, this chapter provides recommendations based on the research findings, suggesting practical implications and potential areas for further investigation. It emphasizes the broader significance of research and its potential impact on the field.

1.20 Research Ethics For Pilot Study 1 (Chapter 2)

The University of Waterloo, research ethics body, has reviewed and approved this research with application # 41958. No invasive or drug intervention was involved in this experiment; therefore, the risk of adverse effects is negligible. This research was carried out according to the University of Waterloo tri-agency research policy TCPS-2 of the government of Canada and adhered to the declaration of Helsinki.

1.21 Research Ethics For Pilot Study 2 (Chapters 3, 4, and 5)

The University of Waterloo, research ethics body, has reviewed and approved this research with application # 44460. No invasive or drug intervention was involved in this experiment; therefore, the risk of adverse effects is negligible. This research was carried out according to the University of Waterloo tri-agency research policy TCPS-2 of the government of Canada and adhered to the declaration of Helsinki.

Chapter 2

Vernier Acuity Test (VAT)

In this chapter, I described developing a software program using modern technology and implementing an advanced and efficient psychophysical technique to measure Vernier acuity quantitatively. Using specialized software, the Vernier acuity measurements validate and standardize the stimuli shape and contrast based on the experiment results achieved through a pilot study.

This work has been presented at SPIE, light in nature conference and I adopted and/or modified figures and tables from the same paper¹⁶⁰.

2.1 Introduction

The macula, a very complex structure, is one of the outstanding aspects of the human visual system that distinguishes it from other organisms on Earth^{14,15,44}. The macular structures should be intact and sufficiently dry for vision to be sharp and for images to be clear in our central vision. Certain diseases, disorders, and abnormal eye conditions involving the macula cause damage or loss of central vision and macular functions. Though macular disorders are most commonly seen in elderly individuals, they can affect individuals of any age⁵⁸. A list of common eye conditions that are known to cause damage to the central vision is mentioned below:

1. Retinal vein occlusions
2. Diabetic retinopathy
3. Central serous retinopathy
4. Age-related Macular degeneration
5. Macular edema
6. Macular hole
7. Retinal Detachment
8. Retinitis Pigmentosa
9. Retinopathy of prematurity
10. Retinoblastoma

Vernier acuity is highly sensitive in detecting subtle changes in the fovea, and poor VeT can indicate disease-related changes much earlier than visual acuity. Therefore, it holds considerable potential to be used in clinics for vision screening of several conditions that can result in permanent blindness. Most studies in the literature measured the VeT using psychophysical procedures and techniques that rely on the observer's behavior in reaction to their visual perception of the stimulus's relative positions. Furthermore, Vernier offsets were measured using several stimuli configurations typically presented on computer screens. Stimuli characteristics, including stimuli shape, size, colour, contrast, and gap size (vertical distance between the two stimuli), may also influence the VeT directly^{148,161-167}. It must be noted from the literature that psychophysical testing and stimuli characteristics can influence the thresholds' accuracy. Consequently, results obtained from such studies are prone to the proportion of inaccurate measurements due to technical limitations and the nature of the psychophysical method itself.

Various psychophysical methods are used in the literature to measure Vernier acuity, including the method of limits, the method of constant stimuli, the method of adjustment, and the modified interleaved staircase. The commonly used psychophysical procedure to determine the VeT for the clinical purpose in the literature is the method of adjustment. According to a study by Abbud and Cruz¹⁶⁸ from 2002, the adjustment method makes it easier to distinguish between Vernier accuracy (mean offset error) and precision (standard deviation). However, a mean precision of 10% can only be achieved after adjusting Vernier stimuli for between 100 and 700 trials. It would take 50 minutes to achieve one hundred trials using such a method. Therefore, the thresholds will likely be measured inaccurately due to fatigue and lack of concentration. In addition, such methods involved using old-fashioned computer input devices such as a ball mouse, joystick, or trackball. These technical tools are outdated as they offer low sensitivity to stimuli adjustments and can be difficult to oversee, particularly for operations like alignment adjustment¹⁶⁸.

Although attempts were made in the literature to provide free tools to measure Vernier acuity on desktops or laptops, they lag standard testing methods and stimuli features⁵⁸. It is crucial to have a standard Vernier acuity testing program with optimized stimuli features to offer rapid, efficient, precise, and, most importantly, reliable Vernier acuity thresholds, particularly for clinical vision screening. Developing a program that can integrate advanced psychophysical testing and technicality is necessary. Such a program can be evaluated and validated for clinical utility, including vision screening, disease monitoring, and treatment assessment. The validation of a standard program for testing Vernier acuity

will help clinicians understand the utility of Vernier testing for clinical consideration. It can serve various clinical needs and normative data for further comparison. Therefore, there is a need to advance and standardize the testing procedure along with technicality and stimuli configuration for Vernier acuity testing.

To address the challenges observed in the literature and improve Vernier acuity testing for diagnostic applications, I attempt to advance Vernier acuity testing by developing a program in three major steps.

- 1. Digitalizing the test:** I planned to advance the test by programming a user-friendly computer-based software application using a modern computer language ‘python’ for testing convenience.
- 2. Implementation of advanced method:** I implement an advanced psychophysical procedure, an adaptive staircase method (ASM)¹⁰⁵, along with an alternative forced-choice technique (AFC) to efficiently record the test responses.
- 3. Stimuli Optimization:** I concentrated on optimizing the Vernier testing with ideal stimuli configurations such as shape and contrast.

2.2 Software Development

Vernier acuity test is programmed in a computer-based software application using an open-source psychophysical experimental development tool, “PsychoPy,” version-3, that runs on a python-3, an advanced computer programming language¹⁶⁹. The PsychoPy platform offers a builder and coder view interface, as shown in the figure. A builder interface is a handy tool with essential materials commonly required for building a psychophysical experiment. The code was developed using builder and code interfaces to access the required experimental settings. It also allows access to the program settings that enable extended control over the experimentations. It is freely available on the official website (<https://www.psychopy.org/download.html>) and installs smoothly on the system but runs efficiently only on the systems that support open graphics library technology. The software program was designed to perform Vernier acuity testing in an organized fashion. The program was built to offer an interactive user experience using a graphical user interface (GUI) window that allows the examiner to input demographic information and set the desired settings at the beginning of the testing.

The program file opens a GUI-based request window for adding subject information, including name, age, gender, and session details. The following window involves experimental setting adjustments before beginning the Vernier acuity measurements. The stimuli and program characteristics were configured for a given viewing distance. It is also programmed to manage the various patient records and experiment details, including patient demographics, experiment data, screen resolution details, viewing distance, Vernier measurements, stimuli positions, responses, date, and testing time. These records are saved immediately at the end of the test in a specified folder in .csv file format and can be easily accessed using Microsoft Excel. This software application program is designed to automate the testing process, record accurate results, and provide a detailed summary of the test results at the end of testing immediately. Overall, it can offer a high-quality testing experience for patients while simultaneously providing convenience, confidence, and adaptability to the examiners.

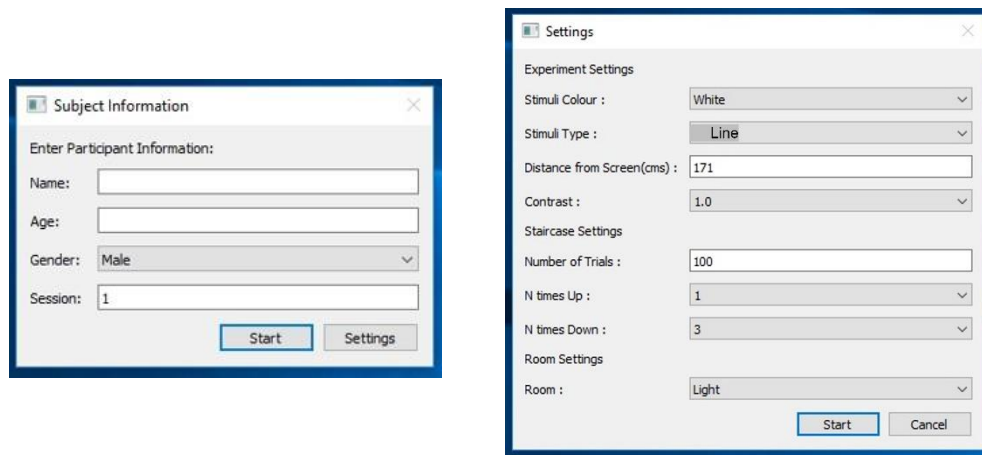


Figure 2-1 The GUI window of the VAT model to add participant information in the left image and experimental settings in the right image.

The software application code was verified for static testing that involves organizing and simplifying code components, finding bugs or code errors. Following that, validation testing was performed to test the program functionality and assess the performance.

2.3 An Adaptive Staircase Method

An adaptive staircase method is known to be an advanced psychophysical testing procedure when compared to the previous methods because of its optimized staircase paradigm^{18,104-106}. It is a staircase method with a condition for every possible response at each step. I applied a 3-down, 1-up (3D-1U) staircase that essentially involves tracking and supervising the stimuli's position depending on the accuracy of the response. For example, suppose the subject registers a correct response for three consecutive stimuli presentations. In that case, the stimulus in the following presentation advances a step toward the alignment, as shown in Figure 2-2. However, if the subject registers an incorrect

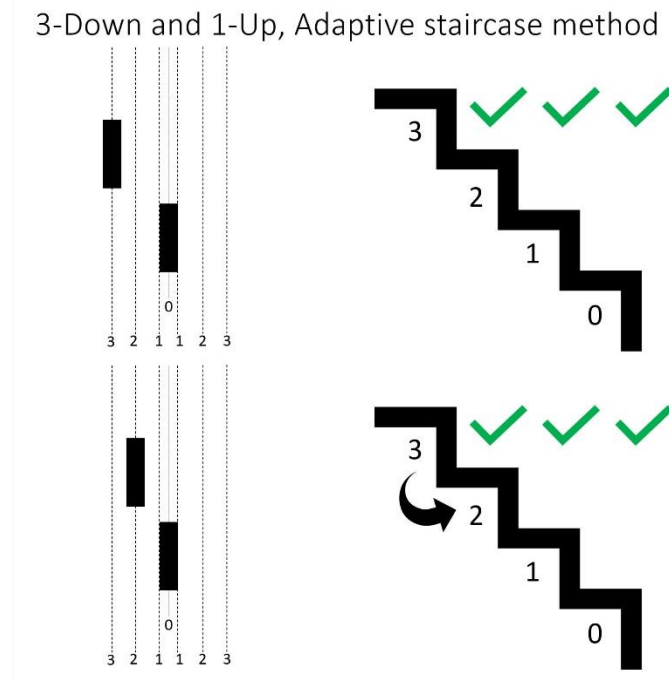


Figure 2-2 Graphical representation of staircase method using stimuli positioning example on the left and response on the right that drives the following presentation of the stimuli.

response, the stimulus in the following presentation moves a step backward from the alignment, as shown in Figure 2-3. This procedure effectively positions the adjustable stimuli closer to the vertical or measurable threshold until the subject experiences Vernier alignment and registers a specific response for alignment. Once the alignment is achieved, the stimulus moves backward, also called the point of reversal, as shown in the figure. The process of testing continues until a set number of reversals are recorded. The lowest threshold number indicates the highest sensitivity. In addition to that, the stimuli

presentations were randomized between the right- or left-hand sides of the reference stimuli to minimize the guessing effect. (Figure 2-4)

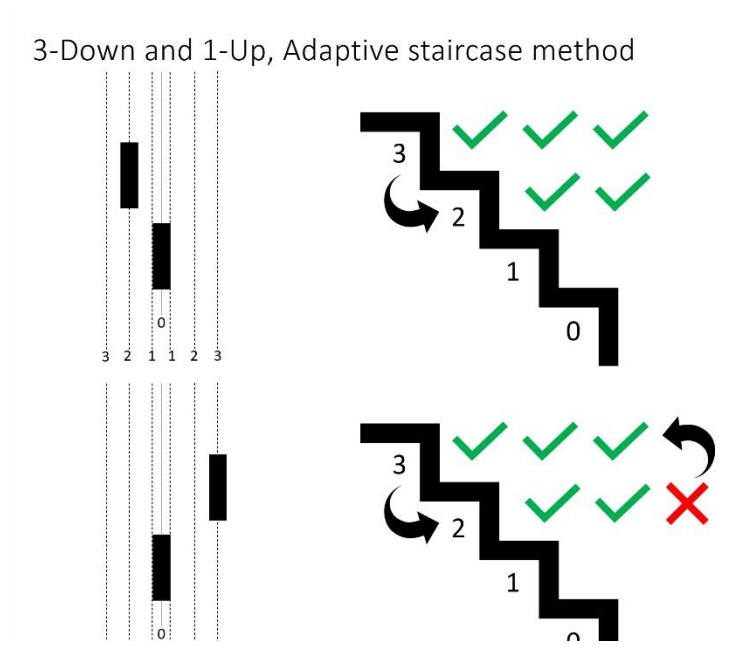


Figure 2-3 An example of incorrect response that drives the stimuli a step back.

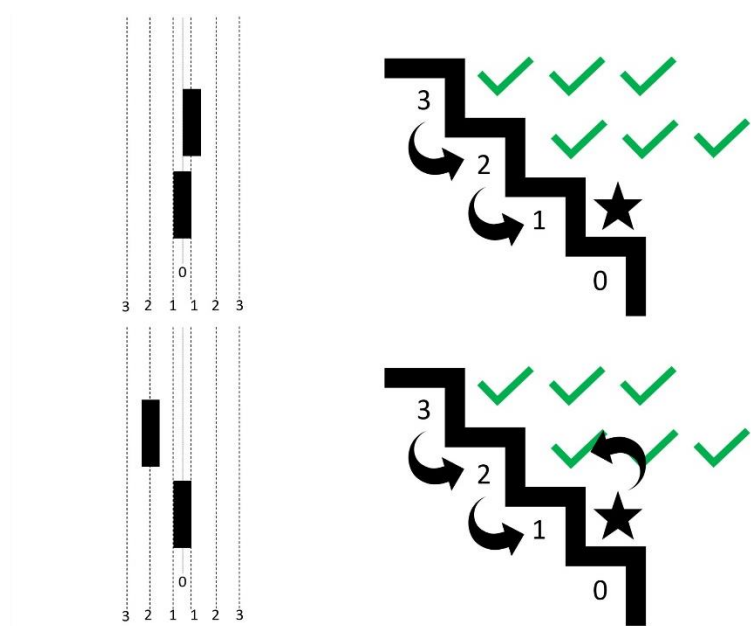


Figure 2-4 For every aligned response the stimuli move a step back.

2.4 Alternative Forced Choice Technique

I employed a three-alternative forced choice (3-AFC) technique to collect subject responses for a given stimulus presentation^{18,104,170}. This means at each stimuli presentation; three options are given to the subject, who are asked to make an alignment judgment and choose the best option that describes the relative position of the adjustable stimuli with the reference stimuli. For instance, when the adjustable stimuli are presented to the left-hand side to the reference stimuli, the subject is instructed to press the left arrow key on the computer keyboard, as shown in Figure 2-5: Similarly, when the adjustable stimuli are presented to the right-hand side of the reference stimuli, the subject is instructed to press the right arrow key on the computer keyboard as shown in figure 2-6. Alternatively, when the subjects perceive adjustable stimuli as relatively aligned with the reference stimuli, the subject is instructed to press the space key on the computer keyboard as shown in Figure 2-7:

This technique generates three types of responses: correct, incorrect, and aligned. Correct responses are achieved when the subject registered response is on the same side in which adjustable stimuli are presented, relatively either the left or right-hand side of the reference stimuli. If the stimuli are presented on the right-hand side of the reference stimuli, and the subject presses the right arrow key, or if the stimuli are presented on the left side, the subject presses the left arrow key. In comparison, incorrect

Graphical representation of 3-AFC

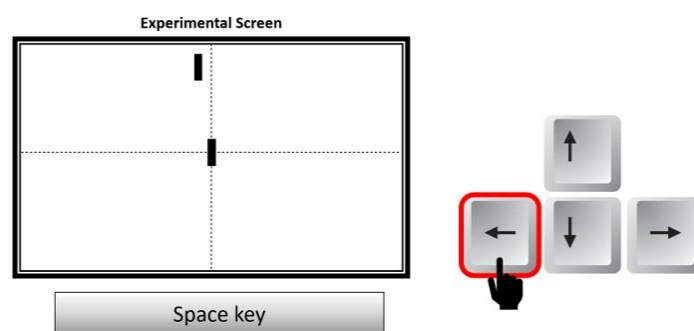


Figure 2-5 The position of the above stimuli on the experimental screen is indicated by pressing the left arrow key on the computer keyboard.

Graphical representation of 3-AFC

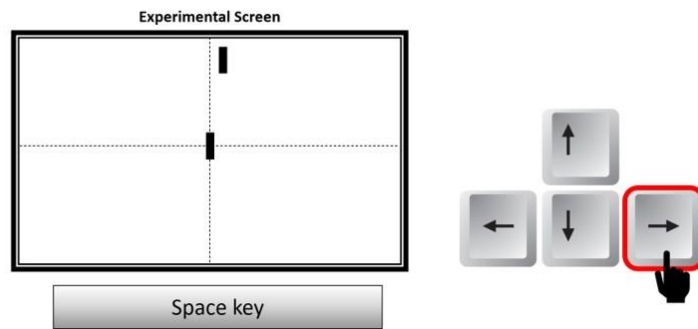


Figure 2-6 The position of the above stimuli on the experimental screen is indicated by pressing the right arrow key on the computer keyboard.

Graphical representation of 3-AFC

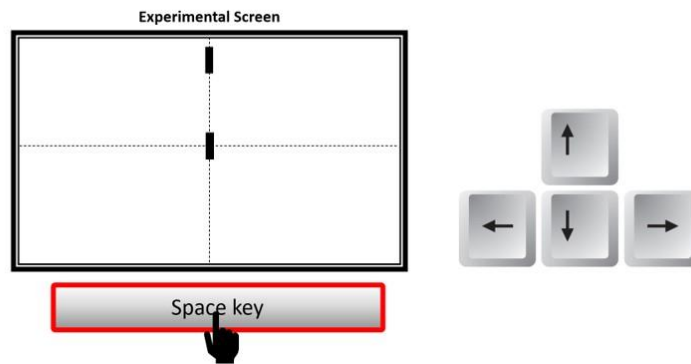


Figure 2-7 The position of the above stimuli on the experimental screen is indicated by pressing the space key on the computer keyboard.

responses are obtained when the subject registered response is opposite to the side on which adjustable stimuli are presented, relatively either the left or right-hand side of the reference stimuli. That is, if the stimuli presented right and the subject pressed the left arrow or vice versa, from either the left or right-hand side of the reference stimuli. Aligned responses are achieved only when the subject perceives the two stimuli as vertically aligned and registers the response by pressing the space key on the keyboard.

This technique is adopted as it limits response bias to 33.3% and helps improve the accuracy when compared with 2-AFC technique where the chance of guessing/response bias is 50% at each presentation. While the 4-AFC technique improves the efficiency and limits the response bias, however,

it increases the testing time, can be tiring and confusing the participants with number of options to choose at each presentation. Hence, the 3-AFC technique was employed to obtain responses with minimal bias in the shortest possible time without compromising the accuracy of the responses. To further minimize the guessing and learning effect, the stimuli presentations were randomized between the right and left-hand sides to the reference stimuli. The order of testing at various gap sizes was also randomized to determine the effect of gap size on the Vernier thresholds.

2.5 Stimuli Configuration

In addition to psychophysical procedures, studies have reported that Vernier acuity is highly susceptible to stimuli characteristics^{78,125,161-163,171}. To optimize Vernier acuity testing, it is essential to optimize stimuli configuration.

2.5.1 Gap Sizes

The figure shows that the vertical separation between the stimuli or inter-stimuli distance is called gap size. To better predict the impact of opacity on Snellen acuity and identify potential retinal/neural dysfunction, researchers have investigated the link between the Vernier acuity thresholds and gap functions^{146,166,172}. We know from the literature that the Vernier acuity thresholds are directly proportional to the gap sizes, implying that thresholds are poor when the separation between the two stimuli increases. To verify the gap effect on Vernier measurements as reported in the literature and support method validation, I planned to measure Vernier measurements at seven gap sizes starting from 128 arcminutes until two arcminutes in log units [128, 64, 32, 16, 8, 4, 2].

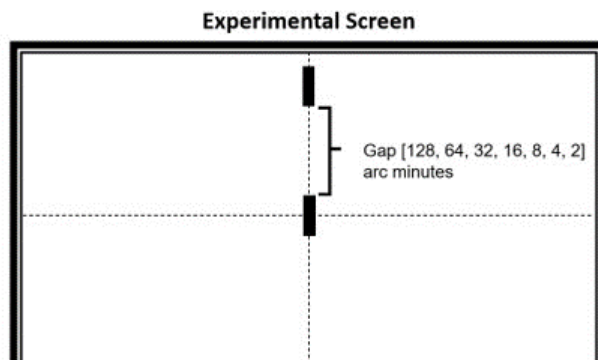


Figure 2-8 The above stimuli was vertically displaced to form separation between the stimuli (gap)

2.5.2 Shapes

It is clear from the literature that the Vernier acuity thresholds are highly dependent on stimuli shapes, particularly between the line and a dot stimulus^{103,163,166,171,173}. As most of the research in the literature used Vernier acuity measurements with either line or a dot stimulus, I planned to run experiments using both stimuli shapes to assess the ideal stimuli shape for Vernier acuity testing.

2.5.3 Contrast Polarity

The literature has examined how stimulus contrast affects Vernier acuity and found that VeT are increased by poor contrast. However, thresholds tend to become independent of contrast when contrast is high^{99,110,161-163,165,174}. Another study used a previously reported formula to evaluate the luminance of the stimulus and the background on the monitor screen to establish a clear relationship between the retinal image contrast and the hyperacuity thresholds. The contrast formula is given below:

$$\text{Contrast } (C) = \frac{(L_{\text{stim}} - L_{\text{surr}})}{(L_{\text{stim}} + L_{\text{surr}})}$$

L_{stim} is the stimulus's luminance, and L_{surr} is that of the surrounding background. Depending on the direction sign of the difference, this definition of contrast predicts values between 1.0 and -1.0. ($L_{\text{stim}} - L_{\text{surr}}$). VeT are about 4-5 arcseconds for contrasts of 0.22 and above, but they exponentially increase (lose sensitivity) as contrast decreases, according to this study¹⁷⁵. Contrast polarity is a property of visual stimulus. It can be classified into two types: positive stimuli contrast has a black stimulus on white background, whereas negative stimuli contrast has a white stimulus with a black background. I planned to assess the effect of positive and negative stimuli contrast on the Vernier acuity thresholds to identify the optimum contrast for Vernier acuity testing.

2.6 Method

2.6.1 Study Subjects

In this pilot study, I planned to perform the test on five healthy adult volunteers between 20-30 years of age. Volunteers with no history of significant medical conditions, any eye diseases or surgery, and who underwent a comprehensive eye examination in the past six months were included. Refractive errors of less than ± 3.00 Diopters sphere and less than 2 Diopters of an astigmatic cylinder with the best-corrected Snellen Visual acuity of 20/20 or better were recruited. Informed consent was acquired

from all the volunteers. The obtained demographic information included name, age, and gender. All the volunteers were naïve to the experimental procedure and Vernier acuity testing.

2.6.2 Experimental Setup

All experiments in this study were performed in the Theoretical and Experimental Epistemology Lab (TEEL), School of Optometry and Vision Science, University of Waterloo. The experimental setup consisted of a long desk with attached chin rest, a keyboard, and a height-adjustable chair on one end. While on the other end of the table had a computer monitor screen positioned at a viewing distance of 171 centimeters. The height-adjustable chin rest was used to avoid the subject's face tilt and support posture, whereas the height-adjustable chair was used to improve seating comfort. A flat LCD Acer® monitor of size 21.5 inches wide (12 height x 20 widths in inches) with a resolution of 1920×1080 was used along with a desktop system with Windows-10 Education, a 64-bit operating system with an Intel® Core™ i7-6700 CPU with clock speed up to 3.40 GHz. This system was supported with 16 Gigabytes of RAM and 2 Gigabytes of Nvidia graphics memory. The experiment was performed under low light conditions. The luminance was adjusted to 100 cd/m², the contrast was set to 1.0 using a digital spectrophotometer, and the screen brightness was adjusted to 50 percent.

2.6.3 Stimuli Configuration

The experimental stimuli characteristics were calibrated in visual angle units. A line stimulus subtended 5×10 (width x height) in arcminutes, whereas a dot stimulus subtended 5×5 in arcminutes. A positive stimuli contrast stimulus had a black stimulus with white background, whereas a negative stimuli contrast had a white stimulus with black background. Both stimuli were presented in synchronized order at every presentation of the testing.

2.6.4 Gap Sizes

The literature shows that the Vernier acuity thresholds are directly proportional to the gap sizes, implying that thresholds are higher (poor) when the separation between stimuli increases. To verify the gap-related Vernier acuity characteristics as reported in the previous literature, I planned to measure Vernier measurements at seven gap sizes starting from 128 arcminutes until 2 arcminutes in log units [128, 64, 32, 16, 8, 4, 2]

2.6.5 Experiment Testing

The experimental testing involved a short learning session at the beginning of the experimentation to ensure the subject was familiar with the instructions and procedure. I used a chin rest to stabilize the head posture and support posture. The testing was performed monocularly in the best eye (dominant) only while the fellow eye was patched. Short breaks were introduced after each gap size to allow stretching and relaxation. The testing was performed in March 2020, a week before the COVID-19 pandemic lockdown. All the testing was conducted during the working hours of weekdays only.

At each gap size, the thresholds were measured at least three times from one hundred stimuli presentations or trials, referred to as reversals. Once the threshold is achieved, the stimuli reposition a step backward, and the test is repeated until the set number of reversals is measured. The start position was set at 1 Degree (3600 arcseconds) off the vertical alignment presented on either the left or right-hand side randomly at the beginning of each trial. The step size of the stimuli was formulated into a slope of a line equation in log units that precisely allows the stimuli to move closer to the vertical alignment but will not reach the point of absolute alignment. The log step size regulates the position of the stimuli. For example, If the stimuli are close to the vertical alignment, the step size is smaller when compared with the step size when the stimuli are farther away from the vertical alignment. This will allow the stimuli position to move close to the vertical alignment and detect the best possible misalignment position visually perceived as aligned.

2.7 Data Analysis

The statistical analysis was performed using GraphPad Prism, version 8.0.1 software (GraphPad Software, Dotmatics, San Diego, California, USA, www.graphpad.com). The Shapiro-Wilk test was performed to estimate the Gaussian distribution of the data (normality) with the alpha value set at 0.05. The values are presented as mean \pm standard deviation and mean difference. A non-parametric test was performed for a data distribution that was not normal. A paired t-test was performed to compare the differences in VeT with a statistical significance (p-value) of less than 0.05. The parametric data were analyzed using a Mann-Whitney U test to estimate the statistical difference between VeT.

2.7.1 Data Interpretation

The precision is the standard deviation of the positions where the aligned response is registered. This thesis refers to it as the ‘Vernier threshold,’ whereas the mean offset error is the Vernier accuracy. The

lowest value of the Vernier threshold means high Vernier sensitivity, and the highest value means low Vernier sensitivity.

2.8 Results

This study was performed on five healthy adult volunteers (4 males and one female) aged 20-30 years (Mean \pm SD, 24.4 \pm 1.1 years). All participants had undergone comprehensive eye examinations within six months of this testing. All the participants had a dominant right eye, with two participants having mild compound myopic astigmatism (< -2.0 Diopter with < -1.0 Cylinder), and rest three were simple hyperopes ($< +0.50$ Diopter). All participants had best-corrected visual acuity of 20/15 with habitual refractive spectacle correction.

2.8.1 Experiment-1: Software Program Testing (Positive Contrast)

The primary objective of this experiment was to develop a software application program that can quantitatively measure the Vernier acuity thresholds across gap sizes using 3D-1U ASM along with the 3-AFC technique to collect responses accurately. The secondary objective was to confirm the finding reported in the literature related to the sensitivity of stimuli shapes (line and dot) on vernier acuity across the gaps.

2.8.1.1 Results

This experiment was performed on a participant (Male) to assess the initial software functionality and compare the outcomes of line and dot stimuli for testing Vernier acuity. The Vernier acuity thresholds measured using line and dot stimuli were plotted against the gap sizes as shown in figure 2-9 to identify the optimum stimuli shape. The thresholds recorded using both stimulus shapes followed similar trends across all the gap sizes with relatively higher variations at 2 and 32 arcminutes of gaps. Both stimulus shapes had the lowest threshold of 6 arcseconds at 4 arcminutes. However, at two arcminutes, the thresholds recorded using dot stimuli were comparably double to those measured with line stimuli. In addition, the thresholds recorded using dot stimuli were relatively higher at most of the gap sizes.

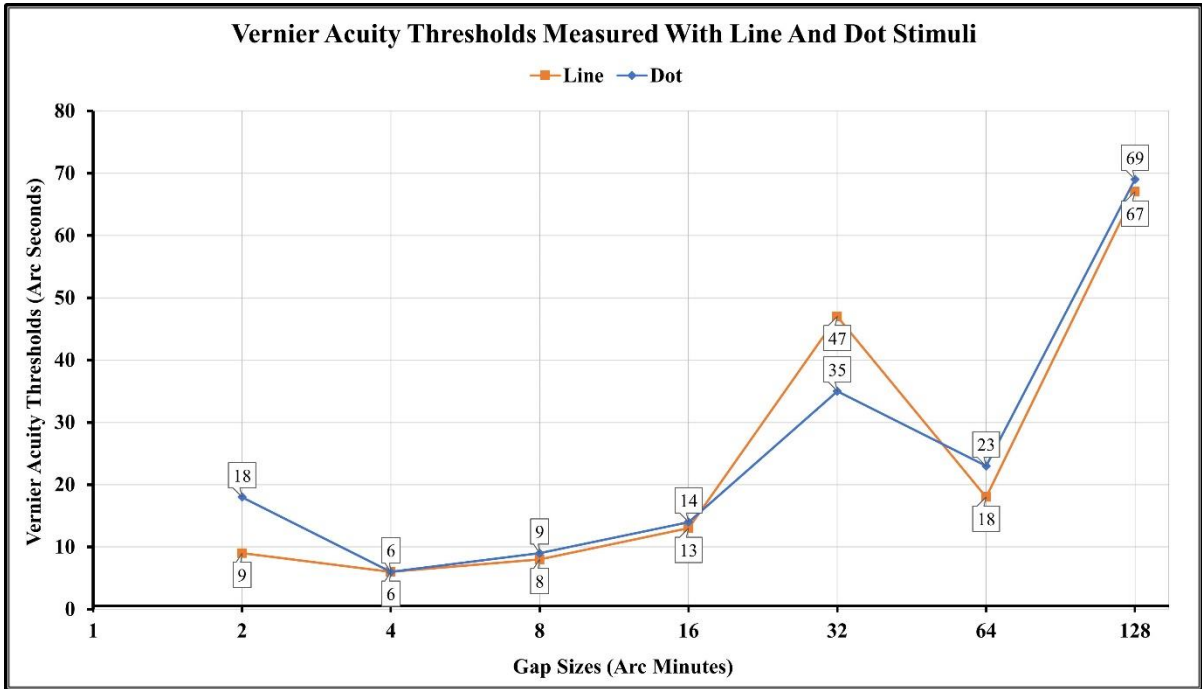


Figure 2-9 VeT using line and dot stimuli across gap sizes.

2.8.2 Experiment-2: Method Validation

This experiment aimed to assess the Vernier acuity thresholds using a positive contrast line stimulus (as line stimuli are observed to perform better in experiment 1) across gap sizes on a small group of volunteers, including 3 Males and 2 Females (n=5).

2.8.2.1 Results

The VeT obtained from all five participants (P1, P2, P3, P4, and P5) were plotted against the gap sizes shown in the figure to assess the method. P4 recorded the lowest threshold of 2 arcseconds at 2 arcminutes of gap size, whereas P1 recorded the highest threshold of 104 arcseconds at 2 arcminutes of gap size.

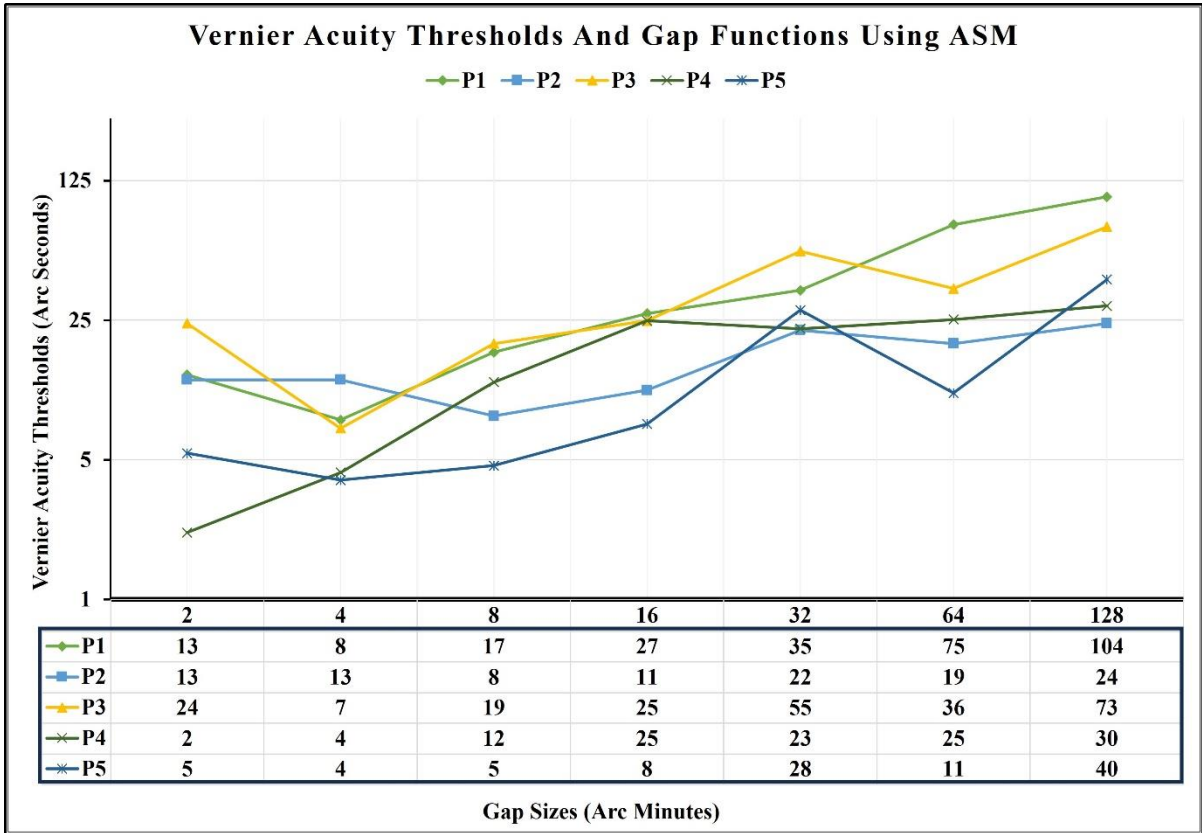


Figure 2-10 Graphical representation of individual participant Vernier acuity thresholds at all gaps.

The mean Vernier acuity thresholds were estimated and plotted against gap sizes, as shown in figure 2-11 to establish the relationship between VeT and gap functions. The highest mean Vernier threshold of 54 arcseconds was measured at the maximum gap size of 128 arcminutes, whereas the lowest mean Vernier threshold of 7 was measured at 4 arcminutes. While the mean VeT measured at 2 arcminutes was relatively higher (almost double), the thresholds measured at 4 arcminutes. The mean thresholds measured at 32 and 64 gap sizes were the same.

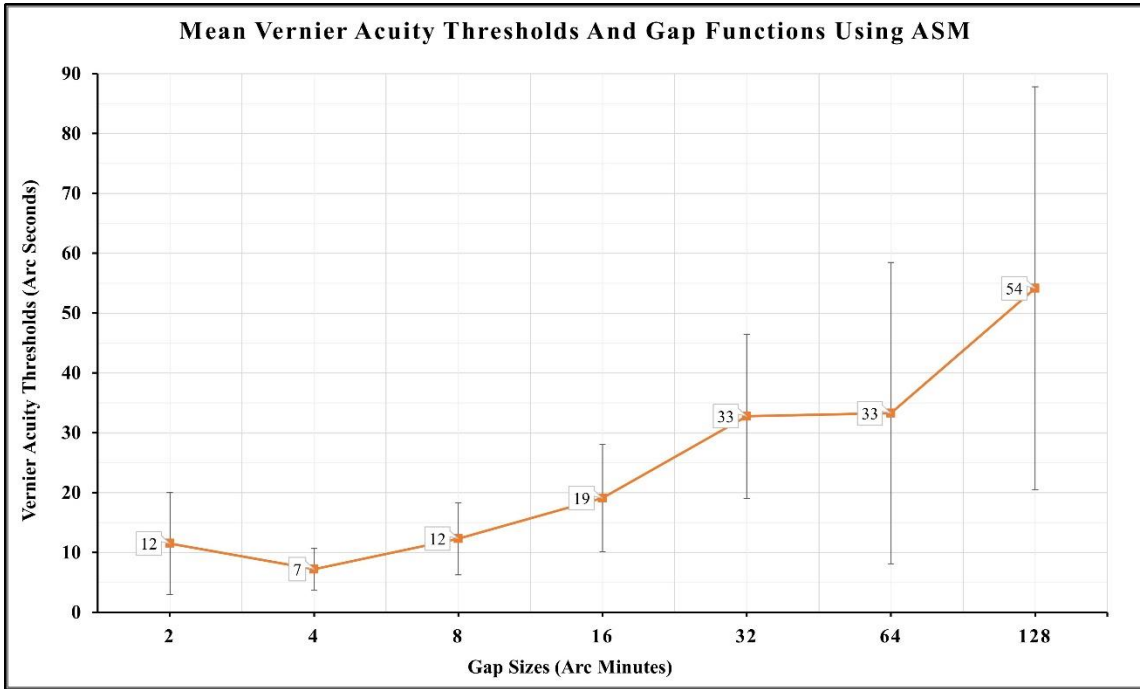


Figure 2-11 Graphical representation of mean Vernier acuity thresholds and gap functions using a positive contrast line stimulus.

The graphical representation of an adaptive staircase method from a participant's responses was plotted to demonstrate the experimental flow of the responses throughout the testing. The blue dots represent correct response, while the black dot represent incorrect response and red dots represent aligned responses.

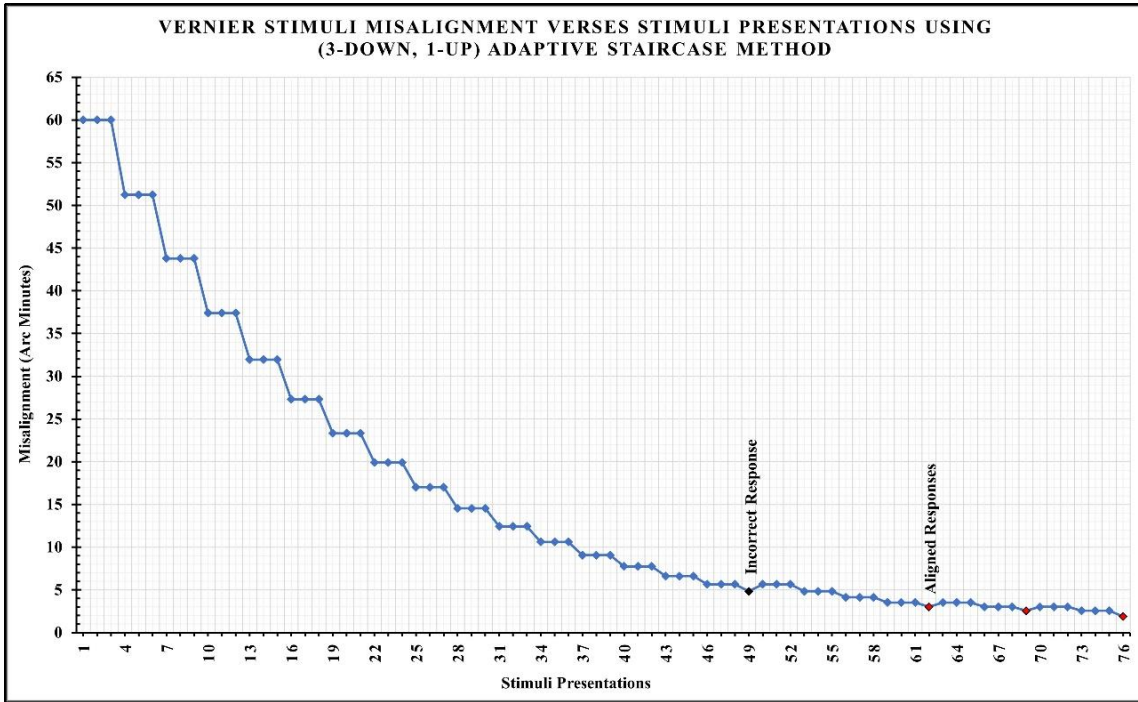


Figure 2-12 Graphical representation of misalignment versus stimuli presentation using 3-Down 1-Up adaptive staircase method.

2.8.3 Experiment-3: Stimuli Contrast Comparison (Positive vs. Negative)

This experiment aimed to measure Vernier acuity thresholds using negative contrast line stimuli and compare them with positive contrast line stimuli to identify the optimum contrast for testing Vernier acuity.

2.8.3.1 Results

The mean VeT for the positive and negative contrast stimuli were estimated and plotted against the gap sizes, and the mean VeT for the positive contrast stimuli were measured in experiment 2. This comparison was drawn to identify the optimum stimuli contrast, as shown in the figure. The thresholds recorded using positive contrast stimuli were comparably higher at most gap sizes than negative contrast stimuli. The mean thresholds measured using negative contrast stimulus had relatively similar trends but only at 64, 16, 8, and 4 gap sizes. The lowest mean threshold measured using positive contrast stimuli was 7 arcseconds at 4 arcminutes, whereas the lowest mean threshold measured using negative contrast stimuli was 5 arcseconds at 2 arcminutes. The mean VeT measured using negative contrast

were lower at 128, 64, 32, 8, and 2, equal at 4, and higher at 16 arcminutes of gap size. Compared with positive contrast stimuli, the thresholds measured using negative contrast stimuli were significantly lower at 32 gap size with a p-value < 0.05, as shown in the table.

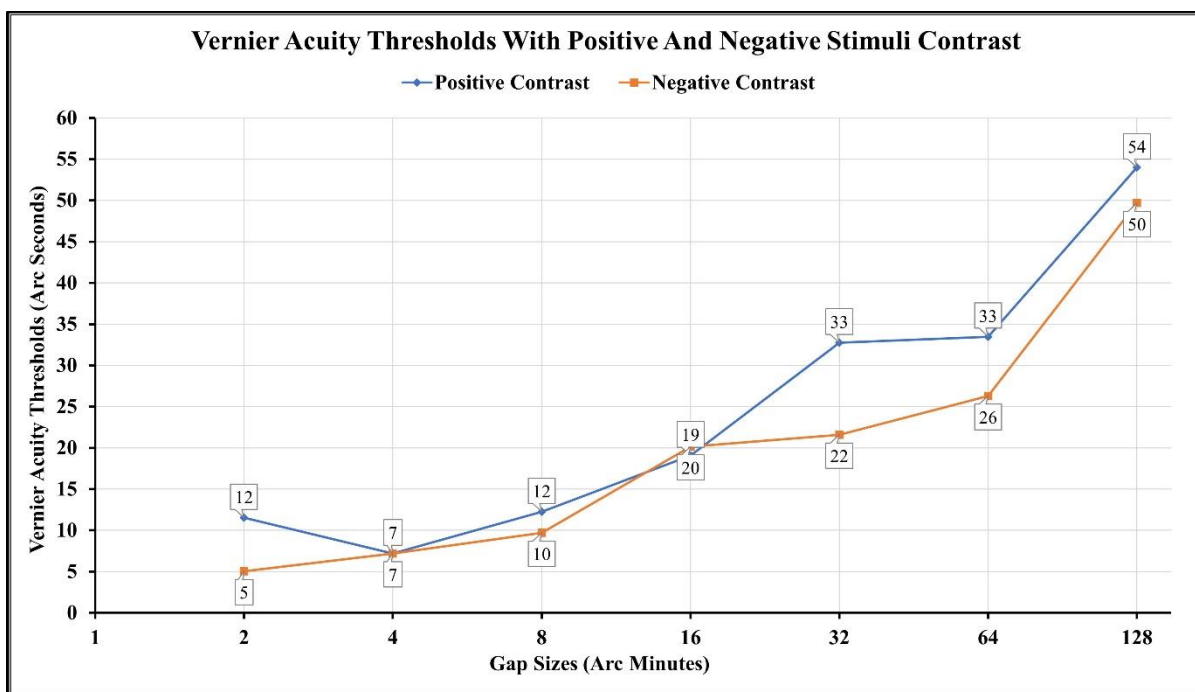


Figure 2-12-3 Graphical representation of mean VeT from positive and negative contrast line stimuli.

Table 2-1 Mean VeT using positive and negative contrast, mean difference, and p-values at all gap sizes.

Gap size (Arcminutes)	Mean Positive Contrast (Arcseconds)	Mean Negative Contrast (Arcseconds)	Mean difference	P-value (<0.05)
128	54	50	-4	0.33
64	33	26	-7	0.23
32	33	22	-11	0.02*
16	19	20	1	0.40
8	12	10	-2	0.19
4	7	7	0	0.47
2	12	5	-7	0.10

2.9 Discussion

In this study, a sophisticated software application program was developed and tested that combines a 3D-1U ASM and 3-AFC approach to quantitatively measure the Vernier acuity thresholds across gap sizes. The software was initially tested using line and dot stimuli, and I observed that line stimuli were relatively sensitive to VeT. The lowest threshold (highest precision) for the VeT estimated using an adaptive staircase method was 2 arcseconds, validating the test's efficiency. The VeT ranged between 1 to 105 arcseconds across the gap sizes, which is relatively sensitive compared to those reported by Lakshminarayanan et al.¹⁴⁵ for similar age groups with thresholds ranging between 20 to 150 arcseconds. However, the difference in VeT between our study and those of Lakshminarayanan et al. could be due to methodology, technical details, and sample size.

I tested the adaptive staircase method using a positive contrast stimulus across gap sizes in the following experiment. The mean lowest Vernier threshold was below 10 arc seconds at 4 gap size, and the highest threshold was below 60 arc seconds or less than the resolution limit at the 128-gap size. The results achieved using 3D-1U ASM were comparatively more than two times more sensitive than the methods used previously in the literature. However, the results from this study might be influenced by the optical magnification for the spectacle correction or the refractive error itself. Although the results are strong and encouraging, further validation with a larger sample size of emmetropic participants is required before reaching any firm conclusions.

Cornsweet¹⁰⁷ in the formulation of the staircase method, emphasized that the method should be changed throughout the experiment. For instance, the steps in the initial stage of dark adaptation should be large, and the final stage should be significantly smaller if the procedure were used to find the absolute, visual, and intensive threshold. It would be ideal from the perspective of careful experimental design for the first stimulus in each staircase to be at the same intensity level. As a result, the starting and final levels in both series would be quite different. To follow his recommendation, I formulated the step size into a slope of a line equation. He also emphasized the staircase method is extremely efficient. It requires the presentation of fewer stimuli than any other psychophysical method for a given reliability of a computed threshold value. This is because, once the first few stimuli are out of the way, all other stimuli are very close to the threshold level, each contributing significantly to the final computed threshold value. Though it resembles the method of limits, the adaptive staircase method is immune to the characteristics of the method- hysteresis^{103,104}.

The three alternatives forced choice (3AFC) technique is known to collect the responses with minimal bias and improved accuracy. This method involves 79% of psychometric function^{18,105}. A lower Vernier threshold indicates better Vernier acuity. For instance, the observer may be asked to indicate whether the adjustable stimuli are offset to the left or the right to the reference stimuli or whether they both are previewed as aligned. It reduces the chance of guessing by dividing the stimuli presentation response into multiple options compared to 2AFC, where the response is divided between two options (yes or no/ 1 or 2), having a 50% guessing effect on the thresholds.

Similarly, the 4AFC technique may offer multiple options at each presentation. However, too many options pose a risk of confusion, and it takes time to decide. An ongoing trial during the experiment may cause stress to the participants, leading to incorrect responses to the presentation.

The last experiment involved estimating VeT using negative contrast stimuli, and the results indicated that VeT were relatively better at most of the gap sizes. Therefore, I assessed the method repeatability using negative contrast line stimuli in the following pilot study (Chapter 3). However, I noticed a few areas of improvement that can be adjusted to achieve thresholds efficiently. In the following study, I enhanced and tested the method on emmetropic participants to achieve optimum precision, responses, time, and repeatability (Chapter 3).

2.10 Conclusion

I developed and validated a software application program that quantitatively measures the Vernier acuity thresholds using an adaptive staircase method, efficient technique, and modern technology. In addition, I standardized ideal stimuli characteristics, including shape and contrast, for testing Vernier acuity. The estimated results are precise and consistent with the previously reported values. Thus, motivating us to further advance the test methods for evaluating. However, the test performance analysis of this study indicated a few adjustments that can improve the test efficiency. I made those adjustments in the following pilot testing study to further validate the VAT program.

Chapter 3

Vernier Acuity Test

3.1 Introduction

Though many studies reported in the literature describe the clinical importance of Vernier acuity, these studies only focused on method application, results interpretations, and possible future directions. It is also observed from the literature that these studies lack the other most critical clinical qualities, such as method repeatability, reliability, and measurement time. Despite having enormous potential to be utilized in clinics as a screening tool, Vernier acuity has remained an experimental tool for laboratory settings. A few major issues raised in the literature include methodology challenges, difficulty to access testing-facilitating equipment and lack of understanding related to Vernier acuity in the clinical community^{13,112}. A study by Li et al. in 2012 reported that measuring the effect of positional noise on VeT using a staircase method in elderly subjects took 60-90 minutes to record 400 responses¹²⁹. Studies in the literature reported a quantitative range of VeT varying between 20 to 200 arcseconds when measured between 4 to 128 arcminutes of stimuli¹⁴⁶. However, these thresholds were determined by various psychophysical procedures and techniques that may have a substantial amount of variability, sensitivity, and testing time.

Program Modifications: As discussed in Chapter 2, experimental results from pilot study 1 of program validation provided insights into program performance and identified the optimum stimuli configuration. In pilot study 2 of program validation, I used the insight obtained from pilot study 1 of testing. I improved the methodology to further advance the program, particularly to achieve better sensitivity and more time efficiency. The program modifications are listed below:

- **Stimuli Size:** I adjusted the stimuli dimensions to 3 x 30 arcminutes (width and height); the line stimuli size was optimized to achieve better thresholds.
- **Reversals:** Increasing the number of reversals from 3 to 5 for more robust results and facilitating five reversals.
- **Presentations:** I extended the stimuli presentations from 100 to 200 at each gap
- **Steps:** I adjusted the staircase for the reversal's response to stimuli, moving 3 steps backward or away at each reversal.

I developed a software application to test Vernier acuity and tested it for stimuli shape and contrast using an adaptive staircase method described in the previous chapter. In this chapter, I describe the enhanced method and assess the performance and repeatability of the VeT on emmetrope individuals.

3.1.1 Impact of Covid-19 on this Research

Initially, this research study was planned to achieve thesis objectives that included the development of a software program using an advanced method to measure Vernier acuity, followed by clinical testing for validation. A month before the pandemic, the VAT program was first assessed for precision, gap functions, and ideal stimuli configuration in the laboratory through a small pilot study (pilot study 1). The program achieved promising results and motivated further testing. However, due to the COVID-19 restrictions, I could not perform the clinical testing of this program for validation. Consequently, I limited program testing to the laboratory for technical validation and assessed performance through the subject's response accuracy and response reaction time. In addition, I further classified the VAT results into age and gender groups to verify similarities and differences. Alternatively, I planned to extend the hyper-acuity paradigms by developing two additional software programs, HP and MMP, and testing them with the VAT program.

3.1.2 Post-Pandemic Research Precautions

Due to pandemic reasons, I set flexible inclusion criteria of unaided vision of 20/20 or better to recruit more participants. The experiments were performed according to the safety standards provided by the University of Waterloo. The room occupancy was limited to 2 persons in each laboratory room with at least 2 meters of social distancing. After testing each participant, the laboratory room was disinfected with 70% alcohol disinfectant spray, and the point of contact surfaces were thoroughly disinfected using alcohol-based disinfection wipes. Both examiner and participants had their nose and mouth covered using an N95 face mask during the testing.

3.1.3 Technical Validation

I tested the VAT program in pilot studies; the first pilot study of testing (pilot study 1) involved a series of experiments primarily focused on evaluating the program's performance and precision. Secondly, to verify the ideal stimuli shape and contrast for stimuli standardization. Results from pilot study 1 allowed us to make method enhancements by identifying methodological and technological issues affecting the efficiency of the test performance. In addition, it helped in estimating the ideal stimuli

characteristics for standardization. In this pilot study 2, the standardized stimuli configuration and enhanced program were used to estimate Vernier acuity thresholds, response accuracy, reaction time, testing time, and repeatability. The testing was performed on both eyes individually; results from individual eyes were assessed for repeatability and compared between eyes at each visit for symmetry. The correlation between the repeated measurements was estimated to verify the result's consistency for reliability. The programs that can produce consistent results were considered for technical validation. In addition, the results obtained from each program can serve as baseline data for future comparisons. A discrepancy between the measurement and prediction implies the presence of a possible retinal/neural dysfunction. In addition, I further classified the results into age and gender groups to verify similarities and differences. This chapter will briefly discuss the pilot study-2 testing of the VAT program.

3.1.4 Factors Affecting Vernier Acuity

3.1.4.1 Symmetry between eyes

Though structural symmetry is observed between the eyes, functional differences may co-exist. Evidence in the literature suggests the presence of functional asymmetry due to wavefront alteration of the eye⁹⁰.

3.1.4.2 Age

Vernier acuity is among the six visual functions resistant to age-related changes¹⁴⁷. Studies discussed the relationship between aging and VeT, and findings showed that Vernier alignment hyperacuity thresholds are not sensitive to age. It has been proposed that hyperacuity (Vernier) thresholds could be used as a benchmark for aging studies and suggest that this measurement can serve as a valuable control and reference for other clinical studies of aging^{145,146,168}. Therefore, I assessed the Vernier acuity thresholds in different age groups and documented the range of thresholds for clinical reference.

3.1.4.3 Gender Differences

In general, most visual functions are similar in males and females. However, certain visual aspects, such as motion perception, may have high variance between males and females⁹⁰. Therefore, I assessed the Vernier differences between males and females.

3.1.5 Reproducibility

In preclinic research, many factors can contribute to irreproducibility. A few common errors include the study design, poor testing material, and inconsistencies in testing protocols. The faulty initial pre-clinic research can lead to the wastage of resources and cost economically¹⁷⁶. Therefore, pre-clinic research must be detailed and thorough to achieve reproducible results. From the literature, I noticed that Vernier acuity is uncommonly used in clinical practice due to several reasons mentioned in the lacunae section, and one such reason is that the clinical community does not understand it well. Though its clinical utility has been suggested in the literature, including for screening various eye conditions and its potential to assess outcome measures in clinical trials of emerging neuro-ophthalmic treatments. The variability concerns of the VeT did not allow it for clinical screening. A recent review paper published in 2021 on the clinical use of Vernier acuity by Monica L. Hu et al.⁵⁸ recommended seven key features for a psychophysical method to achieve the most reproducible results. They are listed below:

1. Application of software programs, including PsychoPy, with optimized staircase paradigms.
2. Testing without crowding markers.
3. For optimum Vernier acuity thresholds, measure it using 4 arcminutes of gap size.
4. Stimuli are to be presented synchronously.
5. Stimuli are to be presented in horizontal and vertical directions rather than oblique directions.
6. Use high contrast levels of over 90%
7. Test monocularly while the fellow eye is patched with a dark occluder to avoid binocular interference.

I incorporated all the suggestions to achieve reproducible Vernier acuity testing.

In this study, I plan to assess test performance through response accuracy, reaction time, testing time, and repeatability of VeT. Additionally, I classified the Vernier acuity measurements into eyes, age, and gender to assess variation and repeatability.

3.2 Method

3.2.1 Program Modification

From pilot study 1, I noticed that 100 stimulus presentations at each gap size are adequate to achieve three reversals. An adequate number of stimuli presentations are necessary to achieve the desired number of reversals. A minimum of three reversals are enough to obtain the precision. However, in this study, I estimated 5 reversals from 200 stimulus presentations at each gap size to improve the precision instead of 3 reversals from 100 stimulus presentations. In addition to that, I reduced the viewing distance from 172 centimeters to 100 centimeters for better screen viewing and field of vision coverage. To detect such a degree of misalignment, I planned to shrink the line stimuli to a standard size optimum enough to detect the subtle difference. The stimuli dimensions were adjusted to 30 x 3 arcminutes from 10 x 5 arcminutes to make it appear lean and long, as suggested in the literature. The software application calculated the experimental and stimuli inputs and maintained the required visual angle of the experimental characteristics for a given viewing distance. The experimental setup and testing were like pilot study 1 of program testing. Both the stimuli were presented synchronously, and a delay of 0.3 seconds was introduced between each stimuli presentation to minimize the error that can occur due to continuous stimuli presentation on the screen.

3.2.2 Study Subjects

This study was planned to include twenty participants. The obtained demographic information included name, age, and gender. Because of the pandemic, I had slightly flexible inclusion criteria for emmetropes (unaided vision of 20/20 or better) using a LogMAR ETDRS chart (calibrated for 3 meters) to recruit maximum participants. The participants were included in this study based on the following inclusion criteria: healthy emmetropic adults between the age of 19-41 years with no history of any ocular or systemic health problem and no history of any ocular surgery or currently on any medication for any systemic conditions. All the volunteers were naïve to the experimental procedure and Vernier acuity testing. These experiments were conducted from November to December 2022. The testing order was randomized between right and left eyes to minimize the learning effect and to minimize the experimentation bias the order of the testing between the three experiments were randomized. In appreciation of time and interest in participating in the Pilot study-2 experiments of the Vernier acuity study, the participants were paid \$20 through the COETF research fund.

3.2.3 Experimental Setup

All experiments in this study were performed in the Theoretical and Experimental Epistemology Lab (TEEL), School of Optometry and Vision Science, University of Waterloo. The experimental setup consisted of a long desk with attached chin rest, a keyboard, and a height-adjustable chair on one end. While on the other end of the table had a computer monitor screen positioned at a viewing distance of 100 centimeters. The height-adjustable chin rest was used to avoid the subject's face tilt and support posture, whereas the height-adjustable chair was used to improve seating comfort. A flat LCD Acer® monitor of size 21.5 inches wide (12 height x 20 widths in inches) with a resolution of 1920×1080 was used along with a desktop system with Windows-10 Education, a 64-bit operating system with an Intel® Core™ i7-6700 CPU with clock speed up to 3.40 GHz. This system was supported with 16 Gigabytes of RAM and 2 Gigabytes of Nvidia graphics memory. The experiment was performed under low light conditions. The luminance was adjusted to 100 cd/m², the contrast was set to 1.0 using a digital spectrophotometer, and the screen brightness was adjusted to 50 percent.

3.3 Data Acquisition

To support the VAT program technical validation metrics, I estimated the program performance using the parameters that are listed below:

1. **VeT:** Vernier Acuity thresholds were measured at various gap sizes to assess the ideal gap size.
2. **Response Accuracy:** The subject responses were assessed for each stimuli presentation at each gap size to estimate the subject attention throughout the Vernier acuity testing. The response accuracy was calculated in percentages for three types of responses: correct, incorrect, and aligned response. (response/total response x 100)
3. **Reaction Time:** The time interval between stimuli presentation and subject response (correct/incorrect/aligned) at each gap size. A sum of all three (correct/incorrect/aligned) response times constitutes a gap size time or the time taken to measure the Vernier acuity at a particular gap size. The time taken at all gap sizes collectively provides a total test time.
4. **Test Time:** Is an important parameter that will help to identify the ideal time efficient gap size based on the Vernier threshold's precision.

3.3.1 Data Categorization

The collected data were categorized into three groups and assessed for thresholds and repeatability.

1. VeT and Eyes; (Right eye versus left eye) 21 Right and Left eyes = total 42 eyes
2. VeT and Ages; (≤ 30 years verses > 30 years) 14 participants (28 eyes) ≤ 30 years and 7 participants (14 eyes) >30 years of age
3. VeT and Gender; (Females versus Males) 10 Males (20 eyes) and 11 Females (22 eyes)

3.3.2 Repeatability

It is very important for a clinical screening test to produce repeatable measurements and to be considered reliable for clinical testing. The Vernier program testing was repeated at least a 6 to 8 days of time interval to assess the repeatability. The mean difference between the VeT measured at visits 1 and 2 was assessed to estimate the leaning effect.

3.3.3 Data Analysis

The statistical analysis was performed using GraphPad Prism, version 8.0.1 (Dotmatics, San Diego, USA). The Shapiro-Wilk test was performed to assess the Gaussian distribution of the data (normality) with the alpha value set at 0.05. The paired t-test was conducted to estimate the statistical difference between the VeT between the visits, and the appropriate test was selected based on the normality test. A non-parametric test was performed for a data distribution that was not normal. The mean, standard deviation, and mean difference are provided, along with the p-value indicating the statistical significance. Repeatability refers to the strength of agreement between repeated measurements obtained under similar circumstances. Interclass correlation (ICC) analysis was performed to determine the strength of linear association or reliability or similarity between measurements from both visits. ICC values can range from 0 to 1, with higher values indicating greater reliability or agreement and lower value indicating no reliability or the measurements are entirely inconsistent or random.

- **0 < ICC < 0.2:** There is slight or poor agreement. The measurements have low reliability, and there is a significant amount of variability.
- **0.2 \leq ICC < 0.4:** There is fair agreement. While there is some reliability, the measurements still have notable variability.

- **0.4 ≤ ICC < 0.6:** There is moderate agreement. The measurements are moderately reliable and show a fair degree of consistency.
- **0.6 ≤ ICC < 0.8:** There is substantial agreement. The measurements have a high level of reliability and demonstrate strong consistency.
- **0.8 ≤ ICC ≤ 1:** There is almost perfect agreement. The measurements are highly reliable, with minimal variability or inconsistency.

The focus of this study was to achieve ICC values between 0.4 and 1 at least.

3.3.4 Data Interpretation

The standard deviation of the mean aligned position is the Vernier acuity threshold. The lower threshold value implies good precision and vice versa.

3.4 Results

A total of twenty-one healthy (n = 21) adult emmetropic participants (10 males, 11 females) aged ranging between 20-39 years (Mean ± SD, 28.7 ± 4.6 years) met the eligibility for this study. The monocularly unaided visual acuity for the right and left eye was -0.10 ± 0.06 (Mean ± SD). The mean and SD of ≤ 30 below age group was 26 ± 2.5 years, whereas >30 age group was 34 ± 2.4 years.

3.4.1 Vernier Acuity Repeatability (Eyes)

3.4.1.1 Right Eyes

The mean VeT estimated with right and left eyes were plotted against the gap sizes for visits 1 and 2, as shown in Figures 3-1 and 3-2.

At Visit 1, the lowest mean Vernier acuity threshold measured with the right eyes was 14 arcseconds at 2 arcminutes, and the highest was 55 arcseconds at 128 arcminutes. The Vernier acuity was observed to deteriorate gradually as the gap between the stimulus increased.

At Visit 2, the lowest Vernier threshold recorded with right eyes was 17 arcseconds at 2 arcminutes, and the highest was 61 arcseconds at 128 arcminutes. The Vernier acuity was observed to deteriorate gradually as the gap between the stimulus increased. However, the Vernier acuity was relatively similar at the initial smallest gap sizes, including 2 and 4 arcminutes.

The mean VeT measured with the right eye at visits 1 and 2 were plotted against the gap sizes, as shown in figure 3-1 to assess the repeatability. The right eye VeT measured at visit 2 were relatively higher than visit 1 across the gap sizes. However, thresholds were statistically significant ($p < 0.05$) only at 32 and 64 arcminutes of gap sizes.

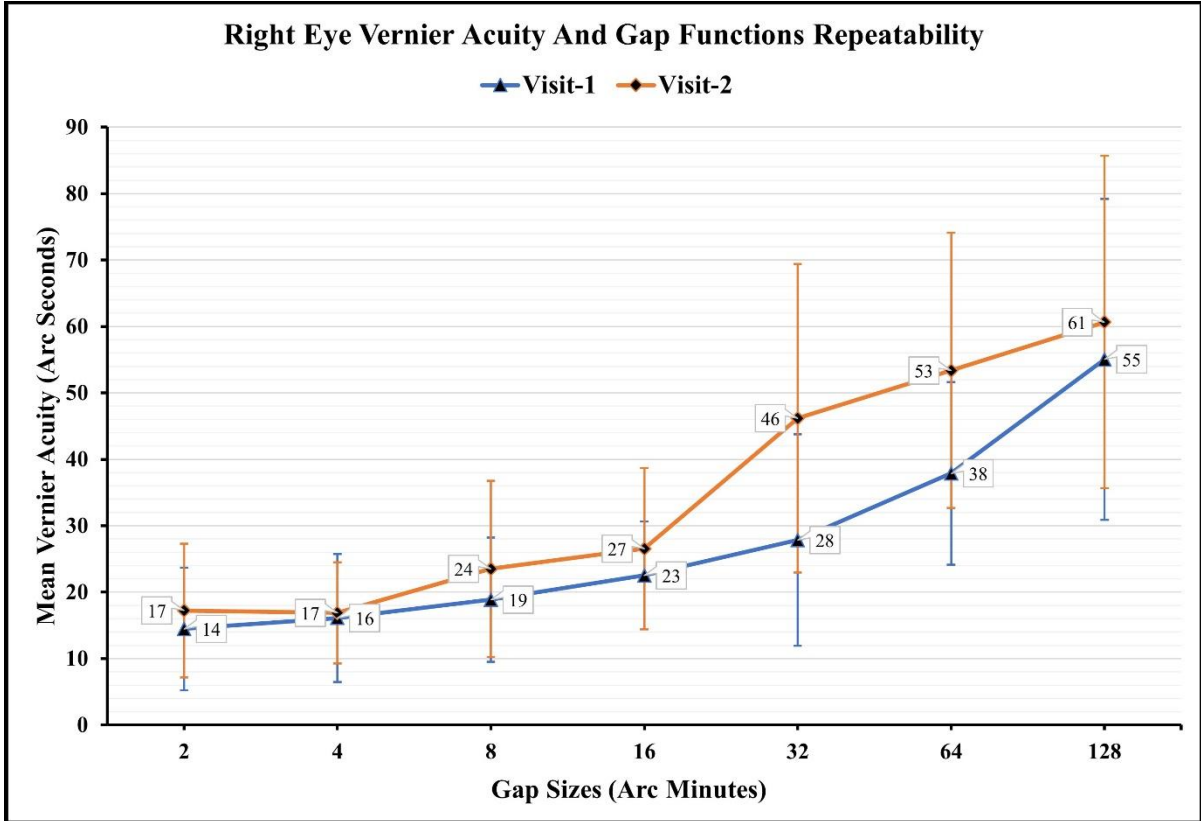


Figure 3-1 Repeatability of the Vernier acuity thresholds measured with right at both visits were plotted against gap sizes.

Table 3-1 Repeatability of Vernier acuity thresholds measured with right eyes at visits 1 and 2, mean difference and statistical significance are provided in the table below.

Right Eyes Mean Vernier Acuity Repeatability					
Gap Sizes (Arc Minutes)	Visit-1	Visit-2	Mean Difference	p-value (<0.05)	ICC
	Mean ± SD (Arc Seconds)	Mean ± SD (Arc Seconds)			
128	55 ± 24	61 ± 25	6	0.43	0.14
64	38 ± 14	53 ± 21	15	0.001*	0.28
32	28 ± 16	46 ± 23	18	0.01*	-0.03
16	23 ± 80	27 ± 12	4	0.19	0.12
8	19 ± 90	24 ± 13	5	0.25	0.02
4	16 ± 10	17 ± 80	1	0.77	0.02
2	14 ± 90	17 ± 10	3	0.47	-0.15

3.4.1.2 Left Eyes

At Visit 1, the lowest mean Vernier acuity threshold measured with the left eye was 19 arcseconds at 2 and 4 arcminutes, and the highest was 49 arcseconds at 64 arcminutes. Thresholds gradually increased with increasing gap sizes except at 4 and 64 arcminutes.

At Visit 2, the lowest mean Vernier acuity threshold measured with the left eye was 17 arcseconds at 2, and the highest was 64 arcseconds at 128 arcminutes. The Vernier acuity was observed to deteriorate gradually as the gap between the stimulus increased.

The mean VeT measured with the left eye at visits 1 and 2 were plotted against the gap sizes, as shown in the figure to assess the repeatability. The left eye VeT measured at visit 2 were relatively higher at 8, 16, 32, and 128 arcminutes, equal at 4 arcminutes, and lower at 2 arcminutes of gap sizes. However, the thresholds were statistically significant only at 128 arcminutes of gap size ($p < 0.05$). Except at 64 gap size, all the gap sizes had poor ICC.

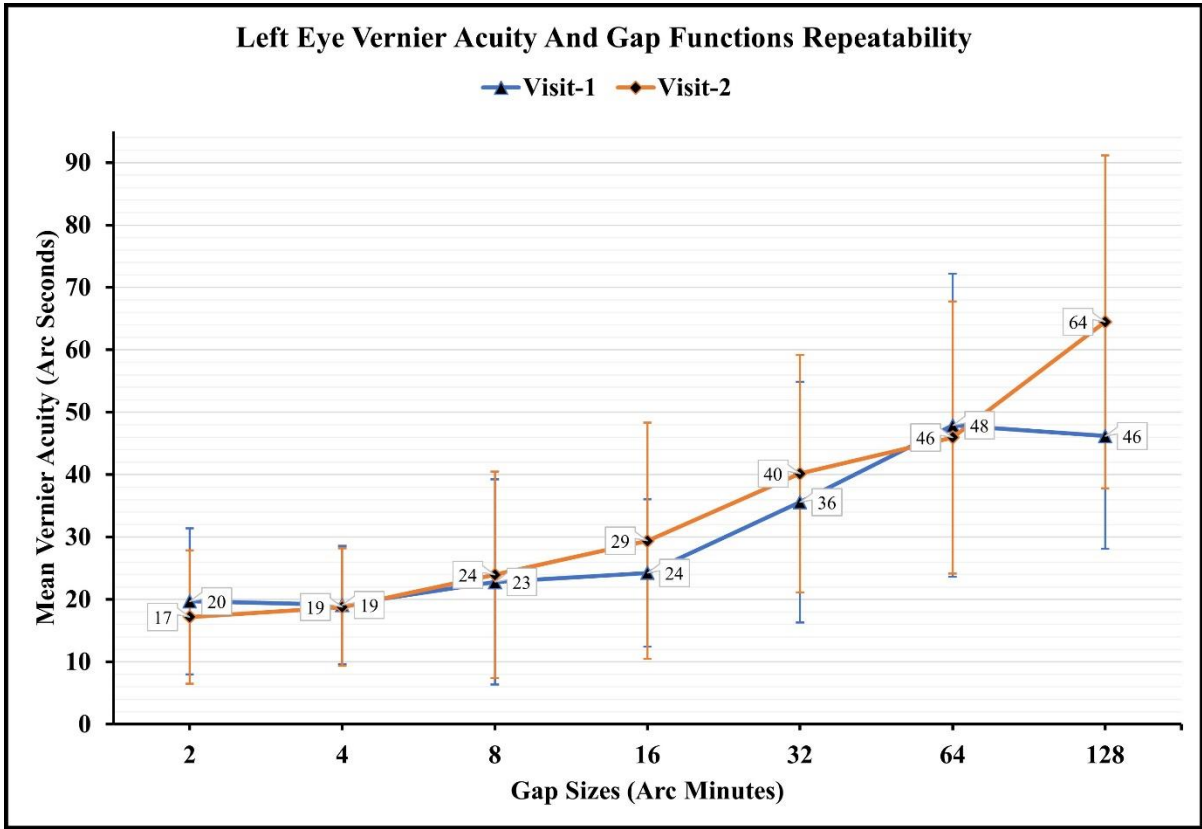


Figure 3-2 Mean VeT measured with the left eye at visits 1 and 2 were plotted against gap sizes.

Table 3-2 Mean VeT measured with left eye at visits 1 and 2, mean difference, and statistical significance.

Left Eyes Mean Vernier Acuity Repeatability					
Gap Sizes (Arc Minutes)	Visit-1	Visit-2	Mean Difference	p-value (<0.05)	ICC
	Mean ± SD (Arc Seconds)	Mean ± SD (Arc Seconds)			
128	46 ± 18	64 ± 27	18	0.01*	0.62
64	48 ± 24	46 ± 22	-2	0.86	-0.06
32	36 ± 19	40 ± 19	4	0.35	0.21
16	24 ± 12	29 ± 19	5	0.44	0.25
8	23 ± 16	24 ± 17	1	0.91	0.57
4	19 ± 90	19 ± 90	0	0.87	0.47
2	20 ± 12	17 ± 11	-3	0.16	0.62

3.4.2 Vernier Acuity Repeatability (Between Eyes)

3.4.2.1 Right vs. Left Eyes (Visit-1)

Between the right and left eyes, at visit 1, the highest and the lowest threshold mean Vernier acuity threshold was measured by the right eye at 128 and 2 arc minutes of gap sizes, respectively. The left eye thresholds were relatively higher at all the gap sizes except at 128 arcminutes of gap size.

The mean VeT measured with the right and left eye at visit 1 were plotted against the gap sizes, as shown in the figure to assess the repeatability. The left eye thresholds were relatively higher at all the gap sizes except at 128 arcminutes of gap size. However, there was no statistical difference ($p > 0.05$) between the eyes at visit 1 across all gap sizes.

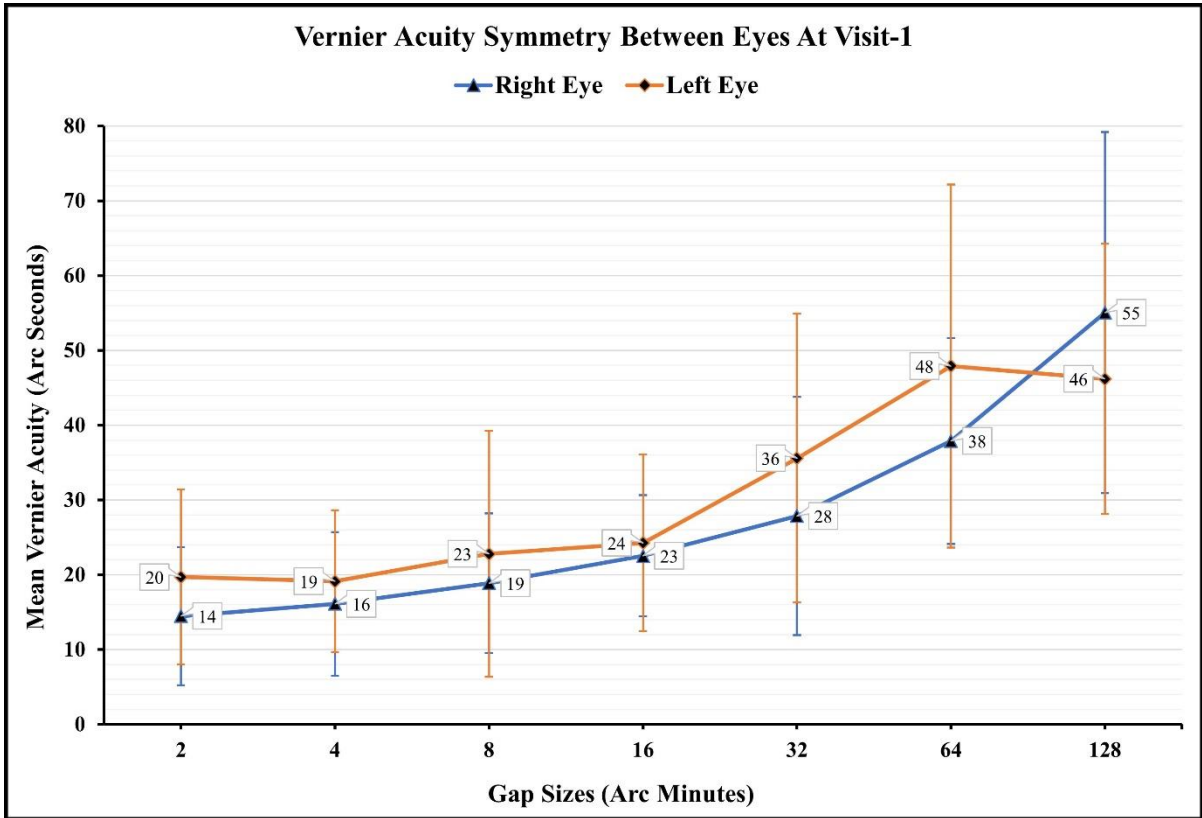


Figure 3-3 Mean VeT measured with the right and left eye at visit 1 were plotted against gap sizes.

Table 3-3 Mean VeT measured with right and left eyes were compared for symmetry between the eyes at visit 1.

Vernier Acuity Symmetry Between Eyes At Visit-1				
Gap Sizes (Arc Minutes)	Right Eyes	Left Eyes	Mean Difference	p-value (<0.05)
	Mean ± SD (Arc Seconds)	Mean ± SD (Arc Seconds)		
128	55 ± 24	46 ± 18	-9	0.21
64	38 ± 14	48 ± 24	10	0.21
32	28 ± 16	36 ± 19	8	0.05
16	23 ± 80	24 ± 12	1	0.81
8	19 ± 90	23 ± 16	4	0.37
4	16 ± 10	19 ± 90	3	0.26
2	14 ± 90	20 ± 12	6	0.19

3.4.2.2 Right vs. Left Eyes (Visit-2)

Between the right and left eyes, at visit 2, the highest mean Vernier acuity threshold was observed by the left eye, while both eyes observed the lowest threshold.

The mean VeT measured with the right and left eye at visit 2 were plotted against the gap sizes, as shown in the figure 3-4 to assess the repeatability. The left eye thresholds were relatively higher at all the gap sizes except 32 and 64 arcminutes of gap size. However, there was no statistical difference ($p > 0.05$) between the eyes at visit 2 across all gap sizes.

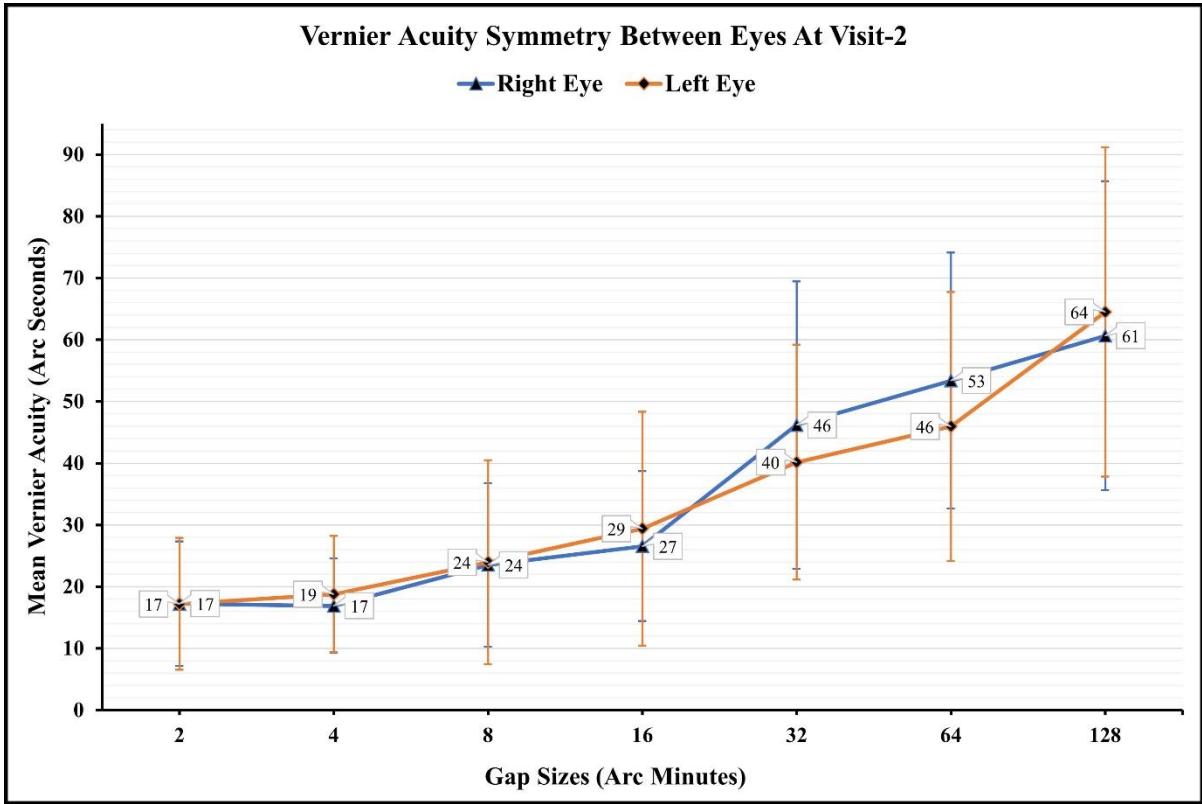


Figure 3-4 Mean VeT measured with the right and left eye at visit 2 were plotted against gap sizes.

Table 3-4 Mean VeT measured with right and left eyes were compared for symmetry between the eyes at visit 2.

Vernier Acuity Symmetry Between Eyes at Visit 2				
Gap Sizes (Arc Minutes)	Right Eyes	Left Eyes	Mean Difference	p-value (<0.05)
	Mean ± SD (Arc Seconds)	Mean ± SD (Arc Seconds)		
128	61 ± 25	64 ± 27	3	0.55
64	53 ± 21	46 ± 22	-7	0.14
32	46 ± 23	40 ± 19	-6	0.29
16	27 ± 12	29 ± 19	2	0.89
8	24 ± 13	24 ± 17	0	0.73
4	17 ± 80	19 ± 90	2	0.28
2	17 ± 10	17 ± 11	0	0.92

3.4.3 Vernier Acuity Repeatability (Compiled)

A total of 42 eyes (21 right and 21 left) were analyzed in this section, the mean highest Vernier threshold measured was 51 arcseconds at 128 arcminutes of gap size, and the lowest threshold measured was 17 arcseconds at 2 arcminutes of gap size. The mean thresholds were under 30 arcseconds for the first four lower gap sizes, 2, 4, 8, and 16 arcminutes, and for the rest of the gap sizes, thresholds were between 31 to 60 arcseconds. This suggests that the VeT are highly sensitive to the gap size below 16 arcminutes in this cohort of participants.

The mean Vernier acuity thresholds indicated similar threshold distribution across the gap sizes at both visits. However, thresholds measured at visit 2 were relatively higher at all the gap sizes except 2 and 4 gap sizes, where thresholds were the same for both visits. A significant difference between the mean VeT at 32, 64, and 128 arcminutes of gap sizes indicated poor repeatability. The mean difference between the visits at smaller gap sizes, including 2, 4, 8, and 16, were not statistically significant, meaning thresholds are highly repeatable. A negative learning effect was observed as the thresholds on visit 2 were relatively higher when compared to visit 1. Although a positive correlation was estimated at all the gap sizes, 128, 64, 32 and 2 gap sizes had weak correlation and 16, 8 and 4 gap sizes had fair correlation.

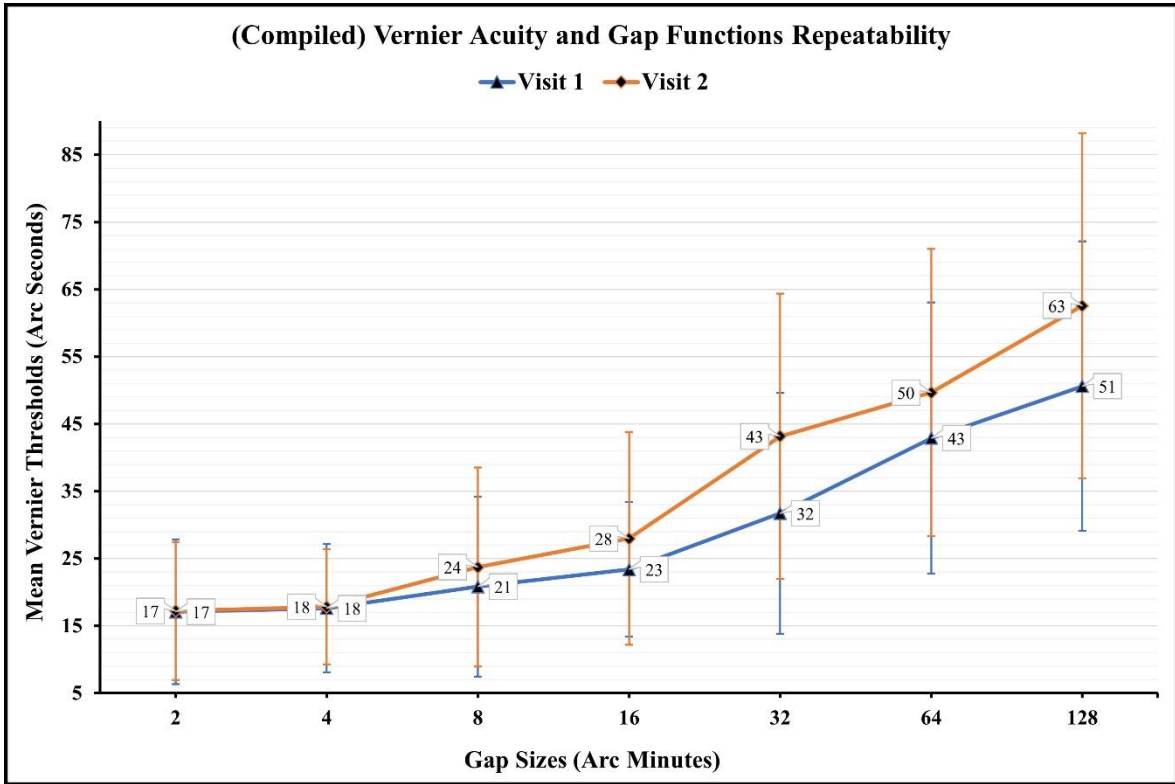


Figure 3-5 The right and left eye (compiled) mean VeT at visits 1 and 2 were plotted against gap sizes.

Table 3-5 The right and left eye (compiled) mean VeT at visits 1 and 2, mean difference, p-value, and interclass correlation (ICC).

(Compiled) Vernier Acuity Repeatability					
Gap Sizes (Arc Minutes)	Visit 1	Visit 2	Mean Difference	p-value (<0.05)	ICC
	Mean ± SD (Arc Seconds)	Mean ± SD (Arc Seconds)			
128	51 ± 22	63 ± 26	12	0.04*	0.08
64	43 ± 20	50 ± 21	7	0.03*	0.19
32	32 ± 18	43 ± 21	11	0.01*	0.16
16	23 ± 10	28 ± 16	5	0.12	0.22
8	21 ± 13	24 ± 15	3	0.42	0.29
4	18 ± 10	18 ± 90	0	0.98	0.28
2	17 ± 11	17 ± 10	0	0.76	0.19

3.4.4 Responses Accuracy Analysis

The mean performance accuracy was estimated in percentages for correct, incorrect, and aligned responses at all gap sizes, as presented in the below table. The program achieved over 92 percent correct responses and less than 3 percent incorrect responses to achieve the VeT from 5 reversals, about 5 percent aligned responses at each gap size. (This indicates the test efficiency and subject attention)

The mean performance accuracy from both visits was analyzed for accuracy repeatability and

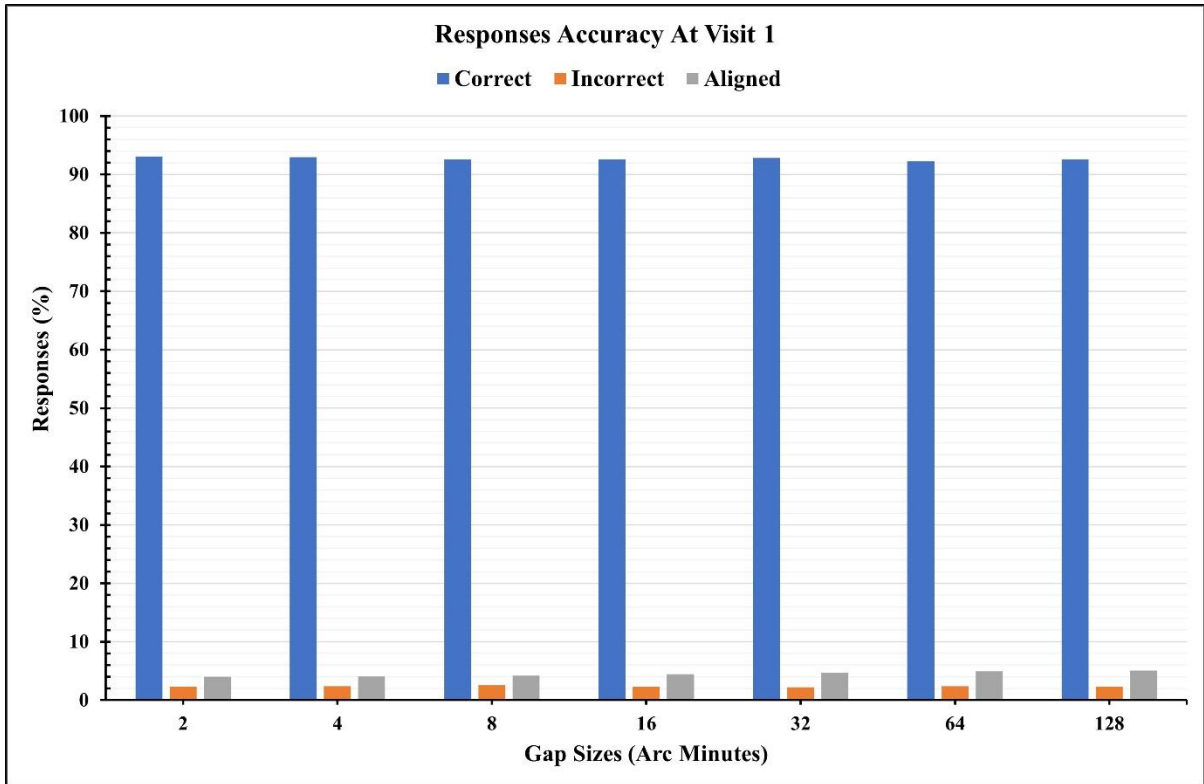


Figure 3-6 Responses percentages across gap sizes estimated using ASM model at visit 1.

secondarily to assess subject attention. At both visits and for all the gap sizes, the program achieved over 91 percent correct responses and less than 3.5 percent incorrect responses to achieve 5 reversals, between 3.9 to 5.3 percent aligned responses. A positive learning effect was observed at most gap sizes for correct responses. However, at 32 gap sizes, the positive learning effect was significantly strong. No learning effect was observed at 128 and 2 arcminutes of gap sizes, and a negative learning effect was observed at 4 arcminutes of gap size. A negative learning effect was observed for incorrect responses at most gap sizes. A positive learning effect was observed only at 128 arcminutes of gap size,

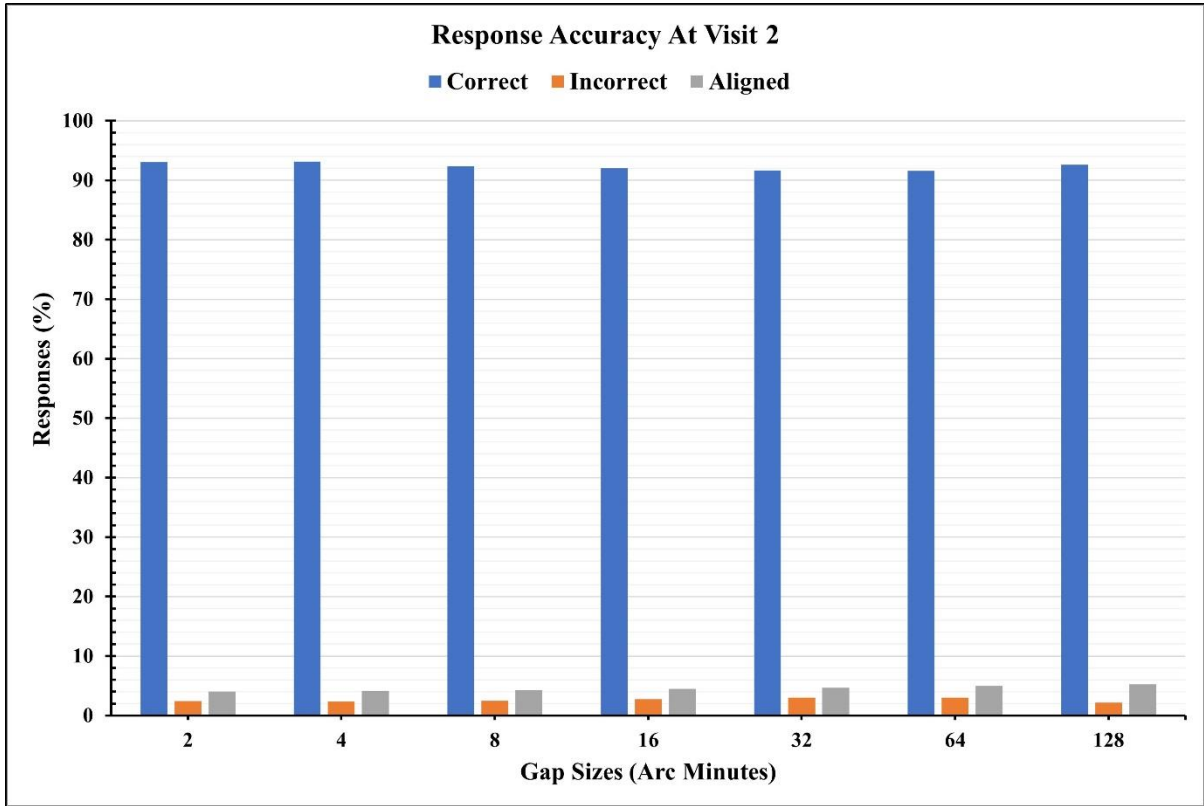


Figure 3-7 Responses percentages across gap sizes estimated using ASM model at visit 2.

while a negative effect was observed at 4 and 8 gap sizes. There was no statistically significant learning effect observed across gap sizes. A negative learning effect was observed for aligned responses at all gap sizes, and no statistically significant learning effect was observed across gap sizes.

Table 3-6 The repeatability of mean percentage correct, incorrect, and aligned responses measured for all gap sizes.

Mean Responses Accuracy Repeatability				
Gap Sizes (Arc Minutes)	Mean Correct Response (%)		Mean Difference	p-value (<0.05)
	Visit-1 (Mean ± SD)	Visit-2 (Mean ± SD)		
128	92.6 ± 2.9	92.6 ± 2.4	0.0	0.50
64	92.3 ± 2.9	91.6 ± 3.6	-0.7	0.43
32	92.8 ± 2.4	91.6 ± 2.9	-1.2	0.02*
16	92.5 ± 2.4	92.0 ± 3.2	-0.5	0.59
8	92.6 ± 3.0	92.4 ± 3.1	-0.2	0.10
4	92.9 ± 2.9	93.1 ± 2.9	0.2	0.10
2	93.1 ± 2.5	93.1 ± 2.4	0.0	0.10
Overall	92.7 ± 2.7	92.3 ± 2.9	-0.3	
Mean Responses Accuracy Repeatability				
Gap Sizes (Arc Minutes)	Mean Incorrect Response (%)		Mean Difference	p-value (<0.05)
	Visit-1 (Mean ± SD)	Visit-2 (Mean ± SD)		
128	2.3 ± 3.8	2.1 ± 2.9	-0.15	0.45
64	2.3 ± 3.3	3.0 ± 4.0	0.66	0.54
32	2.1 ± 2.8	3.0 ± 3.4	0.83	0.11
16	2.3 ± 2.7	2.7 ± 3.5	0.43	0.53
8	2.5 ± 2.9	2.5 ± 3.3	-0.05	0.78
4	2.4 ± 3.0	2.3 ± 3.1	-0.01	0.71
2	2.3 ± 2.8	2.4 ± 2.6	0.12	0.75
Overall	2.3 ± 3.0	2.6 ± 3.3	0.26	
Mean Responses Accuracy Repeatability				
Gap Sizes (Arc Minutes)	Mean Aligned Response (%)		Mean Difference	p-value (<0.05)
	Visit-1 (Mean ± SD)	Visit-2 (Mean ± SD)		
128	5.1 ± 1.1	5.2 ± 0.8	0.1	0.99
64	4.9 ± 0.8	5.0 ± 1.0	0.1	0.56
32	4.7 ± 0.7	4.6 ± 0.8	-0.1	0.62
16	4.4 ± 0.6	4.5 ± 0.8	0.1	0.62
8	4.2 ± 0.6	4.3 ± 0.8	0.1	0.28
4	4.1 ± 0.7	4.2 ± 0.7	0.1	0.42
2	4.0 ± 0.6	4.1 ± 0.7	0.1	0.41
Overall	4.5 ± 0.7	4.6 ± 0.8	0.1	

3.4.5 Reaction Time Analysis

Visit 1: The mean reaction time was estimated in milliseconds for correct, incorrect, and aligned responses at all gap sizes, as presented in the below table. The mean time required to correctly judge a Vernier misalignment at all gap sizes was less than a second; for an incorrect response, it was less than three-fourths of a second; for aligned responses, it was less than two and a half seconds. The fastest reaction for correct responses was recorded at 8 arcminutes, and the slowest reaction was recorded at 128 arcminutes of gap size. The fastest reaction for incorrect responses was recorded at 8 arcminutes, and the slowest was recorded at 128 arcminutes of gap size. The fastest reaction for aligned responses was recorded at 2 arcminutes and the slowest at 128 arcminutes of gap size. At all gap sizes, the wrong responses were observed to be relatively faster than the correct response, whereas aligned responses were the slowest. It means been observed that participants take relatively longer time to visually make alignment judgement and confirm the alignment of lines.

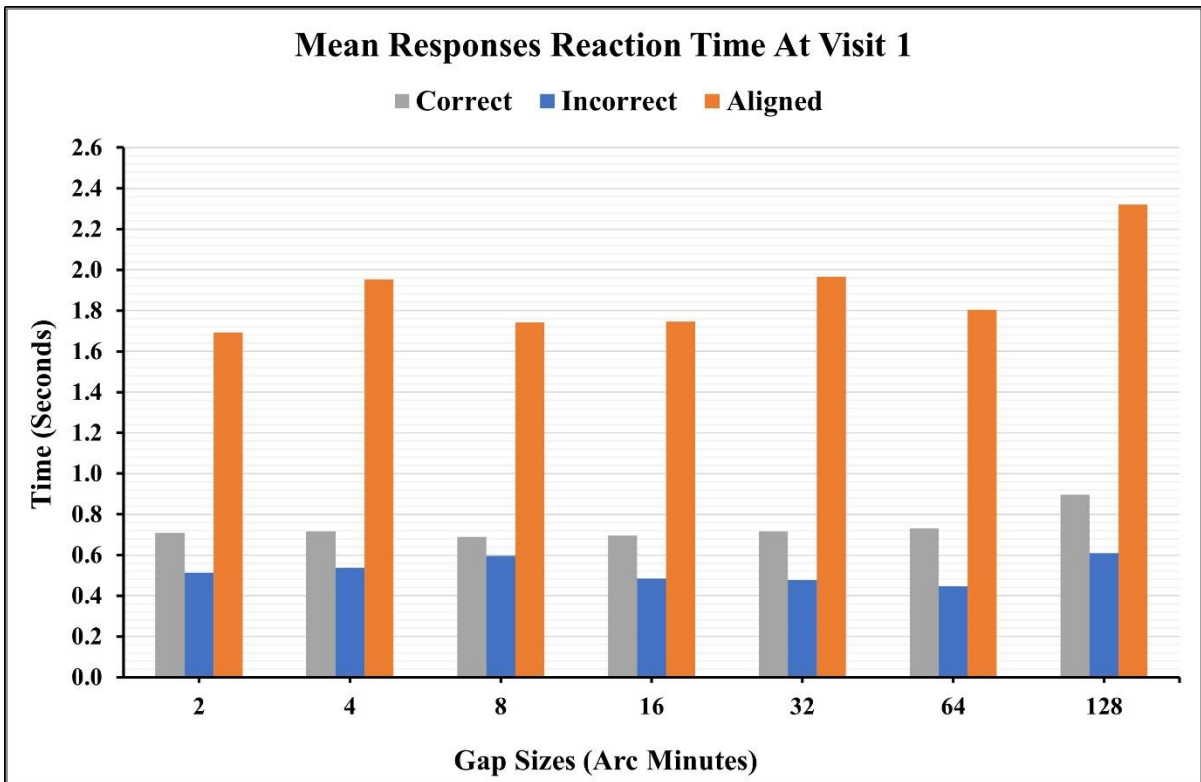


Figure 3-8 Response reaction time across gaps using ASM program at visit 1.

Visit 2: The mean response time estimated in milliseconds for correct, incorrect, and aligned responses at all gap sizes was analyzed to assess the optimum gap size concerning time. The correct and aligned responses were significantly faster at all the gap sizes during the second visit, whereas incorrect responses were significantly faster only at 2 and 4 arcminutes of gap sizes. At all gap sizes, the wrong responses were observed to be relatively faster than the correct response, whereas aligned responses were the slowest.

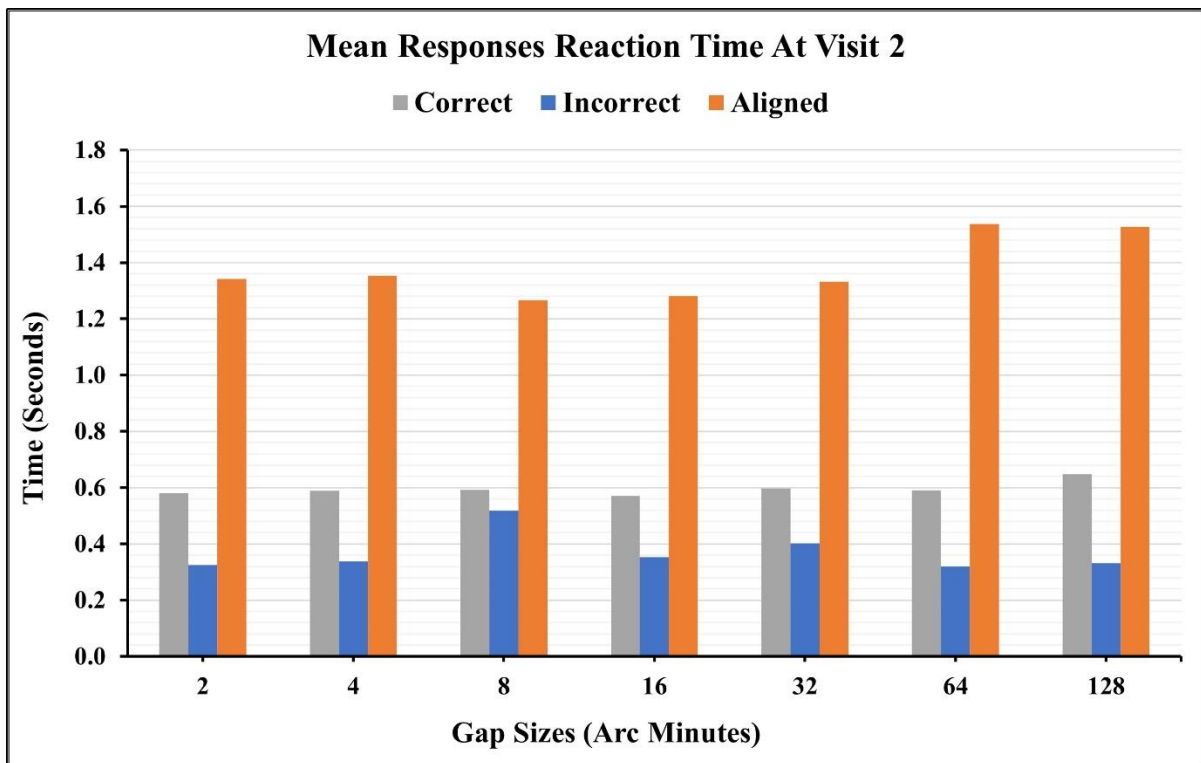


Figure 3-9 Response reaction time across gaps using ASM program at visit 2.

Table 3-7 The mean response reaction time measured for all gap sizes at visits 1 and 2.

Mean Responses Reaction Time (RRT) Repeatability				
Gap Sizes (Arc Minutes)	Mean Correct RRT (Seconds)		Mean Difference	p-value (<0.05)
	Visit-1 (Mean ± SD)	Visit-2 (Mean ± SD)		
128	0.90 ± 0.31	0.65 ± 0.15	-0.25	0.00*
64	0.73 ± 0.20	0.59 ± 0.12	-0.14	0.00*
32	0.72 ± 0.22	0.60 ± 0.21	-0.12	0.00*
16	0.70 ± 0.16	0.57 ± 0.11	-0.13	0.00*
8	0.69 ± 0.17	0.59 ± 0.15	-0.10	0.00*
4	0.72 ± 0.20	0.59 ± 0.12	-0.13	0.00*
2	0.71 ± 0.14	0.58 ± 0.12	-0.13	0.00*
Overall	0.74 ± 0.20	0.60 ± 0.14	-0.14	
Mean Responses Reaction Time (RRT) Repeatability				
Gap Sizes (Arc Minutes)	Mean Incorrect RRT (Seconds)		Mean Difference	p-value (<0.05)
	Visit-1 (Mean ± SD)	Visit-2 (Mean ± SD)		
128	0.61 ± 1.00	0.33 ± 0.40	-0.28	0.24
64	0.45 ± 0.58	0.32 ± 0.29	-0.13	0.25
32	0.48 ± 0.60	0.40 ± 0.32	-0.08	0.50
16	0.48 ± 0.67	0.35 ± 0.34	-0.13	0.58
8	0.60 ± 0.78	0.52 ± 0.86	-0.08	0.54
4	0.54 ± 0.77	0.34 ± 0.38	-0.20	0.02*
2	0.51 ± 0.66	0.33 ± 0.25	-0.19	0.04*
Overall	0.52 ± 0.72	0.37 ± 0.40	-0.15	
Mean Responses Reaction Time (RRT) Repeatability				
Gap Sizes (Arc Minutes)	Mean Aligned RRT (Seconds)		Mean Difference	p-value (<0.05)
	Visit-1 (Mean ± SD)	Visit-2 (Mean ± SD)		
128	2.32 ± 1.38	1.53 ± 0.79	-0.79	0.00*
64	1.80 ± 0.72	1.54 ± 1.00	-0.27	0.00*
32	1.97 ± 1.06	1.33 ± 0.78	-0.63	0.00*
16	1.75 ± 0.90	1.28 ± 0.61	-0.47	0.00*
8	1.74 ± 0.99	1.27 ± 0.78	-0.48	0.00*
4	1.95 ± 1.19	1.35 ± 0.91	-0.60	0.00*
2	1.69 ± 0.69	1.34 ± 0.79	-0.35	0.00*
Overall	1.89 ± 0.99	1.38 ± 0.81	-0.51	

3.4.6 Test Time Analysis

The time taken to measure VeT at each gap size was estimated and plotted to identify the gap size that is time efficient for clinical screening. Vernier acuity thresholds were measured faster at all gap sizes in visit 2 compared to visit 1. This could be an indication of training effect from the first visit. The VeT were measured slowest at the 4-gap size of visit 1 and 2 and 4-gap sizes of visit 2, whereas they were

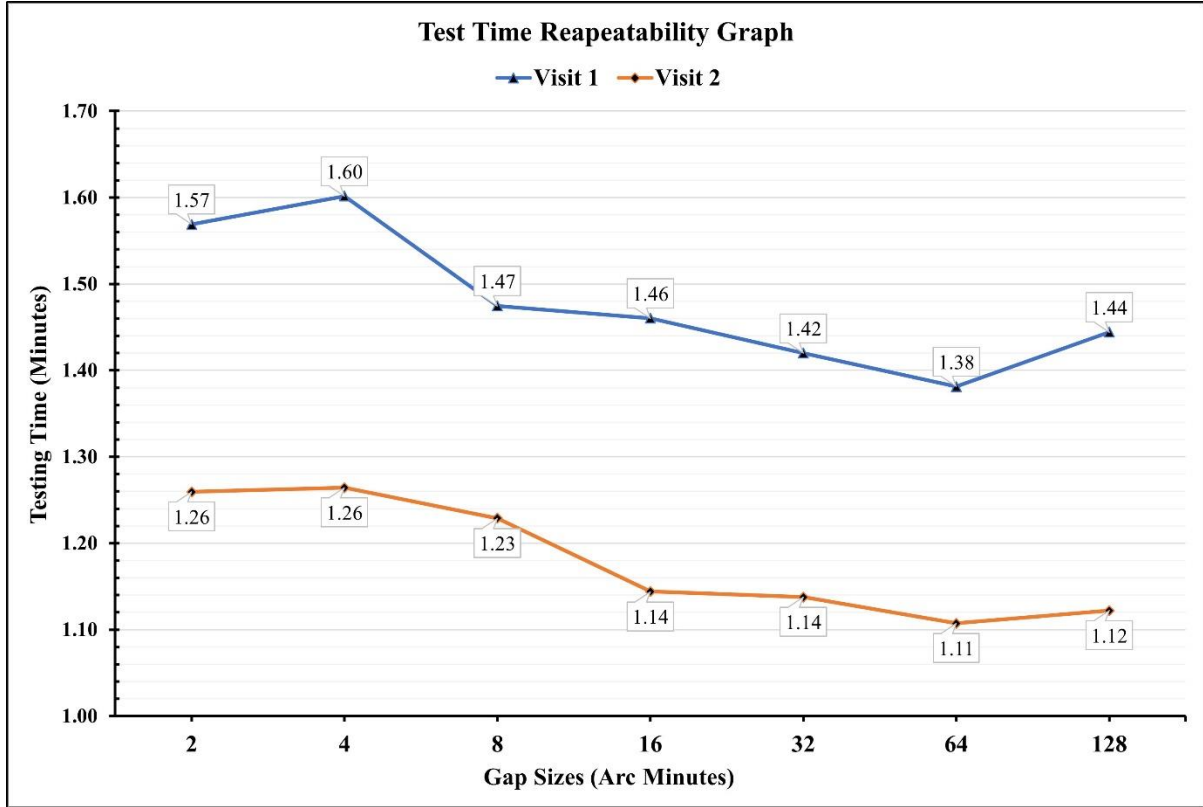


Figure 3-10 VAT testing time across gap sizes at visits 1 and 2.

faster at the 64-gap size for both visits.

3.4.7 Vernier Acuity and Age

As described below, I classified the participants into two groups (A and B) to identify the relationship between the VeT and age. Similar age groups were tested and compared in the past to estimate age related differences between the age groups. Therefore, I planned to compare similar age groups for Vernier acuity differences.

1. The age group of 20 to 30 years

2. The age group of 31 to 39 years

The mean VeT from each group were analyzed for both visits for repeatability and compared between the two age groups to assess variation between the groups. The VeT measured in the > 30 years age group were relatively variable compared to the ≤ 30 years age group.

3.4.7.1 VeT in Age 20 to 30 years (Repeatability)

A total of 28 eyes ($n = 28$), At visit 1, the mean lowest Vernier acuity threshold measured in the 20 to 30 age group was 18 arcseconds at 2 arcminutes, and the highest was 65 arcseconds at 128 arcminutes.

At visit 2, the mean lowest Vernier acuity threshold measured in the 20 to 30 age group was 15 arcseconds at 2 arcminutes, and the highest was 58 arcseconds at 128 arcminutes.

VeT measured in the 20 to 30 age group at visits 1 and 2 were plotted against the gap sizes as shown in the figure to assess the repeatability. The VeT were relatively higher at all gaps except 4 arcminutes on the second visit. However, there was a statistically significant difference only at 32 arcminutes of gap size.

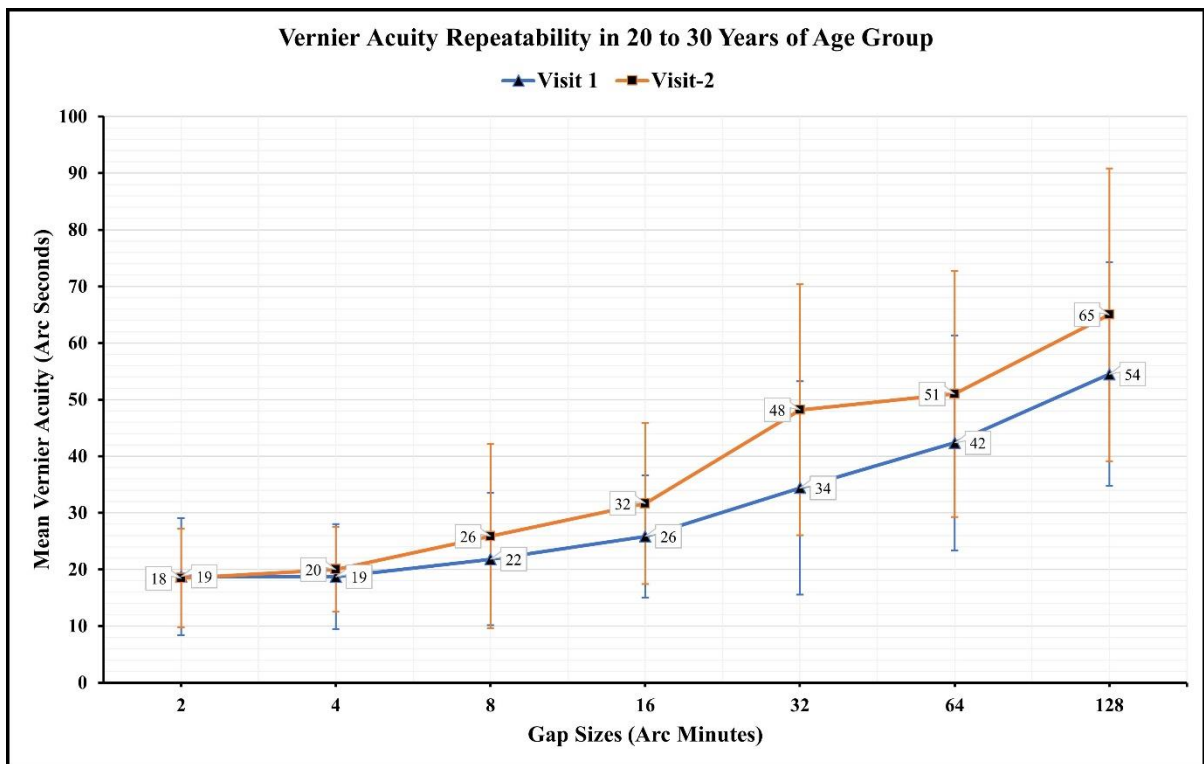


Figure 3-11 Mean VeT measured in the 20 to 30 age group at visits 1 and 2 were plotted against gap sizes.

Table 3-8 Repeatability of Vernier acuity in 20 to 30 age group.

Vernier Acuity Repeatability in 20 to 30 years of Age Group				
Gap Sizes (Arc Minutes)	Visit-1	Visit-2	Mean Difference	p-value (<0.05)
	Mean \pm SD (Arc Seconds)	Mean \pm SD (Arc Seconds)		
128	54 \pm 20	65 \pm 26	11	0.12
64	42 \pm 19	51 \pm 22	9	0.06
32	34 \pm 19	48 \pm 22	14	0.03*
16	26 \pm 11	32 \pm 14	6	0.07
8	22 \pm 12	26 \pm 16	4	0.40
4	19 \pm 90	20 \pm 70	1	0.51
2	19 \pm 10	18 \pm 90	-1	0.81

3.4.7.2 VeT in Age 31 to 40 years (Repeatability)

A total of 14 eyes (n = 14), At visit 1, the mean lowest Vernier acuity threshold measured in the 31 to 40 age group was 14 arcseconds at 2 arcminutes, and the highest was 44 arcseconds at 64 arcminutes.

At visit 2, the mean lowest Vernier acuity threshold measured in the 31 to 40 age group was 15 arcseconds at 2 arcminutes, and the highest was 58 arcseconds at 128 arcminutes.

VeT measured in 31 to 40 years of age group at visits 1 and 2 were plotted against the gap sizes as shown in the figure to assess the repeatability. The VeT were relatively higher at all gaps except 4 arcminutes on the second visit. However, no statistically significant difference was observed at all the gap sizes.

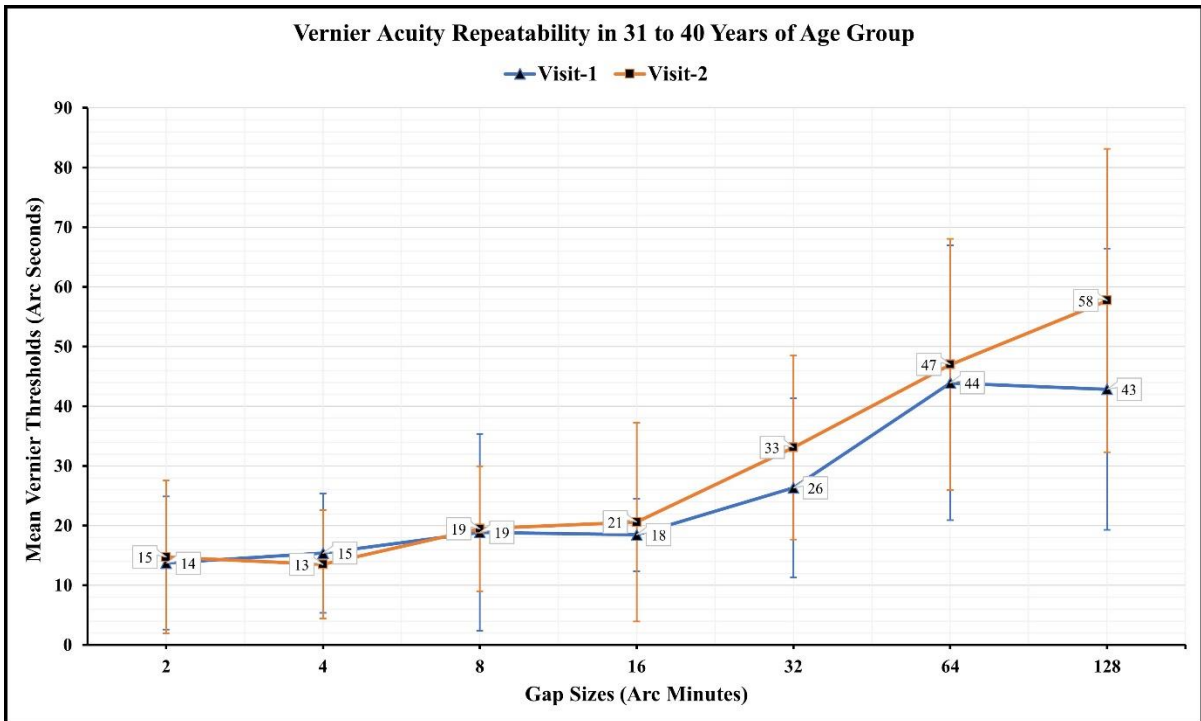


Figure 3-12 Mean VeT measured in 31 to 40 years of age group at visits 1 and 2 were plotted against gap sizes.

Table 3-9 Repeatability of Vernier acuity in 31 to 40 age group.

Vernier Acuity Repeatability in 31 to 40 years of Age Group				
Gap Sizes (Arc Minutes)	Visit-1	Visit-2	Mean Difference	p-value (<0.05)
	Mean ± SD (Arc Seconds)	Mean ± SD (Arc Seconds)		
128	43 ± 24	58 ± 25	15	0.06
64	44 ± 23	47 ± 21	3	0.36
32	26 ± 15	33 ± 15	7	0.24
16	18 ± 60	21 ± 17	3	0.76
8	19 ± 17	19 ± 10	0	0.86
4	15 ± 10	13 ± 90	-2	0.71
2	14 ± 11	15 ± 13	1	0.84

3.4.7.3 VeT Between Age Groups (Repeatability)

Between the age groups, at visit 1, the mean highest Vernier acuity threshold was measured by the 20 to 30 age group at 54 arc seconds at 128 arc minutes of gap size, and the lowest was measured by the 31 to 40 age group 14 arc seconds at 2 arc minutes of gap size. The left eye thresholds were relatively higher at all the gap sizes except at 128 arcminutes of gap size. However, this difference could be potentially due to the unequal number of participants between the groups.

Table 3-10 Comparison of Vernier acuity between the age groups at both visits.

Comparison of Vernier Acuity Between Age Groups at Visit-1				
Gap Sizes (Arc Minutes)	Age 20 to 30	Age 31 to 40	Mean Difference	p-value (<0.05)
	(Mean ± SD) (Arc Seconds)	(Mean ± SD) (Arc Seconds)		
128	54 ± 20	43 ± 24	-11	0.10
64	42 ± 19	44 ± 23	2	0.93
32	34 ± 19	26 ± 15	-8	0.06
16	26 ± 11	18 ± 60	-8	0.02*
8	22 ± 12	19 ± 17	-3	0.11
4	19 ± 90	15 ± 10	-4	0.29
2	19 ± 10	14 ± 11	-5	0.05
Comparison of Vernier Acuity Between Age Groups at Visit-2				
Gap Sizes (Arc Minutes)	Age 20 to 30	Age 31 to 40	Mean Difference	p-value (<0.05)
	(Mean ± SD) (Arc Seconds)	(Mean ± SD) (Arc Seconds)		
128	65 ± 26	58 ± 25	-7	0.39
64	51 ± 22	47 ± 21	-4	0.61
32	48 ± 22	33 ± 15	-15	0.02*
16	32 ± 14	21 ± 17	-11	0.00*
8	26 ± 16	19 ± 10	-7	0.27
4	20 ± 70	13 ± 90	-7	0.00*
2	18 ± 90	15 ± 13	-3	0.09

3.4.8 Vernier Acuity and Gender

3.4.8.1 Vernier Acuity Thresholds in Females (Repeatability)

The mean highest Vernier acuity threshold recorded in females was 52 arcseconds at 128 arcminutes, and the lowest was 17 arcseconds at 2 arcminutes. While at visit 2, the highest Vernier acuity threshold recorded was 68 arcseconds at 128 arcminutes, and the lowest was 17 arcseconds at 2 arcminutes. The VeT measured in the second visit had relatively higher thresholds at all gap sizes except 2 and 4 arcminutes. However, a statistically significant difference was seen only at 128 arcminutes gap size. The mean VeT measured in females at visits 1 and 2 were plotted against the gap sizes shown in the figure to assess the repeatability.

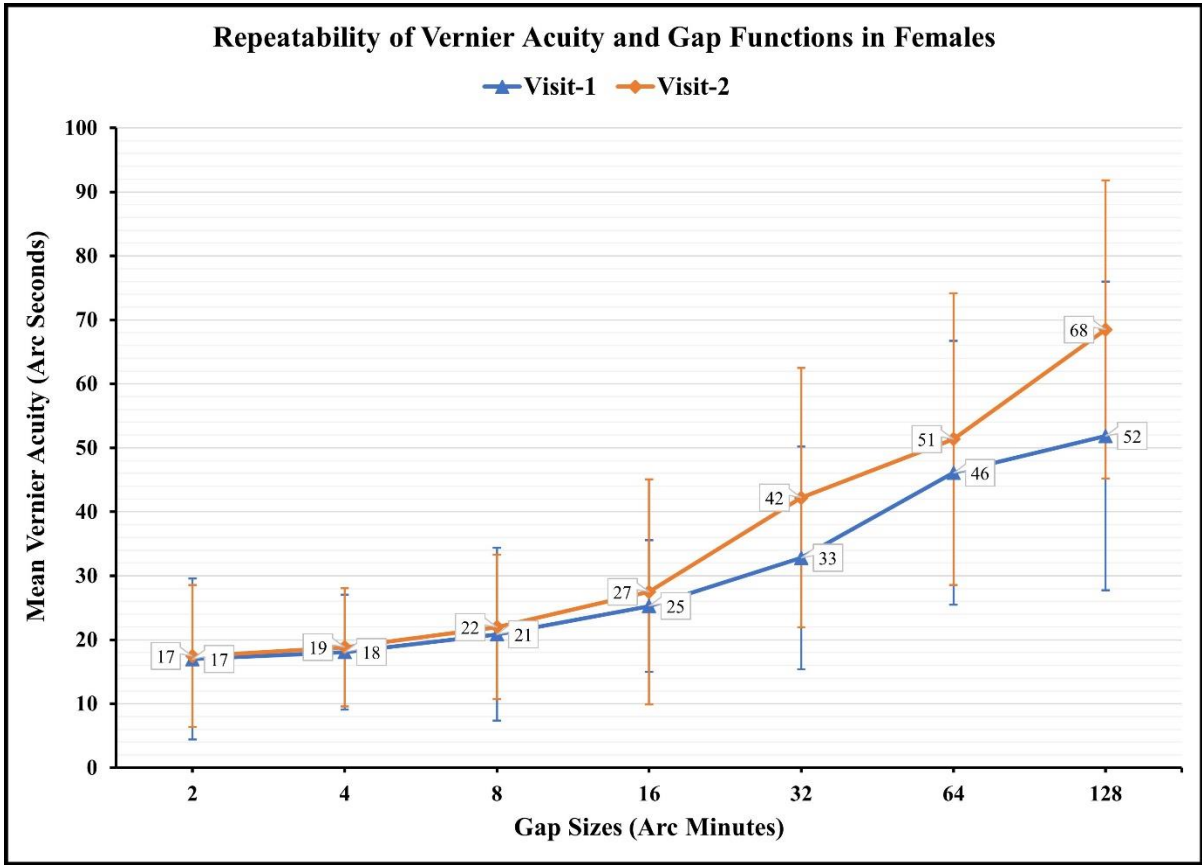


Figure 3-13 Mean VeT measured in females at visits 1 and 2 were plotted against gap sizes.

Table 3-11 Repeatability of Vernier acuity in females

Vernier Acuity Repeatability in Females				
Gap Sizes (Arc Minutes)	Visit-1	Visit-2	Mean Difference	p-value (<0.05)
	Mean \pm SD (Arc Seconds)	(Mean \pm SD) (Arc Seconds)		
128	52 \pm 24	68 \pm 23	16	0.04*
64	46 \pm 21	51 \pm 23	5	0.45
32	33 \pm 17	42 \pm 20	9	0.16
16	25 \pm 10	27 \pm 18	2	0.75
8	21 \pm 14	22 \pm 11	1	0.87
4	18 \pm 90	19 \pm 90	1	0.76
2	17 \pm 13	17 \pm 11	0	0.99

3.4.8.2 Vernier Acuity Thresholds in Males (Repeatability)

At visit 1, the mean highest Vernier acuity threshold recorded in males was 49 arcseconds at 128 arcminutes, and the lowest was 17 arcseconds at 2 arcminutes. While at visit 2, the highest Vernier acuity threshold recorded was 56 arcseconds at 128 arcminutes, and the lowest was 17 arcseconds at 2 arcminutes. The VeT measured in the second visit had relatively higher thresholds at all gap sizes except 2 and 4 arcminutes. However, there was a statistically significant difference at 16, 32, and 64 arcminutes of gap sizes. The mean VeT measured in males at visits 1 and 2 were plotted against the gap sizes shown in the figure to assess the repeatability.

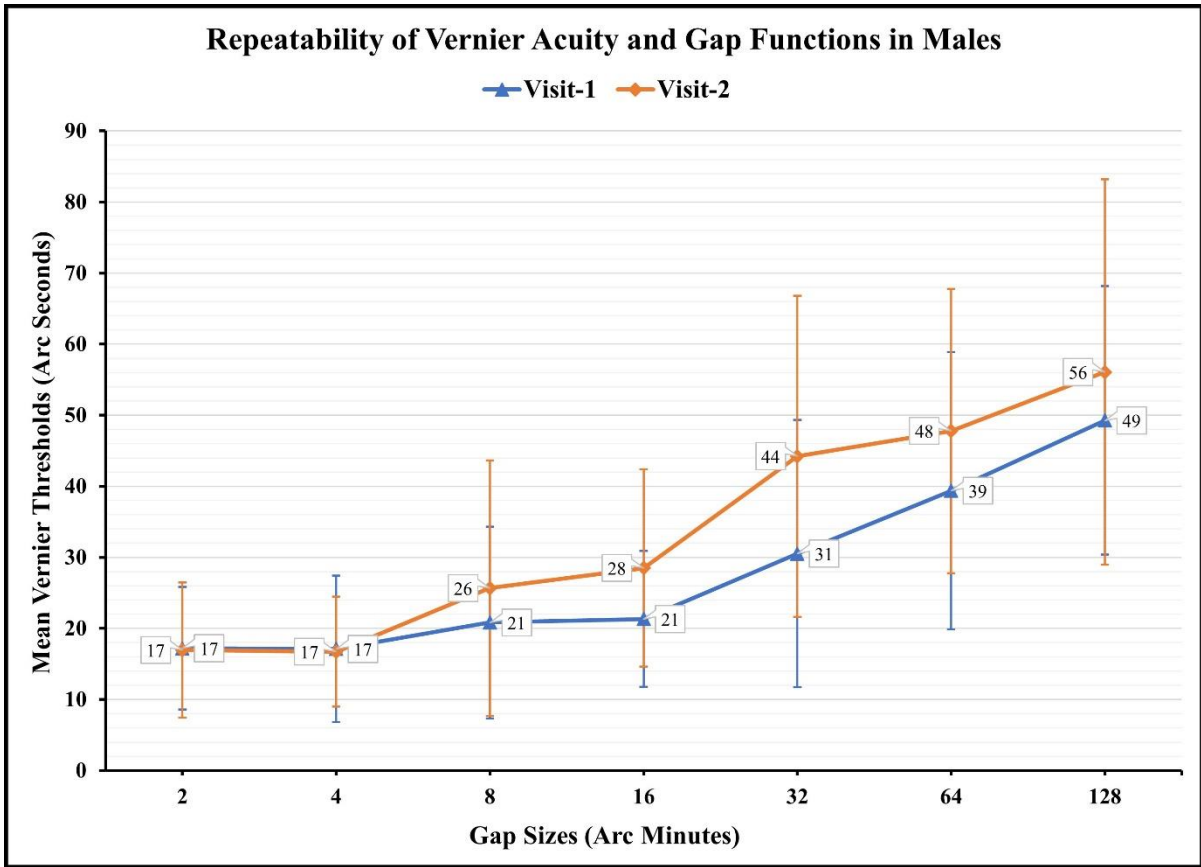


Figure 3-14 Mean VeT measured in males at visits 1 and 2 were plotted against gap sizes.

Table 3-12 Vernier acuity repeatability in males

Vernier Acuity Repeatability in Males				
Gap Sizes (Arc Minutes)	Visit-1	Visit-2	Mean Difference	p-value (<0.05)
	(Mean ± SD) (Arc Seconds)	(Mean ± SD) (Arc Seconds)		
128	49 ± 19	56 ± 27	7	0.43
64	39 ± 20	48 ± 20	9	0.01*
32	31 ± 19	44 ± 23	13	0.04*
16	21 ± 10	28 ± 14	7	0.03*
8	21 ± 14	26 ± 18	5	0.36
4	17 ± 10	17 ± 80	0	0.87
2	17 ± 90	17 ± 10	0	0.92

3.4.8.3 Vernier Acuity Differences Between Females and Males

Though females had relatively higher Vernier acuity thresholds at all gaps at visit 1 and most gaps at visit 2, there was no statistical difference between females' and males' VeT at both visits.

Table 3-13 Comparison of Vernier acuity between gender at both visits.

Comparison of Vernier Acuity Between Gender at Visit-1				
Gap Sizes (Arc Minutes)	Females	Males	Mean Difference	p-value (<0.05)
	(Mean \pm SD) (Arc Seconds)	(Mean \pm SD) (Arc Seconds)		
128	52 \pm 24	49 \pm 19	-3	0.70
64	46 \pm 21	39 \pm 20	-7	0.23
32	33 \pm 17	31 \pm 19	-2	0.63
16	25 \pm 10	21 \pm 10	-4	0.20
8	21 \pm 14	21 \pm 14	0	0.88
4	18 \pm 90	17 \pm 10	-1	0.74
2	17 \pm 13	17 \pm 90	0	0.48
Comparison of Vernier Acuity Between Gender at Visit-2				
Gap Sizes (Arc Minutes)	Females	Males	Mean Difference	p-value (<0.05)
	(Mean \pm SD) (Arc Seconds)	(Mean \pm SD) (Arc Seconds)		
128	68 \pm 23	56 \pm 27	-12	0.12
64	51 \pm 23	48 \pm 20	-3	0.59
32	42 \pm 20	44 \pm 23	2	0.70
16	27 \pm 18	28 \pm 14	1	0.58
8	22 \pm 11	26 \pm 18	4	0.55
4	19 \pm 90	17 \pm 80	-2	0.43
2	17 \pm 11	17 \pm 10	0	0.96

3.5 Discussion

This study aimed to validate the Vernier acuity test with modified changes in the methodology and assess test performance and repeatability. The data from twenty-one emmetropic participants were analyzed for eyes, age, and gender differences.

Performance Analysis:

- 1. Response Accuracy:** Most of the correct and all the incorrect and aligned responses were consistent on both visits suggesting no deficit in subject attention while performing the test. Accuracy of the responses may indicate the subject attention while performing the test. Poor accuracy may indicate lack of understanding, attention, and any possible perception related problems.

- 2. Reaction Time:** Correct and aligned responses were significantly faster at all gap sizes in visit 2 compared to visit 1. In comparison, incorrect responses were significantly faster only at 2 and 4 gap sizes in visit 2 compared to visit 1. Delay in reaction may also indicate subject difficulties in processing the visual stimuli due to visual or cortical abnormalities in impairment.
- 3. Average Test Time:** The average time taken to complete the Vernier acuity testing for all gap sizes with the right and left eye during the first visit was 10.65 minutes. The second visit was 8.26 minutes, and the mean difference was 2.39. However, for the clinical visual screening consideration, a minimum of three gap sizes between 2 and 8 can be tested quickly within 5 to 7 minutes.

VeT Repeatability:

- 1. Eyes:** The VeT measured with the right eye at visits 1 and 2 were highly repeatable for all gap sizes except 32 and 64 arcminutes. Similarly, left-eye VeT were highly repeatable at all gap sizes except 128 arcminutes. It can be noted from the results that the first four lower gap sizes, including 2, 4, 8, and 16 arcminutes, are highly repeatable with both eyes. Therefore, Vernier acuity can be reasonably measured between 2 and 16 gap sizes to shorten the test for the initial testing, if the testing indicates abnormality the gap sizes can be extended up to 128. The thresholds were relatively higher at the second visit at all the gap sizes with the right eye and in most of the gap sizes with the left eye indicating a negative learning effect. However, participants were faster on the second visit compared to the first visit possibly due to the learning effect. The learning effect on Vernier acuity was efficiently minimized through randomization of stimuli presentations. Though there was a slight variation in VeT between the eyes (inter-eye) at both visits, there was no statistical difference suggesting the presence of performance symmetry between the eyes for Vernier acuity. Since there is a symmetry between the eyes for Vernier acuity, I compiled the VeT measured with the right and left eye to strengthen the sample size (n = 42; 21 right and 21 left eyes) and assess repeatability.
- 2. Age:** VeT were repeatable at most gap sizes for the 20 to 30 age group, and all the gap sizes for the 31 to 40 age group. Comparable results were observed between the age groups at visit 1 except at 16 gap size. Similarly, at visit-2 VeT had a poor comparison between the age groups at 32, 16, and 4 arcminutes of gap sizes. This could possibly be due to the considerable amount of difference in the sample sizes.

3. **Gender:** VeT in female participants were highly repeatable at most gap sizes compared to male participants. The VeT were independent when compared between males and females at both visits.
4. **Correlation:** A weak but positive correlation existed between the average VeT compiled between visits.

Table 3-14 Comparisons of Vernier acuity for all variables using statistical significance from repeatability (p-values).

Gap Sizes		128	64	32	16	8	4	2
Overall	HAT	0.04	0.03	0.01	0.12	0.42	0.98	0.76
	Eye							
	Right	0.43	0.00	0.01	0.19	0.25	0.77	0.47
	Left	0.01	0.86	0.35	0.44	0.91	0.87	0.16
Age	<30	0.12	0.06	0.03	0.07	0.40	0.51	0.81
	>30	0.06	0.36	0.24	0.76	0.86	0.72	0.84
Gender	Female	0.04	0.45	0.17	0.75	0.87	0.77	1.00
	Male	0.43	0.02	0.04	0.04	0.37	0.87	0.93

I optimized some aspects of the method, such as the number of reversals, stimuli presentation, and stimuli size. I increased the number of stimuli presentations from 100 to 200 to achieve the required reversals. I changed the stimuli size from 10 x 5 arcminutes to 30 x 3 arcminutes. To make the line stimuli more obvious and obtain an ideal size for Vernier acuity testing.

This test can be further tested using an eye-tracker to follow the eye movements while performing the test and correlate it with the response accuracy to establish the fixation points on the stimuli that contribute to the alignment decision. Vision screening using VAT could be conducted in multiple steps, the initial steps may involve testing VeA at smaller gap sizes particularly 4 and 8 arc minutes. Only if the measurements are within the expected range of age matched normal or control group indicating no sign of vision abnormality, further testing can be skipped. If the estimated Vernier measurements are above the age-matched control group, then the vernier acuity can be further tested at higher gap sizes

to confirm the abnormality and record the severity. In addition, hyperacuity based tests can be performed to quantify associated visual functions that can collectively indicate an abnormality.

3.6 Conclusion

I modified the VAT program and tested it for various validation metrics. The program was robust and efficient to measure the Vernier acuity. However, the reliability of the Vernier measurements in the studied cohort was estimated using interclass correlation to be between and medium ($ICC < 0.75$). Therefore, this program can be further modified and tested to achieve better reliability for clinical application.

Chapter 4

Hyperacuity Perimetry

4.1 Introduction

As noted in Chapter 1, both central and peripheral vision plays a critical role, and people with limited visual fields often face difficulties in meeting job requirements or participating in daily activities. Due to disease or abnormal eye condition certain aspects of vision are likely to be affected, including the visual field. Visual field quantification has been discussed in the earlier chapter. Visual scotoma is a dark patch in the visual field resulting from corresponding retina area abnormality. Usually, the photoreceptors of that area fail to process vision, and the brain interprets the overall vision, excluding the affected area. That area is usually perceived as a dark patch in the visual field. Visual scotomas are commonly observed in glaucoma and age-related macular degeneration conditions^{147,170,175}.

While most clinical evaluations focus on foveal vision, assessing the visual field across the macula is important to understand the severity and extent of any disease. This information cannot be obtained through tests on foveal visual function alone. Therefore, it's vital to detect any abnormalities in both the foveal and parafoveal regions¹⁷⁷.

Perimetry is a crucial diagnostic tool used in clinics to evaluate visual field abnormalities. They can be of two types, static and dynamic. Static perimetry is the most prevalent method that includes projecting light spots of small size onto a uniform background, and the patient determines the minimum amount of light required for detection. It measures the sensitivity of each retinal point; the stimulus is constant and stationary while the luminance varies until it is noticed visually. This test is commonly carried out at 76 locations on a grid throughout the central 30° radius of the visual field, providing valuable insights into vision abnormalities, disease status, and post-treatment progress. In comparison, kinetic perimetry measures the extent of the visual field by plotting the isopters. Stimuli are non-stationary and move from the non-seeing visual field to the seeing field with varying stimulus sizes^{158,172,177,178}. Perimetry is highly beneficial in diagnosing retinal conditions, such as age-related macular degeneration and neurological abnormalities, such as optic nerve damage caused by glaucoma^{177,178}. Additionally, it is frequently utilized for assessing visual ability in driving. Visual field defects are of several types, such as¹⁷⁸:

- 1. Central scotoma:** The loss of visual function in the central visual field, most likely due to macular disease.
- 2. Altitudinal field defects:** The loss of vision in either the superior or inferior half of the visual field, completely or partially, but without crossing the horizontal meridian. These visual defects occur when the ganglion cells that feed into a particular part of the optic nerve head are damaged. It is more frequently observed in cases with glaucoma than in ischemic optic neuropathies and high myopia.
- 3. Bitemporal Hemianopia:** The loss of lateral half visual fields completely or partially, but without crossing the vertical meridian. It is more commonly seen in lesions of the optic chiasm¹⁷⁸.

Difficulties with vision can impact the functioning of the macula, leading to a decline in our ability to perceive things. As a result, it is imperative to assess visual function in both the central and parafoveal regions, which includes measuring Vernier acuity. In the past, Vernier acuity has been used to assess macular function in patients with cataracts or other media opacities¹⁵⁸.

Therefore, to extend the Vernier acuity application to quantify the other visual functions including visual field. I developed a software package that can quantitatively measure Vernier acuity, in the eccentric 5-degrees of central visual field at different positions, including superior, inferior, nasal, and temporal. This program was modified from the VAT program discussed in chapter 3 of this thesis. The experiment details were like the VAT program however, stimuli configuration was adjusted and explained in the method section of this chapter. The test performance was assessed through repeatability of the measurements.

4.2 Method

4.2.1 Study Subjects

Please refer to section 3.2.2

4.2.2 Experimental Setup

Please refer to section 3.2.3

4.2.3 Software Application

Please refer to section 2.4

4.2.4 Stimuli Configuration

The experimental stimuli characteristics were calibrated in visual angle units. The line stimulus had a width of 3 arcminutes and a height of 30 arcminutes, while the fixation cross had a size of 15 arcminutes at the test distance.

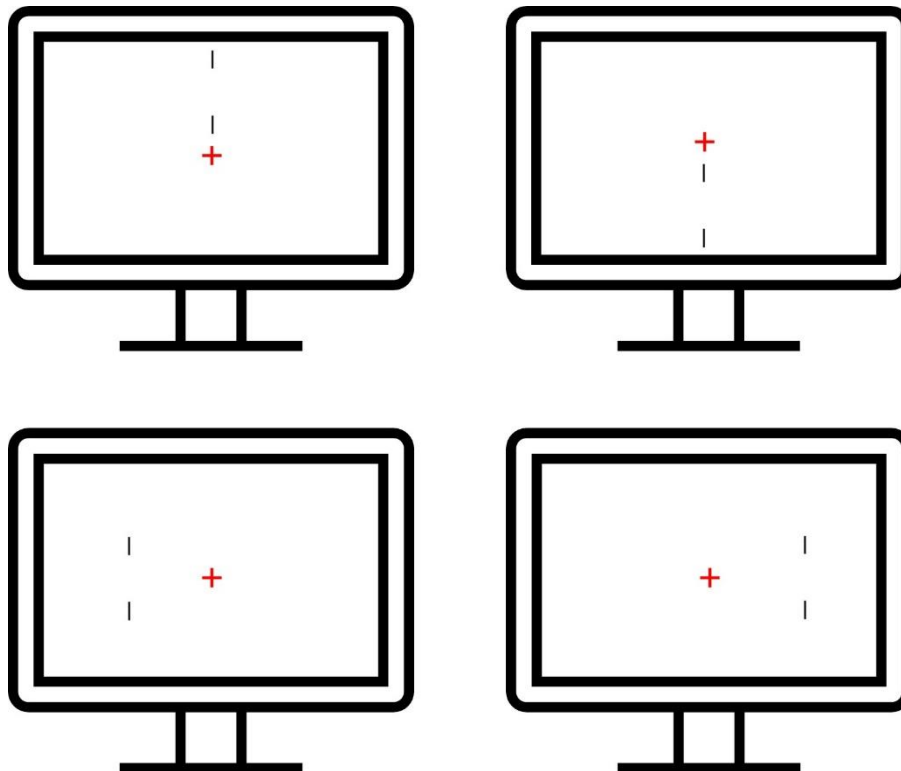


Figure 4-1 Graphical representation of hyperacuity perimetry position on the screen with respective central fixation target.

4.2.5 Gap sizes

As the testing is planned to estimate the VeT across eccentric 5 degrees and the foveal sensitivity gradually reduces towards periphery. I plan to measure the Vernier acuity sensitivity at an eccentricity

5 degrees from the fovea using two gap sizes of 15 and 30 arcminutes only to be in the sensitivity zones and not go beyond the observation limit.

4.2.6 Experiment Testing

Before the initiation of the experiment, all subjects were given a brief training session to familiarize themselves with the instructions and experimental procedures. The test was done monocularly, while Each eye was tested individually, with the fellow eye fully covered with a dark occluder. To reduce the influence of the dominant eye on the test results, the testing order was randomized between the right and left eyes. After each gap size, a short break was provided to allow the subjects to relax and overcome boredom.

During the experimental procedure, a small red cross was presented at the center of the screen. In contrast, the Vernier stimuli were presented in all four quadrants (Superior, Inferior, Nasal, and Temporal) at 5 degrees peripheral from the center. Measurements were taken at each quadrant for two different gap sizes: 15 and 30 arcminutes. The Vernier acuity threshold value was determined by the standard deviation of the positions where the subject registered the response for stimuli alignment. A lower threshold indicates higher sensitivity, while a higher threshold indicates poor sensitivity. To determine the threshold, measurements were taken at each gap size with a minimum of five reversals from two hundred stimuli presentations or trials. Once the threshold was achieved, the stimuli were repositioned three steps backward, and the test was repeated until five reversals were measured.

4.2.7 Data Analysis

Same as section 3.3.3

4.3 Results

4.3.1 Right Eyes HP (Visit 1)

At visit 1, the mean VeT measured with right eyes for eccentric 5 degrees in all four viewing quadrants were plotted at 15 and 30 gap sizes.

The highest thresholds of 73 and 76 arc seconds were observed in the temporal fields at both gap sizes. The lowest threshold for a 15-gap size was 61 arc seconds in the superior field, while the lowest threshold for a 30-gap size was 50 arc seconds in the inferior field. I did not see any significant

difference when the mean right eye thresholds were compared between gap sizes at all visual fields ($p>0.05$).

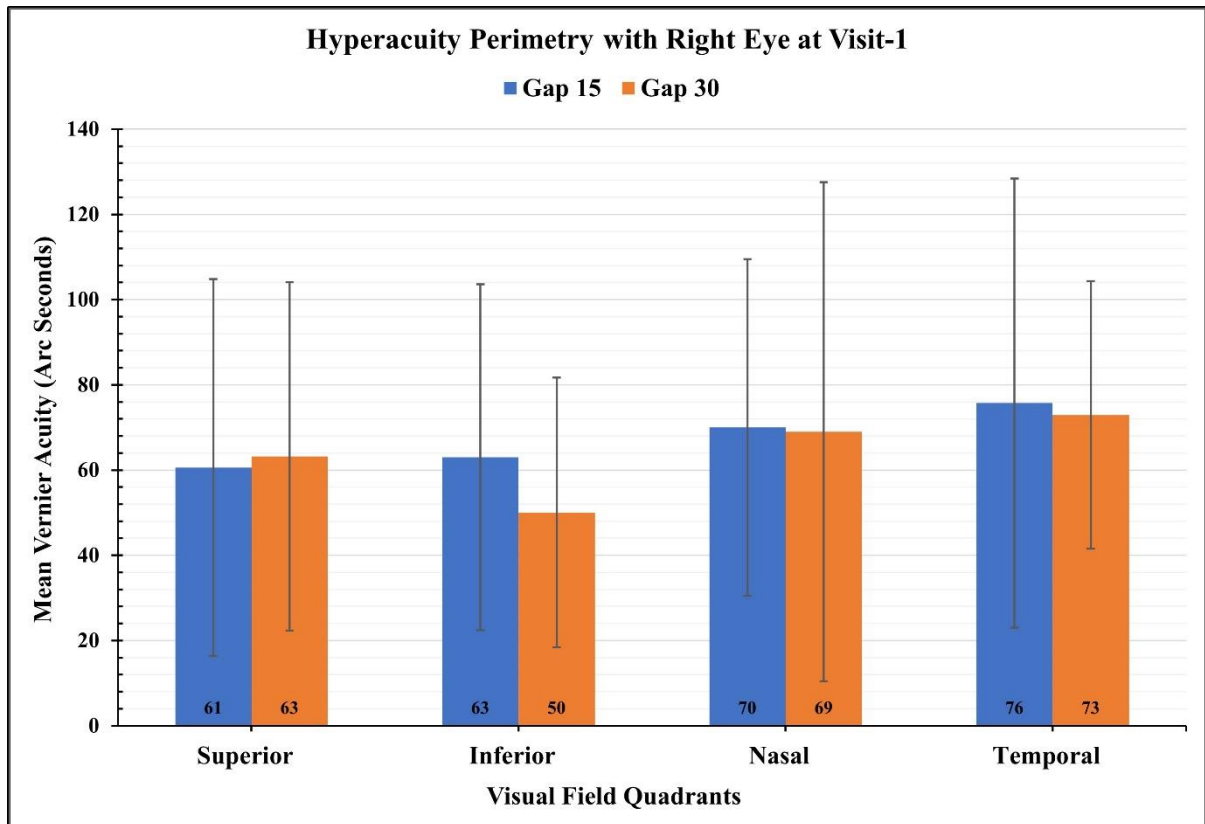


Figure 4-2 Hyperacuity Perimetry with right eyes for eccentric 5 degrees across four viewing quadrants at 15 and 30 gap sizes at Visit 1.

Table 4-1 Hyperacuity Perimetry with Right Eye at Visit 1

Hyperacuity Perimetry with Right Eye at Visit-1				
Visual Fields	Gap 15	Gap 30	Mean Difference	p-value (<0.05)
	Mean ± SD (Arc Seconds)	Mean ± SD (Arc Seconds)		
Superior Field	61 ± 44	63 ± 41	2	0.52
Inferior Field	63 ± 41	50 ± 32	-13	0.17
Nasal Field	70 ± 39	69 ± 59	-1	0.70
Temporal Field	76 ± 53	73 ± 31	-3	0.98

4.3.2 Right Eyes HP (Visit 2)

At visit 2, the mean VeT measured with right eyes for eccentric 5 degrees in all four viewing quadrants were plotted at 15 and 30 gap sizes.

The highest threshold of 73 arc minutes was observed at the temporal field for 15 gap size, while the highest threshold for 30 gap size was 78 arc seconds. The lowest thresholds for both gap sizes were 62 and 71 arc seconds at the inferior field. I did not see any significant difference when the mean right eye thresholds were compared between gap sizes at all visual fields ($p>0.05$).

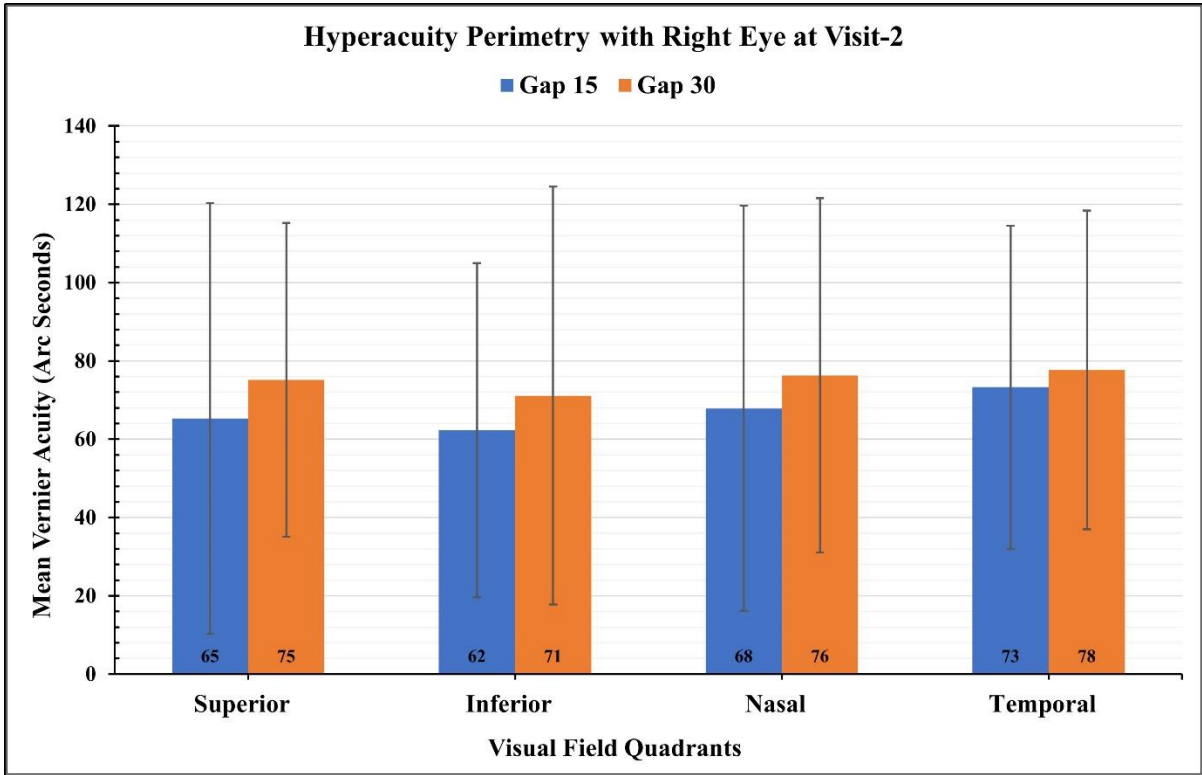


Figure 4-3 The mean VeT measured with right eyes for eccentric 5 degrees across four viewing quadrants at 15 and 30 gap sizes.

Table 4-2 Hyperacuity Perimetry with Right Eye at Visit 2

Hyperacuity Perimetry with Right Eye at Visit-2				
Visual Fields	Gap 15	Gap 30	Mean Difference	p-value (<0.05)
	Mean ± SD (Arc Seconds)	Mean ± SD (Arc Seconds)		
Superior Field	65 ± 55	75 ± 40	10	0.28
Inferior Field	62 ± 43	71 ± 53	9	0.36
Nasal Field	68 ± 52	76 ± 45	8	0.39
Temporal Field	73 ± 41	78 ± 41	5	0.52

4.3.3 Right Eyes HP (Repeatability)

To test for repeatability, the VeT of the right eye was compared between two visits. The thresholds were measured at 15 and 30 gap sizes for the superior, inferior, nasal, and temporal visual fields. At the 15-gap size, the highest thresholds were obtained at the temporal field visits 1 and 2, with 76 and 73 arc seconds, respectively. The lowest thresholds were found at the superior with 61 arc seconds for visit 1 and inferior fields with 62 arc seconds for visit 2. At the 30-gap size, the highest thresholds were observed at the temporal fields for visits 1 and 2, with 73 and 78 arc seconds, respectively. The lowest thresholds were found at the inferior field for visits 1 and 2, with 50 and 71 arc seconds, respectively. No significant difference was seen between the visits of all four visual fields of the right eye for 15-gap size ($p > 0.05$). However, a significant difference was observed between the inferior field of the right eye for the 30-gap size ($p = 0.01$). Interclass correlation (ICC) analysis was performed to test the reliability of the results between visits. The ICC showed positive but poor correlations for all fields except for the superior field at 15 gap size, which showed a negative correlation.

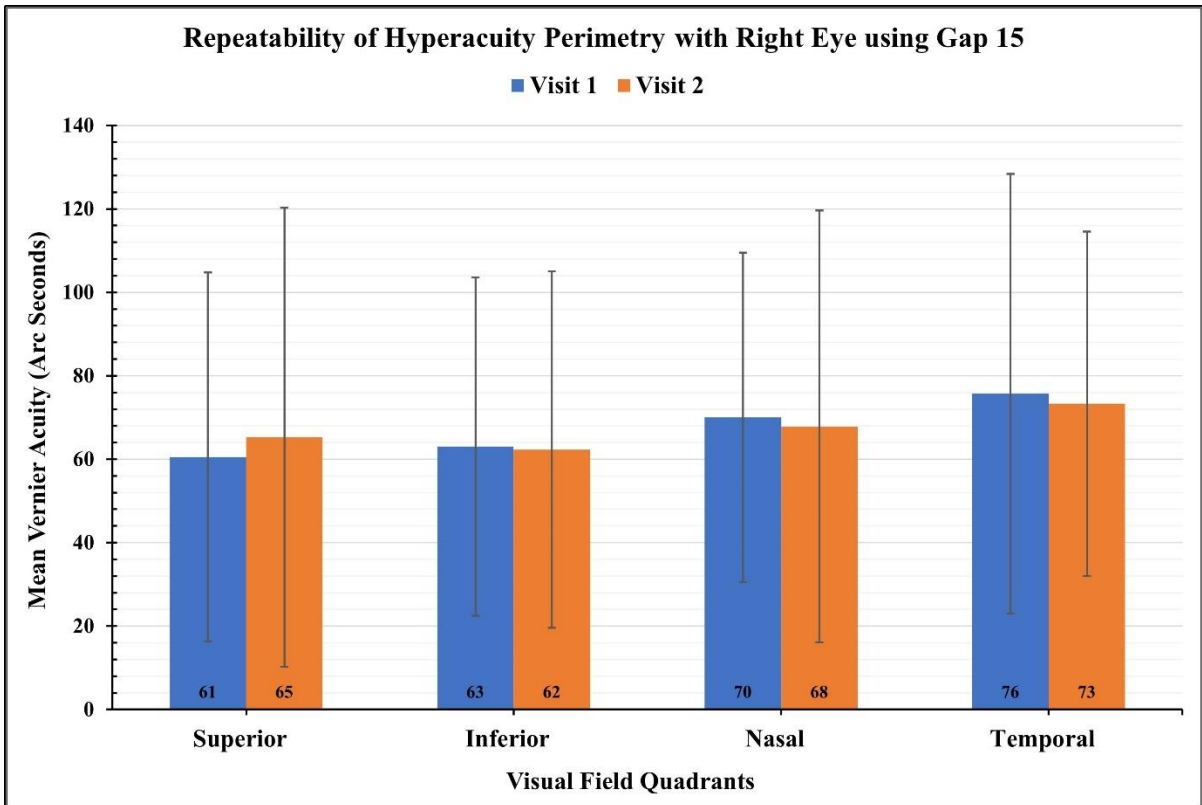


Figure 4-4 Repeatability of Hyperacuity Perimetry with right eye using 15 gap size.

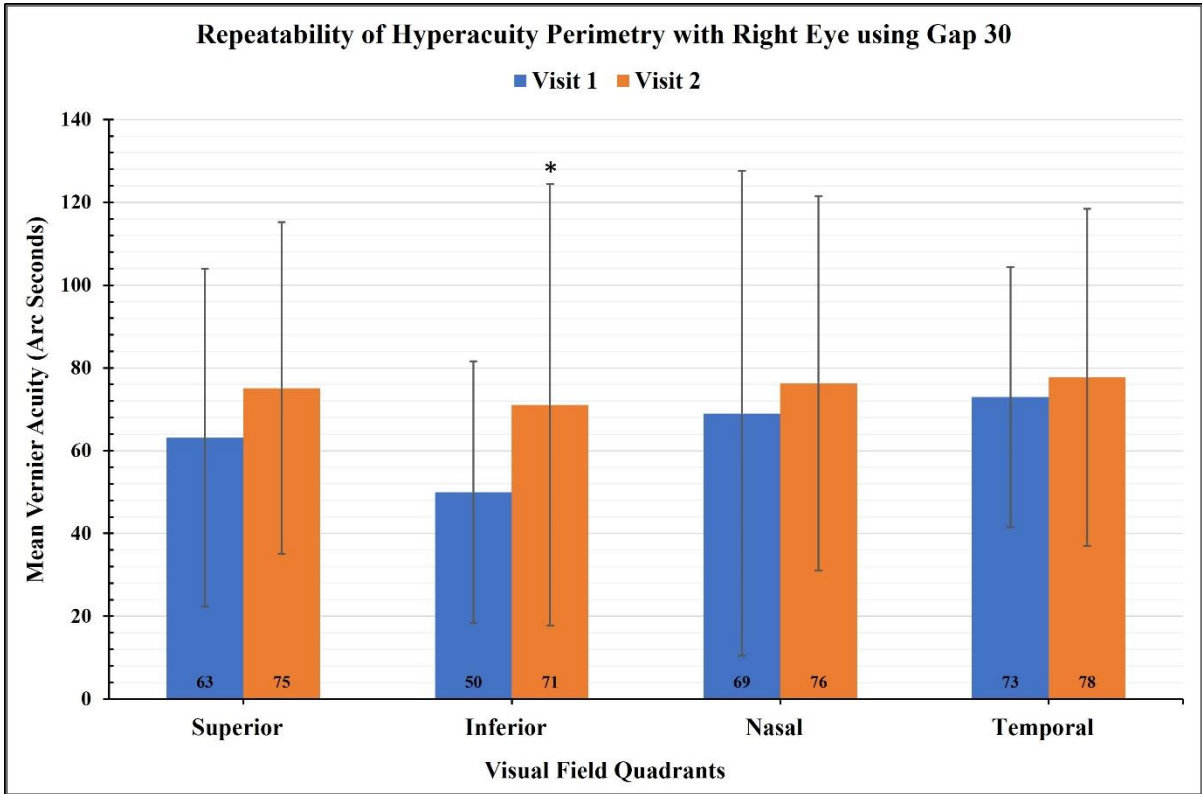


Figure 4-5 Repeatability of Hyperacuity Perimetry with right eye using 30 gap size.

Table 4-3 Repeatability of Hyperacuity Perimetry using right eye.

Right Eye Hyperacuity Perimetry Repeatability					
<i>Gap Size 15</i>			Mean Difference	p-value (<0.05)	ICC
Visual Fields	Visit 1 Mean ± SD (Arc Seconds)	Visit 2 Mean ± SD (Arc Seconds)			
Superior Field	61 ± 44	65 ± 55	4	0.86	-0.31
Inferior Field	63 ± 41	62 ± 43	-1	0.73	0.14
Nasal Field	70 ± 40	68 ± 52	-2	0.75	0.35
Temporal Field	76 ± 53	73 ± 41	-3	0.99	0.41
<i>Gap Size 30</i>					
Superior Field	63 ± 41	75 ± 40	12	0.22	0.53
Inferior Field	50 ± 32	71 ± 53	21	0.01*	0.42
Nasal Field	69 ± 59	76 ± 45	7	0.28	0.28
Temporal Field	73 ± 31	78 ± 41	5	0.86	0.29

4.3.4 Left Eyes HP (Visit 1)

At visit 1, the mean VeT measured with left eyes for eccentric 5 degrees in all four viewing quadrants were plotted at 15 and 30 gap sizes.

The highest thresholds of 71 arc seconds were observed at the temporal fields for 15 gap size and 81 arc seconds for the nasal field at 30 gap size. In the superior field, the lowest thresholds for 15 and 30 gap sizes were 50 and 66 arc seconds, respectively. When the mean left eye thresholds were compared between gap sizes at all visual fields, there was a significant difference seen at superior, inferior, and nasal visual fields (p<0.05)

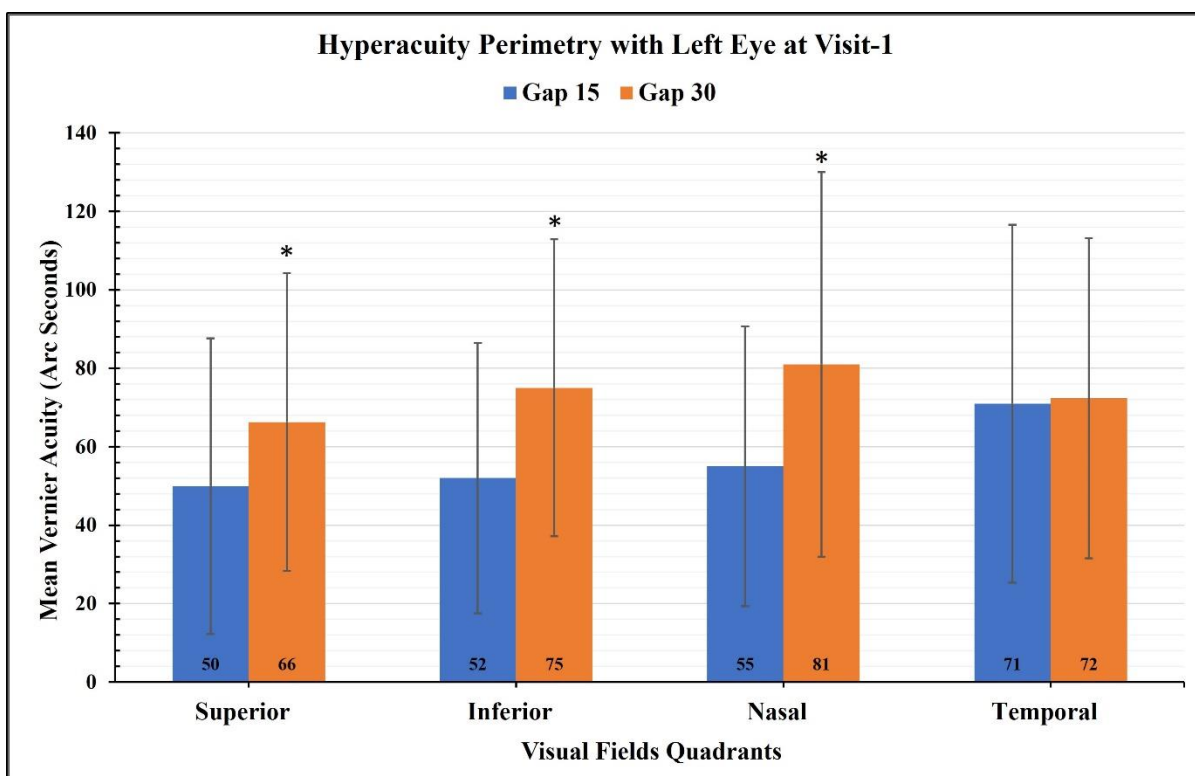


Figure 4-6 Hyperacuity Perimetry with left eyes for eccentric 5 degrees across four viewing quadrants using 15 and 30 gap sizes at Visit 1.

Table 4-4 Left eye Hyperacuity Perimetry comparison between the gap sizes at visit 1.

Hyperacuity Perimetry with Left Eye at Visit-1				
Visual Fields	Gap 15	Gap 30	Mean Difference	p-value (<0.05)
	Mean ± SD (Arc Seconds)	Mean ± SD (Arc Seconds)		
Superior Field	50 ± 38	66 ± 38	16	0.03*
Inferior Field	52 ± 34	75 ± 38	23	0.02*
Nasal Field	55 ± 36	81 ± 49	26	0.00*
Temporal Field	71 ± 46	72 ± 41	1	0.89

4.3.5 Left Eyes HP (Visit 2)

At visit 2, the mean VeT measured with left eyes for eccentric 5 degrees in all four viewing quadrants were plotted at 15 and 30 gap sizes.

The highest thresholds of 87 and 88 arc seconds were observed at the nasal fields for 15 and 30 gap sizes, respectively. The superior field had the lowest threshold of 64 arc seconds for a 15-gap size, whereas the inferior field had the lowest threshold of 77 arc minutes for 30 gap size. No significant difference was found after comparing the visual fields for both gap sizes at visit 2 ($p>0.05$).

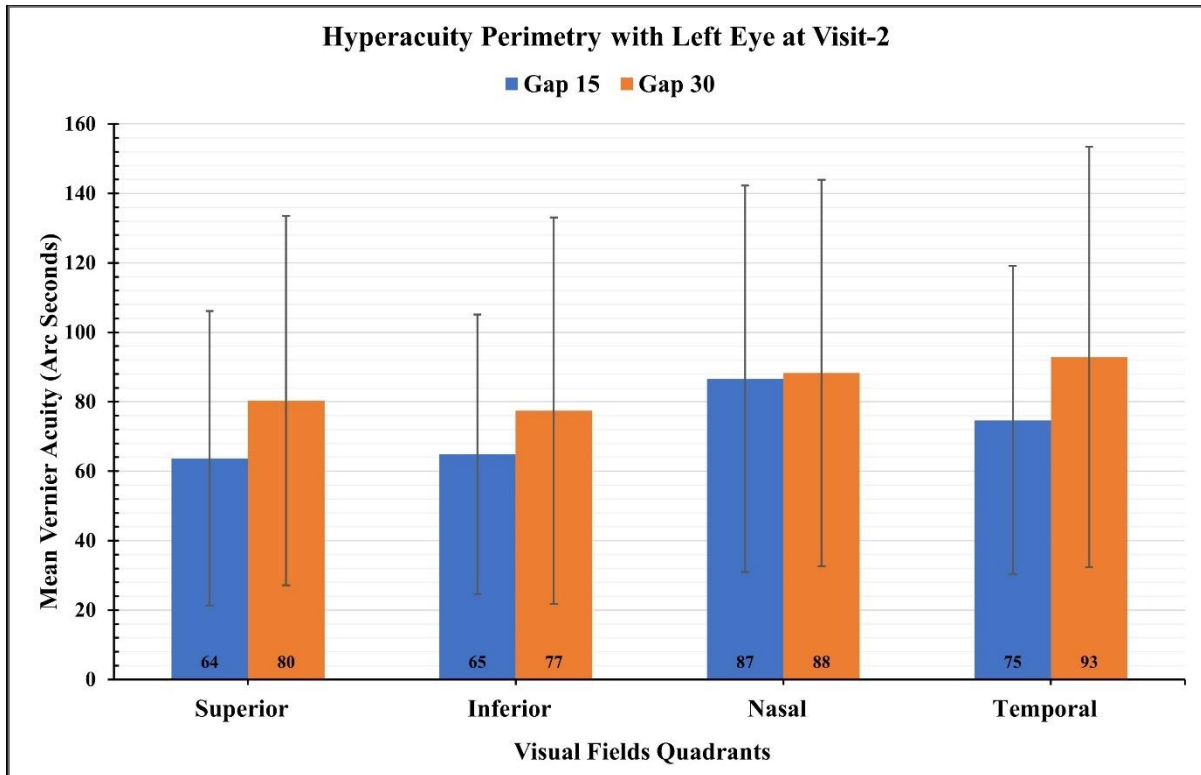


Figure 4-7 Hyperacuity Perimetry with left eyes for eccentric 5 degrees across four viewing quadrants using 15 and 30 gap sizes at Visit 2.

Table 4-4 Left eye Hyperacuity Perimetry comparison between the gap sizes at visit 2.

Hyperacuity Perimetry with Left Eye at Visit-2				
Visual Fields	Gap 15	Gap 30	Mean Difference	p-value (<0.05)
	Mean ± SD (Arc Seconds)	Mean ± SD (Arc Seconds)		
Superior Field	64 ± 42	80 ± 53	16	0.23
Inferior Field	65 ± 40	77 ± 56	12	0.38
Nasal Field	87 ± 56	88 ± 56	1	0.80
Temporal Field	75 ± 44	93 ± 61	18	0.08

4.3.6 Left Eyes (Repeatability)

To test for repeatability, the VeT of the left eye was compared between two visits. At the 15-gap size, the highest thresholds were obtained at the temporal field, with 71 arc seconds for visit 1, and the nasal field, with 87 arc seconds for visit 2. The lowest thresholds were found at the superior and inferior fields, with 61 and 62 arc seconds for visits 1 and 2, respectively. At the 30-gap size, the highest thresholds were obtained at the nasal field, with 81 arc seconds for visit 1 and 93 arc seconds at the temporal field for visit 2. The lowest thresholds were found at the superior field, with 66 arc seconds for visit 1, and inferior fields, with 77 arc seconds for visit 2. A significant difference was observed between the nasal field of the left eye for the 15-gap size ($p = 0.02$). No significant difference was seen between the visits of all four visual fields of the left eye for the 30-gap size ($p > 0.05$). Interclass correlation (ICC) analysis was performed to test the reliability of the results between visits. The ICC showed positive but poor correlations at both gap sizes for all fields.

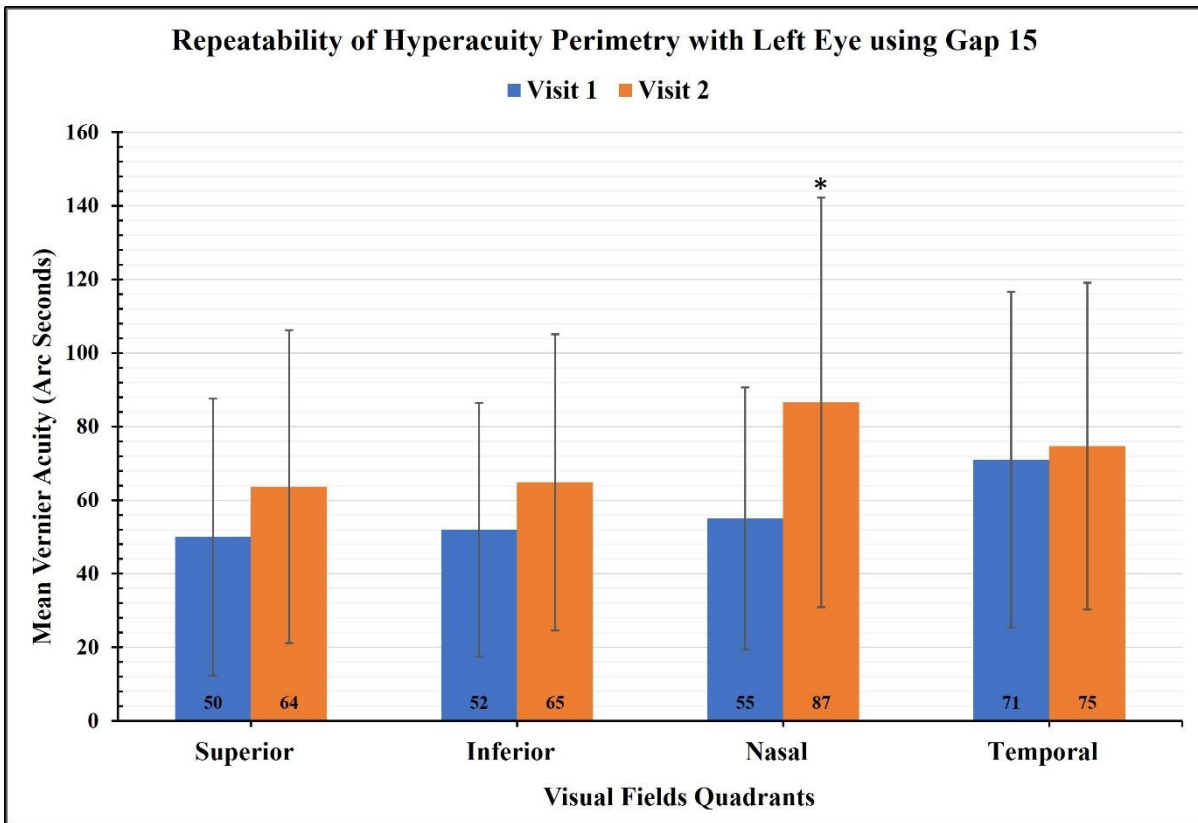


Figure 4-8 Repeatability of Hyperacuity Perimetry with left eye using gap 15.

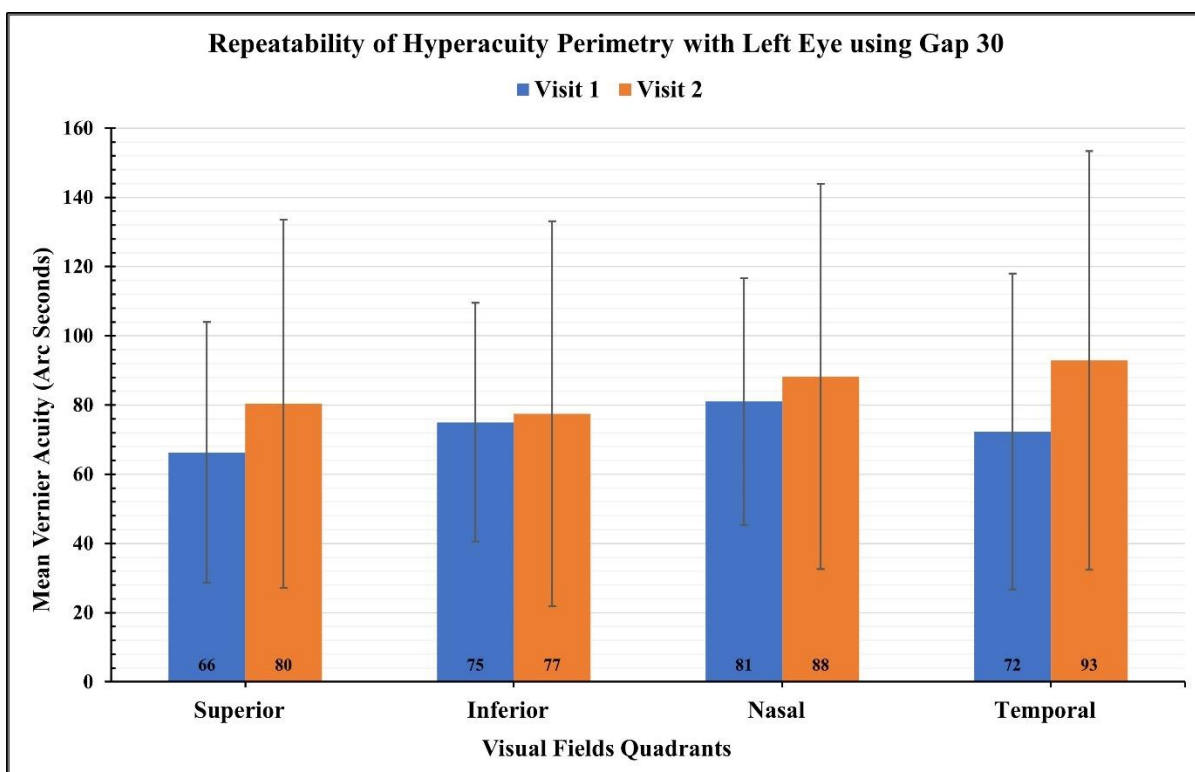


Figure 4-9 Repeatability of Hyperacuity Perimetry with left eye using gap 30.

Table 4-5 Comparison of Hyperacuity Perimetry between the visits for both gap sizes.

Left Eye Hyperacuity Perimetry Repeatability					
<i>Gap Size 15</i>					
Visual Fields	Visit 1	Visit 2	Mean Difference	p-value (<0.05)	ICC
	Mean ± SD (Arc Seconds)	Mean ± SD (Arc Seconds)			
Superior Field	50 ± 38	64 ± 42	14	0.13	0.10
Inferior Field	52 ± 34	65 ± 40	13	0.21	0.29
Nasal Field	55 ± 36	87 ± 56	32	0.02*	0.19
Temporal Field	71 ± 46	75 ± 44	4	0.77	0.13
<i>Gap Size 30</i>					
Superior Field	66 ± 38	80 ± 53	14	0.40	0.31
Inferior Field	75 ± 38	77 ± 56	2	0.86	0.23
Nasal Field	81 ± 49	88 ± 56	7	0.73	0.41
Temporal Field	72 ± 41	93 ± 61	21	0.11	0.35

4.3.7 Right Eyes Verses Left Eyes

4.3.7.1 Visit 1

At visit 1, the mean VeT of all four directional quadrants were compared between the right and left eye at 15 and 30 gap sizes.

At 15 gap size, the highest thresholds of 76 and 71 arc seconds were observed at the temporal field of right and left eye, respectively. While the lowest thresholds of 61 and 50 arc seconds were observed at the superior field for the right and left eye, respectively.

At 30 gap size, the highest threshold of 73 arc seconds was observed in the temporal field of the right eye and 81 arc seconds in the nasal field of the left eye. While the lowest threshold of 50 arc seconds was observed in the nasal field of the right eye and 66 arc seconds in the superior field of the left eye.

There was no statistical difference between the eyes for VeT at all the visual fields of 15 gap size. However, for the 30-gap size, there was a statistical difference between the eyes for VeT only in inferior visual field ($p < 0.05$).

Table 4-6 Comparison of Hyperacuity perimetry between eyes at visit 1.

Hyperacuity Perimetry Symmetry Between Eyes at Visit-1				
<i>Gap Size 15</i>	Right Eye	Left Eye	Mean Difference	p-value (<0.05)
Visual Fields	Mean ± SD (Arc Seconds)	Mean ± SD (Arc Seconds)		
Superior Field	61 ± 44	50 ± 38	-11	0.43
Inferior Field	63 ± 41	52 ± 34	-11	0.20
Nasal Field	70 ± 40	55 ± 36	-15	0.07
Temporal Field	76 ± 53	71 ± 46	-5	0.78
<i>Gap Size 30</i>				
Superior Field	63 ± 41	66 ± 38	3	0.89
Inferior Field	50 ± 32	75 ± 38	25	0.02*
Nasal Field	69 ± 59	81 ± 49	12	0.28
Temporal Field	73 ± 31	72 ± 41	-1	0.94

4.3.7.2 Visit 2

At 15 gap size, the highest threshold of 73 arc seconds was observed in the temporal field of the right eye and 87 arc seconds in the nasal field of the left eye. While the lowest thresholds of 62 arc seconds

were observed in the inferior field of the right eye and 64 arc seconds in the superior field of the left eye. At 30 gap size, the highest threshold of 78 and 93 arc seconds was observed in the right and left eye temporal fields, respectively. At the same time, the lowest thresholds of 71 and 77 arc seconds were observed in the inferior field of the right and left eye, respectively. There was no statistical difference between the eyes for VeT at all the visual fields of 15 and 30 gap sizes.

The test took about half an hour for each participant, approximately 10-15 minutes for each eye. Each gap size took about 2 minutes to complete testing. Therefore, it would take about 5 minutes to complete testing VeT at a given gap size for both eyes.

Table 4-7 Comparison of Hyperacuity perimetry between eyes at visit 2.

Hyperacuity Perimetry Symmetry Between Eyes at Visit-2				
<i>Gap Size 15</i>	Right Eye	Left Eye	Mean Difference	p-value (<0.05)
Visual Fields	Mean ± SD (Arc Seconds)	Mean ± SD (Arc Seconds)		
Superior Field	65 ± 55	64 ± 42	-1	0.95
Inferior Field	62 ± 43	65 ± 40	3	0.45
Nasal Field	68 ± 52	87 ± 56	19	0.08
Temporal Field	73 ± 41	75 ± 44	2	0.91
<i>Gap Size 30</i>				
Superior Field	75 ± 40	80 ± 53	5	0.99
Inferior Field	71 ± 53	77 ± 56	6	0.94
Nasal Field	76 ± 45	88 ± 56	12	0.39
Temporal Field	78 ± 41	93 ± 61	15	0.34

4.4 Discussion

In my investigation, I thoroughly assessed VeT with an eccentricity of 5 degrees in all four quadrants of the retina utilizing gap sizes of 15 and 30 arc minutes. Our analysis revealed some interesting findings. At 15 arc minutes of gap size, the right eyes showed a consistent pattern and demonstrated a positive correlation (weak) in all visual fields except the superior field, where the correlation was negative (weak). When I increased the gap size to 30 arc minutes, the right eyes remained consistent in all visual fields except the inferior field. The correlation remained positive but weak in all visual fields except the superior field, where it was moderate. Similarly, when 15 arc minutes of gap size was used, the left eyes VeT were reliable in all visual fields except the nasal field. The correlation stayed positive

but weak in all visual fields. However, when I increased the gap size to 30 arc minutes, the left eyes were consistent, revealing a positive but weak correlation in all visual fields. However, a detailed study is necessary to provide conclusive results. The results from the study indicate that the software application program can reliably measure VeT in the parafoveal area. Therefore, it can be further tested for clinical validation.

4.5 Conclusion

I developed an HP program to quantify central 5 degrees of eccentricity visual field in four quadrants using Vernier acuity task. The program measured the eccentric Vernier acuity using 15 and 30 gap sizes and the results indicate asymmetry between the eyes for reliability for gap sizes. Additional testing may provide evidence to verify the findings.

Chapter 5

Metamorphopsia

5.1 Introduction

This chapter focuses on another macular function, namely visual distortions, commonly called metamorphopsia (MMP), which means ‘seeing mutated shapes’ in Greek. Visual distortions in certain vision abnormalities, including maculopathies and myopia, are likely to occur in the central visual field. They usually occur in the central visual field when the alignment of photoreceptors in the macula is altered due to underlying pathology resulting in distortions in the vision fields. In addition, they may also occur because of abnormal cortical processing. It can be experienced in several forms, such as misrepresenting the viewing scene, the object appearing wavy, or the shape appearing smaller, called micropsia, or larger, called macropsia^{130,179-182}.

Clinicians commonly rely on the Amsler grid test to evaluate visual field distortions in the central 20 degrees. The test entails projecting a thin vertical and horizontal dark grid on a white background with a central fixation target onto the central retina. An abnormality in the macular region can cause straight lines to appear tilted, wavy, or wiggly in the visual space. Patients can mark any affected areas they perceive on a grid to assess these distortions while focusing on the central target. It is essentially a bisection Vernier task, where the patient is essentially making the alignment judgment of vertical and horizontal lines of a grid. This is a simple and qualitative way to rapidly evaluate macular abnormality within the central 20 degrees of vision^{130,183}.

However, it is important to note that even though the Amsler test can evaluate macular abnormalities, its effectiveness in detecting early MMP is limited. The test relies on subjective responses and is therefore susceptible to errors. Another potential challenge is the crowding effect caused by the surrounding vertical and horizontal lines, making pinpointing the affected area challenging. Peripheral cues may aid in identifying distorted areas, but it is important to consider the patient’s psychological factors, which could potentially influence the test results¹⁷⁹. A recently published systematic review and meta-analysis on the diagnostic accuracy of the Amsler grid test for detecting neovascular age-related macular degeneration concluded that despite being inexpensive and easy for self-assessment use, it is not sensitive enough for monitoring the condition. It offers lower sensitivity and moderate specificity to identify the neovascular AMD population¹⁸⁴.

There are many attempts made in the literature to detect and quantify metamorphopsia early. In addition, several digital testing through computer and smartphone applications were proposed for home monitoring applications^{183,184}. However, most of them are not thoroughly tested and clinically validated^{179,181}. This chapter further extended our Vernier acuity protocols for quantifying MMP.

As I developed and validated Vernier acuity testing programs in this thesis, I plan to extend the Vernier acuity testing in this chapter.

I developed a software application program that can perform Vernier bisection testing with negligible crowding effect and peripheral cues to efficiently measure the MMP. In addition, I measured the thresholds using line stimuli in two different orientation patterns and compared them to assess the optimum pattern for clinical testing. The estimated MMP thresholds from healthy subjects can provide normative data that can be further helpful in determining the disease-related abnormality in the visual function.

5.2 Method

5.2.1 Study Subjects

Please refer to section 3.2.2

5.2.2 Experimental Setup

Please refer to section 3.2.3

5.2.3 Software Application

Please refer to section 2.4

5.2.4 Stimuli Configuration

All the experimental stimuli characteristics were calibrated in visual angle units; a line stimulus subtended 3×30 (width x height) in arcminutes, whereas an adjustable cross stimulus subtended 15 arcminutes.

5.2.5 The Method of Adjustment (MOA)

The MOA is a simple psychophysical procedure that involves stimuli alignment using a computer keyboard at every presentation and does not require repeated measurements. Therefore, it is time

efficient. This test involved a 5 alternative forced choice technique. It should be noted that even though MOA does not give the most reliable thresholds, I used this method in the interest of testing time minimization.

5.2.6 Gap Sizes

To estimate MMP, I employed Vernier acuity-based bi-directional alignment task in the central 5 degrees visual field. (Figure) This study involved extended perpendicular lines with a point of intersection at the center of the screen. A gap is formed between the lines when the middle segment of perpendicular lines is removed from the point of intersection to appear as four-line stimuli equidistant from the screen center (2 vertical and 2 horizontal). These lines form a bi-directional Vernier pattern at the screen center. I used this pattern to measure MMP in two orientations: pattern forming 45 degrees ('×'), and pattern B, forming a 90-degree ('+') angle from the screen center. Both the patterns were measured for 1, 2, 3, 4, and 5 degrees of visual angle. The sequence of stimuli presentations was randomized to minimize the measurement bias.

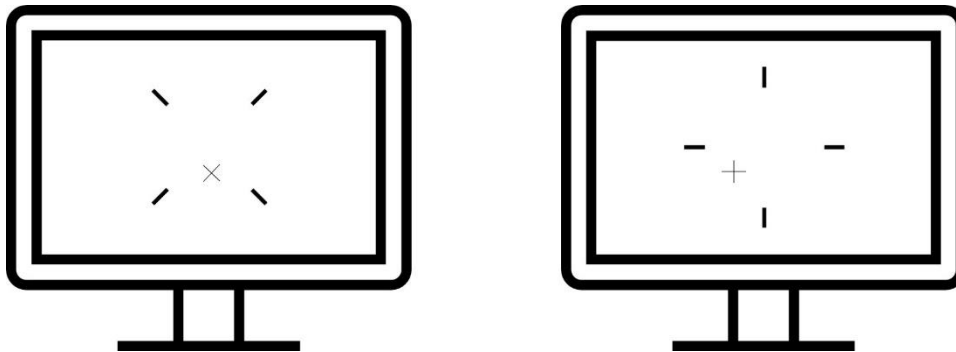


Figure 5-1 Stimuli presentation on screen for pattern A (left) and pattern B (right)

5.2.7 Experiment Testing

The testing was performed monocularly while the fellow eye was completely patched with a dark occluder. The experimental procedure involved 10 stimuli presentations: patterns A and B at ten central visual field locations. A small adjustable plus shape '+' stimuli were positioned randomly within the 1.5 degrees circumference of the screen center. During each presentation, the four-line stimuli and adjustable stimuli were presented together. The subjects were instructed to judge the alignment of

stimuli relating to the surrounding lines and move it to the point of intersection using the four arrow keys on the computer keyboard. After aligning the movable stimuli with the point of intersection, the subjects were instructed to press the space key to confirm their alignment judgment. To ensure visual comparability between the center and surrounding stimuli for proper alignment, the orientation of the adjustable stimuli was paired with the surrounding stimuli pattern.

5.2.8 Data Interpretation

The threshold is the Euclidean distance between the actual center to the subject's adjusted center and is measured in arcminutes of visual angle. The lower threshold value implies good precision and vice versa.

5.2.9 Data Analysis

Same as section 3.3.3

5.3 Results

5.3.1 Right Eye MMP (Visit 1)

At visit 1, the mean thresholds measured with right eyes across central 5 degrees using patterns A and B were plotted. The MMP thresholds measured using pattern-B were relatively lower across central 5 degrees, suggesting the MMP sensitivity for pattern-B is relatively high.

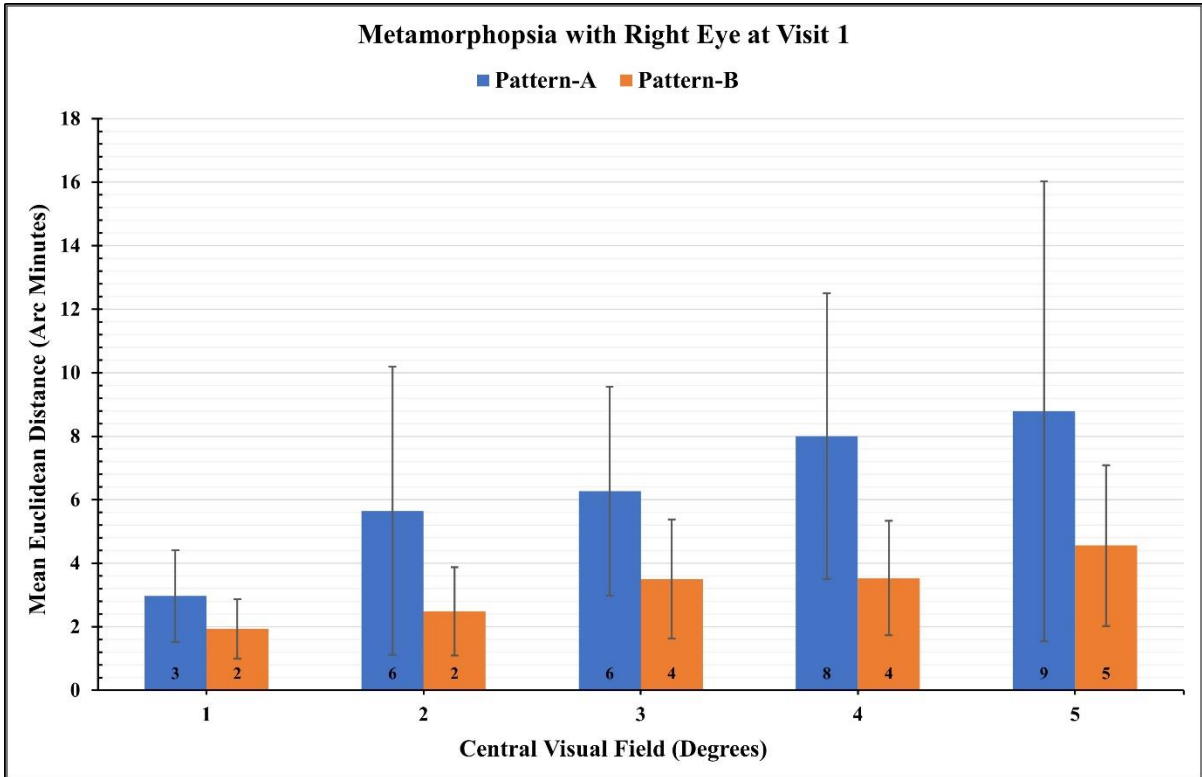


Figure 5-2 Mean MMP thresholds measured with right eyes across central 5 degrees using patterns A and B at visit 1.

5.3.2 Right Eye MMP (Visit 2)

At visit 2, the mean thresholds measured with right eyes across central 5 degrees using patterns A and B were plotted. The MMP thresholds measured using pattern were relatively lower across central 5 degrees, suggesting the MMP sensitivity for pattern-B is relatively high.

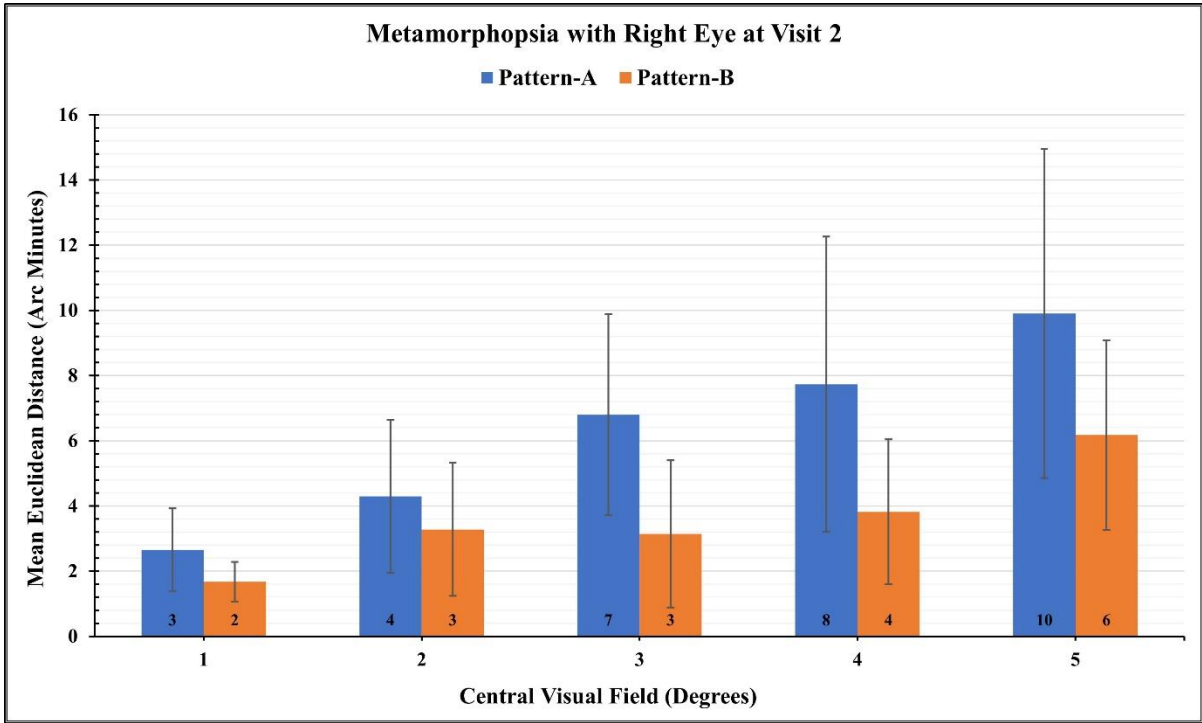


Figure 5-3 Mean MMP thresholds measured with right eyes across central 5 degrees using patterns A and B at visit 2.

5.3.3 Right Eye MMP (Repeatability)

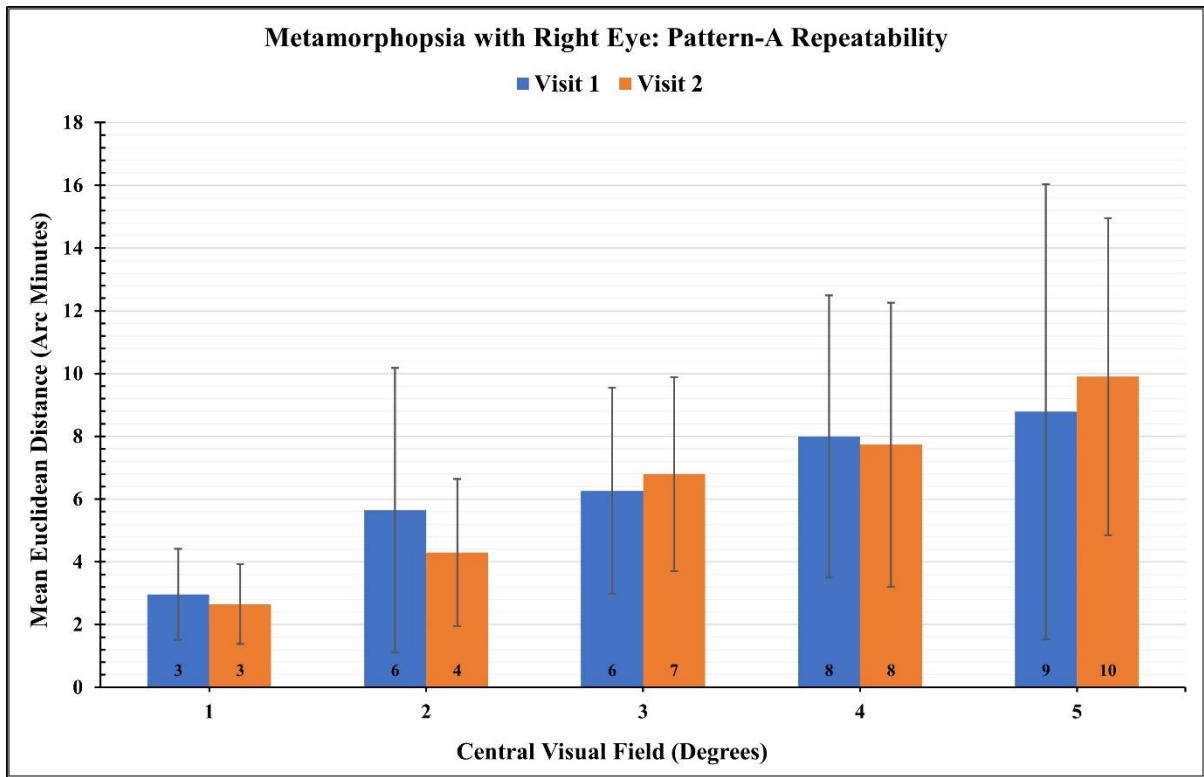


Figure 5-4 Repeatability of Metamorphopsia with right eye for pattern-A.

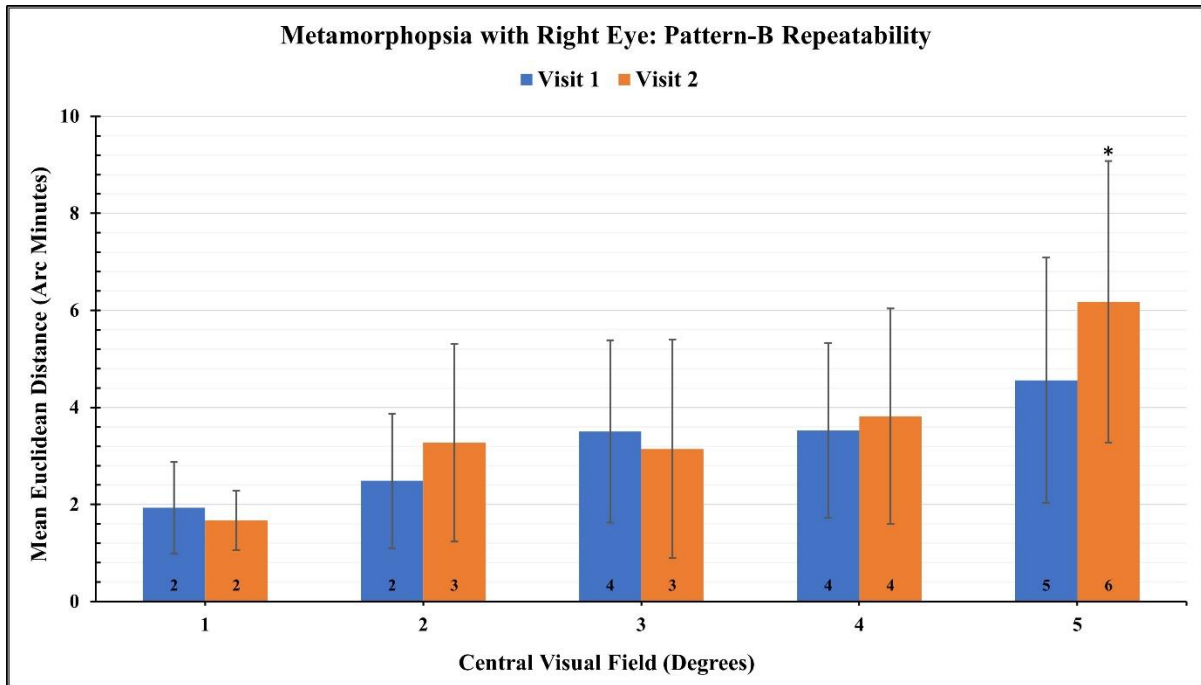


Figure 5-5 Repeatability of Metamorphopsia with right eye for pattern-B.

In the right eyes, the mean thresholds were measured at 5,4,3,2 and 1 degrees from the center at visit 1 and visit 2 for patterns A and B.

For pattern-A, the highest thresholds were observed at 5 degrees with 9 and 10 arcminutes of visit 1 and visit 2, respectively. Similarly, the highest thresholds for pattern B were observed at 5 degrees with 5 and 6 arcminutes of visit 1 and visit 2, respectively. At the same time, the lowest threshold for pattern A was 3 arcminutes at 1 degrees of visits 1 and 2. Similarly, the lowest thresholds for pattern B were observed at 1 degrees with 2 arcminutes of visit 1 and visit 2, respectively. When the mean thresholds from visit 1 and visit 2 were compared for differences for both patterns, there was no significant difference seen ($p > 0.05$) except for the 5 degrees of pattern B, where the thresholds were significantly different ($p = 0.03$). Interclass correlation analysis was performed to assess the reliability of the test results between visit 1 and visit 2; ICC showed positive but weak correlations for all except 5 and 1 degrees for pattern A and 3 and 2 degrees for pattern B which showed a negative correlation.

Table 5-1 Repeatability of MMP using pattern A and pattern B for right eye.

Pattern A		Metamorphopsia with Right Eye			
Visual Field (Degrees)	Visit 1	Visit 2	Mean Difference	p-value (<0.05)	ICC
	Mean ± SD (Arc Minutes)	Mean ± SD (Arc Minutes)			
5	9 ± 7	10 ± 5	1.1	0.39	-0.14
4	8 ± 4	8 ± 5	-0.3	0.81	0.39
3	6 ± 3	7 ± 3	0.5	0.56	0.16
2	6 ± 5	4 ± 2	-1.4	0.35	0.09
1	3 ± 1	3 ± 1	-0.3	0.48	-0.12
Pattern B		Metamorphopsia with Right Eye			
5	5 ± 3	6 ± 3	1.6	0.03*	0.15
4	4 ± 2	4 ± 2	0.3	0.59	0.23
3	4 ± 2	3 ± 2	-0.4	0.53	-0.39
2	2 ± 1	3 ± 2	0.8	0.14	-0.03
1	2 ± 1	2 ± 1	-0.3	0.30	0.24

5.3.4 Left Eye MMP (Visit 1)

At visit 1, the mean thresholds measured with left eyes across central 5 degrees using patterns A and B were plotted. The MMP thresholds measured using pattern-B were relatively lower across central 5 degrees, suggesting the MMP sensitivity for pattern-B is relatively high.

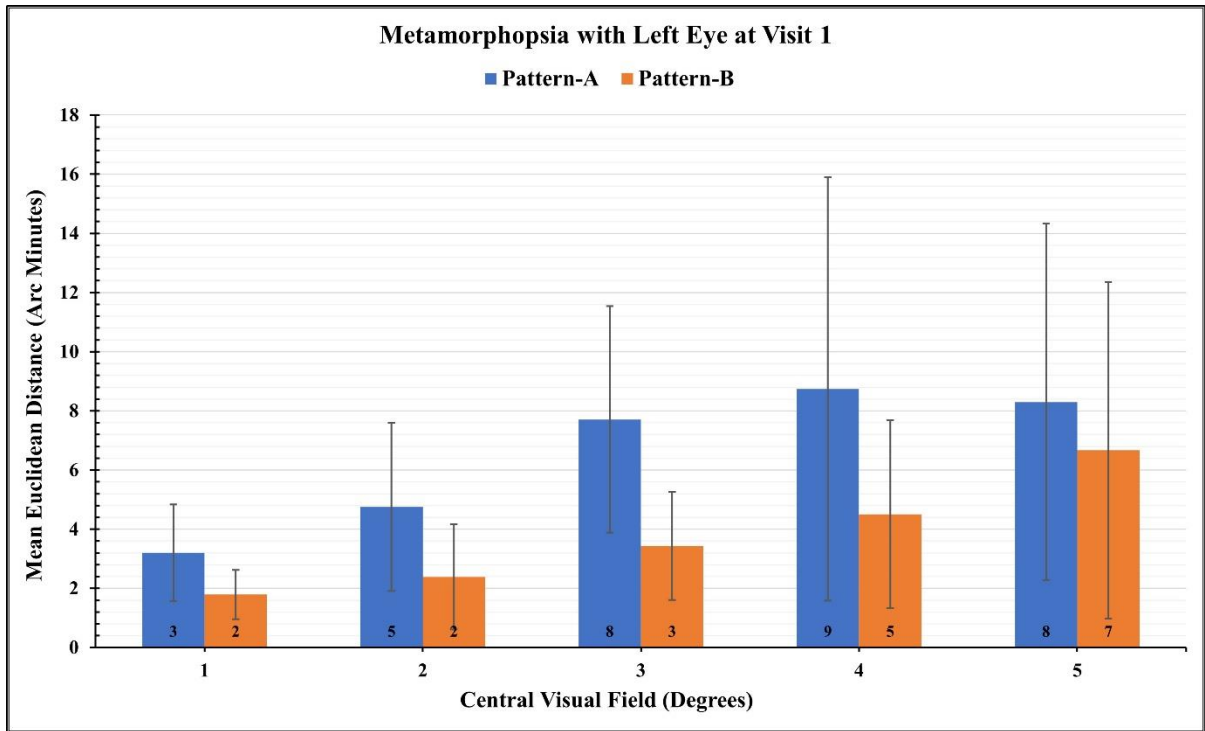


Figure 5-6 Mean MMP thresholds measured with left eye across central 5 degrees using patterns A and B at visit 1.

5.3.5 Left Eye MMP (Visit 2)

At visit 2, the mean thresholds measured with left eyes across central 5 degrees using patterns A and B were plotted. The MMP thresholds measured using pattern-B were relatively lower across central 5 degrees, suggesting the MMP sensitivity for pattern-B is relatively high.

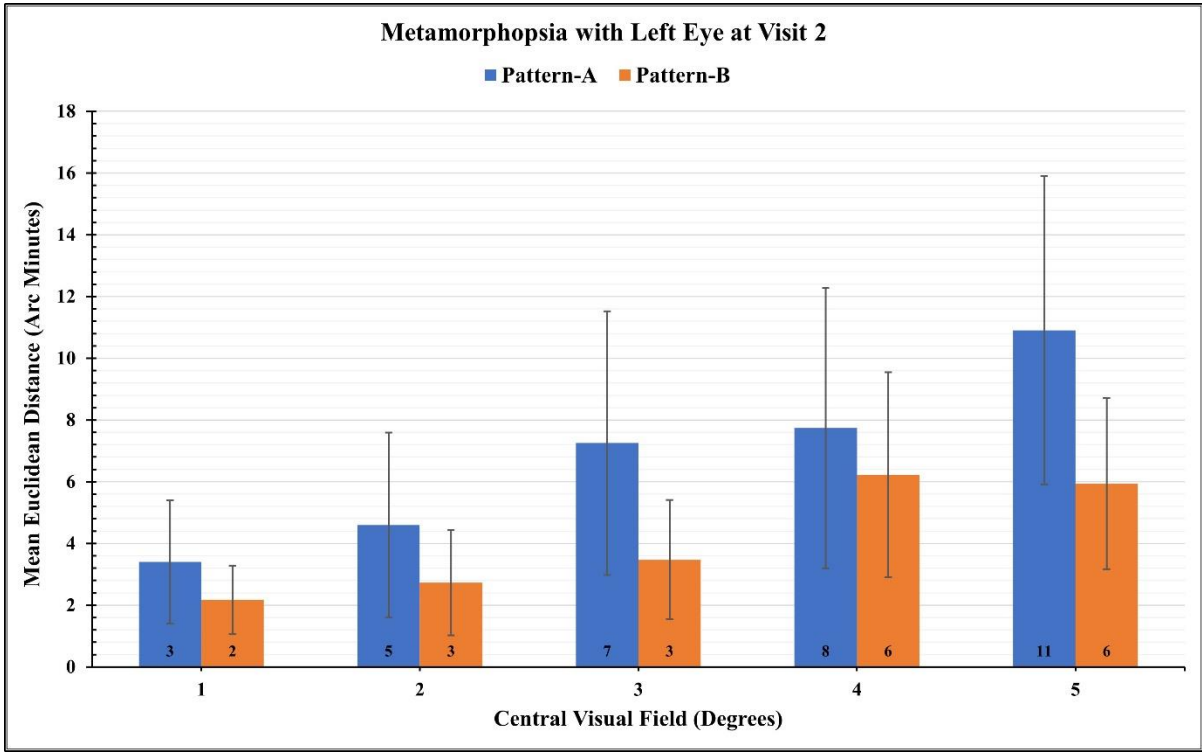


Figure 5-7 Mean MMP thresholds measured with left eye across central 5 degrees using patterns A and B at visit 2.

5.3.6 Left Eye MMP (Repeatability)

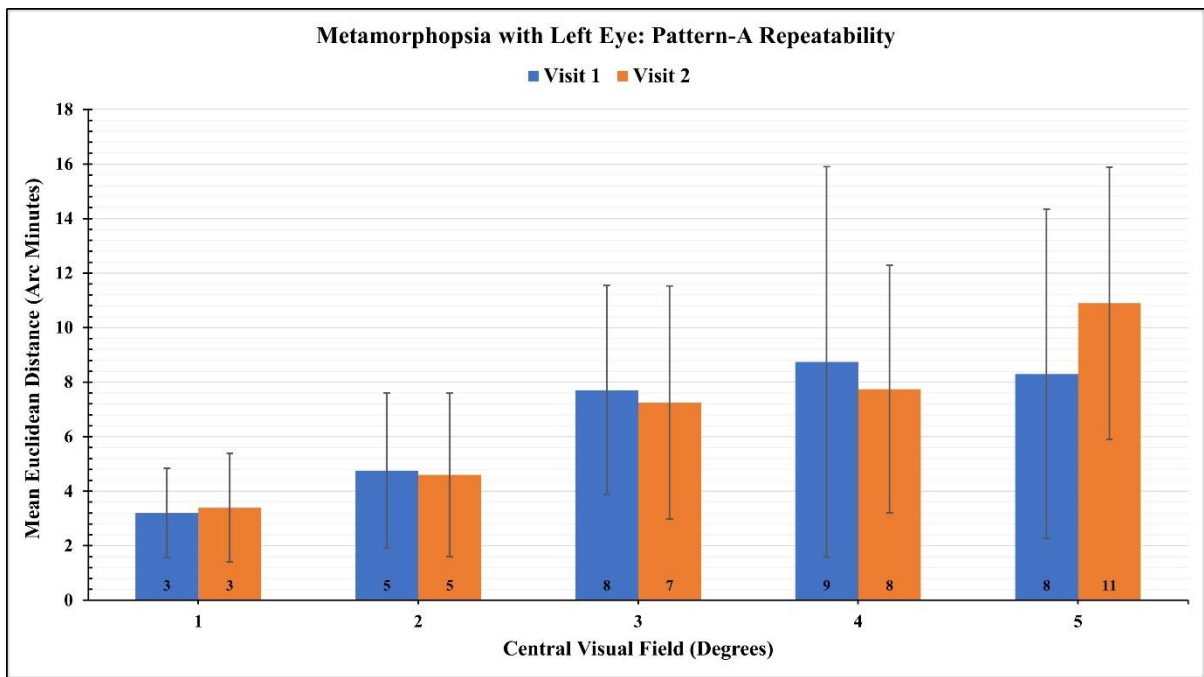


Figure 5-8 Comparison of left eye MMP patter-A.

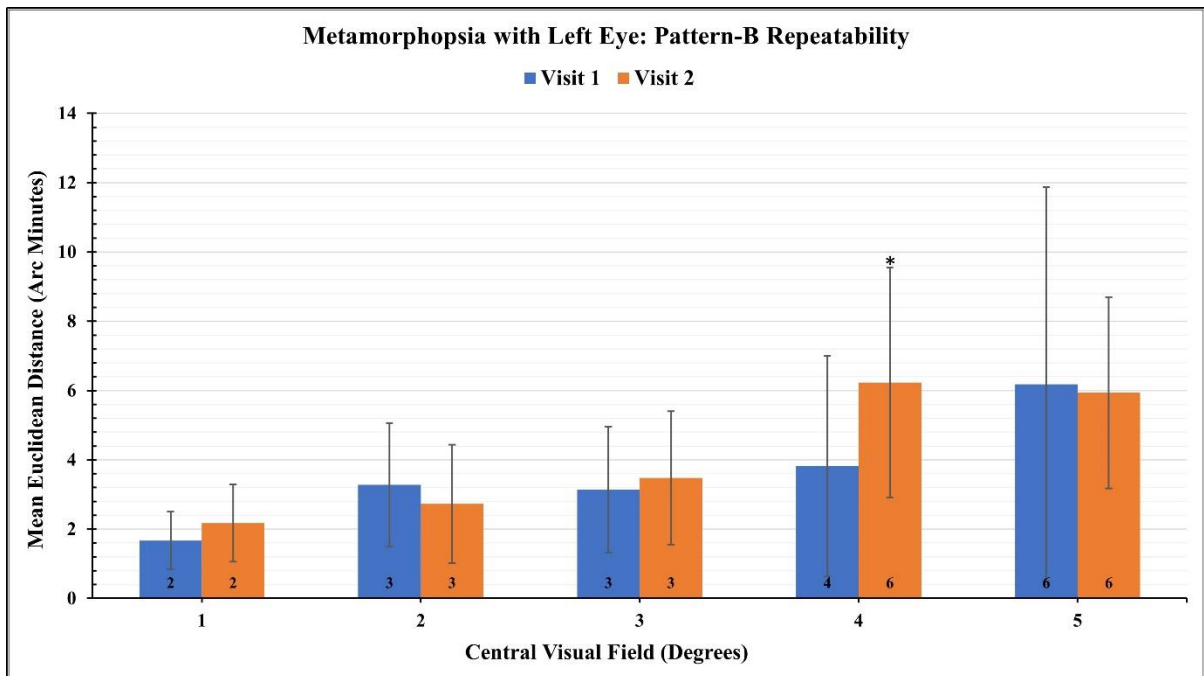


Figure 5-9 Comparison of left eye MMP patter-B.

In the left eyes, the mean thresholds were measured at 5,4,3,2 and 1 degrees of visual angle from the center at visit 1 and visit 2 for patterns A and B.

For pattern A, the highest thresholds were observed at 5 degrees with 8 and 11 arcminutes of visit 1 and visit 2, respectively. Similarly, the highest thresholds for pattern B were observed at 5 degrees with 7 and 6 arcminutes of visit 1 and visit 2, respectively. The lowest threshold for pattern A was 3 arcminutes at 1 degrees of visit 1 and visit 2. Similarly, the lowest thresholds for pattern B were observed at 1 degree with 2 arcminutes of visit 1 and visit 2. When the mean thresholds from visit 1 and visit 2 were compared for differences for both patterns, there was no significant difference seen ($p > 0.05$) except for the 4 degrees of pattern B, where the thresholds were significantly different ($p = 0.03$). Interclass correlation analysis was performed to assess the reliability of the test results between visit 1 and visit 2; ICC showed positive and moderate to strong correlations across 5 degrees for both patterns A and B.

Table 5-2 Repeatability of MMP using pattern A and pattern B for left eye.

Pattern A		Metamorphopsia with Left Eye			
Visual Field (Degrees)	Visit 1	Visit 2	Mean Difference	p-value (<0.05)	ICC
	Mean ± SD (Arc Minutes)	Mean ± SD (Arc Minutes)			
5	8 ± 6	11 ± 5	2.6	0.07	0.38
4	9 ± 7	8 ± 5	-1.0	0.58	0.31
3	8 ± 4	7 ± 4	-0.5	0.61	0.50
2	5 ± 3	5 ± 3	-0.2	0.84	0.24
1	3 ± 2	3 ± 2	0.2	0.93	0.76
Pattern B		Metamorphopsia with Left Eye			
5	7 ± 6	6 ± 3	-0.7	0.73	0.59
4	5 ± 3	6 ± 3	1.7	0.03*	0.39
3	3 ± 2	3 ± 2	0.0	0.68	0.39
2	2 ± 2	3 ± 2	0.3	0.33	0.60
1	2 ± 1	2 ± 1	0.4	0.10	0.45

5.3.7 Symmetry Between Eyes

When compared between the right eye and left eye for visit 1, for pattern A, the highest mean thresholds with the right eyes were 9 arcminutes at 5 degrees, and left eyes were at 9 arcminutes at 4 degrees. Similarly, for pattern B the highest thresholds with the right eyes were 6 arcminutes at 5 degrees and 7 arcminutes at 5 degrees with the left eyes. The lowest thresholds for pattern A were 3 arc minutes at 1 degrees in both the right and left eye, and for pattern B were 2 arc minutes at 1 and 2 degrees in both eyes. When results between the right and left eye were compared from visit 1, no statistically significant difference was seen between eyes for both pattern-A and pattern-B ($p > 0.05$).

Table 5-3 MMP Symmetry between the eyes for patter A and B at visit 1

Pattern A Metamorphopsia Symmetry Between Eyes at Visit 1				
Visual Field (Degrees)	Right Eye	Left Eye	Mean Difference	p-value (<0.05)
	Mean ± SD (Arc Minutes)	Mean ± SD (Arc Minutes)		
5	9 ± 7	8 ± 6	-0.5	0.88
4	8 ± 4	9 ± 7	0.7	0.93
3	6 ± 3	8 ± 4	1.4	0.22
2	6 ± 5	5 ± 3	-0.9	0.83
1	3 ± 1	3 ± 2	0.2	0.62
Pattern B Metamorphopsia Symmetry Between Eyes at Visit 1				
5	5 ± 3	7 ± 6	2.1	0.12
4	4 ± 2	5 ± 3	1.0	0.20
3	4 ± 2	3 ± 2	-0.1	0.97
2	2 ± 1	2 ± 2	-0.1	0.70
1	2 ± 1	2 ± 1	-0.1	0.50

When compared between the right eye and left eye for visit 2, for pattern A, the highest mean thresholds with the right eyes were 10 arc minutes at 5 degrees, and left eyes were at 11 minutes of arc at 5 degrees. Similarly, for pattern B the highest thresholds with the right and left eyes were at 6 minutes of arc at 5 degrees. The lowest thresholds for pattern A were 3 arc minutes at 1 degrees in both the right and left eye, and for pattern B were 2 arc minutes at 1 degrees in both eyes. When results between the right and left eye were compared from visit 2, no statistically significant difference was seen between eyes for pattern-A ($p > 0.05$). While for pattern B, there was no statistically significant difference seen between

the eyes across 5 degrees ($p > 0.05$), except for the 4 and 1 degrees, where a statistically significant difference was seen between the eyes ($p < 0.05$).

Table 5-4 MMP symmetry between eyes for pattenr A and B at visit 2

Pattern A Metamorphopsia Symmetry Between Eyes at Visit 2				
Degrees	Right Eye	Left Eye	Mean Difference	p-value (<0.05)
	Mean ± SD (Arc Minutes)	Mean ± SD (Arc Minutes)		
5	10 ± 5	11 ± 5	1.0	0.58
4	8 ± 5	8 ± 5	0.0	0.97
3	7 ± 3	7 ± 4	0.5	0.65
2	4 ± 2	5 ± 3	0.3	0.71
1	3 ± 1	3 ± 2	0.7	0.11
Pattern B Metamorphopsia Symmetry Between Eyes at Visit 2				
5	6 ± 3	6 ± 3	-0.2	0.75
4	4 ± 2	6 ± 3	2.4	0.00*
3	3 ± 2	3 ± 2	0.3	0.51
2	3 ± 2	3 ± 2	-0.5	0.16
1	2 ± 1	2 ± 1	0.5	0.02*

5.4 Discussion

This study used MOA to measure the MMP in the central 5 degrees of the visual field. MMP thresholds from pattern-A were almost double to those found for pattern B. when measured with the right and left eyes across the central 5 degrees at both visits indicating optimum sensitivity of MMP thresholds for pattern B. This has been investigated in the past and has been discussed briefly in the neural processing of the Vernier acuity section. The pattern-B sensitivity is likely due to the orientation-specific receptive fields in the cortex.

Though the MOA is not the most efficient psychophysical procedure as discussed in the earlier chapters, it was necessary to measure thresholds across multiple locations of visual fields in this study with interest of time. Considering the patient flow in clinical settings, using ASM would have been too time-consuming as it involves measurements from at least 5 to 10 locations. Since I developed a Vernier

acuity software application package, I planned to extend the Vernier acuity utility in the best possible form to quantify the macular functions, including the MMP. Therefore, I chose MOA as it provides rapid threshold readings without repeated measurements, making it more feasible for clinical use. The testing time was measured between 2 to 4 minutes at all 10 locations for an individual eye. The primary objective of this study was to offer a technically advanced tool for assessing MMP than is currently being used.

5.5 Conclusion

I developed MMP software using MOA for 2 different stimuli orientation patterns across central 5 degrees of vision. The testing was rapid and efficient; however, the reliability of the measurements was poor. The program can be further modified to achieve better reliability for clinical applications.

Chapter 6

Conclusion and Future Direction

6.1 Summary of the Dissertation

In this thesis dissertation, the first chapter was focused on providing necessary background information related to the thesis topic. The initial topics highlight the most important structures of the eye that enable vision, including the retina, macula, fovea, and photoreceptors that initiate visual processing. Further, it details the flow of visual information from the eye to the various parts of the brain, where certain vision components, including colour vision, visual fields, and binocular vision, are developed. In addition, the systematic organization of receptive fields at multi-levels facilitates various aspects of visual functions, including visual acuity and visual fields. The following topics emphasize the optical limitations of the eye and discuss sub-topics that contribute as a base for the thesis topic. Before the thesis topic, a brief introduction to visual psychophysics was provided, as it is a tool, I used in this thesis to quantify visual functions. Later, the thesis topic that included hyperacuity, Vernier acuity, the clinical importance of Vernier acuity, and rising global vision impairment due to the lack of sensitive screening tests was introduced. Following that, I discussed the gaps in the literature thoroughly. The conclusion of this chapter includes a thesis plan and a brief overview of the succeeding thesis chapters.

In the second chapter, I briefly discussed a method commonly used in the literature to measure Vernier acuity for clinical testing and noted why it could not meet the clinical needs. To supply the clinical needs, I programmed a user-friendly software program to quantify the Vernier acuity, particularly for clinical utility. I employed 3D-1U ASM paired with the 3-AFC technique for efficient and rapid testing. Vernier acuity was measured as a standard deviation of 3 aligned positions from 100 stimuli presentations, and it was measured at seven different gap sizes to match the results with the previously reported data and compare consistency. I performed technical validation of this test in a small cohort through a pilot study, and the obtained results were consistent with previous studies data. Moreover, the test achieved the lowest value (highest precision) humans can detect. Therefore, I further verified the stimuli characteristics and found line stimuli with reverse contrast are ideal for future testing. As I arrived to set clinical testing, the pandemic outbreak occurred, and unfortunately, I was unable to proceed with clinical validation due to the imposed restrictions. However, during the pandemic, I continued expanding Vernier acuity utility for clinical screening by programming dedicated software

programs to quantify specific visual functions, including visual fields and distortions, which possess significant diagnostics value.

In the third chapter, I modified a few experimental parameters to improve test efficiency and assessed subject responses, testing time, and test reliability through test-retest analysis. The adjusted parameters included adjustment of stimuli dimensions to 3 x 30 (width and height), increasing the reversals to 5 from 200 stimuli presentations, and at each reversal point, stimuli were positioned further away by 3 steps from the point of reversal. There was no significant difference between mean Vernier acuity of right and left eyes at both visits. Therefore, I compiled the data from both eyes to assess test performance. Throughout the study, over 90% of mean correct responses were recorded with a mean reaction time of less than 0.91 seconds. About 3% of mean incorrect responses were recorded with a mean reaction time of fewer than 0.75 seconds and about 5% of mean aligned responses were recorded with a mean reaction time of less than 2.5 seconds. Moreover, the testing time at each gap size was less than 2 minutes at both visits. The interclass correlation between the visits for Vernier acuity was positive but weak. I further analyzed the Vernier acuity between age and gender. The age groups of ≤ 30 and > 30 years were repeatable in almost all gap sizes of both age groups. In comparison, Females were repeatable at almost all gap sizes than males.

The fourth chapter focused on quantifying the visual field using the hyperacuity paradigm. I adopted the VAT program and modified it to assess the Vernier acuity in eccentric 5 degrees across the macula in four visual field locations, including Superior, Inferior, Nasal, and Temporal. This testing involved the presentation of the viewing target at the screen center and the two vertical line stimuli on the respected visual field at 5 degrees from the center. The participants were asked to judge the misalignment of the top stimuli relative to the lower one while holding the fixation on the target and registering the response for each stimuli presentation. At all four visual field locations, I measured the Vernier acuity using two different gap sizes to identify the gap-driven sensitivity of Vernier acuity. I found that both gap sizes achieved a similar degree of thresholds at both visits. Though the results were repeatable at all four visual fields with gap-15, the interclass correlation was negative and weak in the superior field. In contrast, the correlation was positive but weak in all other fields. Whereas, with gap-30, the results were not repeatable only at inferior fields, and there was a positive correlation at all visual fields, yet it was weak. Therefore, the software program can be further improvised to produce reliable results for clinical application.

The fifth chapter focused on quantifying the visual field distortions using the hyperacuity paradigm. I developed a dedicated software program to assess the distortions of visual fields using a method of adjustment. The testing involved bisectional alignment of both vertical and horizontal lines simultaneously in two different orientation patterns, Pattern-A: making an angle of 45 degrees (Oblique) and Pattern-B: making an angle of 90 degrees at the screen center (Straight). The measurements were taken at 10, 8, 6, 4, and 2 degrees from the center. An adjustable plus '+' shaped stimuli were randomly misaligned within the 1.5 degrees circumference of the screen center. Both line stimuli and adjustable stimuli were paired with the order of orientation and presented synchronized at each presentation. The subject was instructed to move the adjustable stimuli to the center of the surrounding line stimuli using the arrow keys on the computer keyboard. The results indicated that the right eyes were repeatable for pattern A; however, there was a negative and weak correlation only at 10 and 2 degrees. Whereas, for pattern B, poor repeatability was at 10 degrees and negative and weak correlation only at 6 and 4 degrees. While the left eye results were repeatable for pattern A, a positive and moderate to strong correlation was observed at all measured degrees. For pattern B, poor repeatability was at 8 degrees, and a positive and moderate to strong correlation was observed at all the measured degrees. Therefore, the software program can be further modified to produce highly reliable results for the clinical application.

6.2 Limitations

In the pilot-2 study, I randomly tested all three programs, and it took about an hour to complete the testing. Though I introduced breaks to maintain steady attention throughout the experimentations, participants may not be attentive during the testing or at the end of the testing due to exhaustion. However, VAT results indicate the participants' accuracy was over 90% throughout the testing at both visits. Therefore, it can be inferred that there was a negligible effect of boredom during the testing.

Due to COVID-19 reasons, I could not test it on a large sample of participants, which might be one reason for the poor reliability of the measurements for all three programs. Overall, the programs are efficient, robust and can serve in the clinics after reliability is verified.

6.3 Future Directions

All three experimental programs were robust and efficient; however, the reliability was weak. This could be due to sample size and methodological factors. Each program can be studied independently and improvised for better reliability. The area of improvement for each program is discussed briefly for future research considerations.

The VAT program was optimized for better performance. However, the results from this study indicated further areas of improvement, including adjusting the start position for individual gap size. As smaller gap sizes between 2 and 8 are highly repeatable, the 4 arcminutes of gap size can be an ideal stimuli position for the quick vision screening. In addition, the start position can be reduced by half (from 60 to 30 arcminutes) that will take a fewer presentations and time for the vision screening. At 4 arcminutes of gap size, the thresholds are relatively sensitive at both visits, therefore, can be recommended for clinical testing. A detailed study with a variety of age groups may provide age-related variability of VeT for this program.

The HP program measured the Vernier acuity across the macula (para-foveal area) using 15 and 30-gap sizes. The right eyes were highly repeatable using a 15-gap size, whereas the left eyes were highly repeatable with a 30-gap size. This can be further verified on a larger sample size to standardize the gap.

The MMP program measured visual field distortions using both A and B patterns were repeatable but reliability was poor at the most measured locations for both eyes. The program can be further modified and assessed on larger sample may provide better reliability results.

References

1. Causes of blindness and vision impairment in 2020 and trends over 30 years, and prevalence of avoidable blindness in relation to VISION 2020: the Right to Sight: an analysis for the Global Burden of Disease Study. *The Lancet Global health*. 2021;9(2):e144-e160.
2. Trends in prevalence of blindness and distance and near vision impairment over 30 years: an analysis for the Global Burden of Disease Study. *The Lancet Global health*. 2021;9(2):e130-e143.
3. Avidor D, Loewenstein A, Waisbourd M, Nutman A. Cost-effectiveness of diabetic retinopathy screening programs using telemedicine: a systematic review. *Cost effectiveness and resource allocation : C/E*. 2020;18:16.
4. World Health O. World report on vision. 2019.
5. Assi L, Chamseddine F, Ibrahim P, et al. A Global Assessment of Eye Health and Quality of Life: A Systematic Review of Systematic Reviews. *JAMA Ophthalmol*. 2021;139(5):526-541.
6. Blindness and vision impairment. <https://www.who.int/news-room/fact-sheets/detail/blindness-and-visual-impairment>.
7. Maberley DA, Hollands H, Chuo J, et al. The prevalence of low vision and blindness in Canada. *Eye (Lond)*. 2006;20(3):341-346.
8. Cruess AF, Gordon KD, Bellan L, Mitchell S, Pezzullo ML. The cost of vision loss in Canada. 2. Results. *Can J Ophthalmol*. 2011;46(4):315-318.
9. Virgili G, Acosta R, Bentley SA, Giacomelli G, Allcock C, Evans JR. Reading aids for adults with low vision. *Cochrane Database Syst Rev*. 2018;4(4):Cd003303.
10. Egunsola O, Dowsett LE, Diaz R, Brent MH, Rac V, Clement FM. Diabetic Retinopathy Screening: A Systematic Review of Qualitative Literature. *Canadian journal of diabetes*. 2021;45(8):725-733.e712.
11. Wandell BA. *Foundations of vision*. sinauer Associates; 1995.
12. Gregory RL. *Eye and brain: The psychology of seeing*. Vol 80: Princeton university press; 2015.
13. Yoshioka T, Sakakibara M. Physical aspects of sensory transduction on seeing, hearing and smelling. *Biophysics (Nagoya-shi, Japan)*. 2013;9:183-191.
14. Dalesio NM, Barreto Ortiz SF, Pluznick JL, Berkowitz DE. Olfactory, Taste, and Photo Sensory Receptors in Non-sensory Organs: It Just Makes Sense. *Frontiers in Physiology*. 2018;9.
15. Marzvanyan A, Alhawaj AF. Physiology, Sensory Receptors. In: *StatPearls*. Treasure Island (FL): StatPearls Publishing; 2023.
16. Remington LA. Chapter 1 - Visual System. In: Remington LA, ed. *Clinical Anatomy and Physiology of the Visual System (Third Edition)*. Saint Louis: Butterworth-Heinemann; 2012:1-9.
17. Rehman I, Hazhirkarzar B, Patel BC. Anatomy, Head and Neck, Eye. In: *StatPearls*. Treasure Island (FL)2022.
18. Lu Z-L, Doshier B. *Visual Psychophysics: From Laboratory to Theory*. The MIT Press; 2013.
19. Levin LA, Nilsson SFE, Hoeve JV, Wu S, Kaufman PL, Alm A. *Adler's Physiology of the Eye E-Book : Expert Consult*. Philadelphia, UNITED STATES: Elsevier; 2011.
20. Ekstrom AD. Why vision is important to how we navigate. *Hippocampus*. 2015;25(6):731-735.
21. Goodale MA, Milner AD. Separate visual pathways for perception and action. *Trends in neurosciences*. 1992;15(1):20-25.

22. Loomis JM, Da Silva JA, Fujita N, Fukusima SS. Visual space perception and visually directed action. *Journal of experimental psychology: Human Perception and Performance*. 1992;18(4):906.
23. Boyer MC. *CyberCities: visual perception in the age of electronic communication*. Princeton Architectural Press; 1996.
24. Chen J, Cranton W, Fihn M. *Handbook of visual display technology*. Springer; 2016.
25. Marmor MF. Vision, eye disease, and art: 2015 Keeler Lecture. *Eye (Lond)*. 2016;30(2):287-303.
26. Chia E-M, Wang JJ, Rochtchina E, Smith W, Cumming RR, Mitchell P. Impact of bilateral visual impairment on health-related quality of life: the Blue Mountains Eye Study. *Investigative ophthalmology & visual science*. 2004;45(1):71-76.
27. Chiang PPC, Zheng Y, Wong TY, Lamoureux EL. Vision impairment and major causes of vision loss impacts on vision-specific functioning independent of socioeconomic factors. *Ophthalmology*. 2013;120(2):415-422.
28. Serviss GP. Curiosities of the Sky. By Garrett P. Serviss (Book Review). In. Vol 103. London: The Spectator Ltd; 1909:1062.
29. Light-Based Science. In: Boudrioua A, Rashed, R., & Lakshminarayanan, V., ed. *Technology and Sustainable Development, The Legacy of Ibn al-Haytham (1st ed.)*. Boca Raton 2017.
30. Unal N, Elcioglu O. Anatomy of the eye from the view of Ibn Al-Haitham (965-1039). The founder of modern optics. *Saudi Med J*. 2009;30(3):323-328.
31. Dartt DA, Besharse JC, Dana R. *Encyclopedia of the eye*. London: Elsevier/Academic Press; 2010.
32. Laios K, Moschos MM, George A. Ocular anatomy in medieval arabic medicine. A review. *Italian journal of anatomy and embryology = Archivio italiano di anatomia ed embriologia*. 2016;121(1):105-111.
33. Daneshfard B, Dalfardi B, Nezhad GS. Ibn al-Haytham (965-1039 AD), the original portrayal of the modern theory of vision. *Journal of medical biography*. 2016;24(2):227-231.
34. Khurana AK, Khurana AK, Khurana B, Khurana AK. *Comprehensive ophthalmology*. Seventh edition. ed. New Delhi: Jaypee Brothers Medical Publishers; 2019.
35. Riordan-Eva P. Chapter 1. Anatomy & Embryology of the Eye. In: Riordan-Eva P, Cunningham ET, eds. *Vaughan & Asbury's General Ophthalmology, 18e*. New York, NY: The McGraw-Hill Companies; 2011.
36. Salazar JJ, Ramírez AI, Hoz Rd, et al. Anatomy of the Human Optic Nerve: Structure and Function. 2018.
37. Malhotra A, Minja FJ, Crum A, Burrowes D. Ocular anatomy and cross-sectional imaging of the eye. *Semin Ultrasound CT MR*. 2011;32(1):2-13.
38. Remington LA. Chapter 4 - Retina. In: Remington LA, ed. *Clinical Anatomy and Physiology of the Visual System (Third Edition)*. Saint Louis: Butterworth-Heinemann; 2012:61-92.
39. Kolb H. Facts and Figures Concerning the Human Retina. In: Kolb H, Fernandez E, Nelson R, eds. *Webvision: The Organization of the Retina and Visual System*. Salt Lake City (UT): University of Utah Health Sciences Center, Copyright: © 2023 Webvision . 1995.
40. Rocher N. [Anatomy and physiology of the human eye]. *Soins*. 2010(744):30-31.
41. Nguyen KH, Patel BC, Tadi P. Anatomy, Head and Neck: Eye Retina. In: *StatPearls*. Treasure Island (FL): StatPearls Publishing; 2023.
42. Kaur C, Foulds WS, Ling EA. Hypoxia-ischemia and retinal ganglion cell damage. *Clin Ophthalmol*. 2008;2(4):879-889.
43. Masland RH. The neuronal organization of the retina. *Neuron*. 2012;76(2):266-280.

44. Rehman I, Mahabadi N, Motlagh M, Ali T. Anatomy, Head and Neck, Eye Fovea. In: *StatPearls*. Treasure Island (FL) ineligible companies.2023.
45. Kaplan HJ. Anatomy and function of the eye. *Chem Immunol Allergy*. 2007;92:4-10.
46. Hirsch LR, Holzer JR, Finnin MS, Cazares SM. Significance of Retinal Lesions Potentially Caused by Dazzling Lasers. 2015.
47. Zimmerman AL. 48 - Visual Transduction. In: Sperelakis N, ed. *Cell Physiology Source Book (Third Edition)*. San Diego: Academic Press; 2001:807-814.
48. Wolf G. The visual cycle of the cone photoreceptors of the retina. *Nutrition reviews*. 2004;62(7 Pt 1):283-286.
49. Lamb TD. Why rods and cones? *Eye (Lond)*. 2016;30(2):179-185.
50. Fain G, Sampath AP. Rod and cone interactions in the retina. *F1000Research*. 2018;7.
51. Kandel E, Kandel ER, Schwartz J, Jessell T. *Principles of Neural Science, Fourth Edition*. McGraw-Hill Companies, Incorporated; 2000.
52. Silverstein LDJCR, Application. *Foundations of Vision*, by Brian A. Wandell, Sinauer Associates, Inc., Sunderland, MA, 1995. xvi + 476 pp., hardcover \$49.95. 2008;21:142-144.
53. Korenbrot JI. Speed, sensitivity, and stability of the light response in rod and cone photoreceptors: facts and models. *Prog Retin Eye Res*. 2012;31(5):442-466.
54. Freundlieb PH, Herbig A, Kramer FH, Bach M, Hoffmann MB. Determination of scotopic and photopic conventional visual acuity and hyperacuity. *Graefes Arch Clin Exp Ophthalmol*. 2020;258(1):129-135.
55. Thoreson WB, Mangel SC. Lateral interactions in the outer retina. *Prog Retin Eye Res*. 2012;31(5):407-441.
56. Hofer H, Carroll J, Neitz J, Neitz M, Williams DR. Organization of the human trichromatic cone mosaic. *The Journal of neuroscience : the official journal of the Society for Neuroscience*. 2005;25(42):9669-9679.
57. Williamson SJ, Cummins HZ. *Light and Color in Nature and Art*. Wiley; 1983.
58. Hu ML, Ayton LN, Jolly JK. The Clinical Use of Vernier Acuity: Resolution of the Visual Cortex Is More Than Meets the Eye. *Front Neurosci*. 2021;15:714843.
59. de Villiers G, Pike ER. *The Limits of Resolution*. Milton, UNITED KINGDOM: Taylor & Francis Group; 2016.
60. Andrei AR, Pojoga S, Janz R, Dragoi V. Integration of cortical population signals for visual perception. *Nat Commun*. 2019;10(1):3832.
61. Song C, Schwarzkopf DS, Kanai R, Rees G. Neural population tuning links visual cortical anatomy to human visual perception. *Neuron*. 2015;85(3):641-656.
62. Bear MF, Connors BW, Paradiso MA. *Neuroscience: Exploring the Brain*. Wolters Kluwer; 2016.
63. Hugrass L, Verhellen T, Morrall-Earney E, Mallon C, Crewther DP. The effects of red surrounds on visual magnocellular and parvocellular cortical processing and perception. *J Vis*. 2018;18(4):8.
64. Malone BJ, Kumar VR, Ringach DL. Dynamics of receptive field size in primary visual cortex. *Journal of neurophysiology*. 2007;97(1):407-414.
65. Celesia GG. *Disorders of visual processing*. Boston, Mass: Elsevier; 2005.
66. DeAngelis GC, Ohzawa I, Freeman RD. Receptive-field dynamics in the central visual pathways. *Trends Neurosci*. 1995;18(10):451-458.
67. Goodale MA, Milner AD. Separate visual pathways for perception and action. *Trends Neurosci*. 1992;15(1):20-25.

68. Fleming RW. Visual perception: Colour brings shape into stark relief. *Curr Biol.* 2022;32(6):R272-R273.
69. Welbourne LE, Morland AB, Wade AR. Human colour perception changes between seasons. *Curr Biol.* 2015;25(15):R646-647.
70. Impairments NRCUCoDDfIwV. Visual Impairments: Determining Eligibility for Social Security Benefits, TESTS OF VISUAL FUNCTIONS. 2002; <https://www.ncbi.nlm.nih.gov/books/NBK207559/>. Accessed 2, 2002.
71. Birch EE, O'Connor AR. Chapter 72 - Binocular vision. In: Lambert SR, Lyons CJ, eds. *Taylor and Hoyt's Pediatric Ophthalmology and Strabismus (Fifth Edition)*. London: Elsevier; 2017:746-753.e742.
72. Roy S, Jun NY, Davis EL, Pearson J, Field GD. Inter-mosaic coordination of retinal receptive fields. *Nature.* 2021;592(7854):409-413.
73. Latham K, Chung ST, Allen PM, Tavassoli T, Baron-Cohen S. Spatial localisation in autism: evidence for differences in early cortical visual processing. *Mol Autism.* 2013;4(1):4.
74. Hubel DH. THE VISUAL CORTEX OF THE BRAIN. *Scientific American.* 1963;209:54-62.
75. Bennett CR, Bex PJ, Bauer CM, Merabet LB. The Assessment of Visual Function and Functional Vision. *Semin Pediatr Neurol.* 2019;31:30-40.
76. Colenbrander A. Visual functions and functional vision. *International Congress Series.* 2005;1282:482-486.
77. Westheimer G. Visual acuity and hyperacuity: resolution, localization, form. *Am J Optom Physiol Opt.* 1987;64(8):567-574.
78. Gwiazda J, Bauer J, Held R. From visual acuity to hyperacuity: a 10-year update. *Can J Psychol.* 1989;43(2):109-120.
79. Westheimer G. Editorial: Visual acuity and hyperacuity. *Invest Ophthalmol.* 1975;14(8):570-572.
80. Westheimer G. VISUAL ACUITY AND HYPERACUITY. In: Bass M, ed. *Handbook of Optics: Volume III - Vision and Vision Optics*. 3rd Edition ed. New York: McGraw-Hill Education; 2010.
81. Westheimer G. Visual Acuity and Hyperacuity: Resolution, Localization, Form. *Optometry and Vision Science.* 1987;64(8).
82. Braddick O. Visual hyperacuity. *Nature.* 1984;308(5956):228-229.
83. Manny RE, Klein SA. The development of vernier acuity in infants. *Curr Eye Res.* 1984;3(3):453-462.
84. Buckingham TJ, Kelly SL. The comparative development of movement hyperacuity and visual acuity in children. *Vision Res.* 1996;36(23):3851-3856.
85. Hrynchak P. CLINICAL PROCEDURES IN OPTOMETRY. *Optometry and Vision Science.* 1992;69(3).
86. Gurnani. KKB. *Contrast Sensitivity.* 2023.
87. Stalin A, Dalton K. Relationship of Contrast Sensitivity Measured Using Quick Contrast Sensitivity Function With Other Visual Functions in a Low Vision Population. *Invest Ophthalmol Vis Sci.* 2020;61(6):21.
88. Limits of Resolution- The Rayleigh Criterion. <https://pressbooks.online.ucf.edu/phy2053bc/chapter/limits-of-resolution-the-rayleigh-criterion/>.
89. Meilan PF, Garavaglia M. Rayleigh criterion of resolution and light sources of different spectral composition. 1997.

90. He JC, Marcos S, Webb RH, Burns SA. Measurement of the wave-front aberration of the eye by a fast psychophysical procedure. *J Opt Soc Am A Opt Image Sci Vis.* 1998;15(9):2449-2456.
91. Westheimer G. Optical superresolution and visual hyperacuity. *Prog Retin Eye Res.* 2012;31(5):467-480.
92. Williams DR. Aliasing in human foveal vision. *Vision research (Oxford).* 1985;25(2):195-205.
93. Martin G. Psychophysics. Limits of visual resolution. *Nature.* 1986;319(6054):540.
94. Advanced Microscopy. <https://advanced-microscopy.utah.edu/education/super-res/>.
95. Barakat R. Application of Apodization to Increase Two-Point Resolution by the Sparrow Criterion. I. Coherent Illumination. *J Opt Soc Am.* 1962;52(3):276-283.
96. Sparrow CMJTAJ. On Spectroscopic Resolving Power. 1916;44:76.
97. Learning to Perceive Features below the Foveal Photoreceptor Spacing. In. *Perceptual Learning: The MIT Press; 2002:0.*
98. Lakshminarayanan V. Aliasing and the human visual system. *Concepts in Neuroscience.* 1992;3(1992):201-212.
99. Tran NC, Wang JH, Vu TH, Tai TC, Wang JC. Anti-aliasing convolution neural network of finger vein recognition for virtual reality (VR) human-robot equipment of metaverse. *J Supercomput.* 2023;79(3):2767-2782.
100. Barron J, Mildenhall B, Matthew T, Peter H, Ricardo M-B, Pratul PS. Mip-NeRF: A Multiscale Representation for Anti-Aliasing Neural Radiance Fields. *IEEE International Conference on Computer Vision.* 2021.
101. Mackin A, Bull D. Characterizing the spatiotemporal envelope of the human visual system through the visibility of temporal aliasing artifacts. *J Opt Soc Am A Opt Image Sci Vis.* 2020;37(7):1116-1127.
102. Williams DR. Aliasing in human foveal vision. *Vision Res.* 1985;25(2):195-205.
103. Lu Z-L, Doshier B, Lu Z-L, Doshier B. 3Understanding Human Visual Function with Psychophysics. In: *Visual Psychophysics: From Laboratory to Theory.* The MIT Press; 2013:0.
104. Kubovy M, Epstein W, Gepshtein S. Visual perception: Theoretical and methodological foundations. In: *Handbook of psychology: Experimental psychology, Vol. 4, 2nd ed.* Hoboken, NJ, US: John Wiley & Sons, Inc.; 2013:85-119.
105. Leek MR. Adaptive procedures in psychophysical research. *Percept Psychophys.* 2001;63(8):1279-1292.
106. Treutwein B. Adaptive psychophysical procedures. *Vision Res.* 1995;35(17):2503-2522.
107. Cornsweet TN. The staircase-method in psychophysics. *Am J Psychol.* 1962;75:485-491.
108. Reiniger JL, Lobecke AC, Sabesan R, et al. Habitual higher order aberrations affect Landolt but not Vernier acuity. *J Vis.* 2019;19(5):11.
109. Alexander KR, Derlacki DJ, Fishman GA, Szlyk JP. Grating, vernier, and letter acuity in retinitis pigmentosa. *Invest Ophthalmol Vis Sci.* 1992;33(12):3400-3406.
110. Hamer RD, Carvalho FA, Ventura DF. Effect of contrast and gaps between Vernier stimulus elements on sweep visual evoked potential measurements of human cortical Vernier responses. *Psychology & Neuroscience.* 2013;6(2):199-212.
111. Gouras P. *Progress in sensory physiology.* 1st ed. 1981. ed. Berlin: Springer Verlag; 1981.
112. Loomis JM. An investigation of tactile hyperacuity. *Sensory processes.* 1979;3(4):289-302.
113. Swindale NV, Cynader MS. Vernier acuity of neurones in cat visual cortex. *Nature.* 1986;319(6054):591-593.
114. Berkley MA. Integration regions for vernier acuity in the cat: Comparative aspects of cortical scaling. *Visual Neuroscience.* 1989;2(5):473-482.

115. Belleville S, Wilkinson F. The development of vernier acuity in the cat. *Invest Ophthalmol Vis Sci.* 1990;31(6):1175-1180.
116. Kiorpes L. Effect of strabismus on the development of vernier acuity and grating acuity in monkeys. *Vis Neurosci.* 1992;9(3-4):253-259.
117. Kiorpes L. Development of vernier acuity and grating acuity in normally reared monkeys. *Vis Neurosci.* 1992;9(3-4):243-251.
118. Harmening WM, Göbbels K, Wagner H. Vernier acuity in barn owls. *Vision Res.* 2007;47(7):1020-1026.
119. Enoch JM, Essock EA, Williams RA. Relating vernier acuity and Snellen acuity in specific clinical populations. *Doc Ophthalmol.* 1984;58(1):71-77.
120. Zanker J, Mohn G, Weber U, Zeitler-Driess K, Fahle M. The development of vernier acuity in human infants. *Vision Res.* 1992;32(8):1557-1564.
121. Holmes JM. Comparison of grating and Vernier acuity in infants with developmental delay. *J Pediatr Ophthalmol Strabismus.* 1996;33(1):31-34.
122. Skoczinski AM, Good WV. Vernier acuity is selectively affected in infants and children with cortical visual impairment. *Dev Med Child Neurol.* 2004;46(8):526-532.
123. Carkeet A, Levi DM, Manny RE. Development of Vernier acuity in childhood. *Optom Vis Sci.* 1997;74(9):741-750.
124. Paradiso MA, Carney T, Freeman RD. Cortical processing of hyperacuity tasks. *Vision Res.* 1989;29(2):247-254.
125. Levi DM, Klein SA, Aitsebaomo AP. Vernier acuity, crowding and cortical magnification. *Vision Res.* 1985;25(7):963-977.
126. Srebro R, Osetinsky MV. The localization of cortical activity evoked by vernier offset. *Vision Res.* 1987;27(8):1387-1390.
127. Fahle M, Edelman S, Poggio T. Fast perceptual learning in hyperacuity. *Vision Res.* 1995;35(21):3003-3013.
128. *Perceptual learning.* Cambridge, MA, US: MIT Press; 2002.
129. Li RW, Brown B, Edwards MH, Ngo CV, Chat SW, Levi DM. Reduced sampling efficiency causes degraded Vernier hyperacuity with normal aging: Vernier acuity in position noise. *Sci Rep.* 2012;2:300.
130. Hanumunthadu D, Lescauwat B, Jaffe M, et al. Clinical Update on Metamorphopsia: Epidemiology, Diagnosis and Imaging. *Curr Eye Res.* 2021;46(12):1777-1791.
131. Hou C, Kim YJ, Verghese P. Cortical sources of Vernier acuity in the human visual system: An EEG-source imaging study. *J Vis.* 2017;17(6):2.
132. Sheth KN, Walker BM, Modestino EJ, et al. Neural correlate of vernier acuity tasks assessed by functional MRI (fMRI). *Curr Eye Res.* 2007;32(7-8):717-728.
133. Hou C, Good WV, Norcia AM. Validation study of VEP vernier acuity in normal-vision and amblyopic adults. *Invest Ophthalmol Vis Sci.* 2007;48(9):4070-4078.
134. Watson T, Orel-Bixler D, Haegerstrom-Portnoy G. VEP vernier, VEP grating, and behavioral grating acuity in patients with cortical visual impairment. *Optom Vis Sci.* 2009;86(6):774-780.
135. Skoczinski AM, Norcia AM. Development of VEP Vernier acuity and grating acuity in human infants. *Invest Ophthalmol Vis Sci.* 1999;40(10):2411-2417.
136. Fankhauser F, Kwasniewska S. Cortical mechanisms of normal and abnormal processing in the visual system, Part 1. Spatial vision, amblyopia, hyperacuity, modal assumptions: a review. *Technology and health care : official journal of the European Society for Engineering and Medicine.* 2009;17(2):77-97.

137. Westheimer G, Pettet MW. Contrast and duration of exposure differentially affect vernier and stereoscopic acuity. *Proceedings Biological sciences*. 1990;241(1300):42-46.
138. Drover JR, Morale SE, Wang YZ, Stager DR, Sr., Birch EE. Vernier acuity cards: examination of development and screening validity. *Optom Vis Sci*. 2010;87(11):E806-812.
139. Poggio T, Fahle M, Edelman S. Fast perceptual learning in visual hyperacuity. *Science (New York, NY)*. 1992;256(5059):1018-1021.
140. Williams RA, Enoch JM, Essock EA. The resistance of selected hyperacuity configurations to retinal image degradation. *Invest Ophthalmol Vis Sci*. 1984;25(4):389-399.
141. Essock EA, Williams RA, Enoch JM, Raphael S. The effects of image degradation by cataract on vernier acuity. *Invest Ophthalmol Vis Sci*. 1984;25(9):1043-1050.
142. Whitaker D, Deady J. Prediction of visual function behind cataract using displacement threshold hyperacuity. *Ophthalmic Physiol Opt*. 1989;9(1):20-24.
143. Enoch JM, Giraldez-Fernandez MJ, Knowles R, et al. Hyperacuity test to evaluate vision through dense cataracts; research preliminary to a clinical study. I. Studies conducted at the University of California at Berkeley before travel to India. *Optom Vis Sci*. 1995;72(9):619-629.
144. Quaid P, Stonier C, Cox MJ. Potential vision testing--the relationship between visual acuity and Vernier acuity in the presence of simulated cataract. *Ophthalmic Physiol Opt*. 2002;22(6):469-481.
145. Lakshminarayanan V, Enoch JM. Vernier acuity and aging. *Int Ophthalmol*. 1995;19(2):109-115.
146. Lakshminarayanan V, Aziz S, Enoch JM. Variation of the hyperacuity gap function with age. *Optom Vis Sci*. 1992;69(6):423-426.
147. Enoch JM, Werner JS, Haegerstrom-Portnoy G, Lakshminarayanan V, Rynders M. Forever young: visual functions not affected or minimally affected by aging: a review. *The journals of gerontology Series A, Biological sciences and medical sciences*. 1999;54(8):B336-351.
148. Yebra-Pimentel Vilar E, Giraldez-Fernandez MJ, Enoch JM, Lakshminarayanan V, Knowles R, Srinivasan R. Performance on three-point vernier acuity targets as a function of age. *J Opt Soc Am A Opt Image Sci Vis*. 1995;12(10):2293-2304.
149. Odom JV, Vasquez RJ, Schwartz TL, Linberg JV. Adult vernier thresholds do not increase with age; vernier bias does. *Invest Ophthalmol Vis Sci*. 1989;30(5):1004-1008.
150. Holmes JM, Archer SM. Vernier acuity cards: a practical method for measuring vernier acuity in infants. *J Pediatr Ophthalmol Strabismus*. 1993;30(5):312-314.
151. Graf M, Dietrich H. [Objective vernier acuity testing in adults, children and infants. Possibilities and limits of a new method]. *Klin Monbl Augenheilkd*. 1994;204(2):98-104.
152. Salmon TO, Horner DG. A new subjective refraction method--the meridional polarized vernier optometer. *J Am Optom Assoc*. 1996;67(10):599-605.
153. Skottun BC, Skoyles JR. Vernier Acuity as a Test of Magnocellular Sensitivity. *Neuro-Ophthalmology*. 2010;34(2):82-87.
154. McKendrick AM, Johnson CA, Anderson AJ, Fortune B. Elevated vernier acuity thresholds in glaucoma. *Invest Ophthalmol Vis Sci*. 2002;43(5):1393-1399.
155. Piltz JR, Swindale NV, Drance SM. Vernier thresholds and alignment bias in control, suspect, and glaucomatous eyes. *J Glaucoma*. 1993;2(2):87-95.
156. Meier K, Giaschi D. Unilateral Amblyopia Affects Two Eyes: Fellow Eye Deficits in Amblyopia. *Invest Ophthalmol Vis Sci*. 2017;58(3):1779-1800.
157. Little JA, Woodhouse JM, Lauritzen JS, Saunders KJ. Vernier acuity in Down syndrome. *Invest Ophthalmol Vis Sci*. 2009;50(2):567-572.

158. Levi DM, Klein SA, Yap YL. Positional uncertainty in peripheral and amblyopic vision. *Vision Res.* 1987;27(4):581-597.
159. Cox JF, Suh S, Leguire LE. Vernier acuity in amblyopic and nonamblyopic children. *J Pediatr Ophthalmol Strabismus.* 1996;33(1):39-46.
160. Abdul Rasheed M, Cathy L, Rajeev N, Kaamran R, Vasudevan L. Hyperacuity thresholds and gap functions using an adaptive staircase method. Paper presented at: Proc.SPIE2020.
161. Wehrhahn C, Westheimer G. How vernier acuity depends on contrast. *Experimental Brain Research.* 1990;80(3):618-620.
162. O'Shea RP, Mitchell DE. Vernier acuity with opposite-contrast stimuli. *Perception.* 1990;19(2):207-221.
163. Krauskopf J, Farell B. Vernier acuity: effects of chromatic content, blur and contrast. *Vision Res.* 1991;31(4):735-749.
164. Waugh SJ, Levi DM. Visibility and vernier acuity for separated targets. *Vision Res.* 1993;33(4):539-552.
165. Rüttiger L, Lee BB. Chromatic and luminance contributions to a hyperacuity task. *Vision Res.* 2000;40(7):817-832.
166. Bedell HE, Chung ST, Patel SS. Elevation of Vernier thresholds during image motion depends on target configuration. *J Opt Soc Am A Opt Image Sci Vis.* 2000;17(6):947-954.
167. Fang MS, Enoch JM, Lakshminarayanan V, et al. The three point vernier alignment or acuity test (3Pt VA test): an analysis of variance. *Ophthalmic Physiol Opt.* 2000;20(3):220-234.
168. Abbud CM, Cruz AA. Variability of Vernier acuity measurements in untrained subjects of different ages. *Braz J Med Biol Res.* 2002;35(2):223-227.
169. Peirce JW. PsychoPy--Psychophysics software in Python. *J Neurosci Methods.* 2007;162(1-2):8-13.
170. Manny RE, Klein SA. A three alternative tracking paradigm to measure vernier acuity of older infants. *Vision Res.* 1985;25(9):1245-1252.
171. Foley-Fisher JA. The effect of target line length on Vernier acuity in white and blue light. *Vision Res.* 1973;13(8):1447-1454.
172. Essock EA, Enoch JM, Williams RA, Barricks M, Raphael S. Joint application of hyperacuity perimetry and gap tests to assess visual function behind cataracts: initial trials. *Doc Ophthalmol.* 1985;60(3):293-312.
173. Westheimer G, Beard BL. Orientation dependency for foveal line stimuli: detection and intensity discrimination, resolution, orientation discrimination and vernier acuity. *Vision Res.* 1998;38(8):1097-1103.
174. McIlhagga W, Pääkkönen A. Effects of contrast and length on vernier acuity explained with noisy templates. *Vision Res.* 2003;43(6):707-716.
175. Wehrhahn C, Westheimer G. How vernier acuity depends on contrast. *Exp Brain Res.* 1990;80(3):618-620.
176. Freedman LP, Cockburn IM, Simcoe TS. The Economics of Reproducibility in Preclinical Research. *PLoS biology.* 2015;13(6):e1002165.
177. Thomas M, Wolfson Y, Chaikitmongkol V, Bressler N. Preferential Hyperacuity Perimetry Monitoring in Patients During Treatment of Neovascular Age-related Macular Degeneration. *Investigative Ophthalmology & Visual Science.* 2013;54(15):4173-4173.
178. Hood CT. The Wills eye manual: office and emergency room diagnosis and treatment of eye disease. *British Journal of Ophthalmology.* 2009;93(8):1127.
179. Midena E, Vujosevic S. Metamorphopsia: An Overlooked Visual Symptom. *Ophthalmic Res.* 2015;55(1):26-36.

180. Manabe K, Tsujikawa A, Osaka R, et al. Metamorphopsia Associated with Branch Retinal Vein Occlusion. *PloS one*. 2016;11(4):e0153817-e0153817.
181. Simunovic MP. METAMORPHOPSIA AND ITS QUANTIFICATION. *Retina*. 2015;35(7):1285-1291.
182. Kampmeier J, Zorn MM, Lang GK, Botros YT, Lang GE. [Comparison of Preferential Hyperacuity Perimeter (PHP) test and Amsler grid test in the diagnosis of different stages of age-related macular degeneration]. *Klin Monbl Augenheilkd*. 2006;223(9):752-756.
183. Schmid MK, Thiel MA, Lienhard K, Schlingemann RO, Faes L, Bachmann LM. Reliability and diagnostic performance of a novel mobile app for hyperacuity self-monitoring in patients with age-related macular degeneration. *Eye (Lond)*. 2019;33(10):1584-1589.
184. Bjerager J, Schneider M, Potapenko I, et al. Diagnostic Accuracy of the Amsler Grid Test for Detecting Neovascular Age-Related Macular Degeneration: A Systematic Review and Meta-analysis. *JAMA Ophthalmol*. 2023;141(4):315-323.

Appendix A
Permissions to Reproduce Figures.

SPRINGER NATURE LICENSE
TERMS AND CONDITIONS

Jul 06, 2023

This Agreement between Mr. Abdul Rasheed Mohammed ("You") and Springer Nature ("Springer Nature") consists of your license details and the terms and conditions provided by Springer Nature and Copyright Clearance Center.

License Number	5583171190161
License date	Jul 06, 2023
Licensed Content Publisher	Springer Nature
Licensed Content Publication	Springer eBook
Licensed Content Title	Retinal Histology and Anatomical Landmarks
Licensed Content Author	Stephen H. Tsang, Tarun Sharma
Licensed Content Date	Jan 1, 2018
Type of Use	Thesis/Dissertation
Requestor type	academic/university or research institute
Format	print and electronic
Portion	figures/tables/illustrations
Number of figures/tables/illustrations	1
Will you be translating?	no

Circulation/distribution	50000 or greater
Author of this Springer Nature content	no
Title	Advancing hyperacuity for vision screening
Institution name	University of Waterloo
Expected presentation date	Sep 2023
Portions	Figure 1.2
Requestor Location	Mr. Abdul Rasheed Mohammed 200 Colombia St W Waterloo, ON N2L 3G1 Canada Attn: Mr. Abdul Rasheed Mohammed
Total	0.00 USD

Terms and Conditions

Springer Nature Customer Service Centre GmbH Terms and Conditions

The following terms and conditions ("Terms and Conditions") together with the terms specified in your [RightsLink] constitute the License ("License") between you as Licensee and Springer Nature Customer Service Centre GmbH as Licensor. By clicking 'accept' and completing the transaction for your use of the material ("Licensed Material"), you confirm your acceptance of and obligation to be bound by these Terms and Conditions.

1. Grant and Scope of License

1. 1. The Licensor grants you a personal, non-exclusive, non-transferable, non-sublicensable, revocable, world-wide License to reproduce, distribute, communicate to the public, make available, broadcast, electronically transmit or create derivative works using the Licensed Material for the purpose(s) specified in your RightsLink Licence Details only. Licenses are granted for the specific use requested in the order and for no other use, subject to these Terms and Conditions. You acknowledge and agree that the rights granted to you under this License do not include the right to modify, edit, translate, include in collective works, or create derivative works of the Licensed Material in whole or in part unless expressly stated in your RightsLink

Licence Details. You may use the Licensed Material only as permitted under this Agreement and will not reproduce, distribute, display, perform, or otherwise use or exploit any Licensed Material in any way, in whole or in part, except as expressly permitted by this License.

1. 2. You may only use the Licensed Content in the manner and to the extent permitted by these Terms and Conditions, by your RightsLink Licence Details and by any applicable laws.

1. 3. A separate license may be required for any additional use of the Licensed Material, e.g. where a license has been purchased for print use only, separate permission must be obtained for electronic re-use. Similarly, a License is only valid in the language selected and does not apply for editions in other languages unless additional translation rights have been granted separately in the License.

1. 4. Any content within the Licensed Material that is owned by third parties is expressly excluded from the License.

1. 5. Rights for additional reuses such as custom editions, computer/mobile applications, film or TV reuses and/or any other derivative rights requests require additional permission and may be subject to an additional fee. Please apply to journalpermissions@springernature.com or bookpermissions@springernature.com for these rights.

2. Reservation of Rights

Licensor reserves all rights not expressly granted to you under this License. You acknowledge and agree that nothing in this License limits or restricts Licensor's rights in or use of the Licensed Material in any way. Neither this License, nor any act, omission, or statement by Licensor or you, conveys any ownership right to you in any Licensed Material, or to any element or portion thereof. As between Licensor and you, Licensor owns and retains all right, title, and interest in and to the Licensed Material subject to the license granted in Section 1.1. Your permission to use the Licensed Material is expressly conditioned on you not impairing Licensor's or the applicable copyright owner's rights in the Licensed Material in any way.

3. Restrictions on use

3. 1. Minor editing privileges are allowed for adaptations for stylistic purposes or formatting purposes provided such alterations do not alter the original meaning or intention of the Licensed Material and the new figure(s) are still accurate and representative of the Licensed Material. Any other changes including but not limited to, cropping, adapting, and/or omitting material that affect the meaning, intention or moral rights of the author(s) are strictly prohibited.

3. 2. You must not use any Licensed Material as part of any design or trademark.

3. 3. Licensed Material may be used in Open Access Publications (OAP), but any such reuse must include a clear acknowledgment of this permission visible at the same time as the figures/tables/illustration or abstract and which must indicate that the Licensed Material is not part of the governing OA license but has been reproduced with permission. This may be indicated according to any standard referencing system but must include at a minimum 'Book/Journal title, Author, Journal Name (if applicable),

Volume (if applicable), Publisher, Year, reproduced with permission from SNCSC'.

4. STM Permission Guidelines

4. 1. An alternative scope of license may apply to signatories of the STM Permissions Guidelines ("STM PG") as amended from time to time and made available at <https://www.stm-assoc.org/intellectual-property/permissions/permissions-guidelines/>.
4. 2. For content reuse requests that qualify for permission under the STM PG, and which may be updated from time to time, the STM PG supersede the terms and conditions contained in this License.
4. 3. If a License has been granted under the STM PG, but the STM PG no longer apply at the time of publication, further permission must be sought from the Rightsholder. Contact journalpermissions@springernature.com or bookpermissions@springernature.com for these rights.

5. Duration of License

5. 1. Unless otherwise indicated on your License, a License is valid from the date of purchase ("License Date") until the end of the relevant period in the below table:

Reuse in a medical communications project	Reuse up to distribution or time period indicated in License
Reuse in a dissertation/thesis	Lifetime of thesis
Reuse in a journal/magazine	Lifetime of journal/magazine
Reuse in a book/textbook	Lifetime of edition
Reuse on a website	1 year unless otherwise specified in the License
Reuse in a presentation/slide kit/poster	Lifetime of presentation/slide kit/poster. Note: publication whether electronic or in print of presentation/slide kit/poster may require further permission.
Reuse in conference proceedings	Lifetime of conference proceedings
Reuse in an annual report	Lifetime of annual report
Reuse in training/CME materials	Reuse up to distribution or time period indicated in License
Reuse in newsmedia	Lifetime of newsmedia
Reuse in coursepack/classroom materials	Reuse up to distribution and/or time period indicated in license

6. Acknowledgement

6. 1. The Licensor's permission must be acknowledged next to the Licensed Material in print. In electronic form, this acknowledgement must be visible at the same time as the figures/tables/illustrations or abstract and must be hyperlinked to the journal/book's homepage.

6. 2. Acknowledgement may be provided according to any standard referencing system and at a minimum should include "Author, Article/Book Title, Journal name/Book imprint, volume, page number, year, Springer Nature".

7. Reuse in a dissertation or thesis

7. 1. Where 'reuse in a dissertation/thesis' has been selected, the following terms apply: Print rights of the Version of Record are provided for; electronic rights for use only on institutional repository as defined by the Sherpa guideline (www.sherpa.ac.uk/romeo/) and only up to what is required by the awarding institution.

7. 2. For theses published under an ISBN or ISSN, separate permission is required. Please contact journalpermissions@springernature.com or bookpermissions@springernature.com for these rights.

7. 3. Authors must properly cite the published manuscript in their thesis according to current citation standards and include the following acknowledgement: '*Reproduced with permission from Springer Nature*'.

8. License Fee

You must pay the fee set forth in the License Agreement (the "License Fees"). All amounts payable by you under this License are exclusive of any sales, use, withholding, value added or similar taxes, government fees or levies or other assessments. Collection and/or remittance of such taxes to the relevant tax authority shall be the responsibility of the party who has the legal obligation to do so.

9. Warranty

9. 1. The Licensor warrants that it has, to the best of its knowledge, the rights to license reuse of the Licensed Material. **You are solely responsible for ensuring that the material you wish to license is original to the Licensor and does not carry the copyright of another entity or third party (as credited in the published version).** If the credit line on any part of the Licensed Material indicates that it was reprinted or adapted with permission from another source, then you should seek additional permission from that source to reuse the material.

9. 2. EXCEPT FOR THE EXPRESS WARRANTY STATED HEREIN AND TO THE EXTENT PERMITTED BY APPLICABLE LAW, LICENSOR PROVIDES THE LICENSED MATERIAL "AS IS" AND MAKES NO OTHER REPRESENTATION OR WARRANTY. LICENSOR EXPRESSLY DISCLAIMS ANY LIABILITY FOR ANY CLAIM ARISING FROM OR OUT OF THE CONTENT, INCLUDING BUT NOT LIMITED TO ANY ERRORS, INACCURACIES, OMISSIONS, OR DEFECTS CONTAINED THEREIN, AND ANY IMPLIED OR EXPRESS WARRANTY AS TO MERCHANTABILITY OR FITNESS FOR A PARTICULAR PURPOSE. IN NO EVENT SHALL LICENSOR BE LIABLE TO YOU OR ANY OTHER PARTY OR ANY OTHER PERSON OR FOR ANY SPECIAL, CONSEQUENTIAL, INCIDENTAL, INDIRECT, PUNITIVE, OR EXEMPLARY DAMAGES, HOWEVER CAUSED, ARISING OUT OF OR IN CONNECTION WITH THE DOWNLOADING, VIEWING OR USE OF THE LICENSED MATERIAL REGARDLESS OF THE FORM OF ACTION, WHETHER FOR BREACH OF CONTRACT, BREACH OF WARRANTY, TORT, NEGLIGENCE, INFRINGEMENT OR OTHERWISE (INCLUDING, WITHOUT LIMITATION,

DAMAGES BASED ON LOSS OF PROFITS, DATA, FILES, USE, BUSINESS OPPORTUNITY OR CLAIMS OF THIRD PARTIES), AND WHETHER OR NOT THE PARTY HAS BEEN ADVISED OF THE POSSIBILITY OF SUCH DAMAGES. THIS LIMITATION APPLIES NOTWITHSTANDING ANY FAILURE OF ESSENTIAL PURPOSE OF ANY LIMITED REMEDY PROVIDED HEREIN.

10. Termination and Cancellation

10. 1. The License and all rights granted hereunder will continue until the end of the applicable period shown in Clause 5.1 above. Thereafter, this license will be terminated and all rights granted hereunder will cease.

10. 2. Licensor reserves the right to terminate the License in the event that payment is not received in full or if you breach the terms of this License.

11. General

11. 1. The License and the rights and obligations of the parties hereto shall be construed, interpreted and determined in accordance with the laws of the Federal Republic of Germany without reference to the stipulations of the CISG (United Nations Convention on Contracts for the International Sale of Goods) or to Germany's choice-of-law principle.

11. 2. The parties acknowledge and agree that any controversies and disputes arising out of this License shall be decided exclusively by the courts of or having jurisdiction for Heidelberg, Germany, as far as legally permissible.

11. 3. This License is solely for Licensor's and Licensee's benefit. It is not for the benefit of any other person or entity.

Questions? For questions on Copyright Clearance Center accounts or website issues please contact springernaturesupport@copyright.com or +1-855-239-3415 (toll free in the US) or +1-978-646-2777. For questions on Springer Nature licensing please visit <https://www.springernature.com/gp/partners/rights-permissions-third-party-distribution>

Other Conditions:

Version 1.4 - Dec 2022

Questions? customercare@copyright.com.

ELSEVIER LICENSE
TERMS AND CONDITIONS

Jul 10, 2023

This Agreement between Mr. Abdul Rasheed Mohammed ("You") and Elsevier ("Elsevier") consists of your license details and the terms and conditions provided by Elsevier and Copyright Clearance Center.

License Number	5585401261445
License date	Jul 10, 2023
Licensed Content Publisher	Elsevier
Licensed Content Publication	Elsevier Books
Licensed Content Title	Clinical Anatomy and Physiology of the Visual System
Licensed Content Author	Lee Ann Remington
Licensed Content Date	Jan 1, 2012
Licensed Content Pages	32
Start Page	61
End Page	92
Type of Use	reuse in a thesis/dissertation
Portion	figures/tables/illustrations

Number of figures/tables/illustrations	3
Format	both print and electronic
Are you the author of this Elsevier chapter?	No
Will you be translating?	No
Title	Advancing hyperacuity for vision screening
Institution name	University of Waterloo
Expected presentation date	Sep 2023
Portions	Figure 4-23, Figure 4-25, Figure 4-26
Requestor Location	Mr. Abdul Rasheed Mohammed 200 Colombia St W Waterloo, ON N2L 3G1 Canada Attn: Mr. Abdul Rasheed Mohammed
Publisher Tax ID	GB 494 6272 12
Total	0.00 USD
Terms and Conditions	

INTRODUCTION

1. The publisher for this copyrighted material is Elsevier. By clicking "accept" in connection with completing this licensing transaction, you agree that the following terms and conditions apply to this transaction (along with the Billing and Payment terms and conditions established by Copyright Clearance Center, Inc. ("CCC"), at the time that you opened your RightsLink account and that are available at any time at <https://myaccount.copyright.com>).

GENERAL TERMS

2. Elsevier hereby grants you permission to reproduce the aforementioned material subject to the terms and conditions indicated.

3. Acknowledgement: If any part of the material to be used (for example, figures) has appeared in our publication with credit or acknowledgement to another source, permission must also be sought from that source. If such permission is not obtained then that material may not be included in your publication/copies. Suitable acknowledgement to the source must be made, either as a footnote or in a reference list at the end of your publication, as follows:

"Reprinted from Publication title, Vol /edition number, Author(s), Title of article / title of chapter, Pages No., Copyright (Year), with permission from Elsevier [OR APPLICABLE SOCIETY COPYRIGHT OWNER]." Also Lancet special credit - "Reprinted from The Lancet, Vol. number, Author(s), Title of article, Pages No., Copyright (Year), with permission from Elsevier."

4. Reproduction of this material is confined to the purpose and/or media for which permission is hereby given. The material may not be reproduced or used in any other way, including use in combination with an artificial intelligence tool (including to train an algorithm, test, process, analyse, generate output and/or develop any form of artificial intelligence tool), or to create any derivative work and/or service (including resulting from the use of artificial intelligence tools).

5. Altering/Modifying Material: Not Permitted. However figures and illustrations may be altered/adapted minimally to serve your work. Any other abbreviations, additions, deletions and/or any other alterations shall be made only with prior written authorization of Elsevier Ltd. (Please contact Elsevier's permissions helpdesk [here](#)). No modifications can be made to any Lancet figures/tables and they must be reproduced in full.

6. If the permission fee for the requested use of our material is waived in this instance, please be advised that your future requests for Elsevier materials may attract a fee.

7. Reservation of Rights: Publisher reserves all rights not specifically granted in the combination of (i) the license details provided by you and accepted in the course of this licensing transaction, (ii) these terms and conditions and (iii) CCC's Billing and Payment terms and conditions.

8. License Contingent Upon Payment: While you may exercise the rights licensed immediately upon issuance of the license at the end of the licensing process for the transaction, provided that you have disclosed complete and accurate details of your proposed use, no license is finally effective unless and until full payment is received from you (either by publisher or by CCC) as provided in CCC's Billing and Payment terms and conditions. If full payment is not received on a timely basis, then any license preliminarily granted shall be deemed automatically revoked and shall be void as if never granted. Further, in the event that you breach any of these terms and conditions or any of CCC's Billing and Payment terms and conditions, the license is automatically revoked and shall be void as if never granted. Use of materials as described in a revoked license, as well as any use of the materials beyond the scope of an unrevoked license, may constitute copyright infringement and publisher reserves the right to take any and all action to protect its copyright in the materials.

9. Warranties: Publisher makes no representations or warranties with respect to the licensed material.

10. **Indemnity:** You hereby indemnify and agree to hold harmless publisher and CCC, and their respective officers, directors, employees and agents, from and against any and all claims arising out of your use of the licensed material other than as specifically authorized pursuant to this license.

11. **No Transfer of License:** This license is personal to you and may not be sublicensed, assigned, or transferred by you to any other person without publisher's written permission.

12. **No Amendment Except in Writing:** This license may not be amended except in a writing signed by both parties (or, in the case of publisher, by CCC on publisher's behalf).

13. **Objection to Contrary Terms:** Publisher hereby objects to any terms contained in any purchase order, acknowledgment, check endorsement or other writing prepared by you, which terms are inconsistent with these terms and conditions or CCC's Billing and Payment terms and conditions. These terms and conditions, together with CCC's Billing and Payment terms and conditions (which are incorporated herein), comprise the entire agreement between you and publisher (and CCC) concerning this licensing transaction. In the event of any conflict between your obligations established by these terms and conditions and those established by CCC's Billing and Payment terms and conditions, these terms and conditions shall control.

14. **Revocation:** Elsevier or Copyright Clearance Center may deny the permissions described in this License at their sole discretion, for any reason or no reason, with a full refund payable to you. Notice of such denial will be made using the contact information provided by you. Failure to receive such notice will not alter or invalidate the denial. In no event will Elsevier or Copyright Clearance Center be responsible or liable for any costs, expenses or damage incurred by you as a result of a denial of your permission request, other than a refund of the amount(s) paid by you to Elsevier and/or Copyright Clearance Center for denied permissions.

LIMITED LICENSE

The following terms and conditions apply only to specific license types:

15. **Translation:** This permission is granted for non-exclusive world **English** rights only unless your license was granted for translation rights. If you licensed translation rights you may only translate this content into the languages you requested. A professional translator must perform all translations and reproduce the content word for word preserving the integrity of the article.

16. **Posting licensed content on any Website:** The following terms and conditions apply as follows: Licensing material from an Elsevier journal: All content posted to the web site must maintain the copyright information line on the bottom of each image; A hyper-text must be included to the Homepage of the journal from which you are licensing at <http://www.sciencedirect.com/science/journal/xxxxx> or the Elsevier homepage for books at <http://www.elsevier.com>; Central Storage: This license does not include permission for a scanned version of the material to be stored in a central repository such as that provided by Heron/XanEdu.

Licensing material from an Elsevier book: A hyper-text link must be included to the Elsevier homepage at <http://www.elsevier.com>. All content posted to the web site must maintain the copyright information line on the bottom of each image.

Posting licensed content on Electronic reserve: In addition to the above the following

clauses are applicable: The web site must be password-protected and made available only to bona fide students registered on a relevant course. This permission is granted for 1 year only. You may obtain a new license for future website posting.

17. **For journal authors:** the following clauses are applicable in addition to the above:

Preprints:

A preprint is an author's own write-up of research results and analysis, it has not been peer-reviewed, nor has it had any other value added to it by a publisher (such as formatting, copyright, technical enhancement etc.).

Authors can share their preprints anywhere at any time. Preprints should not be added to or enhanced in any way in order to appear more like, or to substitute for, the final versions of articles however authors can update their preprints on arXiv or RePEc with their Accepted Author Manuscript (see below).

If accepted for publication, we encourage authors to link from the preprint to their formal publication via its DOI. Millions of researchers have access to the formal publications on ScienceDirect, and so links will help users to find, access, cite and use the best available version. Please note that Cell Press, The Lancet and some society-owned have different preprint policies. Information on these policies is available on the journal homepage.

Accepted Author Manuscripts: An accepted author manuscript is the manuscript of an article that has been accepted for publication and which typically includes author-incorporated changes suggested during submission, peer review and editor-author communications.

Authors can share their accepted author manuscript:

- immediately
 - via their non-commercial person homepage or blog
 - by updating a preprint in arXiv or RePEc with the accepted manuscript
 - via their research institute or institutional repository for internal institutional uses or as part of an invitation-only research collaboration work-group
 - directly by providing copies to their students or to research collaborators for their personal use
 - for private scholarly sharing as part of an invitation-only work group on commercial sites with which Elsevier has an agreement
- After the embargo period
 - via non-commercial hosting platforms such as their institutional repository
 - via commercial sites with which Elsevier has an agreement

In all cases accepted manuscripts should:

- link to the formal publication via its DOI
- bear a CC-BY-NC-ND license - this is easy to do
- if aggregated with other manuscripts, for example in a repository or other site, be shared in alignment with our hosting policy not be added to or enhanced in any way to appear more like, or to substitute for, the published journal article.

Published journal article (JPA): A published journal article (PJA) is the definitive final record of published research that appears or will appear in the journal and embodies all value-adding publishing activities including peer review co-ordination, copy-editing, formatting, (if relevant) pagination and online enrichment.

Policies for sharing publishing journal articles differ for subscription and gold open access articles:

Subscription Articles: If you are an author, please share a link to your article rather than the full-text. Millions of researchers have access to the formal publications on ScienceDirect, and so links will help your users to find, access, cite, and use the best available version.

Theses and dissertations which contain embedded PJAs as part of the formal submission can be posted publicly by the awarding institution with DOI links back to the formal publications on ScienceDirect.

If you are affiliated with a library that subscribes to ScienceDirect you have additional private sharing rights for others' research accessed under that agreement. This includes use for classroom teaching and internal training at the institution (including use in course packs and courseware programs), and inclusion of the article for grant funding purposes.

Gold Open Access Articles: May be shared according to the author-selected end-user license and should contain a [CrossMark logo](#), the end user license, and a DOI link to the formal publication on ScienceDirect.

Please refer to Elsevier's [posting policy](#) for further information.

18. **For book authors** the following clauses are applicable in addition to the above: Authors are permitted to place a brief summary of their work online only. You are not allowed to download and post the published electronic version of your chapter, nor may you scan the printed edition to create an electronic version. **Posting to a repository:** Authors are permitted to post a summary of their chapter only in their institution's repository.

19. **Thesis/Dissertation:** If your license is for use in a thesis/dissertation your thesis may be submitted to your institution in either print or electronic form. Should your thesis be published commercially, please reapply for permission. These requirements include permission for the Library and Archives of Canada to supply single copies, on demand, of the complete thesis and include permission for Proquest/UMI to supply single copies, on demand, of the complete thesis. Should your thesis be published commercially, please reapply for permission. Theses and dissertations which contain embedded PJAs as part of the formal submission can be posted publicly by the awarding institution with DOI links back to the formal publications on ScienceDirect.

Elsevier Open Access Terms and Conditions

You can publish open access with Elsevier in hundreds of open access journals or in nearly 2000 established subscription journals that support open access publishing. Permitted third party re-use of these open access articles is defined by the author's choice of Creative Commons user license. See our [open access license policy](#) for more information.

Terms & Conditions applicable to all Open Access articles published with Elsevier:

Any reuse of the article must not represent the author as endorsing the adaptation of the article nor should the article be modified in such a way as to damage the author's honour or reputation. If any changes have been made, such changes must be clearly indicated.

The author(s) must be appropriately credited and we ask that you include the end user license and a DOI link to the formal publication on ScienceDirect.

If any part of the material to be used (for example, figures) has appeared in our publication with credit or acknowledgement to another source it is the responsibility of the user to ensure their reuse complies with the terms and conditions determined by the rights holder.

Additional Terms & Conditions applicable to each Creative Commons user license:

CC BY: The CC-BY license allows users to copy, to create extracts, abstracts and new works from the Article, to alter and revise the Article and to make commercial use of the Article (including reuse and/or resale of the Article by commercial entities), provided the user gives appropriate credit (with a link to the formal publication through the relevant DOI), provides a link to the license, indicates if changes were made and the licensor is not represented as endorsing the use made of the work. The full details of the license are available at <http://creativecommons.org/licenses/by/4.0>.

CC BY NC SA: The CC BY-NC-SA license allows users to copy, to create extracts, abstracts and new works from the Article, to alter and revise the Article, provided this is not done for commercial purposes, and that the user gives appropriate credit (with a link to the formal publication through the relevant DOI), provides a link to the license, indicates if changes were made and the licensor is not represented as endorsing the use made of the work. Further, any new works must be made available on the same conditions. The full details of the license are available at <http://creativecommons.org/licenses/by-nc-sa/4.0>.

CC BY NC ND: The CC BY-NC-ND license allows users to copy and distribute the Article, provided this is not done for commercial purposes and further does not permit distribution of the Article if it is changed or edited in any way, and provided the user gives appropriate credit (with a link to the formal publication through the relevant DOI), provides a link to the license, and that the licensor is not represented as endorsing the use made of the work. The full details of the license are available at <http://creativecommons.org/licenses/by-nc-nd/4.0>. Any commercial reuse of Open Access articles published with a CC BY NC SA or CC BY NC ND license requires permission from Elsevier and will be subject to a fee.

Commercial reuse includes:

- Associating advertising with the full text of the Article
- Charging fees for document delivery or access
- Article aggregation
- Systematic distribution via e-mail lists or share buttons

Posting or linking by commercial companies for use by customers of those companies.

20. Other Conditions:

v1.10

Questions? customercare@copyright.com.

Appendix B
Conference Presentations

1. Abdul Rasheed Mohammed, Cathy Le, Rajeev Narayanan, Kaamran Raahemifar, and Vasudevan Lakshminarayanan "Hyperacuity thresholds and gap functions using an adaptive staircase method", Proc. SPIE 11481, Light in Nature VIII, 1148106 (21 August 2020); <https://doi.org/10.1117/12.2566771>

Appendix C

Software Program Codes

Vernier Acuity Test Program Code

```
from __future__ import absolute_import, division

import psychopy
psychopy.useVersion('2022.2')

from psychopy.hardware import keyboard
from psychopy import locale_setup
from psychopy import prefs
from psychopy import sound, gui, visual, monitors, core, data, event,
logging, clock
from psychopy.constants import (NOT_STARTED, STARTED, PLAYING, PAUSED,
                                STOPPED, FINISHED, PRESSED, RELEASED,
                                FOREVER)

import numpy as np # whole numpy lib is available, prepend 'np.'
from numpy import (sin, cos, tan, log, log10, pi, average,
                  sqrt, std, deg2rad, rad2deg, linspace, asarray)
from numpy.random import random, randint, normal, shuffle

import matplotlib.pyplot as plt
import pandas as pd
import xlswriter
import io
import random
import time
import math
from math import floor

import os # handy system and path functions
import sys # to get file system encoding

from win32api import GetSystemMetrics
import statistics
from statistics import stdev, mean
from datetime import datetime
import ctypes
from PyQt5.QtWidgets import QApplication

# Ensure that relative paths start from the same directory as this
script
_thisDir = os.path.dirname(os.path.abspath(__file__))
```

```

os.chdir(_thisDir)

#Demographic GUI
infoGui = psychopy.gui.Dlg (title = "Participant's Information",
labelButtonCancel=' Cancel ', labelButtonOK=' Settings ')

infoGui.addField("Name: ") #0
infoGui.addField("Age: ") #1
infoGui.addField("Gender: ", choices=["Other", "Male", "Female"]) #2
infoGui.addField("Eye: ", choices=["Left", "Right", "Both"]) #3
infoGui.addField("Session:", choices=["1", "2"]) #4

###Experimental setting GUI
settingsGui=psychopy.gui.Dlg (title = "Experimental Settings",
labelButtonCancel=' Back ', labelButtonOK=' Gap Size Settings ')

settingsGui.addText('Stimuli Settings', color = "Red")

settingsGui.addField("Stimuli Type :", choices=["Line"]) #0
settingsGui.addField("Stimuli Colour :", choices=["White", "Black"]) #1
settingsGui.addField("Stimuli Opacity (0-1) :", choices=[1]) #2

settingsGui.addField("Line height (moa) :", choices=[30]) #3
settingsGui.addField("Line width (moa) :", choices=[3]) #4

settingsGui.addText('Staircase Settings', color = "Red")

settingsGui.addField("Number of steps Up :", choices=[1]) # 5
settingsGui.addField("Number of steps Down :", choices=[3]) #6
settingsGui.addField("Number of Reversals :", choices=[5]) #7
settingsGui.addField("Number of trials :", choices=[200]) #8

settingsGui.addText('Display Settings: 0-Default Screen, 1-Extended
Screen', color = "Red")

settingsGui.addField("Screen :", choices=[0]) #9
settingsGui.addField("Distance from Screen(cms) :", choices=[100]) #10

###Gap size setting GUI
gapGui=psychopy.gui.Dlg (title = "Select Gap sizes", labelButtonOK='
Start ', labelButtonCancel=' Back ')

gapGui.addField("Selection :", choices=["All", "Select below"]) #0

gapGui.addText("Select 3 option", color = "Red")
gapGui.addText("Will only run distinct gap sizes", color = "Red")
gapGui.addField("Gap size 1: ", 128) #1

```

```

gapGui.addField("Gap size 2: ", 32) #2
gapGui.addField("Gap size 3: ", 4) #3

flag = True
while(flag):
    infoGui.show()
    if(infoGui.OK == True): # Pressed on Settings
        while(True):
            settingsGui.show()
            if(settingsGui.OK == True): # Pressed Gap size settings
                gapGui.show()
                if(gapGui.OK == True): # Pressed Cancel experiment in
Gap Gui
                    flag = False
                    break
            else: #pressed back in Gap GUI
                pass # DO nothing go back to loop 1
            else: # Pressed back in settings
                break # break out of loop 2 and go back to loop 1
        else: # Pressed on Start experiment in Info GUI
            core.quit()

# Store info about the experiment session
psychopyVersion = '2022.2'
expName = 'HAT'
expDate = data.getDateStr()

# Data file name stem = absolute path + name; later add .psyexp, .csv,
.log, etc
filename = _thisDir + os.sep + u'HAT Data/%s_%s_%s' % (infoGui.data[0],
expName, expDate)

# Open data file
fileName = filename
dataFile = open(fileName+'.csv', 'w')
dataFile.write((18 * "{}\n").format(
    "Date", datetime.now(),
    "Name", infoGui.data[0],
    "Age", infoGui.data[1],
    "Gender", infoGui.data[2],
    "Eye", infoGui.data[3],
    "Session", infoGui.data[4],
    "Stimuli Type", settingsGui.data[0],
    "Stimuli Colour", settingsGui.data[1],
    "Opacity", settingsGui.data[2],
    "Stimuli width", settingsGui.data[3],
    "Stimuli height", settingsGui.data[4],

```

```

"Number of steps Up", settingsGui.data[5],
"Number of steps Down", settingsGui.data[6],
"Number of Reversals", settingsGui.data[7],
"Number of Trials", settingsGui.data[8],
"Screen", settingsGui.data[9],
"Distance from screen", settingsGui.data[10],
"Display resolution (px)", str(GetSystemMetrics(0)) + " x " +
str(GetSystemMetrics(1)))
#"Display Size (cm)",

# Converts minutes of arc to cm
def arc2cm(arc):
    return settingsGui.data[10] * math.tan(arc * math.pi / 60/180)

# Converts minutes of arc to cm
def cm2arc(length):
    return math.atan(length/settingsGui.data[10]) * 60 *
180/math.pi

def removeDup(array):
    for i in range(0, len(array)):
        for j in range(i, len(array)):
            if ((j+1) == len(array)):
                break
            if array[i] == array[j+1]:
                del array[j+1]
    return array

def checkUndet(array):
    for i in range(0, len(array)):
        if array[i] == "Undetermined":
            array[i] = 0
    return array

#Stimuli $ Staircase settings
One = settingsGui.data[5]
Three = settingsGui.data[6]
Reversals = settingsGui.data[7]

Stim_Opacity = settingsGui.data[2]
Stim_Contrast = 1 #(1.0: unchanged, 0.5: decrease, 0.0: uniform, 0.5
slightly inverted, -1.0: totally inverted)
Stim_Orientation = 0

# Assign Stimuli variables
if (settingsGui.data[1] == "White"):
    stimuliColor = 'white'
    backgroundColor = 'black'

```

```

else:
    stimuliColor = 'black'
    backgroundColor = 'white'

#Defining the stimuli in MINUTES OF ARC
height_moa = settingsGui.data[3]
width_moa = settingsGui.data[4]

##Converting MOA into Cms
line_height = arc2cm(height_moa)
line_width = arc2cm(width_moa)

Presentations = settingsGui.data[8] - 1

# Define global variables
recordedResponses = []
responseCounter = 0
wrongCounter = 0
spaceCounter = 0
reversalCounter = 0
stdevDistance = []
averages = []
CorRespTime = []
IncRespTime = []
SpaRespTime = []
CorLevelRT = []
IncLevelRT = []
SpaLevelRT = []

# Monitor calibration is (Checked and verified okay)
# Get actual DPI (Pixels per inch) of screen monitor
app = QApplication(sys.argv)
screen = app.screens()[0]
dpi = screen.physicalDotsPerInch() # Pixels per inch
app.quit()

#Finds user's native resolution
user32 = ctypes.windll.user32
user32.SetProcessDPIAware()
[Width, Height] = [user32.GetSystemMetrics(0),
user32.GetSystemMetrics(1)]

#Calculate width of screen monitor
width_cm = (Width/dpi)*2.54 # There are 2.54 cm in an inch

# Define a monitor that adapts to resolution
testMonitor = monitors.Monitor(name='testMonitor')

```

```

testMonitor.setSizePix((Width, Height))
testMonitor.setWidth(width_cm)
testMonitor.setDistance(settingsGui.data[10])
testMonitor.saveMon()

# Define static variables
win = visual.Window(
    size=[Width,Height], fullscr=True, screen=int(settingsGui.data[9]),
    winType='pyglet', allowGUI=False, allowStencil=True,
    monitor='testMonitor', color=backgroundColor, colorSpace='rgb',
    blendMode='avg', useFBO=True, units='cm')

trialClock = core.Clock()

top = visual.Rect(win=win, units='cm', anchor='center',
    colorSpace='rgb', lineColor=backgroundColor, lineColorSpace='rgb',
    opacity=Stim_Opacity, contrast=Stim_Contrast,
    ori=Stim_Orientation, depth=0.0, interpolate=True )

#Dynamic stimuli
bot = visual.Rect(win=win, units='cm', anchor='center',
    colorSpace='rgb', lineColor=backgroundColor, lineColorSpace='rgb',
    opacity=Stim_Opacity, contrast=Stim_Contrast,
    ori=Stim_Orientation, depth=0.0, interpolate=True )

startgap = [128]
gaps = [64, 32, 16, 8, 4, 2]
random.shuffle(gaps)

if (gapGui.data[0] == "All"):
    gap_sizes = []
    gap_sizes.append(startgap[0])
    gap_sizes.append(gaps[0])
    gap_sizes.append(gaps[1])
    gap_sizes.append(gaps[2])
    gap_sizes.append(gaps[3])
    gap_sizes.append(gaps[4])
    gap_sizes.append(gaps[5])
else:
    gap_sizes = []
    gap_sizes.append(gapGui.data[1])
    gap_sizes.append(gapGui.data[2])
    gap_sizes.append(gapGui.data[3])
    gap_sizes = removeDup(gap_sizes)

# Create some handy timers
globalClock = core.Clock() # to track the time since experiment
started

```



```

routineTimer = core.CountdownTimer() # to track time remaining of each
(non-slip) routine

# Define strings
welcomeText = "Welcome to Vernier Acuity Test.\n\n Press Enter to
continue."
breakText = "Take a quick break.\n\n Press Enter to continue..."
exitText = "Excellent!!!\n\n This experiment is complete.\n\n Thank you
for participating! :)"

# draws current level
def drawLevel(level, stimuliLeft, gapSize):
    array = []
    drawTop(level, gapSize, array)
    win.flip()

    def Accurate():
        if (getExpectedResponse(emptylist[0]) == (keyEntered[0])[0]):
            return "Correct"
        else:
            if "space" in (keyEntered[0]):
                return "Aligned"
            else:
                return "Incorrect"

    def Gap():
        return (floor((math.tan((gapSize - line_height) /
settingsGui.data[10])) * (10800/math.pi))) # (10800/3 = 3600)???)

    globalClock.reset()
    keyEntered = psychopy.event.waitKeys(keyList = ["left", "space",
"right"], timeStamped=globalClock)
    if (keyEntered[0][0] == "space"):
        SpaRespTime.append((keyEntered[0])[1])
        SpaLevelRT.append((keyEntered[0])[1])
    elif (Accurate() == "Correct"):
        CorRespTime.append((keyEntered[0])[1])
        CorLevelRT.append((keyEntered[0])[1])
    else:
        IncRespTime.append((keyEntered[0])[1])
        IncLevelRT.append((keyEntered[0])[1])
    dataFile.write("{} , {} , {} , {} , {} , {} , {} \n".format(
Gap(),
Presentations - stimuliLeft + 1,
array[0]*60,
getExpectedResponse(array[0]),

```

```

(keyEntered[0])[0],
Accurate(),
(keyEntered[0])[1]))

# keeps track of thresholds for the current visual angle
if "space" in (keyEntered[0]):
    global recordedResponses
    global reversalCounter
    recordedResponses.append(abs(getHorizontalPosition(level,
emptylist))*60)
    reversalCounter += 1

    if (stimuliLeft != 0) and (reversalCounter != settingsGui.data[7]):
        level += updateLevel(getExpectedResponse(array[0]),
(keyEntered[0])[0])
        drawLevel(level, stimuliLeft -1, gapSize)

    else:
        if (len(recordedResponses) > 1):
            global stdevDistance
            dataFile.write((2*"{},{}\n").format("Averages (arc
seconds)", str(mean(recordedResponses)), "Standard Deviations (arc
seconds)", str(stdev(recordedResponses)) + "\n"))
            averages.append(mean(recordedResponses))
            stdevDistance.append(stdev(recordedResponses))

        elif (len(recordedResponses) == 1):
            dataFile.write((2*"{},{}\n").format("Averages (arc
seconds)", str(mean(recordedResponses)), "Standard Deviations (arc
seconds)", "Undetermined\n"))
            averages.append(mean(recordedResponses))
            stdevDistance.append("Undetermined")

        else:
            dataFile.write((2*"{},{}\n").format("Averages (arc
seconds)", "Undetermined", "Standard Deviations (arc seconds)",
"Undetermined\n"))
            averages.append("Undetermined")
            stdevDistance.append("Undetermined")

    recordedResponses = []
    level = -17
    responseCounter= 0
    reversalCounter = 0

# Selection sort based
def mySort(RespT, T):
    for i in range(len(RespT)):

```

```

    min_i = i
    for j in range(i+1, len(RespT)):
        if RespT[j] < RespT[min_i]:
            min_i = j

    tmp = RespT[i]
    RespT[i] = RespT[min_i]
    RespT[min_i] = tmp
    tmp2 = T[i]
    T[i] = T[min_i]
    T[min_i] = tmp2
    return T, RespT

# draws rectangular stimulus on random side on the exponential scale
def drawTop(level, gapSize, array):
    win.flip()
    time.sleep(0.3) #0.5
    drawBot()
    if (settingsGui.data[0] == "Line"):
        top.width = line_width
        top.height = line_height
    array.append(getHorizontalPosition(level, emptylist))
    top.pos = [arc2cm(array[0]), gapSize]
    top.draw()

# draws center stimulus
def drawBot():
    if (settingsGui.data[0] == "Line"):
        bot.width = line_width
        bot.height = line_height
    bot.pos = [0,0]
    bot.draw()

# draws text stimulus
def drawText(text):
    stim = visual.TextStim(win, text, font='Arial',
        color= stimuliColor, languageStyle='LTR', wrapWidth=None,
        alignText='center')
    stim.draw()
    win.flip()
    psychopy.event.waitKeys(keyList = ["return"])

def drawTextAlt(text):
    stim = visual.TextStim(win, text, font='Arial',
        color= stimuliColor, languageStyle='LTR', wrapWidth=None,
        alignText='center')
    stim.draw()

```

```

win.flip()
psychopy.event.waitKeys(keyList = ["return"])

emptylist = []

# returns x position based on level on a logarithmic scale
def getHorizontalPosition(level, listnum):
    randint = 0
    listnum.clear()
    while (randint == 0):
        randint = random.randint(-1,1)
        listnum.append((randint * math.pow(math.e, -0.1574748 * (level))))
# Maximum misalignment left/right (-0.12 to -0.16) (-0.1574748 = 3600
or 1 Degree start position) level = -17
    return listnum[0]

# returns expected responses
def getExpectedResponse(horizontalPosition):
    if (horizontalPosition > 0):
        return "right"
    elif (horizontalPosition < 0):
        return "left"
    else:
        return "space"

#####
#####
# increases level for every 3 correct responses
# decreases level for every incorrect response
# decreases level by 3 steps for every space response

def updateLevel(expectedKey, responseKey):
    global responseCounter
    global wrongCounter
    global spaceCounter

    if (expectedKey == responseKey):
        responseCounter += 1
        if (responseCounter == 3): #(Three correct inputs in row)
            responseCounter = 0
            return settingsGui.data[5] #(1 step close)
        else:
            return 0
    else:
        if "space" in responseKey:
            spaceCounter += 1

```

```

        if (spaceCounter == 1): #(Each time Space input)
            spaceCounter = 0
            return -settingsGui.data[6] #(-3 steps away)
        else:
            return 0
    else:
        wrongCounter += 1
        if (wrongCounter == 1): #(step = 1)
            wrongCounter = 0
            return -settingsGui.data[5] #(-1 step away)
        else:
            return 0

# converts visual angle to cms of given stimulus height
def getGapSizeDistance(gap_size, height):
    return settingsGui.data[10] * math.tan(gap_size * math.pi / 60/180)
+ line_height

def read_cell(x, y):
    with open(fileName + '.csv', 'r') as f:
        reader = csv.reader(f)
        y_count = 0
        for n in reader:
            if y_count == y:
                cell = n[x]
                return cell
            y_count += 1

def main():
    win.mouseVisible = False
    drawText(welcomeText)
    SpaAvgRT = []
    CorAvgRT = []
    IncAvgRT = []
    win.flip()
    for x in range(0, len(gap_sizes)):
        dataFile.write("{} , {} , {} , {} , {} , {} , {}" .format("\nGap Size",
"Presentation Number", "Stimuli Position (arc seconds)", "Correct
Response" , "Key Response", "Accuracy", "Response Time\n"))
        drawLevel(-26, Presentations,
getGapSizeDistance(gap_sizes[x],line_height))
        win.flip()
        win.callOnFlip(globalClock.reset)
        if not SpaLevelRT: # Check if it is empty
            SpaAvgRT.append(0)
        else:

```

```

        SpaAvgRT.append(mean(SpaLevelRT))

    if not CorLevelRT: # Check if it is empty
        CorAvgRT.append(0)
    else:
        CorAvgRT.append(mean(CorLevelRT))

    if not IncLevelRT: # Check if it is empty
        IncAvgRT.append(0)
    else:
        IncAvgRT.append(mean(IncLevelRT))
        SpaLevelRT.clear()
        CorLevelRT.clear()
        IncLevelRT.clear()
        if (len(gap_sizes) != x+1):
            drawTextAlt(breakText)
        drawText(exitText)
        dataFile.write(("{}{}{}{}{}").format("Summary", "\nGapSizes",
"Averages (arc seconds)", "Standard Dev (Thresholds in arc seconds)
\n"))
        for i in range(0, len(gap_sizes)):

dataFile.write("{}{}{}{}{}").format(gap_sizes[i], str(averages[i]), str(
stdevDistance[i]))
        dataFile.close()

    win.flip()

    win.close()

    #format summary tables
    def filter_rows_by_strings(df, col, strings):
        return df[df[col].isin(strings) == False]

    def filter_rows_by_col_val(df, col, strings):
        return df[df[col].isin(strings) == True]

    df = pd.read_csv(filename+".csv", skiprows=18)
    df = df[:-5]
    filter_strings = ["Averages (arc seconds)", "Standard Deviations
(arc seconds)"]
    df = filter_rows_by_strings(df, "Gap Size", filter_strings)

    f = df.eq(df.columns)
    groups = [g.reset_index(drop=True) for _, g in df[~f.iloc[:,
0]].groupby(f.cumsum()[~f.iloc[:, 0]].iloc[:, 0])]

    #numerical table

```

```

gap_size = []
standarddev = []
correct = []
incorrect = []
aligned = []

for i in range(len(groups)):

    gf = groups[i].copy()
    gapsz = gf["Gap Size"].tolist()[0]
    gap_size.append(gapsz)

    pf = groups[i].copy()
    pf = filter_rows_by_col_val(pf, "Key Response", ["space"])
    stdev = pf["Stimuli Position (arc seconds)"].tolist()
    stdev = statistics.stdev([float(x) for x in stdev])
    standarddev.append(stdev)

    cf = groups[i].copy()
    cf = filter_rows_by_col_val(cf, "Accuracy", ["Correct"])
    acc = cf["Response Time"].tolist()
    try:
        acc = statistics.mean([float(x) for x in acc])

    except statistics.StatisticsError:
        acc = 0

    correct.append(acc)

    nf = groups[i].copy()
    nf = filter_rows_by_col_val(nf, "Accuracy", ["Incorrect"])
    nacc = nf["Response Time"].tolist()
    try:
        nacc = statistics.mean([float(x) for x in nacc])

    except statistics.StatisticsError:
        nacc = 0

    incorrect.append(nacc)

    af = groups[i].copy()
    af = filter_rows_by_col_val(af, "Accuracy", ["Aligned"])
    aln = af["Response Time"].tolist()
    try:
        aln = statistics.mean([float(x) for x in aln])

    except statistics.StatisticsError:

```

```

        aln = 0

    aligned.append(aln)

#percent table
correctp = []
incorrectp = []
alignedp = []

for i in range(len(groups)):

    cf = groups[i].copy()
    lencf = len(cf["Response Time"].tolist())
    if lencf == 0:
        acc_percent = 0
    else:
        cf = filter_rows_by_col_val(cf, "Accuracy", ["Correct"])
        acc = len(cf["Response Time"].tolist())
        acc_percent = (acc/lencf)*100
    correctp.append(acc_percent)

    nf = groups[i].copy()
    lennf = len(nf["Response Time"].tolist())
    if lennf == 0:
        nacc_percent = 0
    else:
        nf = filter_rows_by_col_val(nf, "Accuracy", ["Incorrect"])
        nacc = len(nf["Response Time"].tolist())
        nacc_percent = (nacc/lennf)*100

    incorrectp.append(nacc_percent)

    af = groups[i].copy()
    lenaf = len(af["Response Time"].tolist())
    if lenaf == 0:
        aln_percent = 0
    else:
        af = filter_rows_by_col_val(af, "Accuracy", ["Aligned"])
        aln = len(af["Response Time"].tolist())
        aln_percent = (aln/lenaf)*100

    alignedp.append(aln_percent)

# Data file name stem = absolute path + name; later add .psyexp,
.csv, .log, etc

```



```

    data_tables = _thisDir + os.sep + u'HAT Data/%s_%s_%s_%s' %
(infoGui.data[0], "tables", expName, expDate)
    workbook = xlswriter.Workbook(data_tables+'.xlsx')

    summary = workbook.add_worksheet()

    row_a = ["Gap Size", "Thresholds (SD)", "Correct Resp. Avg.",
"Incorrect Resp. Avg.", "Aligned Resp. Avg."]

    summary.write_row('A1', row_a)
    summary.write_column('A2', gap_size)
    summary.write_column('B2', standarddev)
    summary.write_column('C2', correct)
    summary.write_column('D2', incorrect)
    summary.write_column('E2', aligned)

    summarypercent = workbook.add_worksheet()
    p_row_a = ["Gap Size", "Correct Resp. Avg. (%)", "Incorrect Resp.
Avg. (%)", "Aligned Resp. Avg. (%)"]

    summarypercent.write_row('A1', p_row_a)
    summarypercent.write_column('A2', gap_size)
    summarypercent.write_column('B2', correctp)
    summarypercent.write_column('C2', incorrectp)
    summarypercent.write_column('D2', alignedp)

    workbook.close()
    core.quit()

if __name__ == "__main__":
    main()

```

Hyperacuity Perimetry Program Code

```
from __future__ import absolute_import, division

import psychopy
psychopy.useVersion('2022.2')

from psychopy import locale_setup
from psychopy import prefs

from psychopy import sound, gui, visual, monitors, core, data, event,
logging, clock
from psychopy.constants import (NOT_STARTED, STARTED, PLAYING, PAUSED,
                               STOPPED, FINISHED, PRESSED, RELEASED,
FOREVER)

import numpy as np # whole numpy lib is available, prepend 'np.'
from numpy import (sin, cos, tan, log, log10, pi, average,
                  sqrt, std, deg2rad, rad2deg, linspace, asarray)
from numpy.random import random, randint, normal, shuffle

import matplotlib.pyplot as plt
import pandas as pd
import xlswriter
import io
import random
import time
import math
from math import floor

import os # handy system and path functions
import sys # to get file system encoding

from win32api import GetSystemMetrics
from statistics import stdev, mean
from datetime import datetime
import ctypes
from PyQt5.QtWidgets import QApplication

# Ensure that relative paths start from the same directory as this script
_thisDir = os.path.dirname(os.path.abspath(__file__))
os.chdir(_thisDir)

# GUI
infoGui = psychopy.gui.Dlg (title = "Participant Information",
labelButtonCancel=' Cancel ', labelButtonOK=' Settings ')
infoGui.addField("Name: ") # 0
infoGui.addField("Age: ") # 1
```

```

infoGui.addField("Gender: ", choices=["Other", "Male", "Female"]) # 2
infoGui.addField("Session:", 1) # 3

settingsGui=psychopy.gui.Dlg (title = "Experiment Settings",
labelButtonCancel=' Back ', labelButtonOK=' Start ')
settingsGui.addField("Stimuli Colour :", choices=["White", "Black"]) # 0
settingsGui.addField("Stimuli Type :", choices=["Line"]) #1
settingsGui.addField("Opacity :", choices=[1]) #2
settingsGui.addField("Line height (moa) :", choices=[30]) #3
settingsGui.addField("Line width (moa) :", choices=[3]) #4

settingsGui.addText('Staircase Settings', color = "Red")

settingsGui.addField("Number of steps Up :", choices=[1]) #5
settingsGui.addField("Number of steps Down :", choices=[3]) #6
settingsGui.addField("Number of Reversals :", choices=[3]) #7

settingsGui.addField("Eye :", choices=["LEFT", "RIGHT"]) #8
settingsGui.addField("Degrees :", choices=[5]) #9

settingsGui.addText('Display Settings: 0-Default Screen, 1-Extended
Screen', color = "Red")
settingsGui.addField("Screen :", choices=[0]) #10
settingsGui.addField("Distance from Screen(cms) :", choices=[100]) #11

#GUI loop
flag = True
while(flag):
    infoGui.show()
    if(infoGui.OK == True):
        settingsGui.show() # Pressed settings
        if(settingsGui.OK == True): # Pressed Gap size settings
            flag = False
            break
        else: #pressed back in settings GUI
            pass # DO nothing go back to loop 1
    else: # Pressed Cancel in Info GUI
        core.quit()

# Store info about the experiment session
psychopyVersion = '2022.2'
expName = 'HP'
expDate = data.getDateStr()

# Data file name stem = absolute path + name; later add .psyexp, .csv,
.log, etc
filename = _thisDir + os.sep + u'HP Data/%s_%s_%s' % (infoGui.data[0],
expName, expDate)

```

```

# Open data file
fileName = filename
dataFile = open(fileName+'.csv', 'w')
dataFile.write((18 * "{}\n").format(
    "Date", datetime.now(),
    "Name", infoGui.data[0],
    "Age", infoGui.data[1],
    "Gender", infoGui.data[2],
    "Session", infoGui.data[3],
    "Stimuli Colour", settingsGui.data[0],
    "Stimuli Type", settingsGui.data[1],
    "Opacity", settingsGui.data[2],
    "Line height (moa)", settingsGui.data[3],
    "Line width (moa)", settingsGui.data[4],
    "Number of steps Up", settingsGui.data[5],
    "Number of steps Down", settingsGui.data[6],
    "Number of Reversals", settingsGui.data[7],
    "Eye", settingsGui.data[8],
    "Degrees", settingsGui.data[9],
    "Screen", settingsGui.data[10],
    "Distance from screen", settingsGui.data[11],
    "Display resolution (px)", str(GetSystemMetrics(0)) + " x " +
    str(GetSystemMetrics(1))))

# Converts minutes of arc to cm
def arc2cm(arc):
    return settingsGui.data[11] * math.tan(arc * math.pi / 60 / 180)

# Converts Degrees to cm
def deg2cm(degree):
    return settingsGui.data[11] * math.tan(degree * math.pi / 180)

# Converts cm to minutes of arc
def cm2arc(length):
    return math.atan(length/settingsGui.data[11]) * 60 * 180/math.pi

#Stim config
Stim_Opacity = settingsGui.data[2]
Stim_Contrast = 1 #(1.0: unchanged, 0.5: decrease, 0.0: uniform, 0.5
slightly inverted, -1.0: totally inverted)
Stim_Orientation = 0
Red = [1.0, -1, -1]
Presentations = 200 - 1

# Staircase settings
Reversals = settingsGui.data[7]

```

```

#Defining the line stimuli in MINUTES OF ARC
height_moa = settingsGui.data[3]
width_moa = settingsGui.data[4]

##Converting MOA into Cms
line_height = arc2cm(height_moa)
line_width = arc2cm(width_moa)

#Cross stimuli config
cross_moa = 15
Cross = arc2cm(cross_moa)

# Assign Stimuli variables
if (settingsGui.data[0] == "White"):
    stimuliColor = 'white'
    backgroundColor = 'black'
else:
    stimuliColor = 'black'
    backgroundColor = 'white'

Degrees = settingsGui.data[9]
Deg = deg2cm(Degrees)

VisualFields = ["Top", "Nasal", "Bottom", "Temporal"]
xPos = 0
yPos = 0
radius = Deg

def getPosition(visField): # Visual field refers to nasal, temporal,
inferior, superior.
    if (visField == "Top"):
        xPos = 0
        yPos = radius
    elif (visField == "Bottom"):
        xPos = 0
        yPos = -radius
    elif (visField == "Nasal"):
        if (settingsGui.data[8] == "LEFT"):
            xPos = radius
            yPos = 0
        else: # Eye is right
            xPos = -radius
            yPos = 0
    else: # visField == Temporal
        if (settingsGui.data[8] == "LEFT"):

```

```

        xPos = -radius
        yPos = 0
    else: # Eye is right
        xPos = radius
        yPos = 0
    return xPos, yPos

# Define global variables
recordedResponses = []
responseCounter = 0
wrongCounter = 0
spaceCounter = 0
reversalCounter = 0
stdevDistance = []
averages = []
CorRespTime = []
IncRespTime = []
SpaRespTime = []
CorLevelRT = []
IncLevelRT = []
SpaLevelRT = []

# Get actual DPI (Pixels per inch) of screen monitor
app = QApplication(sys.argv)
screen = app.screens()[0]
dpi = screen.physicalDotsPerInch() # Pixels per inch
app.quit()

#Finds user's native resolution
user32 = ctypes.windll.user32
user32.SetProcessDPIAware()
[Width, Height] = [user32.GetSystemMetrics(0),
user32.GetSystemMetrics(1)]

#Calculate width of screen monitor
width_cm = (Width/dpi)*2.54 # There are 2.54 cm in an inch

# Define a monitor that adapts to resolution
testMonitor = monitors.Monitor(name='testMonitor')
testMonitor.setSizePix((Width, Height))
testMonitor.setWidth(width_cm)
testMonitor.setDistance(settingsGui.data[11])
testMonitor.saveMon()

# Define static variables
win = visual.Window(

```

```

    size=[Width,Height], fullscr=True, screen=int(settingsGui.data[10]),
    winType='pyglet', allowGUI=False, allowStencil=True,
    monitor='testMonitor', color=backgroundColor, colorSpace='rgb',
    blendMode='avg', useFBO=True, units='cm')
win.mouseVisible= False
event.globalKeys.add(key='escape', func=sys.exit)
trialClock = core.Clock()

top = visual.Rect(win=win, units='cm', anchor='center',
    colorSpace='rgb', lineColor=backgroundColor, lineColorSpace='rgb',
    fillColor=stimuliColor, opacity=Stim_Opacity, depth=0.0,
    interpolate=True )

bot = visual.Rect(win=win, units='cm', anchor='center',
    colorSpace='rgb', lineColor=backgroundColor, lineColorSpace='rgb',
    fillColor=stimuliColor, opacity=Stim_Opacity, depth=0.0,
    interpolate=True )

fix = psychopy.visual.ShapeStim(win=win, units='cm', vertices='cross',
    anchor='center', colorSpace='rgb', lineColor=backgroundColor,
    lineColorSpace='rgb',
    fillColor=Red, opacity=Stim_Opacity, depth=0.0, interpolate=True )

gap_sizes = [30, 15]
random.shuffle(gap_sizes)

# Create some handy timers
globalClock = core.Clock() # to track the time since experiment started
routineTimer = core.CountdownTimer() # to track time remaining of each
(non-slip) routine

# Define strings
welcomeText = "Welcome to Hyperacuity Perimetry Test\n Testing your
"+settingsGui.data[8] + " eye\n Press Enter to continue..."
breakText = "Take a quick break!\n Press Enter to continue..."
exitText = "Excellent!!!\n\n This experiment is complete.\n\n Thank you
for participating! :)"

# draws current level
def drawLevel(level, stimuliLeft, gapSize, visField):
    array = []
    drawRectangle(level, gapSize, array, visField)
    win.flip()

    def Accurate():
        if (getExpectedResponse(emptylist[0]) == (keyEntered[0])[0]):
            return "Correct"
        else:

```

```

        if "space" in (keyEntered[0]):
            return "Aligned"
        else:
            return "Incorrect"

    def Gap():
        return (floor((math.tan((gapSize - line_height) /
settingsGui.data[11])) * (10800/math.pi)))

    globalClock.reset()
    keyEntered = psychopy.event.waitKeys(keyList = ["left", "space",
"right"], timeStamped=globalClock)
    if (keyEntered[0][0] == "space"):
        SpaRespTime.append((keyEntered[0])[1])
        SpaLevelRT.append((keyEntered[0])[1])
    elif (Accurate() == "Correct"):
        CorRespTime.append((keyEntered[0])[1])
        CorLevelRT.append((keyEntered[0])[1])
    else:
        IncRespTime.append((keyEntered[0])[1])
        IncLevelRT.append((keyEntered[0])[1])
    dataFile.write("{} , {} , {} , {} , {} , {} , {} \n" .format (
Gap(),
Presentations - stimuliLeft + 1,
array[0]*60,
getExpectedResponse(array[0]),
(keyEntered[0])[0],
Accurate(),
(keyEntered[0])[1]))

    # keeps track of thresholds for the current visual angle
    if "space" in (keyEntered[0]):
        global recordedResponses
        global reversalCounter
        recordedResponses.append(abs(getHorizontalPosition(level,
emptylist))*60)
        reversalCounter += 1

    if (stimuliLeft != 0) and (reversalCounter != Reversals):
        level += updateLevel(getExpectedResponse(array[0]),
(keyEntered[0])[0])
        drawLevel(level, stimuliLeft -1, gapSize, visField)
    else:
        if (len(recordedResponses) > 1):
            global stdevDistance

```



```

        dataFile.write((2*"{}, {}").format("Averages",
str(mean(recordedResponses)), "\nStandard Deviations",
str(stdev(recordedResponses)) + "\n"))
        averages.append(mean(recordedResponses))
        stdevDistance.append(stdev(recordedResponses))

    elif (len(recordedResponses) == 1):
        dataFile.write((2*"{}, {}").format("Averages",
str(mean(recordedResponses)), "\nStandard Deviations", "Undetermined\n"))
        averages.append(mean(recordedResponses))
        stdevDistance.append("Undetermined")

    else:
        dataFile.write((2*"{}, {}").format("Averages", "Undetermined",
"\nStandard Deviations", "Undetermined\n"))
        averages.append("Undetermined")
        stdevDistance.append("Undetermined")

recordedResponses = []
level = -17
responseCounter= 0
reversalCounter = 0

# Selection sort based
def mySort(RespT, T):
    for i in range(len(RespT)):
        min_i = i
        for j in range(i+1, len(RespT)):
            if RespT[j] < RespT[min_i]:
                min_i = j

        tmp = RespT[i]
        RespT[i] = RespT[min_i]
        RespT[min_i] = tmp
        tmp2 = T[i]
        T[i] = T[min_i]
        T[min_i] = tmp2
    return T, RespT

# draws rectangular stimulus on random side on the exponential scale
def drawRectangle(level, gapSize, array, visField):
    drawCentre()
    win.flip()
    drawCentre()
    time.sleep(0.3)
    drawAxis(visField, gapSize)
    top.width = line_width

```

```

top.height = line_height
top.ori = Stim_Orientation
array.append(getHorizontalPosition(level, emptylist))
x, y = getPosition(visField)
top.pos = [x + arc2cm(array[0]), y + gapSize/2] #####
top.draw()

# draws static stimuli
def drawAxis(visField, gapSize):
    bot.width = line_width
    bot.height = line_height
    bot.ori = Stim_Orientation
    x, y = getPosition(visField)
    bot.pos = [x, y - gapSize/2]#####
    bot.draw()

def drawCentre():
    fix.size= (Cross, Cross)
    fix.pos= (0,0)
    fix.draw()

# draws text stimulus
def drawText(text):
    stim = visual.TextStim(win, text, font='Arial',
        languageStyle='LTR', wrapWidth=None,
        color= stimuliColor, colorSpace='rgb', alignText='center')
    stim.draw()
    win.flip()
    psychopy.event.waitKeys(keyList = ["return"])

emptylist = []

# returns x position based on level on a logarithmic scale. In degrees of
arc
def getHorizontalPosition(level, listnum):
    randint = 0
    listnum.clear()
    while (randint == 0):
        randint = random.randint(-1,1)
    listnum.append((randint * math.pow(math.e, -0.1574748 * (level))))
    return listnum[0]

# returns expected responses
def getExpectedResponse(horizontalPosition):

```

```

if (horizontalPosition > 0):
    return "right"
elif (horizontalPosition < 0):
    return "left"
else:
    return "space"

#####
#####
# increases level for every 3 correct responses
# decreases level for every incorrect response
# decreases level by 3 steps for every space response

def updateLevel(expectedKey, responseKey):
    global responseCounter
    global wrongCounter
    global spaceCounter

    if (expectedKey == responseKey):
        responseCounter += 1
        if (responseCounter == settingsGui.data[6]): #(Three correct
inputs in row)
            responseCounter = 0
            return 1 #(1 step close)
        else:
            return 0
    else:
        if "space" in responseKey:
            spaceCounter += 1
            if (spaceCounter == 1): #(Each time Space input)
                spaceCounter = 0
                return -3 #(-3 steps away)
            else:
                return 0
        else:
            wrongCounter += 1
            if (wrongCounter == settingsGui.data[5]): #(step = 1)
                wrongCounter = 0
                return -1 #(-1 step away)
            else:
                return 0

# converts visual angle to cms of given stimulus height
def getGapSizeDistance(gap_size, height):
    return settingsGui.data[11] * math.tan(gap_size * math.pi /60/180) +
line_height

```

```

def read_cell(x, y):
    with open(fileName + '.csv', 'r') as f:
        reader = csv.reader(f)
        y_count = 0
        for n in reader:
            if y_count == y:
                cell = n[x]
                return cell
            y_count += 1

def main():
    win.mouseVisible = False
    drawText(welcomeText)
    win.flip()
    for i in range(4):
        visField = VisualFields[i]
        VisFieldText = "Testing the "+ visField+" view of your
"+settingsGui.data[8]+" eye"
        drawText(VisFieldText)
        SpaAvgRT = []
        CorAvgRT = []
        IncAvgRT = []
        win.flip
        dataFile.write(("\\n\\n{},{},{}").format("Visual Field", visField))
        for x in range(0, len(gap_sizes)):
            drawCentre()
            dataFile.write(("{},{},{},{},{},{},{},{}").format("\\nGap Size",
"Presentation Number", "Stimuli Position (arc seconds)", "Correct
Response" ,"Key Response", "Accuracy", "Response Time\\n"))
            drawLevel(-26, Presentations,
getGapSizeDistance(gap_sizes[x],line_height), visField)
            win.flip()
            win.callOnFlip(globalClock.reset)
            if not SpaLevelRT: # Check if it is empty
                SpaAvgRT.append(0)
            else:
                SpaAvgRT.append(mean(SpaLevelRT))

            if not CorLevelRT: # Check if it is empty
                CorAvgRT.append(0)
            else:
                CorAvgRT.append(mean(CorLevelRT))

            if not IncLevelRT: # Check if it is empty
                IncAvgRT.append(0)
            else:

```

```

        IncAvgRT.append(mean(IncLevelRT))
        SpaLevelRT.clear()
        CorLevelRT.clear()
        IncLevelRT.clear()
        if (len(gap_sizes) != x+1):
            drawText(breakText)
        drawText(exitText)
        dataFile.write(("{}{}{}{}").format("Summary", "\nGapSizes",
"Averages (arc seconds)", "Standard Dev (Thresholds in arc seconds) \n"))
        for i in range(0, len(gap_sizes)):
dataFile.write(("{}{}{}").format(gap_sizes[i], str(averages[i]), str(stdev
Distance[i])))
        dataFile.close()

        win.flip()

        win.close()

# #format summary tables
# def filter_rows_by_strings(df, col, strings):
#     return df[df[col].isin(strings) == False]
#
# def filter_rows_by_col_val(df, col, strings):
#     return df[df[col].isin(strings) == True]
#
# df = pd.read_csv(filename+".csv", skiprows=18)
# df = df[:5]
# filter_strings = ["Averages (arc seconds)", "Standard Deviations
(arc seconds)"]
# df = filter_rows_by_strings(df, "Gap Size", filter_strings)
#
# f = df.eq(df.columns)
# groups = [g.reset_index(drop=True) for _, g in df[~f.iloc[:,
0]].groupby(f.cumsum()[~f.iloc[:, 0]].iloc[:, 0])]
#
# #numerical table
# gap_size = []
# standarddev = []
# correct = []
# incorrect = []
# aligned = []
#
#
# for i in range(len(groups)):
#
#     gf = groups[i].copy()
#     gapsz = gf["Gap Size"].tolist()[0]

```

```

#         gap_size.append(gapsz)
#
#         pf = groups[i].copy()
#         pf = filter_rows_by_col_val(pf, "Key Response", ["space"])
#         stdev = pf["Stimuli Position (arc seconds)"].tolist()
#         stdev = statistics.stdev([float(x) for x in stdev])
#         standardev.append(stdev)
#
#         cf = groups[i].copy()
#         cf = filter_rows_by_col_val(cf, "Accuracy", ["Correct"])
#         acc = cf["Response Time"].tolist()
#         try:
#             acc = statistics.mean([float(x) for x in acc])
#
#         except statistics.StatisticsError:
#             acc = 0
#
#         correct.append(acc)
#
#         nf = groups[i].copy()
#         nf = filter_rows_by_col_val(nf, "Accuracy", ["Incorrect"])
#         nacc = nf["Response Time"].tolist()
#         try:
#             nacc = statistics.mean([float(x) for x in nacc])
#
#         except statistics.StatisticsError:
#             nacc = 0
#
#         incorrect.append(nacc)
#
#         af = groups[i].copy()
#         af = filter_rows_by_col_val(af, "Accuracy", ["Aligned"])
#         aln = af["Response Time"].tolist()
#         try:
#             aln = statistics.mean([float(x) for x in aln])
#
#         except statistics.StatisticsError:
#             aln = 0
#
#         aligned.append(aln)
#
#
#         #percent table
#         correctp = []
#         incorrectp = []
#         alignedp = []
#
#
#

```

```

#     for i in range(len(groups)):
#
#         cf = groups[i].copy()
#         lengf = len(cf["Response Time"].tolist())
#         if lengf == 0:
#             acc_percent = 0
#         else:
#             cf = filter_rows_by_col_val(cf, "Accuracy", ["Correct"])
#             acc = len(cf["Response Time"].tolist())
#             acc_percent = (acc/lengf)*100
#         correctp.append(acc_percent)
#
#         nf = groups[i].copy()
#         lennf = len(nf["Response Time"].tolist())
#         if lennf == 0:
#             nacc_percent = 0
#         else:
#             nf = filter_rows_by_col_val(nf, "Accuracy", ["Incorrect"])
#             nacc = len(nf["Response Time"].tolist())
#             nacc_percent = (nacc/lennf)*100
#
#         incorrectp.append(nacc_percent)
#
#         af = groups[i].copy()
#         lenaf = len(af["Response Time"].tolist())
#         if lenaf == 0:
#             aln_percent = 0
#         else:
#             af = filter_rows_by_col_val(af, "Accuracy", ["Aligned"])
#             aln = len(af["Response Time"].tolist())
#             aln_percent = (aln/lenaf)*100
#
#         alignedp.append(aln_percent)
#
#     # Data file name stem = absolute path + name; later add .psyexp,
#     .csv, .log, etc
#     data_tables = _thisDir + os.sep + u'HAT Data/%s_%s_%s_%s' %
# (infoGui.data[0], "tables", expName, expDate)
#     workbook = xlswriter.Workbook(data_tables+'.xlsx')
#
#     summary = workbook.add_worksheet()
#
#     row_a = ["Gap Size", "Thresholds (SD)", "Correct Resp. Avg.",
# "Incorrect Resp. Avg.", "Aligned Resp. Avg."]
#
#     summary.write_row('A1', row_a)
#     summary.write_column('A2', gap_size)
#     summary.write_column('B2', standarddev)

```

```

# summary.write_column('C2', correct)
# summary.write_column('D2', incorrect)
# summary.write_column('E2', aligned)
#
# summarypercent = workbook.add_worksheet()
# p_row_a = ["Gap Size", "Correct Resp. Avg. (%)", "Incorrect Resp.
Avg. (%)", "Aligned Resp. Avg. (%)"]
#
# summarypercent.write_row('A1', p_row_a)
# summarypercent.write_column('A2', gap_size)
# summarypercent.write_column('B2', correctp)
# summarypercent.write_column('C2', incorrectp)
# summarypercent.write_column('D2', alignedp)
#
# workbook.close()
core.quit()

if __name__ == "__main__":
    main()

```


Metamorphopsia Program Code

```
from __future__ import absolute_import, division

import psychopy
psychopy.useVersion('2022.2')

from psychopy.tools.monitorunittools import posToPix
from psychopy.hardware import keyboard
from psychopy import locale_setup
from psychopy import prefs
from psychopy import sound, gui, visual, monitors, core, data, event,
logging, clock
from psychopy.constants import (NOT_STARTED, STARTED, PLAYING, PAUSED,
                                STOPPED, FINISHED, PRESSED, RELEASED,
                                FOREVER)

import numpy as np # whole numpy lib is available, prepend 'np.'
from numpy import (sin, cos, tan, log, log10, pi, average,
                  sqrt, std, deg2rad, rad2deg, linspace, asarray)
from numpy.random import random, randint, normal, shuffle

import os # handy system and path functions
import pandas as pd
import xlswriter
import io
import random
import time
import math
from math import floor
import sys
import matplotlib.pyplot as plt
from win32api import GetSystemMetrics
from statistics import stdev, mean
from datetime import datetime
import ctypes
from PyQt5.QtWidgets import QApplication

#define lists for polygon coordinates
init_x = []
init_y = []
fin_x = []
fin_y = []

# Ensure that relative paths start from the same directory as this
script
_thisDir = os.path.dirname(os.path.abspath(__file__))
```

```

os.chdir(_thisDir)

# Below we add the GUI components. What is added is self explanatory.

infoGui = psychopy.gui.Dlg (title = "Participant Information",
labelButtonCancel=' Cancel ', labelButtonOK=' Settings ')

infoGui.addText("Enter Participant Information: ")
infoGui.addField("Name:") #0
infoGui.addField("Age:") #1
infoGui.addField("Gender:", choices=["Other", "Male", "Female"]) #2
infoGui.addField("Eye:", choices=["Left", "Right", "Both"]) #3
infoGui.addField("Session:", 1) #4

#Settings menu on GUI
settingsGui=psychopy.gui.Dlg (title = "Experiment Settings",
labelButtonCancel=' Back ', labelButtonOK=' Start ')

settingsGui.addField("Stimuli Colour :", choices=["White", "Black"]) #0
settingsGui.addField("Stimuli Type :", choices=["Both"]) #1

settingsGui.addText('Display Settings: 0-Default Screen, 1-Extended
Screen', color = "Red")
settingsGui.addField("Screen :", choices=[0]) #2
settingsGui.addField("Distance from Screen(cms) :", 100)#3

#GUI loop
flag = True
while(flag):
    infoGui.show()
    if(infoGui.OK == True):
        settingsGui.show() # Pressed settings
        if(settingsGui.OK == True): # Pressed Gap size settings
            flag = False
            break
        else: #pressed back in settings GUI
            pass # DO nothing go back to loop 1
    else: # Pressed Cancel in Info GUI
        core.quit()

# Store info about the experiment session
psychopyVersion = '2022.2'
expName = 'MMP'
expDate = data.getDateStr()

# Data file name stem = absolute path + name; later add .psyexp, .csv,
.log, etc

```

```

fileName = _thisDir + os.sep + u'MMP Data/%s_%s_%s' % (infoGui.data[0],
expName, expDate)

# Open data file
fileName = fileName
dataFile = open(fileName+'.csv', 'w')
dataFile.write((11 * "{}\n").format(
    "Date", datetime.now(),
    "Name", infoGui.data[0],
    "Age", infoGui.data[1],
    "Gender", infoGui.data[2],
    "Eye", infoGui.data[3],
    "Session", infoGui.data[4],
    "Stimuli Colour", settingsGui.data[0],
    "Stimuli Type", settingsGui.data[1],
    "Display resolution (px)", str(GetSystemMetrics(0)) + " x " +
    str(GetSystemMetrics(1)),
    "Screen", settingsGui.data[2],
    "Distance from screen", settingsGui.data[3]))

# Assign Stimuli variables
if (settingsGui.data[0] == "White"):
    stimuliColor = 'white'
    backgroundColor = 'black'
else:
    stimuliColor = 'black'
    backgroundColor = 'white'

# Get actual DPI (Pixels per inch) of screen monitor
app = QApplication(sys.argv)
screen = app.screens()[0]
dpi = screen.physicalDotsPerInch() # Pixels per inch
app.quit()

#Finds user's native resolution
user32 = ctypes.windll.user32
user32.SetProcessDPIAware()
[Width, Height] = [user32.GetSystemMetrics(0),
user32.GetSystemMetrics(1)]

#Calculate width of screen monitor
width_cm = (Width/dpi)*2.54 # There are 2.54 cm in an inch

# Define a monitor that adapts to the user's resolution
testMonitor = monitors.Monitor(name='testMonitor')
testMonitor.setSizePix((Width, Height))

```

```

testMonitor.setWidth(width_cm)
testMonitor.setDistance(settingsGui.data[3])
testMonitor.saveMon()

# Create window
win = visual.Window(
    size=[Width,Height], fullscr=True, screen=int(settingsGui.data[2]),
    winType='pyglet', allowGUI=False, allowStencil=True,
    monitor='testMonitor', color=backgroundColor, colorSpace='rgb',
    blendMode='avg', useFBO=True, units='cm')

mouse = event.Mouse(win=win)
x, y = [None, None]

# Create some handy timers
globalClock = core.Clock() # to track the time since experiment
started
resp = [] #list for global response time

someClock = core.Clock()

# Converts minutes of arc to cm
def arc2cm(arc):
    return settingsGui.data[3] * math.tan(arc * math.pi /60/180)

# Converts Degrees to cm
def deg2cm(degree):
    return settingsGui.data[3] * math.tan(degree * math.pi /180)

# Converts cm to minutes of arc
def cm2arc(length):
    return math.atan(length/settingsGui.data[3]) * 60 * 180/math.pi

#Stimuli in minutes of arc to cms.
height_moa = 30
width_moa = 3
#Conversion
line_h = int(settingsGui.data[3]) * math.tan(height_moa * math.pi
/60/180)
line_w = int(settingsGui.data[3]) * math.tan(width_moa * math.pi
/60/180)

#Cross or Target stimuli config
Cross_moa = 15
Plus = int(settingsGui.data[3]) * math.tan(Cross_moa * math.pi /60/180)

```

```

#define keyboard
kb = keyboard.Keyboard()

#minutes of arc variable and variable to determine height of still
stimuli.
Degrees = [5, 4, 3, 2, 1]
Deg = [deg2cm(x) for x in Degrees]

def main():
    cm_gaps = [(x)+line_h/2 for x in Deg]

    def coordcalc(r):
        #cartesian coordinates for vertical & horizontal orientation
        #upper rect
        x1 = 0
        y1 = r

        #bottom rect
        x2 = 0
        y2 = -r

        #left rect
        x3 = -r
        y3 = 0

        #right rect
        x4 = r
        y4 = 0

        #polar coordinates for diagonal orientation
        #top right rect
        x5 = r*np.cos(np.pi/4)
        y5 = r*np.sin(np.pi/4)

        #top left rect
        x6 = r*np.cos(3*np.pi/4)
        y6 = r*np.sin(3*np.pi/4)

        #bottom left rect
        x7 = r*np.cos(5*np.pi/4)
        y7 = r*np.sin(5*np.pi/4)

        #bottom right rect
        x8 = r*np.cos(7*np.pi/4)
        y8 = r*np.sin(7*np.pi/4)

        #list of every coordinate calc

```

```

    return
[(x1,y1), (x2,y2), (x3,y3), (x4,y4), (x5,y5), (x6,y6), (x7,y7), (x8,y8)]

#cgap = cross orientation coords
cgap1 = coordcalc(cm_gaps[0])[0:4] #5 deg
cgap2 = coordcalc(cm_gaps[1])[0:4] #4 deg
cgap3 = coordcalc(cm_gaps[2])[0:4] #3 deg
cgap4 = coordcalc(cm_gaps[3])[0:4] #2 deg
cgap5 = coordcalc(cm_gaps[4])[0:4] #1 deg

#dgap = diagonal orientation coords
dgap1 = coordcalc(cm_gaps[0])[4:] #5 deg
dgap2 = coordcalc(cm_gaps[1])[4:] #4 deg
dgap3 = coordcalc(cm_gaps[2])[4:] #3 deg
dgap4 = coordcalc(cm_gaps[3])[4:] #2 deg
dgap5 = coordcalc(cm_gaps[4])[4:] #1 deg

#cross orientation, diagonal orientation
ori0 = [0,0,0,0]
ori1 = [45,135,-45,-135]

#permutations of all orientations + coords
permutations =
[cgap1,cgap2,cgap3,cgap4,cgap5,dgap1,dgap2,dgap3,dgap4,dgap5]
permutations_str = ["5 (Cross)", "4 (Cross)", "3 (Cross)", "2
(Cross)", "1 (Cross)", "5 (Diag)", "4 (Diag)", "3 (Diag)", "2 (Diag)", "1
(Diag)"]
orientationlist =
[ori0,ori0,ori0,ori0,ori0,ori1,ori1,ori1,ori1,ori1]

#shuffle both together without replacement
coordandorient = list(zip(permutations, orientationlist,
permutations_str))
random.shuffle(coordandorient)
trialpermutations, trialorientations, trialpermutations_s =
zip(*coordandorient)

counter = 0

for trial in range(0, 10):

    #randomization factor for movable stimuli
    randInt1 = random.uniform(-1.5, 1.5)
    #
    randInt2 = random.uniform(1.0, -1.0)
    polygon = visual.ShapeStim(
        win=win, vertices='cross', units='cm', size=(Plus, Plus),
        ori=trialorientations[counter][1], pos=(randInt1,
randInt1),

```

```

        lineColor=backgroundColor, lineColorSpace='rgb',
        fillColor=stimuliColor, fillColorSpace='rgb',
        opacity=1, depth=0.0, interpolate=True)

    if event.getKeys('left'):
        polygon.pos = (polygon.pos[0]+0.1,polygon.pos[1])
        #obtain the coordinates of the initial position of the stimulus
and add append them
        initial_pix = posToPix(polygon)
        initial_cm =
psychopy.tools.monitorunittools.pix2cm(initial_pix, testMonitor)

    #convert to minutes of arc
    init_x.append(cm2arc(initial_cm[0]))
    init_y.append(cm2arc(initial_cm[1]))

    #draw the still stimuli
    StillStimuli1 = visual.Rect(
        win=win, name='StillStimuli1',units='cm',
        width=line_w, height=line_h,
        ori=trialorientations[counter][0],
pos=trialpermuations[counter][0],
        lineColor=backgroundColor, lineColorSpace='rgb',
        fillColor=stimuliColor, fillColorSpace='rgb',
        opacity=1, depth=0.0, interpolate=True)

    StillStimuli2 = visual.Rect(
        win=win, name='StillStimuli2',units='cm',
        width=line_w, height=line_h,
        ori=trialorientations[counter][1],
pos=trialpermuations[counter][1],
        lineColor=backgroundColor, lineColorSpace='rgb',
        fillColor=stimuliColor, fillColorSpace='rgb',
        opacity=1, depth=0.0, interpolate=True)

    StillStimuli3 = visual.Rect(
        win=win, name='StillStimuli3',units='cm',
        width=line_h, height=line_w,
        ori=trialorientations[counter][2],
pos=trialpermuations[counter][2],
        lineColor=backgroundColor, lineColorSpace='rgb',
        fillColor=stimuliColor, fillColorSpace='rgb',
        opacity=1, depth=0.0, interpolate=True)

    StillStimuli4 = visual.Rect(
        win=win, name='StillStimuli4',units='cm',
        width=line_h, height=line_w,

```

```

        ori=trialorientations[counter][3],
pos=trialpermutations[counter][3],
        lineColor=backgroundColor, lineColorSpace='rgb',
        fillColor=stimuliColor, fillColorSpace='rgb',
        opacity=1, depth=0.0, interpolate=True)

counter += 1

# -----Prepare to start Routine "TrialPhase"-----
#drag_in_process = False
continueRoutine = True
# update component parameters for each repeat

#gotValidClick = False # until a click is received
# keep track of which components have finished

if settingsGui.data[1] == "Both":
    TrialPhaseComponents = [polygon, StillStimuli1,
StillStimuli2, StillStimuli3, StillStimuli4, mouse]

for thisComponent in TrialPhaseComponents:
    if hasattr(thisComponent, 'status'):
        thisComponent.status = NOT_STARTED

#         # Define strings
#         welcomeText = "Welcome to Modified Amsler Test\n Testing
your "+infoGui.data[3] + " eye\n Press Enter to continue..."
#         breakText = "Take a quick break!\n Press Enter to
continue..."
#         exitText = "Excellent!!!\n\n This experiment is
complete.\n\n Thank you for participating! :)"
#
while continueRoutine:
    # during your trial
    kb.clock.reset() # when you want to start the timer from
keys = kb.getKeys(['up', 'down', 'left', 'right', 'space',
'escape'], waitRelease=True)
    if 'escape' in keys:
        core.quit()
    if 'up' in keys:
        polygon.pos = (polygon.pos[0],polygon.pos[1]+0.05)
    if 'down' in keys:
        polygon.pos = (polygon.pos[0],polygon.pos[1]-0.05)
    if 'left' in keys:
        polygon.pos = (polygon.pos[0]-0.05,polygon.pos[1])
    if 'right' in keys:
        polygon.pos = (polygon.pos[0]+0.05,polygon.pos[1])

```



```

        if 'space' in keys:
            continueRoutine = False

        #Below determines what the mouse clicks do during the trial

#         if mouse.isPressedIn(polygon, buttons=[2]): #right mouse
button moves to next routine
#             continueRoutine = False #right mouse advances trial
#
#         if not drag_in_process: # check if one should be
#             if mouse.isPressedIn(polygon):
#                 drag_in_process = True
#
#         if True in mouse.getPressed():
#             if drag_in_process and mouse.getPressed()[0]: # left
mouse button moves polygon
#                 polygon.pos = mouse.getPos() # this gives you
direct feedback anyway
#
#         else:
#             drag_in_process = False

##### Polygon Component
Updates

        # *polygon* updates
if polygon.status == NOT_STARTED:
            polygon.setAutoDraw(True)

##### Stimuli Component
Updates for "Both" Case

        elif settingsGui.data[1] == "Both":
            if StillStimuli1.status == NOT_STARTED:
                StillStimuli1.setAutoDraw(True)

            # *StillStimuli2* updates
if StillStimuli2.status == NOT_STARTED:
                StillStimuli2.setAutoDraw(True)

            # *StillStimuli3* updates
if StillStimuli3.status == NOT_STARTED:
                StillStimuli3.setAutoDraw(True)

            # *StillStimuli4* updates
if StillStimuli4.status == NOT_STARTED:
                StillStimuli4.setAutoDraw(True)

```

```

##### Mouse Component Updates

#           # *mouse* updates
#           if mouse.status == NOT_STARTED:
#               mouse.status = STARTED
#               prevButtonState = mouse.getPressed() # if button is
down already this ISN'T a new click
#
#           if mouse.status == STARTED: # only update if started and
not finished!
#               buttons = mouse.getPressed()
#               if buttons != prevButtonState: # button state
changed?
#                   prevButtonState = buttons
#                   if sum(buttons) > 0: # state changed to a new
click
#                       # abort routine on response
#                       continueRoutine = True #left click does not
move to next phase

#####

# check if all components have finished
if not continueRoutine: # a component has requested a
forced-end of Routine
    break
    continueRoutine = False # will revert to True if at least
one component still running
    for thisComponent in TrialPhaseComponents:
        if hasattr(thisComponent, "status") and
thisComponent.status != FINISHED:
            continueRoutine = True
            break # at least one component has not yet
finished

# refresh the screen
if continueRoutine: # don't flip if this routine is over
or we'll get a blank screen
    win.flip()

# -----Ending Routine "TrialPhase"-----
for thisComponent in TrialPhaseComponents:
    if hasattr(thisComponent, "setAutoDraw"):
        thisComponent.setAutoDraw(False)
x

```

```

if continueRoutine == False:
    resp.append(someClock.getTime())
    someClock.reset()

    #obtain the coordinates of the final position of the stimulus
    and add append them
    final_pix = posToPix(polygon)
    final_cm = psychopy.tools.monitorunittools.pix2cm(final_pix,
testMonitor)

    #convert to minutes of arc
    fin_x.append(cm2arc(final_cm[0]))
    fin_y.append(cm2arc(final_cm[1]))

    trial_num = [1,2,3,4,5,6,7,8,9,10] #list

    #calculates euclidian distance (final position relative to origin)
    euc = []
    for i in range(10):
        euc.append(sqrt((fin_x[i])**2+(fin_y[i])**2))
    #calculates euclidian distance (initial position relative to
    origin)
    init_euc = []
    for i in range(10):
        init_euc.append(sqrt((init_x[i])**2+(init_y[i])**2))

    #write again to data file
    dataFile.write("{} , {} , {} , {} , {} , {} , {} , {} , {}" .format("\nTrial #",
"Presentation (Degrees)", "initial x-position (moa)", "initial y-
position (moa)" , "final x-position (moa)", "final y-position (moa)" ,
"Final Distance from Origin (moa)", "Response Time (s)\n"))

    #prints all the elements of the provided lists into excel under the
    columns made above ^
    for i in range(0,10):
        dataFile.write("{} , {} , {} , {} , {} , {} , {} , {} , {}" .format(
            trial_num[i],
            trialpermutations_s[i],
            init_x[i],
            init_y[i],
            fin_x[i],
            fin_y[i],
            euc[i],
            resp[i]))

    #standard deviation and mean

```

```

Mean = mean(euc)
Stdev = stdev(euc)

#add stdev and mean to data file
dataFile.write((2 * "{}\n").format(
"Average Distance from Origin (moa)", Mean,
"Standard Deviation (Distance)", Stdev))

# completed 10 repeats of 'trials_2'
dataFile.close()

# Flip one final time so any remaining win.callOnFlip()
# and win.timeOnFlip() tasks get executed before quitting
win.flip()

win.close()

# Data file name stem = absolute path + name; later add .psyexp,
.csv, .log, etc
main_data = _thisDir + os.sep + u'MMP Data/%s_%s_%s' %
(infoGui.data[0], expName, expDate)
workbook = xlsxwriter.Workbook(main_data+'.xlsx')

patient_info = workbook.add_worksheet()
col_a = ["Date", "Name", "Age", "Gender", "Eye", "Session",
"Stimuli Colour", "Stimuli Type", "Display resolution (px)", "Screen",
"Distance from screen"]
col_b = [expDate, infoGui.data[0], infoGui.data[1],
infoGui.data[2], infoGui.data[3], infoGui.data[4], settingsGui.data[0],
settingsGui.data[1], str(GetSystemMetrics(0)) + " x " +
str(GetSystemMetrics(1)), settingsGui.data[2], settingsGui.data[3]]

patient_info.write_column('A1', col_a)
patient_info.write_column('B1', col_b)

exp_data = workbook.add_worksheet()

df_values = pd.read_csv(fileName + ".csv", skiprows=11)
df_values = df_values[:-2]
df_values = df_values.sort_values('Presentation (Degrees)',
ascending=False)
print(df_values)

trials = ['Trial #'] + df_values['Trial #'].tolist()

```

```

    pres = ['Presentation (Degrees)'] + df_values['Presentation
(Degrees)'].tolist()
    init_x_moa = ['initial x-position (moa)'] + df_values['initial x-
position (moa)'].tolist()
    init_y_moa = ['initial y-position (moa)'] + df_values['initial y-
position (moa)'].tolist()
    fin_x_moa = ['final x-position (moa)'] + df_values['final x-
position (moa)'].tolist()
    fin_y_moa = ['final y-position (moa)'] + df_values['final y-
position (moa)'].tolist()
    dist_moa = ['Final Distance from Origin (moa)'] + df_values['Final
Distance from Origin (moa)'].tolist()
    response = ['Response Time (s)'] + df_values['Response Time
(s)'].tolist()

    exp_data.write_column('A1', trials)
    exp_data.write_column('B1', pres)
    exp_data.write_column('C1', init_x_moa)
    exp_data.write_column('D1', init_y_moa)
    exp_data.write_column('E1', fin_x_moa)
    exp_data.write_column('F1', fin_y_moa)
    exp_data.write_column('G1', dist_moa)
    exp_data.write_column('H1', response)

    # Create a new Chart object.
    chart = workbook.add_chart({'type': 'line'})

    # Configure the chart. In simplest case we add one or more data
series.
    chart.add_series({'categories': '=Sheet2!$B$2:$B$11', 'values':
'=Sheet2!$G$2:$G$11', 'name': 'Distance from Origin (moa)', 'marker':
{'type': 'circle'}})
    chart.add_series({'categories': '=Sheet2!$B$2:$B$11', 'values':
'=Sheet2!$H$2:$H$11', 'name': 'Response Time (s)', 'marker': {'type':
'circle'}})

    chart.set_title({'name': 'Final Distance from Origin and Response
Time vs Presentation'})
    chart.set_x_axis({'name': 'Presentations (Degrees)'})

    # Insert the chart into the worksheet.
    exp_data.insert_chart('B17', chart)
    #write averages ()

workbook.close()

file = fileName + ".csv"
if os.path.exists(file) and os.path.isfile(file)):

```

```
    os.remove(file)
    print("file deleted")
else:
    print("file not found")

core.quit()

if __name__ == "__main__":
    main()
```